Geology of Organ Mountains and southern San Andres Mountains, New Mexico

by WILLIAM R. SEAGER



See page i

MEMOIR 36 New Mexico Bureau of Mines & Mineral Resources 1981

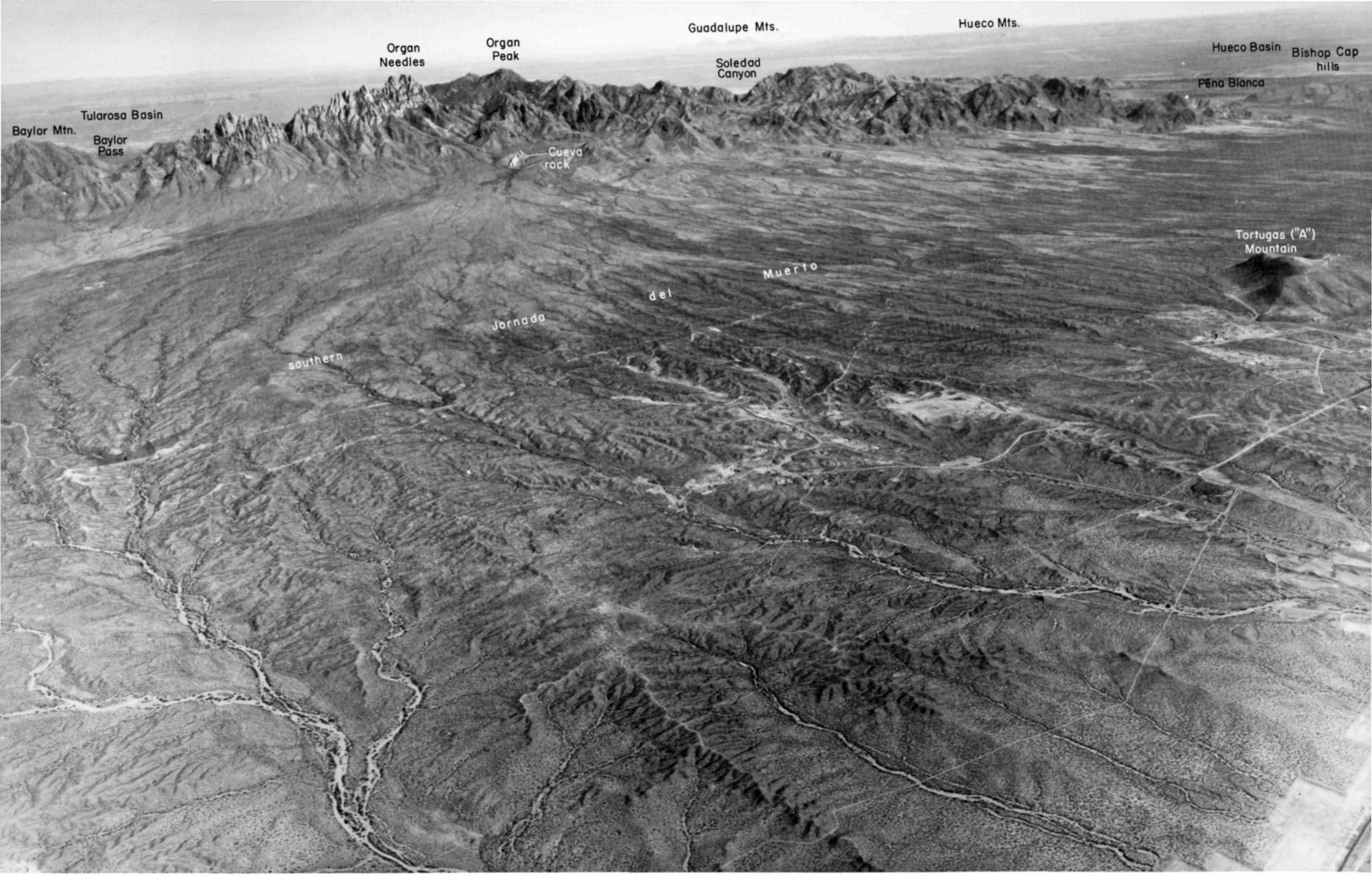
A DIVISION OF

NEW MEXICO INSTITUTE OF MINING & TECHNOLOGY

Geology of Organ Mountains and southern San Andres Mountains, New Mexico

COVER—"THE 'SIERRA DE LOS ORGANOS' OR ORGAN MOUNTAINS are so named from their pinnacled summits and sides which resemble the pipes of an organ. They are of a light gray granite, and rise to the height of 3,000 feet above the river. The defiles are filled with large pines and the more open valley, with live oaks. From the place where we halted and lunched, I took a sketch of these mountains and of the defile through which I had passed."

(from Bartlett, 1854)



FRONTISPIECE: Organ Mountains and southern Jornada del Muerto; view to east-southeast (photo courtesy of Rollag and Associates, El Paso, Texas).

Memoir 36



New Mexico Bureau of Mines & Mineral Resources

A DIVISION OF
NEW MEXICO INSTITUTE OF MINING & TECHNOLOGY

Geology of Organ Mountains and southern San Andres Mountains, New Mexico

by William R. Seager

SOCORRO 1981

NEW MEXICO INSTITUTE OF MINING & TECHNOLOGY
KENNETH W. FORD, *President*

NEW MEXICO BUREAU OF MINES & MINERAL RESOURCES
FRANK E. KOTTLOWSKI, *Director*
GEORGE S. AUSTIN, *Deputy Director*

BOARD OF REGENTS
Ex Officio
Bruce King, *Governor of New Mexico*
Leonard DeLayo, *Superintendent of Public Instruction*

Appointed
William G. Abbott, President, 1961-1985, *Hobbs*
Judy Floyd, 1977-1987, *Las Cruces*
Owen Lopez, 1977-1983, *Santa Fe*
Dave Rice, 1972-1983, *Carlsbad*
Steve Torres, Secretary-Treasurer, 1967-1985, *Socorro*

BUREAU STAFF

Full Time

MARLA D. ADKINS, *Assistant Editor*
ORIN J. ANDERSON, *Geologist*
RUBEN ARCHULETA, *Technician I*
KEVIN C. BAKER, *Field Researcher*
ROBERT A. BIEBERMAN, *Senior Petrol. Geologist*
STEVE BLODGETT, *Assistant Editor*
LYNN A. BRANDVOLD, *Chemist*
JAMES C. BRANNAN, *Draftsperson*
CORALE BRIERLEY, *Chemical Microbiologist*
BRENDA R. BROADWELL, *Assoc. Lab Geoscientist*
FRANK CAMPBELL, *Coal Geologist*
RICHARD CHAMBERLIN, *Economic Geologist*
CHARLES E. CHAPIN, *Senior Geologist*
JEANETTE CHAVEZ, *Admin. Secretary I*
RICHARD R. CHAVEZ, *Assistant Head, Petroleum*
RUBEN A. CRESPIN, *Laboratory Technician II*
LOIS M. DEVLIN, *Director, Bus.–Pub. Office*
KATHY C. EDEN, *Editorial Technician*
ROBERT W. EVELETH, *Mining Engineer*
K. BABETTE FARIS, *X-ray Lab. Manager*
ROUSSEAU H. FLOWER, *Sr. Emeritus Paleontologist*
STEPHEN J. FROST, *Coal Geologist*
JOHN W. HAWLEY, *Environmental Geologist*
DANA M. HELJESON, *Editorial Technician*
STEPHEN C. HOOK, *Paleontologist*
MELVIN JENNINGS, *Metallurgist*
BARBARA J. JOHNSON, *Staff Secretary*
ROBERT W. KELLEY, *Editor & Geologist*
SHERRY A. KRUKOWSKI, *Record Manager*
MARK LOGSDON, *Economic Geologist*
ANNABELLE LOPEZ, *Clerk Typist*
DAVID W. LOVE, *Environmental Geologist*
WESS MAULDIN, *Driller's Helper*
VIRGINIA MCLEMORE, *Geologist*
LYNNE MCNEIL, *Staff Secretary*
NORMA J. MEEKS, *Department Secretary*
DAVID MENZIE, *Geologist*
ARLEEN MONTOYA, *Librarian/Typist*
TERESA A. MUELLER, *Draftsperson*
SUE NESS, *Receptionist*
ROBERT M. NORTH, *Mineralogist*
KEITH O'BRIEN, *Hydrologist*
JOANNE C. OSBURN, *Coal Geologist*
GLENN R. OSBURN, *Volcanologist*
JOAN C. PENDLETON, *Associate Editor*
BARBARA R. POPP, *Lab. Biotechnologist*
ROBERT QUICK, *Driller*
MARSHALL A. REITER, *Senior Geophysicist*
JACQUES R. RENAULT, *Senior Geologist*
JAMES M. ROBERTSON, *Mining Geologist*
GRETCHEN H. ROYBAL, *Coal Geologist*
AMY SHACKLETT, *Asst. Lab Biotechnologist*
JACKIE H. SMITH, *Laboratory Technician IV*
DALE STALEY, *Driller's Helper*
WILLIAM J. STONE, *Hydrogeologist*
SAMUEL THOMPSON III, *Petroleum Geologist*
JUDY M. VAIZA, *Executive Secretary*
DEBRA VETTERMAN, *Draftsperson*
ROBERT H. WEBER, *Senior Geologist*
DONALD WOLBERG, *Vertebrate Paleontologist*
MICHAEL W. WOOLDRIDGE, *Scientific Illustrator*

Part Time

CHRISTINA L. BALK, *Geologist*
HOWARD B. NICKELSON, *Coal Geologist*
BEVERLY OHLINE, *Newswriter, Information Services*
THOMAS E. ZIMMERMAN, *Chief Security Officer*

Graduate Students

BRUCE W. BAKER
INDIRA BALKISSOON
GERRY W. CLARKSON
ROBERTA EGGLESTON
TED EGGLESTON
ADRIAN HUNT
TOM MCANULTY
LAWRENCE NELSON
JOHN YOUNG

Plus about 50 undergraduate assistants

First Printing, 1981

Published by Authority of State of New Mexico, NMSA 1953 Sec. 63-1-4
Printed by University of New Mexico Printing Plant, May, 1981

Available from New Mexico Bureau of Mines & Mineral Resources, Socorro, NM 87801 Price $20.00

Preface

Forty-five years have passed since Sir Kingsley Charles Dunham wrote *Geology of the Organ Mountains,* yet his account of the geology of the range is as timely today as it was in 1935 and his writing style is as much a pleasure to read now as then. His description of the ore deposits and his petrographic work with the igneous and metamorphic rocks are not likely to be improved upon for many years. Besides being of interest for the local geology, the book is also of general value because Dunham carefully martials evidence from the Organs on such topics as the emplacement of batholiths, structural and lithologic controls of orebodies, metamorphic mineral equilibrium assemblages, and alteration processes. *Geology of the Organ Mountains* has justly become a classic in the geology of New Mexico.

The quality of Dunham's work is such that few additional geologic studies in the Organ district were published between 1935 and 1980, although many individuals and mining companies used Dunham's report as a basis for mineral exploration during the same period. The present study was undertaken partly to integrate the results of recent exploration activity, geophysical studies, and radiometric dating into Dunham's geologic framework and partly to show geologic details on greatly improved 7½-min topographic base maps. Additional objectives were: 1) to map previously unmapped portions of the northern Organ and southern San Andres Mountains that contain features of structural significance, 2) to describe sections of Paleozoic rocks that had not been described in detail or subdivided into up-to-date stratigraphic units, and finally 3) to investigate relationships between the Organ batholith and volcanic rocks in the southern Organ range, which recently were shown to be of the same age. During the course of mapping and from many discussions with John Hawley, I realized that there were many kinds and ages of alluvial deposits mantling the edge of the mountains and that they were related to the general geomorphic evolution of the range and to repeated movements on the boundary fault along its eastern margin. Another objective in this study was to distinguish among these deposits and relate them to the Quaternary erosional and faulting history of the range.

Field work was done between 1975 and 1978, mostly during the summer months. Working in the summer in the Organ Mountains can be exhilarating, discouraging, rewarding, frightening, or satisfying, and is always different from day to day. Aside from the steep slopes, rocky precipices, and occasional rattlesnakes (mostly black-tailed rattlers), nature uses other ways to insure that geologic information does not come easily from the mountains. Many of the higher slopes are covered with dense tangles of brush, cactus, and stiff-tipped yucca that require more than average stubbornness to thrash through. Once the brush has been negotiated and high ridges conquered, usually about noon or a little after, thunderstorms frequently appear and within minutes lightning invariably forces a hasty retreat—with little or no work accomplished—back down the exposed ridges to the comparative safety of ravine or canyon bottoms. The thunder that follows is deafening, unlike that heard in more open spaces, and reverberates for many seconds off the sheer granite walls of the Needles or rolls from canyon to canyon. Soaking rain follows. All kinds of bad weather seem to be attracted to the high peaks. More than once I struggled 2,000 ft to the summit ready to continue the previous day's work, when instead of lightning, low clouds would promptly gather, engulf me, and make it impossible to see more than a few feet around. Again, nothing to do but go back down and chalk up the day's effort to good exercise.

Even in pleasant weather one can be driven off the rocky summits of the range. For short times during the summer, swarms of gnats and small flies infest every bush and rocky crevice along the higher peaks. They can be set into motion just by a person's presence and they seem indifferent to insect repellent. They come at you in clouds, and shortly your ears, eyes, nose, and mouth are full. Retreat from the ridge top is the only effective antidote. At least once in each summer swarms of ladybugs also take over the highest peaks, rendering the rocks orange by their numbers.

Satisfying experiences far outweigh the disagreeable ones, however. Reaching the summit of the range and looking out over the vast stretches of canyons and ridges below to the broad desert beyond is always exhilarating. To come upon unexpected springs or groves of aspen or Douglas fir is a pleasant surprise and a walk through a flattish stretch of canyon floor shaded by high Ponderosa pines or ancient juniper trees is a pleasure. Golden eagles swooping up a canyon toward you, bighorn rams or huge deer clashing and locking horns in front of you, newly born, unafraid fawns motionless beneath a bush at your side—these are all occasional rewards which more than compensate for the bugs and for the spells of disagreeable weather. Of course, over the long run, the daily variety for a geologist working in the Organ or San Andres Mountains is provided by the geology itself. Even if there were nothing else to make field work a pleasure, the geologic relations among rocks and structures are sufficiently challenging and revealing to insure boredom as an impossibility. Putting together a picture of the geologic relationships and history of the range can be likened to assembling a huge, complex puzzle with half (or more?) of the pieces missing. For a geologist the best part of the field experience—aspen, eagles, and fawns notwithstanding—is putting that puzzle together.

ACKNOWLEDGMENTS—Many people have directly or indirectly contributed to this effort through their advice, critical readings of the text, or with other kinds of help and cooperation. I thank Sam Thompson III, Pete Lipman, Dick Chamberlin, Jerry Mueller, John Hawley, Tom Giordano, Charles Chapin, Glenn R. Osburn, and D. D. Seager for reviewing various chapters of the book, Charles B. Hunt for reviewing an early version of the manuscript and for his help with fig. 83, and especially Vincent C. Kelley for reviewing the manuscript in its entirety. The New Mexico Bureau of Mines and Mineral Resources funded chemical analyses, and I thank Lynn Brandvold for running those analyses. The University of Arizona geochronology laboratory also provided some chemical analyses, a radiometric date, and computer analysis of the chemical data; I am grateful to M. Shafiqullah for obtaining that data for me. Dan Barker and Ted Bornhorst kindly used their computer programs to supply me with norms and other statistical data. I would also like to thank Rich Loring for introducing me to some of the problems of the Organ district and him and CONOCO for releasing radiometric dates in advance of publication. I am grateful to Bill King for his identification of fusulinids, to Steve Hook and George Bachman for their help with the Cretaceous stratigraphy, and to Russ Clemons for his help with petrographic problems. Chan Swanberg and Phil Goodell generously released unpublished K-Th-U analyses to me. I gratefully acknowledge the many helpful discussions and field trips with John Hawley and Lee Gile that enabled me to better understand the Quaternary stratigraphy and geomorphology of the range. Dave Herrell and Nancy Stoll both spent many hours making modal analyses of the Organ batholith and volcanic rocks. I also acknowledge the major effort contributed by Lionel Brown towards the understanding of the range—the complete bouguer gravity map which appears in fig. 66.

Dave Reiter, Mark Parchman, Shari Alexander Kelley, Rick Kelley, and Pat Laney served as very able, helpful, and

enthusiastic field assistants, and I thank them for their considerable effort. I would also like to acknowledge Jonathan T. Wright of the National Geographic Society; Bob Sigmon and the Las Cruces Sun-News; and Rollag and Associates for allowing me use of their photographs. For the outstanding job of drafting and production of the geologic map, I thank Williams and Heintz Map Corporation. For typing of the manuscript (several times) I am indebted to Mitty Dixon and Marilynn Wilson. Thanks also are due Mrs. A. B. Cox, Mrs. Bonnie Ligon, Mr. Rob Cox and Mr. D. Hopkins for allowing me access to their lands. I am especially grateful to R. H. Duncan, chief scientist at the White Sands Missile Range, for permission to make geologic studies on Missile Range lands, and to Felix Sedillo, Fred Perea, and Ismael Rel for their assistance in carrying out the work. Finally, I want to express my appreciation to Frank Kottlowski, Director of the New Mexico Bureau of Mines and Mineral Resources, for his support of the project.

William R. Seager
Professor of Geology
Department of Earth Sciences
New Mexico State University

Las Cruces
January 4, 1980

Contents

ABSTRACT 11

INTRODUCTION 11
- LOCATION 11
- ACCESS AND LAND OWNERSHIP 13
- NAME 13
- PHYSIOGRAPHY 13
- PREVIOUS WORK 19
- PLAN OF BOOK 19

PRECAMBRIAN, PALEOZOIC, AND MESOZOIC ROCKS 20
- PRECAMBRIAN ROCKS 20
- CAMBRIAN AND ORDOVICIAN ROCKS 21
  - Bliss Sandstone 21
  - El Paso Group 22
  - Montoya Group 22
- SILURIAN ROCKS 23
  - Fusselman Dolomite 23
- DEVONIAN ROCKS 24
  - Canutillo Formation 24
  - Percha Shale 24
- MISSISSIPPIAN ROCKS 25
  - Caballero (?) Formation 25
  - Lake Valley Formation 27
  - Las Cruces Formation 27
  - Rancheria Formation 28
  - Helms Formation 29
- PENNSYLVANIAN AND PERMIAN ROCKS 29
  - Lead Camp Limestone 29
  - La Tuna Formation 30
  - Berino Formation 30
  - Panther Seep Formation 30
  - Hueco Limestone 31
  - Abo and Yeso Formations 33
  - Yeso and San Andres Formations 33
- CRETACEOUS ROCKS 33
  - Sarten–Dakota Sandstone 33
  - Strata correlative with Mancos Shale and Gallup Sandstone 33
- SUMMARY OF PRECAMBRIAN, PALEOZOIC, AND MESOZOIC HISTORY 34

LARAMIDE OROGENY 36
- LARAMIDE TECTONIC SETTING 36
- STRUCTURAL FEATURES 37
  - Bear Peak thrust and fold belt 37
  - Torpedo–Bennett fault zone 38
  - Black Prince fault zone 39
  - Mechanics of Laramide uplift 39
  - Origin 40
- LOVE RANCH FORMATION 40
  - Age and correlation 41
  - Interpretation of Laramide history 41

EOCENE OR OLIGOCENE ANDESITIC VOLCANISM 43

MIDDLE TERTIARY SILICIC MAGMATISM AND VOLCANO-TECTONICS 46
- VOLCANIC SEQUENCE 46
  - Cueva Tuff 47
  - Tuff of Cox Ranch 49
  - Tuff of Achenback Park 51
  - Tuff of Squaw Mountain 52
  - West-side lavas 53
- ORGAN BATHOLITH 55
  - Age and relation to volcanic rocks 55
  - Batholith geometry and emplacement 56
  - Batholith rocks 58
- SUMMARY AND DISCUSSION 65
  - Zoning in the magma chamber 65
  - Depth, water-vapor pressure, and temperature of the magma chamber 65
  - Organ cauldron 66
  - Organ batholith 68

METAMORPHIC EFFECTS 69

LATE TERTIARY DEFORMATION 70
- OLDER FAULT SYSTEMS 70
  - Southern San Andres Mountains 70
  - Organ Mountains 71
  - Bishop Cap–northern Franklin Mountains 71
- YOUNGER FAULTS 72
  - Organ Mountains and Artillery Range fault zones 72
  - West-side boundary fault 74
  - Jornada fault 74
  - Westward tilting of the ranges 74
- DISCUSSION 75
- VOLCANIC AND SEDIMENTARY ROCKS PROBABLY RELATED TO EARLY STAGES OF RIFTING 77

LATE PLIOCENE AND QUATERNARY DEPOSITS 78
- CAMP RICE FORMATION 78
  - Basal piedmont-slope facies 78
  - Fluvial facies 79
  - Upper piedmont-slope facies 80
  - Age of the Camp Rice Formation 81
- LATE PLEISTOCENE DEPOSITS 81
- LATEST PLEISTOCENE AND HOLOCENE DEPOSITS 82

MINERAL DEPOSITS 83
- MINERAL DEPOSITS RELATED TO ORGAN BATHOLITH 83
  - Segregations in pegmatites 84
  - Veins in Precambrian rocks 84
  - Mineralized veins and dikes in the Organ batholith 84
  - Replacement deposits 85
- MINERAL DEPOSITS PROBABLY RELATED TO LATE TERTIARY RIFTING 88
  - Ruby mine (Hayner mine) 88
  - Bishop Cap area 88
  - Devil's Canyon area 89
- RECENT DRILLING AND FUTURE POTENTIAL OF THE ORGAN DISTRICT 89

REFERENCES 91

INDEX 95

APPENDIX A—Measured sections (microfiche) **pocket**

APPENDIX B—Chemical analyses and norms of igneous rocks **pocket**

TABLES

1—Thicknesses of Paleozoic and Cretaceous strata **28**
2—Radiometric dates of rocks associated with Organ batholith **46**
3—Electron-microprobe analyses of glasses in west-side lavas **54**
4—Modal analyses of west-side lavas **54**
5—Electron-microprobe analyses of plagioclase phenocrysts **55**
6—Modal analyses of Organ batholith and related rocks **59**
7—Age relations, rock types, and silica content of Organ batholith **60**
8—Drill-hole data in Organ area **89**

FIGURES

1—Location map, south-central New Mexico **x**
2—Organ Mountains viewed from Tortugas Mountain **11**
3—Location map of Organ, San Agustin, and southernmost San Andres Mountains **12**
4—East side of Organ Mountains **13**
5—Organ and San Andres Mountains viewed from White Sands near Lake Lucero **14**
6—Organ Needles viewed from northwest **14**
7—"Needles" along west-central Organ Mountains **14**
8—"Rabbit Ears" section of Organ Needles **15**
9—Organ Needle viewed from area of Organ Peak **15**
10—Sugarloaf Peak **15**
11—Mouth of nearly vertical-walled Ice Canyon **15**
12—Ruins of Dripping Springs resort near mouth of Ice Canyon **16**
13—Mouth of Long Canyon **16**
14—Headwater region of Boulder Canyon **16**
15—Possible evolution of transverse canyons in San Andres and Organ Mountains **17**
16—Central part of Soledad Canyon **17**
17—Southern wall of Fillmore Canyon **17**
18—Northern contact of Organ batholith with metamorphosed lower Paleozoic rocks **18**
19—San Agustin Peak exfoliation dome **18**
20—Eastern reaches of Bear Canyon **18**
21—An effective attention-getter **19**
22—Correlation and nomenclature of pre-Tertiary rock units **20**
23—Lower and middle Paleozoic rocks **22**
24—Lower Paleozoic rocks **22**
25—Lake Valley Limestone filling channel **24**
26—Middle and lower Paleozoic rocks at Bishop Cap **25**
27—Devonian and Mississippian formations **25**
28—Correlation of Mississippian formations **26**
29—Composite columnar section of Hueco Limestone **back pocket**
30—Planispiral gastropod **32**
31—Echinoid **32**
32—Diagrammatic sections of Permian rocks **32**
33—Cordilleran orogenic belt **36**
34—Major Laramide structural features **36**
35—Geologic map of Laramide uplift in Organ Mountains **37**
36—Eastward view toward Bear Peak **37**
37—Westward view along Bear Peak fold and thrust zone **38**
38—Overturned syncline on southern slopes of Black Mountain **38**
39—Diagrammatic cross section through Laramide block uplift **40**
40—Evolution of Bear Peak fold and thrust belt **42**
41—Orejon Andesite lava flows in Fillmore Canyon **43**
42—Chemical classification of Organ Mountain igneous rocks **44**
43—Variation diagram for Orejon Andesite **45**
44—Composite section of volcanic rocks **48**
45—Chemical and mineralogic variations with age in Cueva Tuff **49**
46—Cueva rock **49**
47—Cueva Tuff exposed on Peña Blanca ridge **49**
48—Columnar section of Cueva Tuff and tuff of Cox Ranch **50**
49—Tuff of Achenback Park **51**
50—Tuffs exposed south of Cueva rock **51**
51—North-south cross section along southwest edge of Organ Mountains **52**
52—Tuff of Squaw Mountain in North Canyon **53**
53—East-central part of Organ batholith **56**
54—Composition of Oligocene volcanic and plutonic rocks of Organ Mountains **56**
55—Diagrammatic sections through Organ batholith **57**
56—Classification of rocks from Organ batholith **58**
57—Organ Needle quartz monzonite **60**
58—Organ Needles **60**
59—Vertical mineral and chemical variations within Organ Needle quartz monzonite **61**
60—Lateral mineral and chemical variations within Organ Needle quartz monzonite (mafic facies) **62**
61—Swarm of mafic xenoliths **63**
62—Cluster of twinned albite crystals **64**
63—Twinned orthoclase crystals **64**
64—Large roof pendant of Orejon Andesite **64**
65—Compositional trend of Oligocene ash-flow tuffs and lavas **66**
66—Complete Bouguer gravity map of Organ Mountains area **67**
67—SiO_2-age relations of volcanic and plutonic rocks **68**
68—Possible evolutionary sequence for Organ Mountains volcanic-plutonic cycle **68**
69—Modoc fault **69**
70—Goat Mountain fault **70**
71—Eastern mouth of Bear Canyon looking south **70**
72—Eastern mouth of Bear Canyon looking north **71**
73—Cross section of low-angle faults in northern Franklin Mountains **72**
74—Minor antithetic faults and rifts **72**

75—Composite Organ Mountains fault scarp **73**
76—Composite Organ Mountains scarp displacing fan **73**
77—Vertical aerial photo of Organ Mountains fault scarp **73**
78—Gravity profile and geologic section **74**
79—East-west section from Tularosa Basin to Mesilla Basin **75**
80—Interpretation of sequential evolution in late Tertiary **76**
81—Clay-model experiment **76**
82—Orientation of shear fractures and strain ellipsoid **76**
83—Geomorphic relationships among fans **79**
84—Camp Rice fan delta **80**
85—Progressive shallowing of fan gradients **80**
86—Spheroidally weathered boulders on Jornada I surface **81**
87—Metal-ore zoning in Organ district **83**
88—Wulfenite from Stevenson-Bennett mine **85**

SHEETS (*in pocket*)

1—Geologic map
2—Cross sections
3—Columnar and short cross sections
4—Chemical analyses

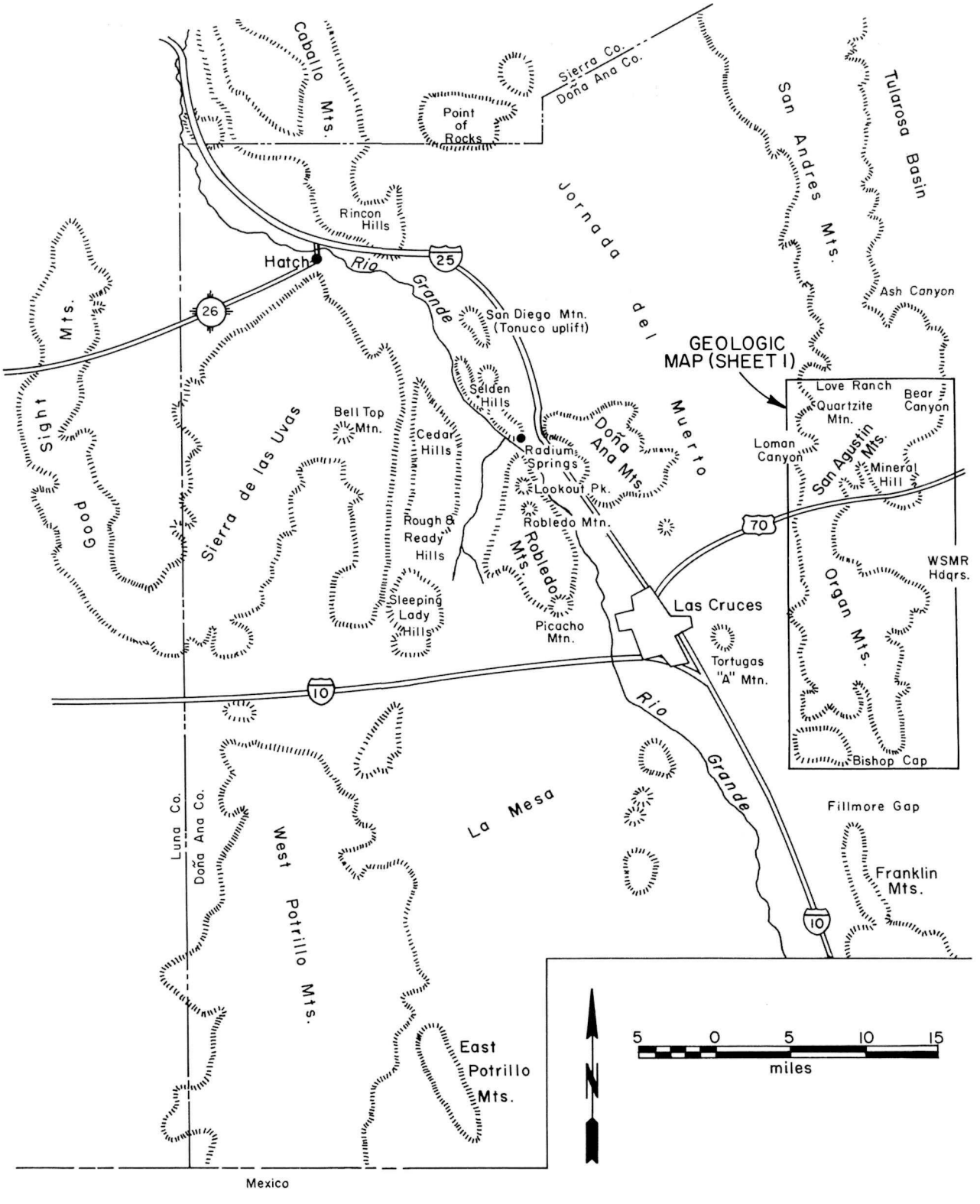


FIGURE 1—LOCATION MAP, SOUTH-CENTRAL NEW MEXICO.

Abstract

The Organ and southernmost San Andres Mountains in south-central New Mexico are part of a 150-mi long, west-tilted fault block extending from El Paso, Texas, northward to central New Mexico. The Organ Mountains tower nearly a mile above the floor of the Tularosa Basin on the east and the Rio Grande valley on the west. Oldest rocks exposed are Precambrian granite, overlain by as much as 8,500 ft of mostly marine Paleozoic and Cretaceous strata. In Laramide time, these rocks were deformed along the faulted margins of a basement-cored block uplift which was ancestral to the modern Organ–San Andres range. Lower Tertiary fanglomerate, at least 2,000 ft thick, records the erosional "unroofing" of the Laramide uplift and was sharply deformed as uplift progressed. Magmatism profoundly affected the area in middle Tertiary time. Intermediate-composition lava and mudflow breccia of late Eocene or early Oligocene age buried the deeply eroded Laramide uplift. The Organ batholith (about 32.8 m.y. old) is interpreted to be an exposure of the upper, outer part of a magma chamber whose silicic cap erupted as pyroclastic flows and lavas 33.0–33.7 m.y. ago. The pyroclastic rocks, approximately 2 mi thick, subsided to form the Organ cauldron, only a piece of which is exposed in the Organ Mountains today. The pyroclastic rocks also formed the roof beneath which the batholith crystallized. Compositional zoning within the volcanics indicates that the erupted magma volume was also zoned, ranging from 77 percent SiO_2 at the top to about 65 percent at lowest levels. The batholith represents deeper, less silicic (56–68 percent) levels of the magma chamber, and late-stage mineralized plutons within the batholith are interpreted to be products of the progressive crystallization of the magma chamber. Undated tristanite-trachybasalt flows interbedded with fanglomerate may indicate onset of late Tertiary block faulting in the area. Subsequent uplift of the modern ranges involved an early stage of closely spaced faulting associated with moderate west tilting or, locally, east downwarping. Some faults, initially steep, were rotated into low-angle positions as tilting progressed. The more recent stage of uplift is distinguished by development of the modern, widely spaced range-boundary faults and their associated horsts, west-tilted blocks, and grabens. Movement on the eastern range-boundary fault of the Organ and southern San Andres fault block has persisted to within the last 4,000–5,000 yrs. Several generations of alluvial fans, as old as middle Pliocene, are products of repeated movement on these faults. Mineral deposits related to the Organ batholith include base-metal deposits as replacements in limestone and dolomite, and as disseminations, vein fillings, and pegmatite minerals in the batholith.

Introduction

Location

The Organ Mountains, one of the most picturesque and rugged mountain ranges in the Southwest, form the skyline approximately 10 mi east of Las Cruces, New Mexico (frontispiece), in southern Doña Ana County (fig. 1). The row of jutting, fluted, bare-rock pinnacles known as the Needles—the backbone of the range—can be seen on a favorable day from nearly 100 mi away, making them probably the most familiar landmark in the region (fig. 2). Their stark, sawtooth profile, their challenging slopes and changing moods have made the Needles a favorite of artists, photographers, and mountain climbers (Ames, 1892; Ingraham, 1979), as well as a daily pleasure to the people who live within their view. From their summit a broad expanse of southern New Mexico, Texas, and Mexico spreads out below—from the Magdalena Mountains on the north to far into Mex-

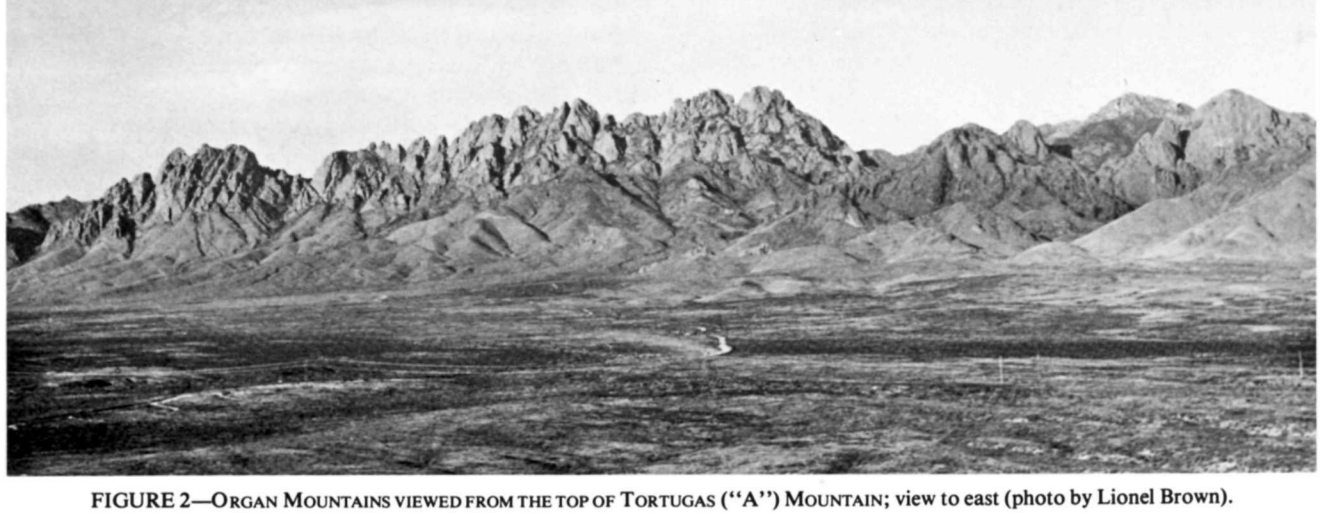


FIGURE 2—ORGAN MOUNTAINS VIEWED FROM THE TOP OF TORTUGAS ("A") MOUNTAIN; view to east (photo by Lionel Brown).

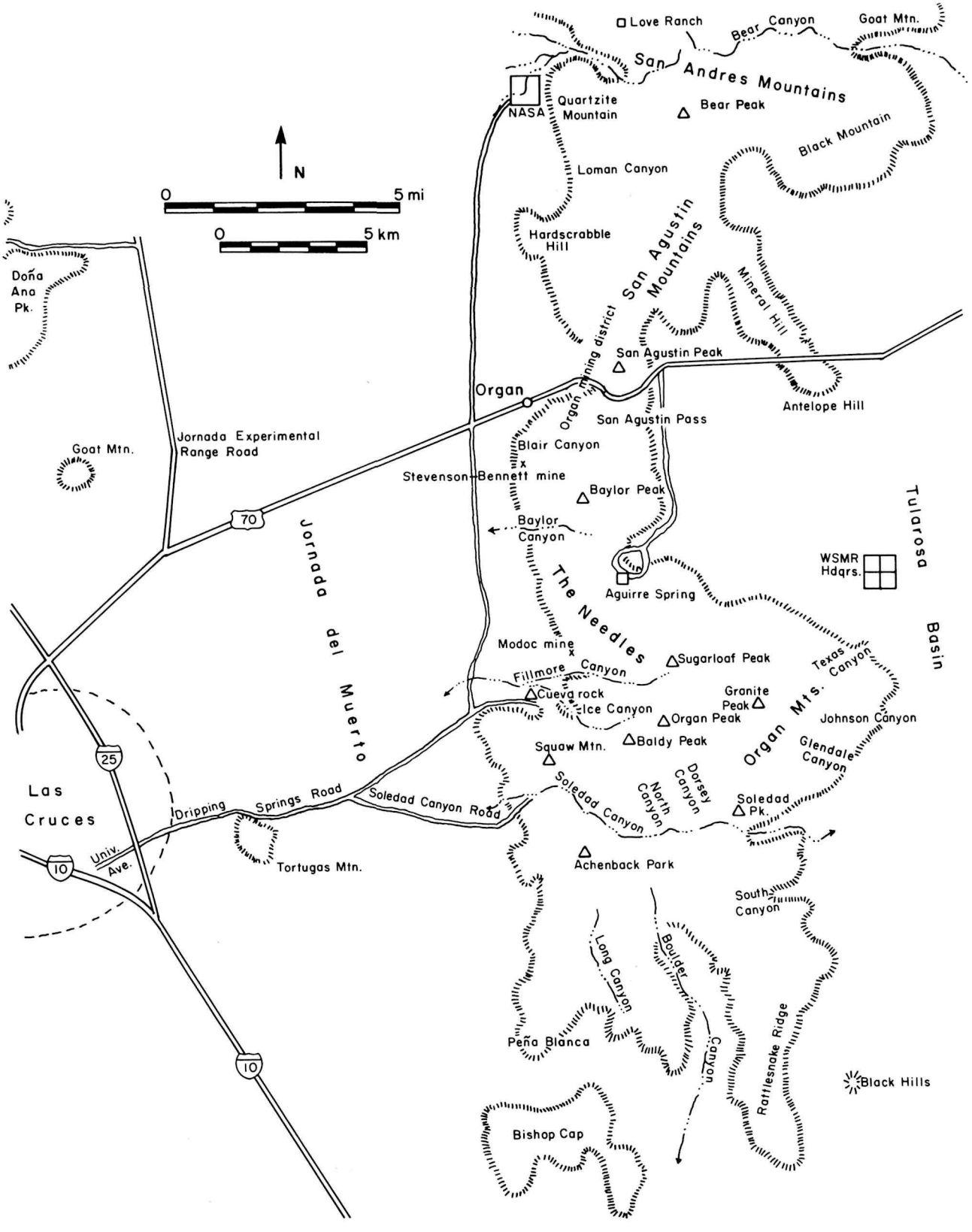


FIGURE 3—LOCATION MAP OF ORGAN, SAN AGUSTIN, AND SOUTHERNMOST SAN ANDRES MOUNTAINS.

ico and from the Arizona border to the Guadalupe Mountains. Yet the Needles are just the crown of a jumbled range of stark peaks, rugged ridges, and deep canyons that stretches for 150 mi from El Paso, Texas, to central New Mexico.

The lofty central peaks of the Organ Mountains gradually become less imposing northward, finally giving way to the high cuestas and deep canyons of the San Agustin and southern San Andres Mountains, also described in this report (fig. 3). The San Agustin Mountains extend northward from San Agustin Pass to Quartzite Mountain, and from there the San Andres Mountains continue for nearly 100 mi. Only the southernmost part of the San Andres Mountains was made a part of this study, specifically the area encompassing Bear Canyon, the southernmost east-west drainage. To the south of the Organ Mountains, the group of outlying hills and ridges known as the Bishop Cap hills is also an important part of this report. Still farther south lie the Franklin Mountains and considerable reference is made to them although they were not mapped. Parts or all of the following USGS (U.S. Geological Survey) 7½- or 15-minute quadrangles were mapped: Bear Peak, Lake Lucero SW, White Sands, Organ, Organ Peak, Davies Tank, Newman NW, Bishop Cap, and Tortugas. The geologic map (sheet 1, in pocket) was compiled from these maps.

Access and land ownership

Parts of the mountain range are easily accessible while entry into many other areas is made only with considerable effort. US-70 passes through the range at San Agustin Pass, and access to the western base of the mountains and to Aguirre Spring on the eastern side is by maintained roads connected with this highway. A hiking trail across Baylor Pass also connects Aguirre Spring with the western side of the mountains. Other dirt roads provide access to the western side of the Organs, notably the Soledad Canyon road, its branch trail along the southwest base of the range, and the road into Bishop Cap and the Peña Blanca–Finlay Canyon area. The latter road joins I-25 at the Mesquite interchange. The central part of the Organ range is inaccessible except by foot. Access to this region is best from Fillmore Canyon or Aguirre Spring. Poor foot trails farther south lead into the picturesque Achenback Park area and Long Canyon. Most of the San Agustin–southern San Andres area is on WSMR (White Sands Missile Range), as is the northeast flank of the Organ Mountains. The west-central and southeast part of the Organs is administered by Fort Bliss. In all these areas permission for entry is required. Furthermore, parts of the west slope of the Organ range are private property, particularly the La Cueva–Ice Canyon–Soledad Canyon area, the Organ area, the area of the Stevenson–Bennett mine, and the Cox Ranch, the latter located 1 mi west of WSMR headquarters. Visitors should contact owners before crossing these lands.

Name

Dunham (1935) summarized views on the origin of the name Organ Mountains as follows: "It is generally supposed that the Organ Mountains owe their name to a resemblance between the jagged spires which are their most striking feature and the pipes of an organ. Marcy, writing in 1850, says, 'The Organ range of mountains takes its name from the supposed similarity of the high-pointed peaks to the pipes of an organ.' However, some local disagreement exists as to which part of the mountains actually resembles an organ. Some hold that the great aiguilles in the center of the west front of the range were the inspiration for its name, while others point to the steep, columnar-faced cliff south of San Agustin Pass on the east side [figs. 4 and 86]. G. A. Feather has suggested an alternative theory to me, namely that the mountains were formerly inhabited by a tribe of Indians whom the Spaniards called 'los Orejones' (referring to their gnarled and wrinkled faces), and that that name was applied to the mountains, becoming corrupted to 'los Organos' in the course of time." Ingraham (1979) points out that the mountains appear on old Spanish maps as "la Sierra de la Soledad"—the Mountains of Solitude.

Physiography

Physical features of each of the three parts of the area studied—the Organ Mountains, San Agustin Mountains, and southern San Andres Mountains—are sufficiently different to warrant separate descriptions.

The Organ Mountains dominate the landscape in south-central New Mexico (figs. 5 and 6). They rise abruptly from the expansive desert plains to 9,012 ft on Organ Needle, which towers approximately 1 mi above the floodplain of the Rio Grande 10 mi to the west and almost a mile above the flat floor of the Tularosa Basin just a few miles to the east. Aprons of alluvial fans mantle the foot of the range on both sides, and locally the slope of mountain bedrock declines abruptly at the mountains' base to become rock pediments. In the area east of Baylor Pass and at Organ, pediment plains are broad; elsewhere, high bedrock ridges slope directly down to the frontal fault of the range and essentially no pediment has developed. In general, the pediments are covered with a thin veneer of gravel; if not for the occasional islands of bedrock or exposures in gully bottoms, the pediments would be difficult to distinguish from alluvial fans of constructional origin. On the east side of the range, fault scarps more than 150 ft high displace both fans and pediments, but more will be said about them and their relation to the Quaternary erosional and depositional history of the range in later sections of this book.

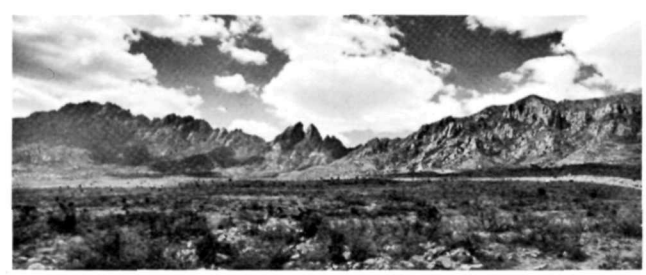


FIGURE 4—EAST SIDE OF THE ORGAN MOUNTAINS; from left to right are Organ Needles, Rabbit Ears, and Baylor Mountain. Note columnar-jointed Needles quartz monzonite on Baylor Mountain. View looks southwest from US-70; (photo by Bob Sigmon, courtesy *Las Cruces Sun News*).



FIGURE 5—ORGAN AND SOUTHERNMOST SAN ANDRES MOUNTAINS AS VIEWED FROM WHITE SANDS NEAR LAKE LUCERO. Organ Needles form central skyline and just left of them is pyramidal Sugarloaf Peak; view to southwest (photo by Walter M. Edwards, courtesy of National Geographic *World,* © 1977).

Spectacular as the Organ Mountains are when viewed from the west side, largely because of the near-vertical, fluted spires of the needles or aiguilles (fig. 7), local relief is greater on the eastern side of the range. This greater relief is mostly due to the floor of the Tularosa Basin lying 1,000 ft lower than the western edge of the range. From Granite Peak to the eastern base of the mountain, a horizontal distance of only 3 mi, the mountain falls away 4,500 ft in a series of precipitous cliffs and steep, brushy ravines carved in Tertiary quartz monzonite and Precambrian granite. In large part the Organs owe their dramatic scenery to the quartz monzonite of the Organ batholith, weathering of which has yielded the rock monoliths known as the Needles, Soledad Peak, Sugarloaf Peak, and San Agustin Peak (figs. 8 and 9). In particular, these monoliths are the products of exfoliation of massive but jointed crystalline rock, and Sugarloaf Peak is a nearly perfect example of an exfoliation dome (fig. 10). In contrast, ridge tops in the rugged, central backbone of the Organs are narrow, only a few feet wide in general, and drop away abruptly in cliffs or steep slopes which descend to adjacent, equally narrow canyon bottoms. Locally, as in Glendale Canyon, these ravines drain to the edge of granite cliffs, then drop in a series of cliffs a few hundred feet high.

Peaks and canyons that nearly rival the Needles in beauty and difficulty of access form the high ground between Fillmore and Soledad Canyons (fig. 11). Underlain by thick, massive rhyolite tuffs rather than quartz monzonite, the high divide is flanked by deep ravines and surmounted by the rounded, barren knob

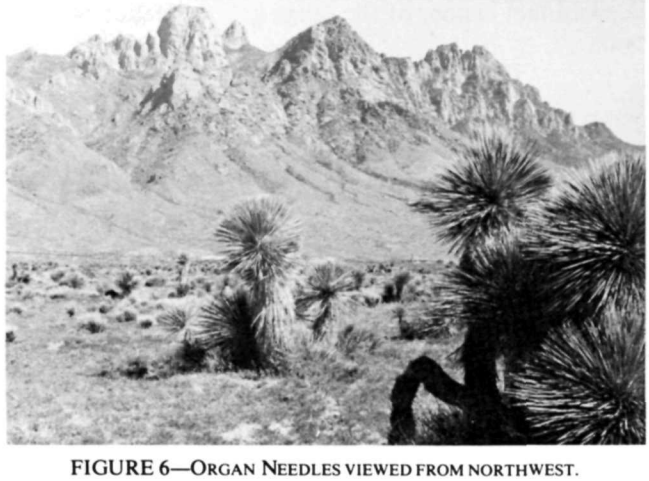


FIGURE 6—ORGAN NEEDLES VIEWED FROM NORTHWEST.



FIGURE 7—"NEEDLES" OF QUARTZ SYENITE AND QUARTZ-ALKALAI FELDSPAR SYENITE along west-central edge of Organ Mountains; southern Jornada del Muerto Basin in foreground.

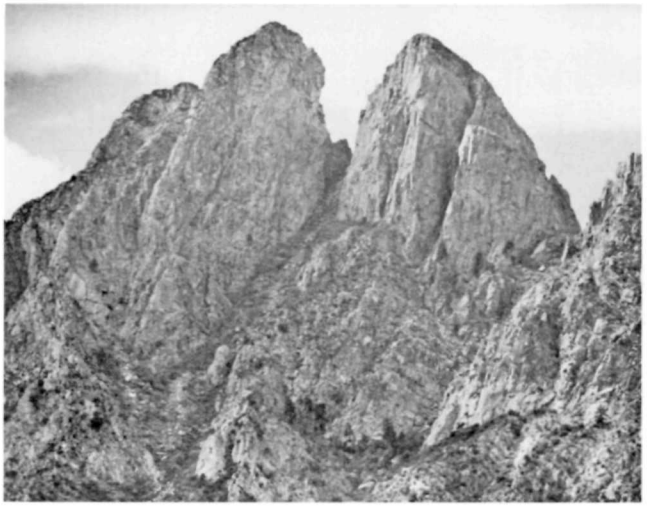


FIGURE 8—"RABBIT EARS" SECTION OF THE ORGAN NEEDLES, ELEV. 8,150 FT; view to east (photo by Bob Sigman, courtesy *Las Cruces Sun News*).

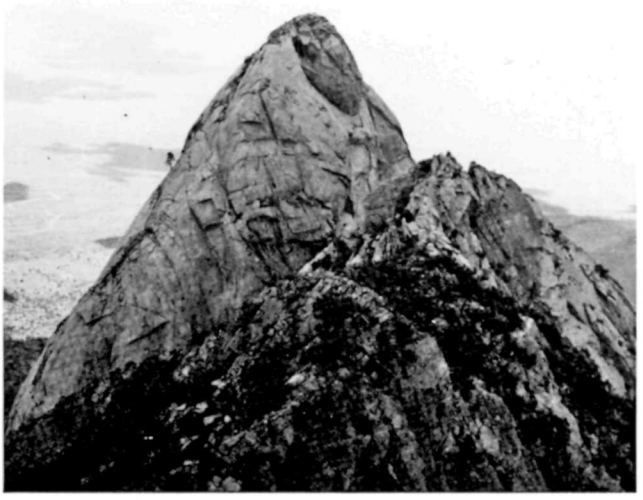


FIGURE 10—SUGARLOAF PEAK, ELEV. 8,150 FT, AN EXCELLENT EXAMPLE OF AN EXFOLIATION DOME; bedrock is quartz monzonite porphyry of Sugarloaf Peak, view to north.

known as Baldy Peak, nearly 8,500 ft in elevation. Rugged, brushy Ice Canyon lies just below the peak to the north, and from Ice Canyon a remarkable vertical-walled, slot-shaped tributary rises steeply to the vertical faces on the west side of Baldy Peak. The narrow canyon, at whose mouth the popular Dripping Springs resort flourished in the early 1900's (fig. 12), is confined by walls nearly 600 ft high; locally, width at the canyon bottom is 50 ft or less. The rhyolite tuff typically weathers to cliffs, although usually not in so dramatic a manner. The cliffy walls of Fillmore and North Canyons are also carved in this rock.

Except for the hogback ridges of Paleozoic limestone and Precambrian granite called Rattlesnake Ridge, the Organ Mountains south of Soledad Canyon have more of a plateaulike aspect. This characteristic is best seen between Boulder Canyon and the western edge of the range where the plateau stands 2,000 ft above the adjacent alluvial fans, dropping off to the desert below in a series of cliffs, steep slopes, and ravines. Long Canyon drains the plateau, but on top it is scarcely a canyon. There it occupies a broad, flat, grassy valley that faithfully follows the arcuate Long Canyon fault zone. The canyon is only shallowly incised into the plateau surface, but at the southern edge of the plateau the drainage spills over a 100-ft-high falls before entering the Finlay Canyon drainage (fig. 13). The walls of the canyon below the falls rise nearly 600 ft to the summit of the plateau. Across Boulder Canyon to the east, what appears to be a remnant of the plateau lies atop the broad, square-shaped mass of quartz monzonite that forms the divide between Boulder and Soledad Canyons. Viewed northward from the lower reaches of Boulder Canyon, the quartz monzonite mountain looms like a huge fortress above the grassy headwater region of the canyon (fig. 14). The eastern scarp of the range descends abruptly from this mass and is carved in quartz monzonite or granite here as it is northward along the whole length of the Organ Mountains. However, relief on the mountain front gradually diminishes southward and at this point, south of Soledad Canyon, is approximately 3,000 ft.

Perhaps the two most notable drainages in the Organ Mountains are Soledad Canyon and Fillmore Canyon. Together they drain most of the central, high part of the mountain range. Soledad has by far the greatest water-



FIGURE 9—ORGAN NEEDLE, ELEV. 9,012 FT, VIEWED FROM AREA OF ORGAN PEAK; view looks northwest.

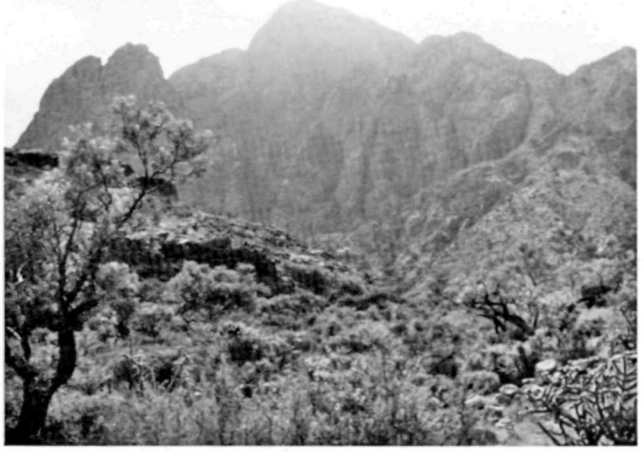


FIGURE 11—MOUTH OF NEARLY VERTICAL-WALLED ICE CANYON LOOKING EAST TOWARD BALDY PEAK, ELEV. 8,445 FT; ridges beyond are in clouds.

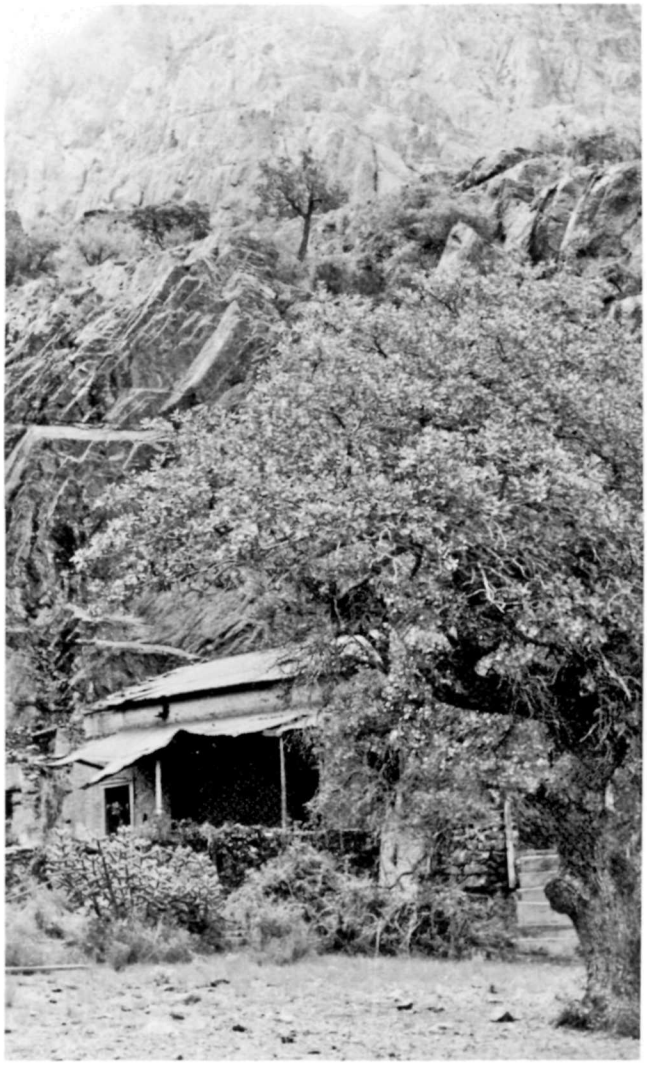


FIGURE 12—RUINS OF DRIPPING SPRINGS RESORT NEAR THE MOUTH OF ICE CANYON; resort flourished as a popular vacation spot in early 1900's, view to southeast.

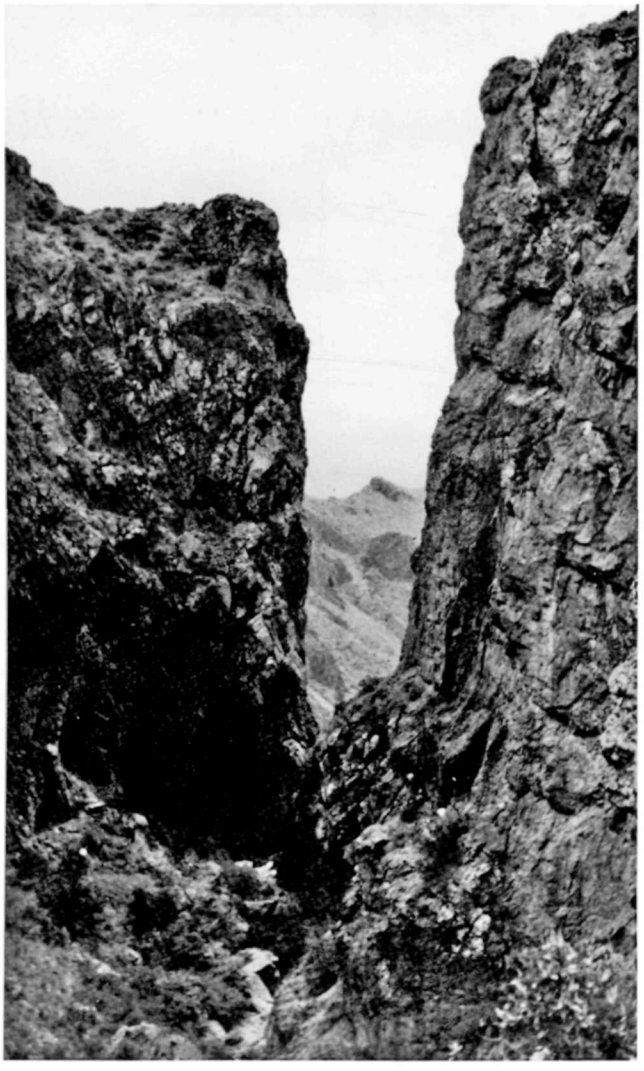


FIGURE 13—MOUTH OF LONG CANYON WHERE IT JOINS FINLAY CANYON DRAINAGE AT SOUTHERN END OF ORGAN MOUNTAINS; walls, formed of Soledad Rhyolite, are nearly 600 ft high; view to east.

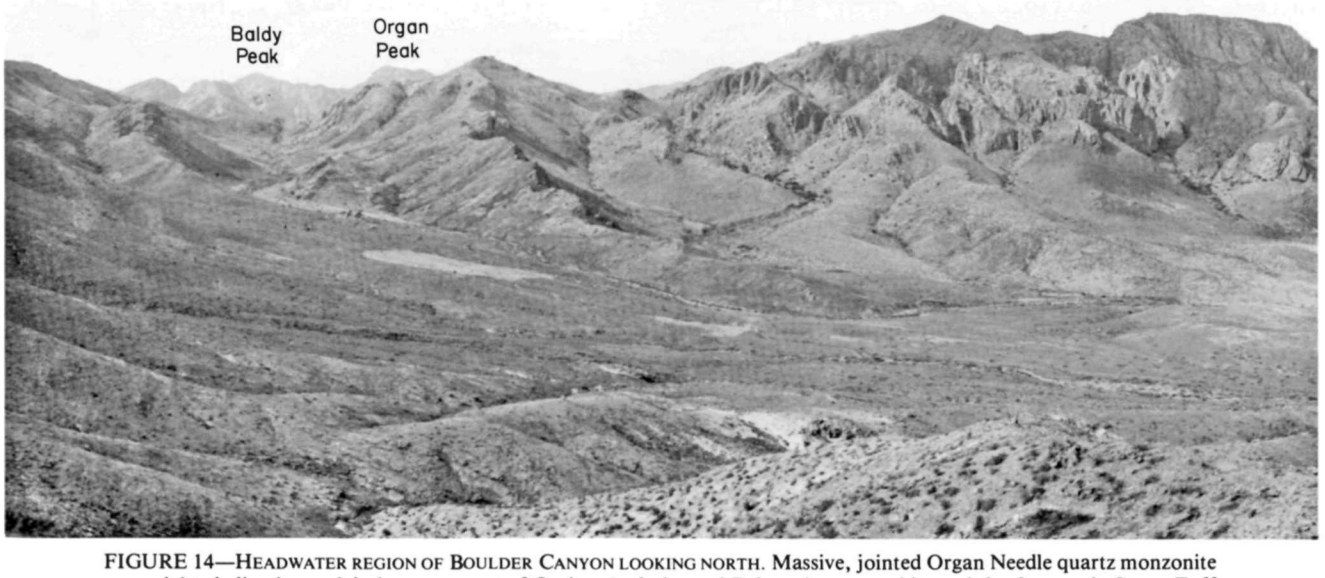


FIGURE 14—HEADWATER REGION OF BOULDER CANYON LOOKING NORTH. Massive, jointed Organ Needle quartz monzonite on right skyline is overlain by a remnant of Orejon Andesite and Paleozoic strata; ridge at left of center is Cueva Tuff and ridges at far left are ash-flow tuff units in the lower part of the Soledad Rhyolite.

shed. A low divide along the western side of the canyon separates it into a short west-flowing segment and a major east-flowing drainage system that empties onto a huge fan at the canyon's eastern mouth. Hunt (1975) pointed out the series of transverse valleys (like Soledad Canyon) in the Organ–San Andres chain, most with divides on their western side. He noted that they were unusual in the Basin and Range province, and suggested that they reflected some event or condition in the late Cenozoic evolution of the range. In the case of Soledad Canyon, the upper and middle part of the canyon is located on sheared and fractured rock along the east-trending part of a major fault zone (Modoc fault). Other transverse drainages may have evolved as illustrated in fig. 15.

Soledad Canyon is one of the most beautiful canyons in the entire range (fig. 16). Floored by a broad, grassy valley spotted with huge, old oak, juniper, and piñon trees, Soledad Canyon seems a different world from the brushy, precipitous canyons and ridges in adjacent parts of the mountains. North Canyon, the main tributary of Soledad, while beautiful in its own way, epitomizes the narrow, V-shaped, brushy canyons characteristic of most of the Organ range. Even Soledad Canyon loses its pastoral flavor in its lower reaches where it cuts narrow, V-shaped slots through bedrock sills. Soledad Peak, a massive monolith of syenitic rock, guards the eastern entrance to the canyon.

Fillmore Canyon, which drains westward from the central, high part of the range past Cueva rock (a sentinel at the mouth of Fillmore Canyon in the manner of Soledad Peak) is full of pleasant surprises. Walled in by cliffs of tuff on one side and spires of quartz monzonite on the other, the canyon is steeper and more rugged and rocky than Soledad (fig. 17). Fillmore's V-shaped tributaries head beneath the highest peaks in the range, Organ Needle and Orejon. What makes the canyon surprising, however, are the springs that run much of the year and especially the stands of ponderosa and piñon pines, juniper, Douglas fir, and at least one spruce—located high on a north-facing slope. (No aspen are present in the canyon, but two small groves were noted elsewhere in the range, one in a tributary to North Canyon and one in a small ravine draining the northwest side of Sugarloaf Peak.) In contrast, south-facing slopes in Fillmore Canyon, like most other south-facing slopes in the higher part of the Organs, support a tangle of cholla, sharp-tipped yucca, mountain mahogany, and other thorny or dense brush, locally almost impossible to thrash through. Further, Fillmore Canyon is clogged in many places by huge boulders of quartz monzonite of the same size and type that constitute much of the broad fan at the canyon's mouth. Plainly, massive mudflows discharged down this and other canyons in relatively recent times as well as during the Pleistocene, when periglacial conditions (permanent snowfields?) existed beneath the peaks in the upper reaches of the canyon.

North of San Agustin Pass, the group of relatively low, narrow mountain ridges that extend to the Loman Canyon area are called San Agustin Mountains on most maps. Structurally they represent a transition from the Organ Mountains, dominated by the batholith, and the

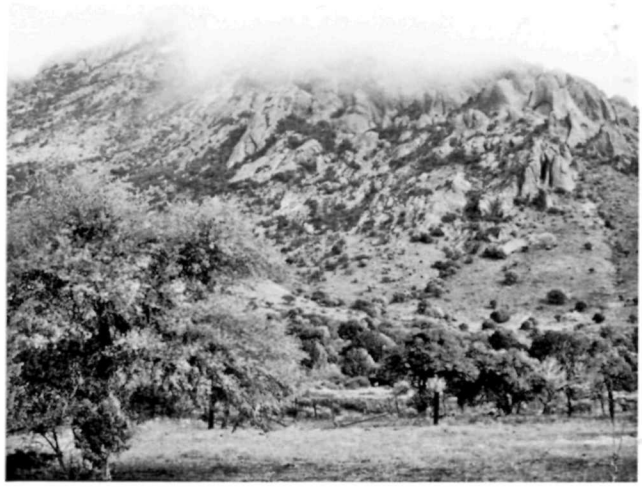


FIGURE 16—CENTRAL PART OF SOLEDAD CANYON NEAR ITS JUNCTION WITH NORTH CANYON. Tuffs within Cueva Tuff form mountain beneath low clouds; trees are frosted with ice; view looks north.

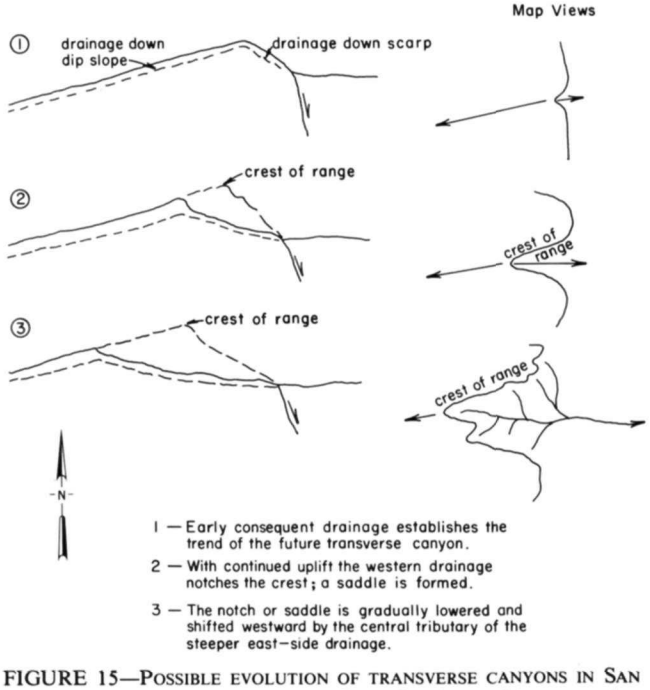


FIGURE 15—POSSIBLE EVOLUTION OF TRANSVERSE CANYONS IN SAN ANDRES AND ORGAN MOUNTAINS (from sketches and interpretation by V. C. Kelley, personal communication, 1979).



FIGURE 17—SOUTHERN WALL OF FILLMORE CANYON EXPOSING TUFFS OF SQUAW MOUNTAIN AND ACHENBACK PARK, both members of the Soledad Rhyolite.



FIGURE 18—NORTHERN CONTACT OF ORGAN BATHOLITH WITH METAMORPHOSED LOWER PALEOZOIC ROCKS; contact plunges north (left) at 35-40 degrees.

San Andres Mountains, composed mostly of tilted and faulted Paleozoic rocks. Most of the San Agustin Mountains comprise the north-plunging northern end of the Organ batholith (fig. 18), together with adjacent metamorphosed Paleozoic rocks that form its roof. The highest peak, San Agustin Peak, has an elevation of 7,020 ft and is another in the series of exfoliation domes eroded on the batholith (fig. 19). The Paleozoic roof rocks form a series of west-dipping hogbacks and cuestas, discontinuous along strike because of extensive faulting. They form the high ridge west of Black Prince Canyon as well as Hardscrabble Hill. Perhaps the most notable feature of the San Agustin Mountains area, however, is the broad pediment that slopes both east and west from San Agustin Peak. The pediment is cut almost entirely on the batholith and at its widest is approximately 8 mi across (including San Agustin Pass), by far the widest pediment in the Organ–San Andres–Franklin chain. At this point the Organ–San Agustin Mountains have been reduced to a low ridge, only 1–3 mi wide, in contrast to their 6–8 mi width farther north and south. Covered by less than 200 ft of gravel, bedrock is exposed over broad areas on parts of the pediment, and bedrock islands project above its general level. The pediment abruptly terminates to the north where Paleozoic strata crop out; these rocks are apparently much less susceptible to lateral planation than are the crystalline ones.

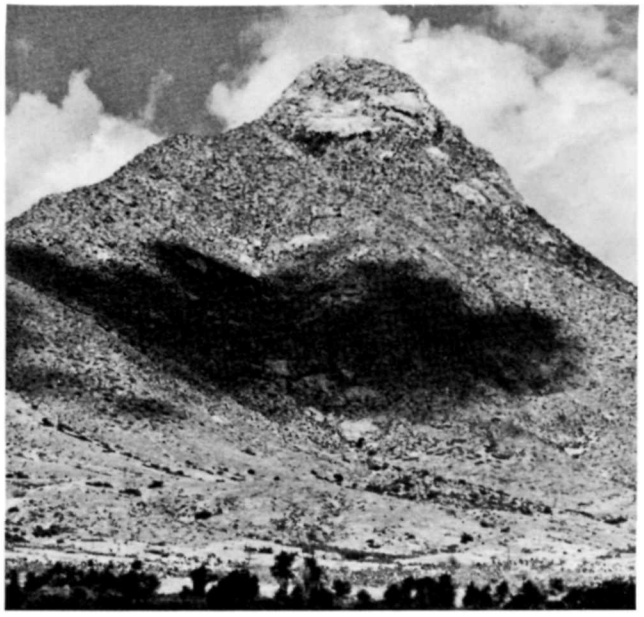


FIGURE 19—SAN AGUSTIN PEAK EXFOLIATION DOME, ELEV. 7,030 FT, JUST NORTH OF SAN AGUSTIN PASS. Bedrock is Sugarloaf Peak quartz monzonite porphyry phase of Organ batholith; view to north (photo by Bob Sigmon, courtesy *Las Cruces Sun News*).

As used in this report, the southern San Andres Mountains are centered around Bear Canyon, a major, deep, transverse canyon that flows from an intracanyon divide both to the east and to the west in the manner of Soledad Canyon. The mountains on either side of the canyon are quite different in their topographic form because of differences in geologic structure. Those on the south comprise a jumble of peaks, hills, and ridges whose shapes and orientation weakly reflect the west-northwest-trending folds and faults in stratified Paleozoic rocks within the Bear Peak fold and thrust belt. On the northeast side of the canyon the strata are less deformed and the mountains are more plateaulike, gradually changing toward the west into a series of west-dipping hogbacks and cuestas. The eastern part of Bear Canyon is incised nearly 2,500 ft into broadly arched Paleozoic strata and Precambrian granite; when viewed from the tops of adjacent mountains it is reminiscent of a small Grand Canyon (fig. 20), albeit one that is basic-

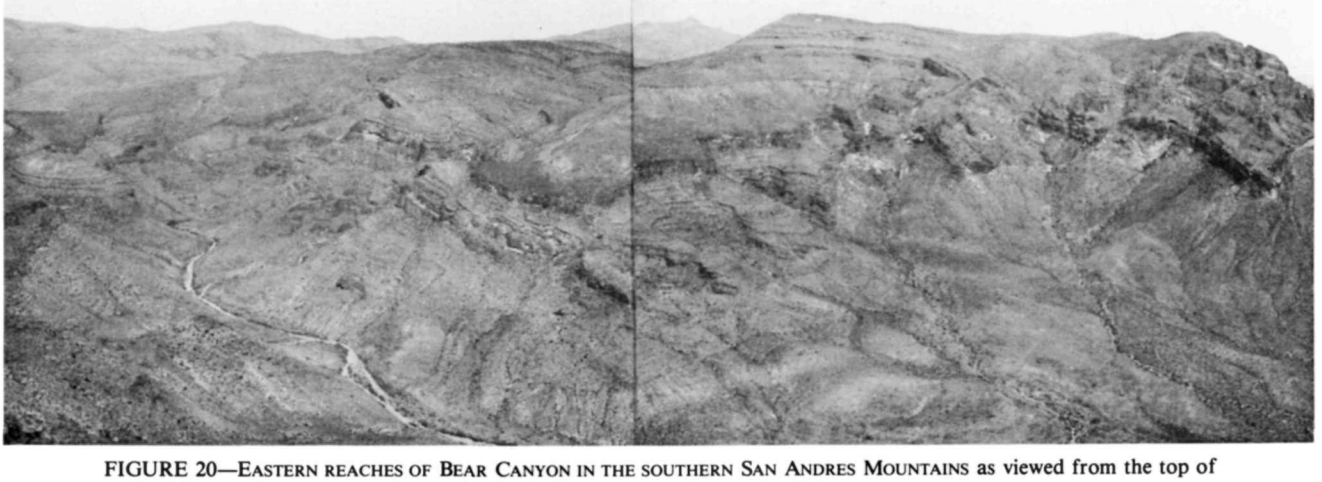


FIGURE 20—EASTERN REACHES OF BEAR CANYON IN THE SOUTHERN SAN ANDRES MOUNTAINS as viewed from the top of Black Mountain looking northward; local relief here is approximately 2,300 ft.

ally gray rather than multicolored. Locally, cliffs hundreds of feet high form the canyon walls, but more typically the walls are stepped in a series of cliffs and benches. Although the strata and granite are tilted and intricately faulted, the overall drainage pattern, a mix of dendritic and poorly developed trellis patterns, is only locally well adjusted to the bedrock structure.

Previous work

So many authors have made observations about the Organ Mountains that an exhaustive list of previous workers would be long indeed. The interested reader should consult Dunham (1935) for one such list; however, a few on that list as well as some more recent workers who made especially important contributions toward understanding the geology of the range should be recognized. Among these are Antisell (1856), who described the Stevenson mine; Wheeler (1879), who also described the mine and gave an account of the geology of the Organs; Jones (1904), who was the first to describe the Organ mining district; Lindgren and Graton (1906) and Lindgren and others (1910), who described the geology and ore deposits; and Keyes (1905), Welsh (1914), Darton (1928), and Johnston (1928), all of whom contributed to an early understanding of the stratigraphy and ore deposits of the range. Of course, the principal contribution to the geology of the Organ Mountains came in 1935 from K. C. Dunham, and acknowledgment of his study was given in the preface to this report. In 1943, Albritton and Nelson described in some detail the geology of the mines in the Organ mining district and presented their results in a USGS open-file report. In 1951, Soulé summarized the results of core drilling by the U.S. Bureau of Mines at the Torpedo property, and in 1975, Glover mapped the western edge of the central part of the range and presented his results in a M.S. thesis at the University of Texas (El Paso). The Organ caldera was recognized in 1975 (Seager, 1975), and in 1978, Seager and Brown published an interpretation of it. Finally, in 1978, Macer interpreted the origin of fluorspar deposits in the Organ Mountains in another M.S. thesis at the University of Texas (El Paso).

Plan of the book

In organizing this book, the idea was to follow the chronologic sequence of events so far as possible. Instead of describing all the rock units in one section and all the structural features of vastly different ages and origins in another, related rocks and structures are treated together in order from oldest to youngest. Precambrian, Paleozoic, and Mesozoic rocks are described first and the geologic history they represent is summarized. Next, Laramide rocks and structures are detailed and interpreted, followed by the products of volcanism during the Eocene. The Organ batholith (Oligocene) and its associated volcanic rocks and cauldrons are treated together because they are the product of one cycle of igneous activity. Late Tertiary deformation and its associated rocks follow, and a summary of the late Pliocene and Quaternary deposits brings the story of the Organs up to date (almost). Mineral deposits, a product of both Oligocene and late Tertiary magmatic and tectonic activity, are a story by themselves and so were removed from their place in the chronologic scheme of things and treated separately at the end.

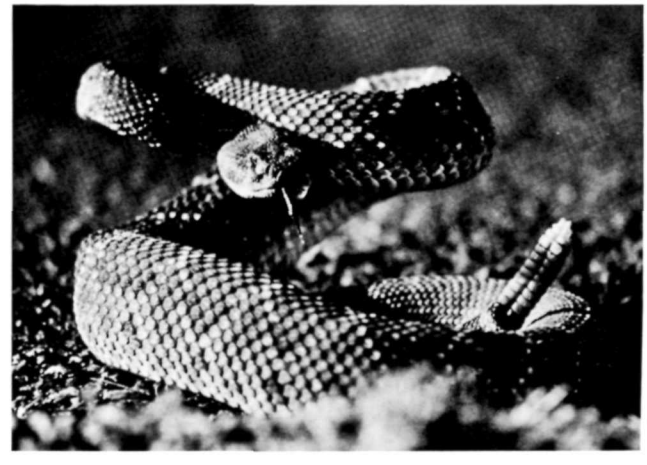


FIGURE 21—ONE OF THE MOST EFFECTIVE ATTENTION-GETTERS IN THE ORGAN MOUNTAINS (photo by Jonathan T. Wright, © National Geographic Society).

Precambrian, Paleozoic, and Mesozoic rocks

Paleozoic and Mesozoic sedimentary rocks at least 8,500 ft thick were deposited on Precambrian granitic crust in the area of the Organ and San Andres ranges. Nearly all the strata are marine and, with few exceptions, were formed in shallow, warm, shelf waters. Almost two-thirds were laid down during the Pennsylvanian and Permian Periods; these appear to be the product of almost continuous deposition during that time. The rest of the section contains numerous unconformities that separate formations and that may represent more time than the rocks themselves. All lower Paleozoic formations thin northward owing to both deposition and erosional truncation. The middle and upper Paleozoic sequence, on the other hand, maintains a comparatively uniform thickness throughout the area, although individual formations may thicken into basins of subsidence or thin by erosion or deposition on stable shelves. Widespread deep erosion during the Cenozoic drastically thinned or completely removed Paleozoic or Mesozoic rocks in many areas.

In places, Paleozoic and Mesozoic strata are thoroughly altered or deformed. Within 1 mi of the Organ batholith, original lithologies are obscured by metamorphism; some rock units are anomalously thin or thick, owing perhaps to ductile flow. Elsewhere, as on parts of Black Mountain or Bear Peak, the strata are segmented and thoroughly brecciated by closely spaced faults. Nevertheless, relatively undeformed exposures of all formations are comparatively common in the range. Fifteen exposures were selected to be measured and described. These make up appendix A. Summaries of the Paleozoic and Mesozoic formations in the area are given in sheet 3 (back pocket), fig. 22, and table 1. Readers interested in further detailed studies of Paleozoic and Mesozoic rocks in the San Andres–Organ–Franklin Mountains area should refer to Laudon and Bowsher (1949), Kottlowski and others (1956), Bachman and Myers (1969), and Harbour (1972) among others. Regional interpretations of the Paleozoic and Mesozoic rocks can be found in Kottlowski (1963), Hayes (1975), and Greenwood and others (1977).

Precambrian rocks

Precambrian rocks crop out over a large portion of the southernmost San Andres range, north of US-70, where they form the core of an early Tertiary (Laramide) uplift bordered by the Bear Peak fold and thrust zone. Less extensive outcrops compose the eastern slopes of Rattlesnake Ridge, the east-central foothills of the Organ Mountains, and the eastern walls of Bear Canyon. Near the Stevenson-Bennett mine, a few patches of Precambrian rock, nearly surrounded by the Organ batholith, are interpreted as roof pendants. The Precambrian rocks nonconformably underlie the Bliss Sandstone, but in many places they are in fault contact with younger Paleozoic strata or are in intrusive contact with the Organ batholith.

The Bear Peak fold and thrust zone of Laramide age separates two different kinds of Precambrian terrane that probably represent different levels of erosion into the same Precambrian batholithic complex. South of the thrust zone, in the deeply eroded core region of the Laramide uplift, massive, homogenous, coarse-grained granite is exposed. It probably represents an interior facies of the Precambrian batholith. North of the Bear Peak thrust zone, at a structurally much lower position, the granite has not been as deeply eroded. At this level it contains numerous irregular patches of granitic gneiss, schist, and amphibolite that are well exposed in the Bear Canyon area. Consistently northeast foliation trends in these patches suggest that the patches are remnants of

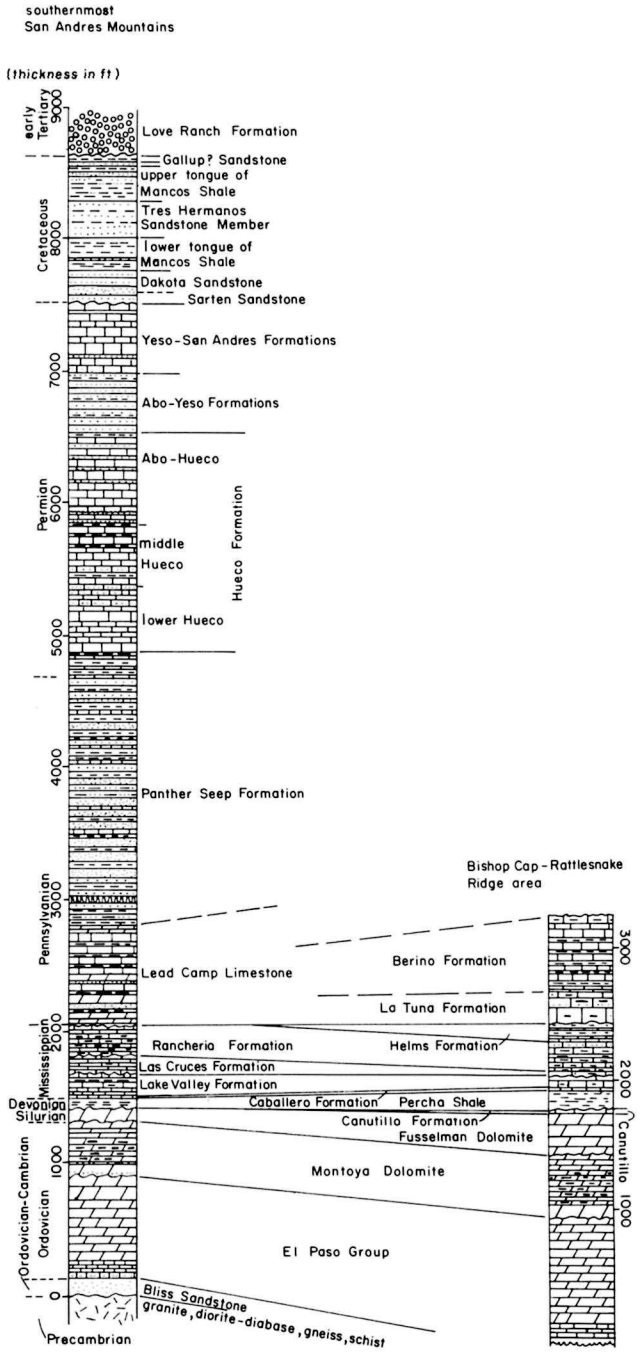


FIGURE 22—Correlation and nomenclature of pre-Tertiary rock units from southern San Andres Mountains to Bishop Cap.

roof pendants near the top of the batholith rather than xenoliths. Both terranes contain many younger mafic dikes, but north of the thrust zone the dikes have been shredded by closely spaced normal faulting of late Tertiary age.

Most of the Precambrian granite is brown or gray, coarse grained, and somewhat porphyritic. A second type of granite contains abundant, coarse-grained, pink orthoclase and has a distinct bright-red color; it is extensively exposed along the southeast edge of the Bear Peak thrust, in Bear Canyon, and in the northern part of Rattlesnake Ridge. A few dikes of the red granite intrude the brown; however, a gradational contact appears likely in most places, although no contacts between the two were observed. A third type is brown-weathering, highly porphyritic, gray granite that forms the massive shoulder of rock at the base of the Organ Mountains 1 mi south of WSMR headquarters. Condie and Budding (1979) believe this granite to be chemically and texturally distinct from the red and brown granite farther north. Outcrops near Texas Canyon and Antelope Hill, however, contain both porphyritic and equigranular varieties that are thoroughly mixed and gradational into each other. They appear to be different facies of the same batholith.

Pink to gray orthoclase crystals up to 3 cm in length are the most conspicuous feature of the gray to brown granite. These crystals are set in a matrix of finer grained quartz, biotite, and plagioclase. Near the Stevenson-Bennett mine, a finer grained equigranular facies that grades into porphyritic rock is exposed. This facies is distinctly pinker owing to an abundance of pink feldspar amid gray quartz. The average grain size is 2-3 mm. Pegmatite lenses or dikes and swarms of aplite dikes are common in several places in the Precambrian batholith. Unlike the rocks of the Tertiary batholith, which usually contain many autoliths, inclusions are rare or lacking in Precambrian rocks. The granite is closely jointed and upon granular disintegration, exfoliation, and spheroidal weathering, produces rounded hills and knobs.

Of special interest are diorite-amphibolite dikes that intrude the granite almost everywhere. The dikes trend generally east or northeast, and may be several miles long and up to 100 ft wide. Some groups appear to be en echelon, while others occur in parallel swarms, like those at Rattlesnake Ridge. Chilled margins can be found along well-exposed contacts. The dikes are truncated by the unconformity at the base of the Bliss Sandstone and are therefore of Precambrian age.

Principal minerals in the dikes are green amphibole and plagioclase. The latter ranges in composition from labradorite to oligoclase (Dunham, 1935), and the color index is 50-70. In hand specimen, the rock appears to be diabase or diorite and thin sections reveal an ophitic texture. The dikes are somewhat altered and locally are greenish, probably from actinolite and chlorite. In Bear Canyon, amphibolite dikes, shredded by faulting, have developed an incipient schistosity. Gold-copper-quartz mineralization is associated with the dikes north of US-70. The mineral deposits may have been introduced with the dikes during the Precambrian or, as Dunham (1935) suggests, they may be of Tertiary age and simply localized in shear zones along dike contacts.

None of the Precambrian rocks in the Organ or southern San Andres Mountains are known to have been dated by radiometric techniques. However, the granites and metamorphic rocks are lithologically similar to Precambrian rocks in the northern San Andres and Oscura Mountains that were described by Budding and Condie (1975) and Condie and Budding (1979), and dated by Muehlberger and others (1966) as 1.3-1.4 b.y. old. They are dissimilar to the rocks in the Franklin Mountains reported to be 1.0 b.y. old. Consequently, the granitic and gneissic rocks in the Organ and southern San Andres Mountains probably are about 1.3-1.4 b.y. old. The diorite-diabase dikes are definitely younger, but they predate the Bliss Sandstone.

Cambrian and Ordovician rocks

The Bliss Sandstone, El Paso Group, and Montoya Group comprise the Cambrian-Ordovician Systems in the San Andres and Organ Mountains. Approximately 30-40 ft of quartzite near the base of the Bliss may be correlative with strata containing upper Cambrian fossils at San Diego Mountain and in the Caballo Mountains (Flower, 1953; Kottlowski and others, 1956).

Bliss Sandstone

The Bliss Sandstone is a transgressive, coastal to shallow-marine deposit that nonconformably overlies Precambrian rocks and grades upward into limestone or dolomite beds of the El Paso Group. From a distance, the two formations are easily separated. The Bliss forms a dark, almost black, band and the lower El Paso weathers to an orange or brown series of ledges or cliffs (fig. 23). The top of the Bliss is placed at the lowest occurrence of light-gray- to orange-weathering sandy limestone containing brown, siliceous streaks—a lithology typical of the lower El Paso strata. As previous workers have pointed out (Kottlowski and others, 1956; Kottlowski, 1963; Bachman and Myers, 1969; Hayes, 1975), the Bliss thins gradually northward from 250 ft thick in the Franklin Mountains to its pinchout in the Oscura Mountains, 150 mi to the north. In the southernmost San Andres-northern Organ Mountains, the formation ranges in thickness from 145 ft near the Hilltop mine to 125 ft in Bear Canyon. The northward thinning must be entirely of depositional origin because no erosion surface is seen at the top of the Bliss.

Lithologically, the Bliss can be divided into two parts. The lower part is 30-40 ft thick and consists mostly of gray to tan, medium-bedded, cross-stratified orthoquartzite interbedded with thin, shaley or flaggy sandstone units. As mentioned earlier, this part of the Bliss may be Late Cambrian in age, based on lithologic correlation with outcrops farther west at San Diego Mountain and in the southern Caballo Mountains. The upper part consists of 80-100 ft of thin- to medium-bedded quartzite, sandstone, and silty shale, much of which is hematitic and siliceous and weathers to shades of dark brown, greenish black, or brown. The bedding is generally parallel, but some cross-stratified or laminated units are present. Kottlowski and others (1956) reported an Ordovician fauna from upper parts of this sequence farther north. Bachman and Myers (1969) indicate the unit has a basal conglomerate.



FIGURE 23—LOWER AND MIDDLE PALEOZOIC ROCKS EXPOSED NEAR THE EASTERN MOUTH OF BEAR CANYON. A strand of the Black Mountain fault zone separates Bliss Sandstone (**€Ob**), El Paso Group (**Oe**), and Montoya Group (**Om**) on right from upper El Paso, Montoya, Fusselman Dolomite (**Sf**), Percha Shale (**Dp**), Las Cruces and Lake Valley Formations (**Ml**), Rancheria Formation (**Mr**), and Lead Camp Limestone (**IPlc**); view looks north.



FIGURE 24—LOWER PALEOZOIC ROCKS EXPOSED ALONG EASTERN SIDE OF SOUTHERN SAN ANDRES MOUNTAINS. Exposure is on northern wall of first canyon south of Bear Canyon; **p€**—Precambrian granite, **€Ob**—Bliss Sandstone, **Oe**—El Paso Group, **Om**—Montoya Group.

El Paso Group

Although the El Paso Group has been divided into several formations in the El Paso area (LeMone, 1969) and Caballo Mountains (Kelley and Silver, 1952), it is treated as a single unit here. The lower contact is gradational with the Bliss, but the upper contact with the Montoya Group is an important disconformity. This erosion surface gently truncates the El Paso beds and is mostly responsible for the northward thinning of the El Paso from 1,000 ft on Rattlesnake Ridge to 780 ft at Bear Canyon (fig. 24). The El Paso wedges out 90 mi farther north in the Oscura Mountains.

The lower 150-200 ft of the El Paso, roughly correlative with the Sierrite Limestone of Kelley and Silver (1952), usually forms a distinctive orange- to brown-weathering series of ledgy slopes or rugged cliffs above the Bliss and below the gray dolomitic rocks of the rest of the El Paso. This lower sequence includes much sandy limestone, especially at the base, but is distinguished primarily by its color and by the planar, thin to medium beds and abundant siliceous streaks, flakes, chips, and laminae, some of which fill twig-shaped burrows. The dominant lithology is fine- to coarse-grained limestone that locally is partly dolomitized.

A transition zone 50-100 ft thick containing lithologies representative of lower as well as upper parts of the El Paso is present at the base of the upper part. Above this, 500-600 ft of gray, coarse-grained dolomite constitutes the upper two-thirds of the El Paso. The thick to medium beds form imposing cliffs in the walls of Bear Canyon, but elsewhere weather to ledgy slopes interrupted by cliffs. Much of the upper El Paso weathers brownish gray, light to dark gray, or pale orange. Branching burrows in many beds weather with a distinctive mottled pattern. Several beds are rich in chert nodules, recrystallized skeletal grains, or stromatolites. In the Bishop Cap hills and near the Hilltop mine, beds of coarse-grained dolomitic sandstone were noted in the upper part of the El Paso.

Faunal studies made by several workers show the El Paso to be of Early Ordovician age (Kottlowski and others, 1956).

Montoya Group

The Montoya Group is separated from El Paso strata by the regional unconformity described earlier. The contact is easy to spot even from a distance; the dark-gray, massive, and banded dolomites of the lower and middle Montoya contrast sharply with the thinner bedded light-gray or pale-brown El Paso strata. Similarly, the upper contact of the Montoya with the overlying Fusselman Dolomite is conspicuous; however, in this case, light-gray, medium-bedded upper Montoya units contrast with darker, massive Fusselman. The Montoya–Fusselman contact is an unconformity that truncates Montoya strata, resulting in thinning of the Montoya Group northward. The Montoya is 400-450 ft thick in the Franklin–Organ Mountains area, 368 ft thick in Bear Canyon, and wedges out in the Oscura Mountains 90 mi to the north. Some of the thinning may be depositional, as pointed out in the following paragraphs.

The four formations which compose the Montoya Group, first described in the Caballo Mountains by

Kelley and Silver (1952), are easily recognized throughout the Organ and San Andres Mountains. These formations are: basal Cable Canyon Sandstone, Upham Dolomite, Aleman Dolomite, and Cutter Dolomite. None are thick enough to be shown at the scale of the map; indeed, some authors (Harbour, 1972; Bachman and Myers, 1969) have treated the four units as members of the Montoya Dolomite, a formation. Hayes (1975) considered the Upham and Cable Canyon units to be members of the Second Value Dolomite, a name introduced by Entwistle in 1944.

The Montoya includes a distinctive group of rocks. The Cable Canyon Sandstone, thin to absent in the Bishop Cap–Rattlesnake Ridge area, is 10-15 ft thick in the Bear Canyon–Black Mountain area where it forms a conspicuous brown-weathering band at the base of the nearly black Upham cliffs. The sandstone consists of coarse-grained, subrounded, frosted quartz cemented by both silica and dolomite. The sandstone is actually a transgressive basal sand of the Upham, into which it grades. The Upham is a single massive unit of dark-gray-weathering, coarsely crystalline, thick-bedded dolomite, more than 100 ft thick in the southern part of the map area and approximately 80 ft thick in the northern part. An abrupt change to black, thin-bedded chert and dolomite marks the base of the overlying Aleman Dolomite.

Most of the Aleman is distinguished by abundant chert in the form of thin layers or elliptical to irregular nodules. Parts of the Aleman may contain 30-60 percent chert, while other parts are comparatively free of it. The Aleman Dolomite is typically medium bedded, fine to medium grained, and may range from light to dark gray. A distinctive light- and dark-gray banding marks the upper part of the Aleman, a result of intertonguing of dark Aleman and light Cutter beds. The difficulty of picking the top of the Aleman consistently within this transition probably accounts in part for the variable thickness reported for both Cutter and Aleman units throughout south-central New Mexico. In this study, the top of the Aleman was placed at the top of the highest bed containing more than 25 percent chert. The thickness of the Aleman within the map area ranges from 198 ft at Bishop Cap to 171-152 ft in the southern San Andres Mountains. According to Kottlowski and others (1956), the Aleman continues to thin northward through the San Andres Mountains. Therefore, in spite of the uncertainties in identification of the top of the formation, the Aleman appears to indicate depositional thinning northward within the Montoya Group.

Uppermost beds of the Montoya are nearly chert-free, fine-grained dolomite of the Cutter Dolomite. The very even, parallel bedding and light-gray color are diagnostic of the unit as is the ledgy slope to which it weathers between the more cliffy strata above and below. The Cutter ranges in thickness within the map area from 156 ft in the south to 100-125 ft in the north at Bear Canyon. The unconformable contact with overlying Fusselman beds is sharp, with 2-3 ft of erosional relief.

Many beds within the Montoya contain comminuted and recrystallized fossil debris. Elsewhere in the region fossils have been identified that indicate that the Cable Canyon and Upham units are of Middle to earliest Late Ordovician age, and the Aleman and Cutter are of Late Ordovician age (Kottlowski and others, 1956; Flower, 1969; Hayes, 1975).

Silurian rocks

Fusselman Dolomite

The Silurian System is represented by the Fusselman Dolomite in the Organ and San Andres Mountains and throughout south-central New Mexico. The massive, homogenous unit forms dark cliffs beneath slope-forming Devonian beds in the southern San Andres Mountains (fig. 23), but forms pale-tan ridge crests and dip slopes at the southern end of the Organs. Upper and lower contacts are sharp unconformities, marked both by distinct color and topographic changes. The upper surface of the Fusselman is a knobby, somewhat siliceous erosion surface in contact with Devonian shale, siltstone, or limestone. According to Kottlowski and others (1956), this erosion surface of Early Devonian age regionally truncates Fusselman, Montoya, El Paso, and Bliss strata from the Franklin Mountains north to the Oscura Mountains. Most, if not all, of the northward thinning of the Fusselman, from 840 ft in the Franklins to 310 ft at Bishop Cap to 110 ft at Bear Canyon, is a result of the Early Devonian erosion. The Fusselman pinches out about 45 mi north of Bear Canyon (Kottlowski and others, 1956).

Bachman and Myers (1969) describe two distinctive dolomite units within the Fusselman from the Sacramento Mountains and note that both are present in the southern San Andres range. In Bear Canyon, I also recognized two kinds of dolomite, separated by a sharp, apparently disconformable surface. The lower unit, only present locally, is a light-gray, pearly, coarse-grained dolomite that weathers to pale grayish orange or light tan; it is relatively chert-free, and is usually less than 20 ft thick. The main part of the Fusselman near Bear Canyon consists of massive, medium- to dark-gray-weathering, very cherty, coarse-grained dolomite. Reworked clasts of the lower member can be found locally near the base of the upper member, indicating an intraformational unconformity between the two members. The thick, massive beds of Fusselman Dolomite in the southern Organ and northern Franklin Mountains are identical with the lower member; beds representative of the upper member were not seen in those areas. Possibly, compensating wedges exist, with the lower member thickening to the south and the upper member thickening to the north. However, Early Devonian erosion may have removed the upper member south of US-70.

The two Fusselman units, together with the disconformable surface between them, suggest that the Fusselman is not a simple formation. Kottlowski and others (1956) point out that fossil evidence also indicates this; fossils ranging in age from Lower to Middle Silurian have been collected from different parts of the formation (Harbour, 1972).

The uppermost Fusselman is the host for many of the barite-fluorite and base-metal deposits in the region. Hydrothermal fluids apparently were prevented from moving into higher Paleozoic rocks in most places by the impermeable Devonian shales. The lines of pros-

pects and the bleaching-alteration effects in uppermost Fusselman beds clearly mark the top of the formation in several areas.

Devonian rocks

Devonian strata in the southern San Andres and Organ Mountains were mapped as the Canutillo Formation (present only in the southern part of the area) and the overlying Percha Shale. The Percha map unit includes not only Percha Shale, but also beds probably correlative with the Oñate, Sly Gap, and Contadero Formations, as described by Stevenson (1945), Laudon and Bowsher (1949), and Kottlowski and others (1956). The latter three units are defined biostratigraphically and are not mappable formations in the southern San Andres and Organ Mountains. Therefore, all of the slope-forming, mostly shaley Devonian strata between the Fusselman and the Mississippian limestones were lumped into the Percha unit following widespread usage in southern New Mexico.

In contrast to the Ordovician and Silurian rocks, which probably were deposited on warm, shallow, normal-marine shelves, the black, nonfossiliferous Devonian shales were the product of deposition in lagoons or shallow-marine seas with muddy bottoms and restricted circulation of water. Conditions improved from time to time, and a normal fauna flourished in parts of the region; within the map area such agreeable conditions apparently were lacking in the Devonian, because fossils are generally scarce and only the nondiscriminating phosphatic brachiopods are occasionally found.

Canutillo Formation

The Canutillo Formation (Nelson, 1940; Laudon and Bowsher, 1949) was recognized at Bishop Cap and on Rattlesnake Ridge. It overlies massive Fusselman Dolomite on what has been described in the Franklin Mountains as a channeled surface marked by potholes (Harbour, 1972). The upper contact with the Percha Shale may also be an unconformity at Bishop Cap judging from the abrupt change from cherty limestone to black shale. In the Franklin Mountains, however, the Canutillo-Percha contact appears to be gradational (Harbour, 1972).

In the central Franklin Mountains the Canutillo is 116 ft thick (Harbour, 1972). At Bishop Cap the Canutillo has thinned to 45 ft thick, and northward it either pinches out or changes facies into a few feet of basal limestone of the Percha noted at Black Mountain and Bear Canyon.

Two informal members of the Canutillo can be recognized at Bishop Cap. The lower member, 18 ft thick, is mostly fissile, thin-bedded, calcareous or dolomitic siltstone that weathers light-brownish-gray. The upper member, 27 ft thick, is thin bedded, very cherty limestone and dolomite. The chert, in thin beds or nodules, is black and constitutes up to 90 percent of several beds. One or two feet of medium-bedded, yellow, brown-weathering dolomite mark the top of the upper member; this is overlain by fissile Percha Shale.

Percha Shale

In a landscape otherwise dominated by cliffs or ledgy slopes, the Percha Shale is easily recognized by the smooth erosional slope, saddle, or bench to which it weathers (fig. 23). The Percha being an exceptionally soft unit, scarce exposures are confined to gullies. On the other hand, fragments of gray, black, or purple fissile shale are common in colluvium on any slope underlain by Percha, and these are useful in identifying the formation where it might not ordinarily be expected, as in the thrust sheets on Black Mountain. In addition to the thrusts, bedding-plane faults are common in the Percha, especially in the folded rocks adjacent to the Bear Peak fold and thrust zone. Drastic thickening or thinning over short distances and complex internal deformation of the Percha has resulted from movement on such faults.

Accurate thicknesses of the Percha range from 140 ft at Bishop Cap to about 70 ft in Bear Canyon. Thicknesses of 70-85 ft are common in the northern Organ–southern San Andres Mountains; however, at one place on Black Mountain, the Percha was completely removed by pre-Lake Valley erosion. At this locality Lake Valley carbonates fill a broad channel cut through the Percha into upper Fusselman beds (fig. 25). While basal contacts of Percha Shale with the Canutillo Formation or Fusselman Dolomite are widespread disconformities, upper contacts with the Mississippian Caballero Formation appear to be conformable in most places.

Dark- to medium-gray or purplish-gray fissile shale composes most of the Percha. There are thin beds of siltstone or, more rarely, limestone at several horizons. At the base through most of the Bear Canyon–Black Mountain area is 10-20 ft of yellow-weathering, hard, fine-grained, medium-bedded limestone that contains scattered comminuted fossils. This limestone unit may be correlative with the Oñate Formation, the basal part of the Devonian system described farther north in the San Andres Mountains (Kottlowski and others, 1956; Bachman and Myers, 1969), or with the Canutillo Formation farther south. The latter correlation would require substantial facies change within the Canutillo.

Fossils have been collected from many units within

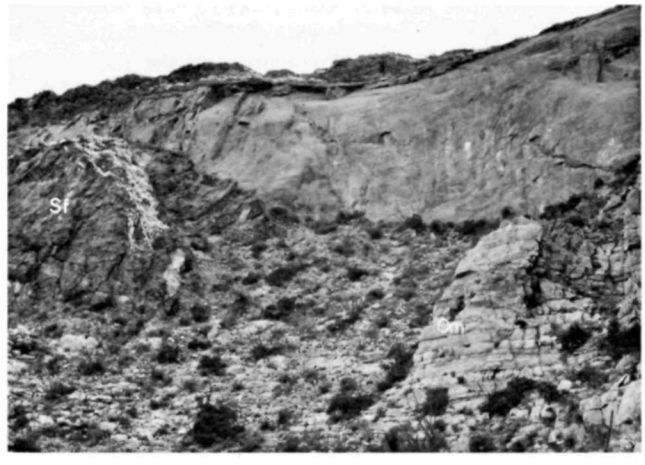


FIGURE 25—MASSIVE, CLIFF-FORMING, CRINOIDAL LAKE VALLEY LIMESTONE filling channel cut through Percha Shale into Fusselman Dolomite **(Sf)**; **Om**—Montoya Dolomite; view to north.

the Percha of the San Andres Mountains. These fauna are complexly distributed and are associated with complex facies changes. Nevertheless, they show that the Percha (as used here) ranges in age from late Middle Devonian to Late Devonian (Kottlowski and others, 1956; Bachman and Myers, 1969). At Bishop Cap the only fossils found in the black shales were linguloid brachipods.

Mississippian rocks

Mississippian strata overlying the Percha Shale have been divided into five formations in the Organ–southern San Andres area (Laudon and Bowsher, 1949). In ascending order the formations are: Caballero, Lake Valley, Las Cruces, Rancheria, and Helms Formations; they represent parts of all four series of the Mississippian System. However, all formations are exposed only at Bishop Cap (figs. 26 and 27) and Rattlesnake Ridge. South of these areas the Lake Valley Formation pinches out, while to the north the Helms Formation thins to a feather edge beneath basal Pennsylvanian limestone. In spite of these variations and the considerable thickening and thinning of the Rancheria, Las Cruces, and Lake Valley Formations, the overall thicknesses of Mississippian strata remain relatively constant across the map area, ranging from approximately 500 ft at Bishop Cap to 450 ft at Bear Canyon.

Fig. 28 shows correlation of Mississippian formations from Bishop Cap to Bear Canyon. The correlation is based mainly on physical characteristics inasmuch as fossil collections were made only locally.

The Mississippian section at Bear Canyon differs in at least three important respects from the section described by Laudon and Bowsher (1949) from the same general area (SW¼NW¼ sec. 30, T. 20 S., R. 5 E.). First, distinctive, laminated, sandy, crinoidal limestone beds, assigned by Laudon and Bowsher (1949) to the Derryan Series, occur beneath the Helms Formation at Bishop Cap and are therefore uppermost Rancheria beds. Such strata cap the Rancheria throughout the Organ and southern San Andres Mountains. Second, Laudon and Bowsher's (1949) Rancheria Formation at Bear Canyon includes a basal sequence of blue- to light-gray-weathering, slightly cherty, even-bedded, black micrite that is assigned to the Las Cruces Formation in this report. The unit is perhaps the most distinctive of the Mississippian formations and upper and lower contacts are clear unconformities. Third, Lake Valley strata differ in both thickness and lithology from the published descriptions by Laudon and Bowsher (1949). These differences may be caused by rapid facies changes, pinching out of units, and the irregular erosion surface at the top of the Lake Valley. This lithostratigraphic combination produces drastic changes in exposures of the Lake Valley from place to place in the Bear Canyon–Black Mountain area. Boundaries between the Lake Valley, Las Cruces, and Rancheria formations are thought to be regionally important erosional unconformities separating distinctive lithologic units. However, correlations were based on lithostratigraphic characteristics and no faunal collections were made for biostratigraphic support.



FIGURE 26—Middle and lower Paleozoic rocks exposed at Bishop Cap (the peak at left). IPb—Berino Formation, IPlt—La Tuna Formation, **Mh**—Helms shale, **Mr**—Rancheria Formation, **Dp**—Percha Shale, **Sf**—Fusselman Dolomite; view looks north.



FIGURE 27—Devonian and Mississippian formations exposed in the south-central Bishop Cap hills. **Dp**—Percha Shale, **Mc**—Caballero Formation, **Mlv**—Lake Valley Formation, **Mr**—Rancheria Formation, **Dc**—Canutillo Formation; view looks southwest.

Caballero(?) Formation

Basal beds of the Mississippian System in this area are correlated with the Caballero Formation (Kinderhookian) of Laudon and Bowsher (1949). The contact with the underlying Percha Shale appears gradational at Bishop Cap and Bear Canyon; however, the abrupt change at the contact in the northwest Organ Mountains indicates a possible disconformity. The formation ranges up to 28 ft thick.

Lithology of the Caballero varies between the northern and southern parts of the map area. At Bishop Cap and Rattlesnake Ridge, Caballero(?) beds are brown-weathering, dolomitic siltstone and interbedded, nodular, argillaceous dolomite that form ledges and slopes at the top of the Percha slope. Some green to gray shale of Percha type is also present; therefore, this Caballero(?) may actually be younger Percha. No

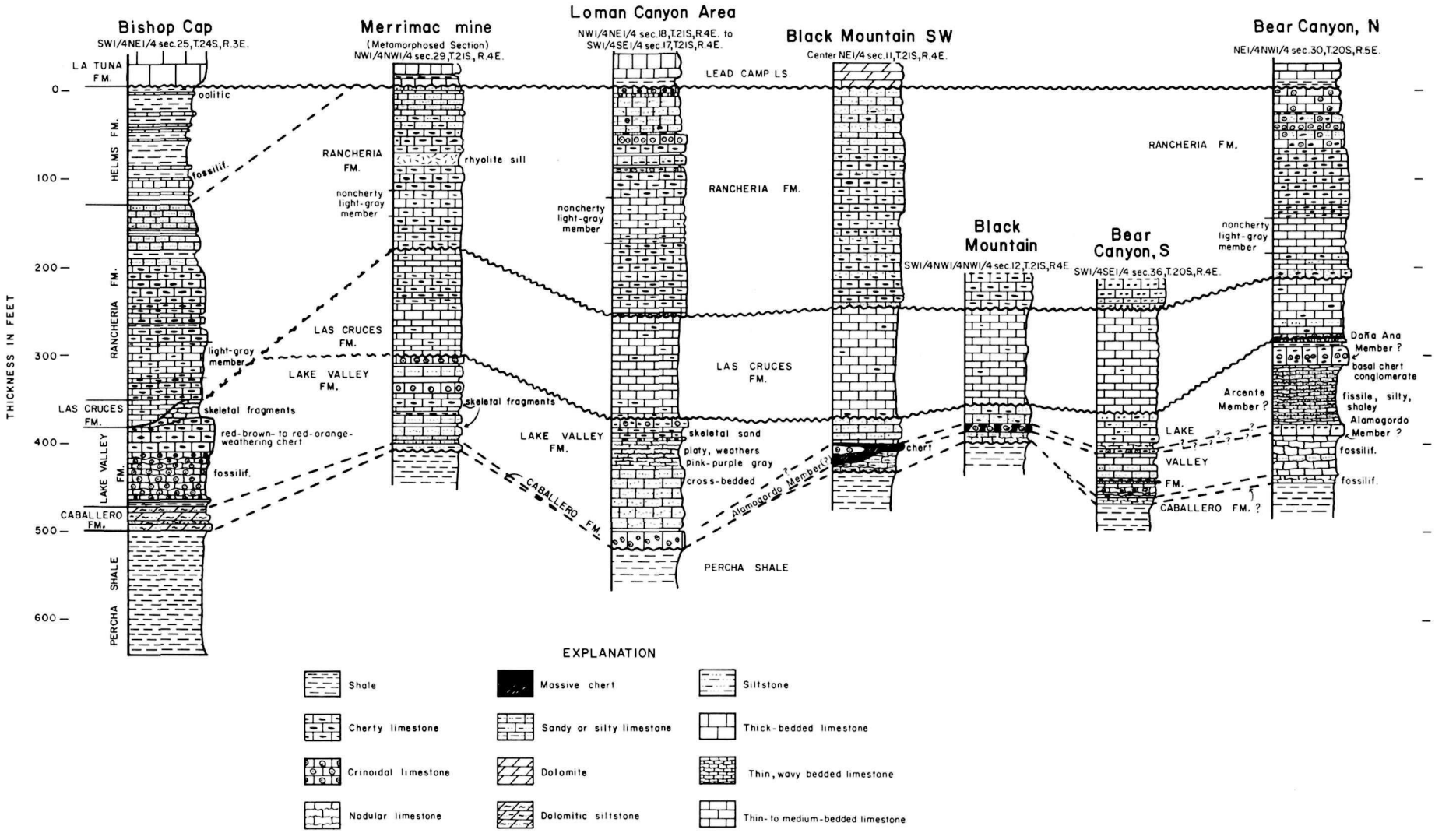


FIGURE 28—CORRELATION OF MISSISSIPPIAN FORMATIONS BETWEEN SOUTHERN SAN ANDRES MOUNTAINS AND BISHOP CAP.

fossils were found, hence the Mississippian age is tentative. Flih (1976) also identified Caballero in the Bishop Cap hills and mentioned an important fauna contained in them, but described no details. Similar siltstones occur between Percha and the Lake Valley north of San Agustin Pass, but there the Percha–Caballero contact is not gradational and may be disconformable.

To the north, in the Black Mountain–Bear Canyon area, lithologies are more representative of the Caballero described by Laudon and Bowsher (1949). Interbedded soft, nodular limestone, fissile shale, and marl compose the Caballero there. Some of the limestone is sandy, and several varieties of rugose corals and brachiopods can be found locally. In this locality, upper and lower contacts of the Caballero are chosen with difficulty because they appear to be gradational. In contrast, regional evidence cited by Kottlowski (1957) indicates that these contacts are significant unconformities. Additional biostratigraphic studies are needed to resolve these problems.

Lake Valley Formation

By far the most complex Mississippian formation in the southern San Andres–Organ Mountain area is the Lake Valley Formation. The combination of abrupt facies changes, rapid thickening and thinning and intertonguing of units, and a locally deep, irregular erosion surface at the top of the formation accounts for the complexity. The six members into which Laudon and Bowsher (1949) subdivided the formation farther north in the range were not identified, except as local possibilities. To attempt such identification in the absence of faunal evidence seemed futile inasmuch as lithologies and thicknesses vary so drastically from place to place. However, Flih (1976), in his study of the Lake Valley Formation at Bishop Cap, reports the presence there of (from oldest to youngest) the Andrecito, Alamogordo, Nunn, and Arcente Members. The Tierra Blanca (between the Nunn and Arcente) and Doña Ana (above the Arcente) were not identified by him. Fossils collected during this study from the Lake Valley Formation at Bishop Cap are "definitely Osage and appear to represent examples from the Nunn" according to A. K. Armstrong (personal communication to S. C. Hook, 1978), thus confirming the presence of Lake Valley strata.

Maximum thickness of Lake Valley strata in the map area is approximately 225 ft, measured on the northern slopes of Bear Canyon. Southward the formation thins somewhat in an irregular manner, and locally at Bishop Cap as much as 181 ft of Lake Valley still remain (Flih, 1976). However, the formation is very thin along the southern edge of the Bishop Cap hills and has not been reported in the Franklin Mountains.

Massive beds of crinoidal limestone are probably the most representative lithology of the Lake Valley. Such strata, containing black chert, form a prominent basal ledge, 5-20 ft thick, throughout most of the Black Mountain–Bear Peak–Hilltop mine area. Younger units include: 1) brown, sandy limestone; 2) more crinoidal limestone ledges; and 3) locally, pink- to purplish-gray-weathering, platy micrite. In some areas these units have been removed by pre–Las Cruces erosion.

In Bear Canyon, a thicker, more complete section is preserved, but it is lithologically dissimilar to sections farther south and west. The sequence here includes: 1) fossiliferous, thin-bedded, nodular to blocky limestone at the base; 2) a massive ledge of slightly cherty, noncrinoidal, well-bedded limestone that may be the Alamogordo Member; 3) 67 ft of pink to purplish-gray, platy, slope-forming, unfossiliferous micrite that is unlike typical Nunn; and 4) massive, cherty, crinoidal limestone, similar to that forming the base of the Lake Valley on Black Mountain.

At Bishop Cap, approximately 60 ft of nodular, soft, yellowish-gray, crinoidal limestone is lithologically similar to the Nunn Member and contains an Osagian fauna. It is overlain in many places by as much as 50 ft of massive, cliff-forming, cherty limestone. The chert constitutes up to 70 percent of the unit and weathers reddish-brown or orange. Along strike, the massive cherty beds build into lens-shaped bioherms as much as 50 ft thick, described in detail by Flih (1976). In a few places, thin-bedded, shaley limestone and shale containing fossil debris overlie the bioherms or the massive, cherty limestone. In most places these upper strata were removed completely by pre–Las Cruces erosion, which left an irregular surface with as much as 50 ft of relief.

Laudon and Bowsher (1949) established an Osagian (early Middle Mississippian) age for the Lake Valley Formation throughout south-central New Mexico. The following forms collected at Bishop Cap were identified by A. K. Armstrong (written communication to S. C. Hook, 1978) and determined to be part of an Osagian fauna: *Ovatia?* aff *Ovatus* (Hall), *Athyris lamellosa* Leveille, *Spirifer rowleyi* Weller, and *Amplexiazaphrentis* or *Hapsiphyllum*.

Las Cruces Formation

Overlying Devonian rocks in the Franklin Mountains are 50-90 ft of light-gray-weathering, even-bedded limestone named Las Cruces Formation (Laudon and Bowsher, 1949; Harbour, 1972). At Vinton Canyon in the northern Franklins, the Las Cruces was studied in detail by Setra (1976). The unit thins northward toward Bishop Cap, where it forms a band of light-colored, ledgy limestones between the Lake Valley and Rancheria Formations. Las Cruces strata in this area fill erosional depressions in the underlying Lake Valley; the strata thicken to 50 ft where the Lake Valley was deeply eroded and are thin or missing altogether where the Lake Valley was less deeply scoured. The Las Cruces is also exposed near the Stevenson–Bennett mine and throughout the southern San Andres Mountains. In this region the formation also forms a distinctive sequence of light-gray- or blue-gray-weathering ledges that unconformably overlie the Lake Valley Formation.

Throughout the region the upper contact also appears to be an unconformity that separates blue-gray-weathering, slightly cherty Las Cruces micrite from brown-weathering, cherty, sandy Rancheria strata. However, the unconformity lacks appreciable relief and has been described by Pray (1961) and Yurewicz (1973) as a diastem, thus indicating only a sedimentation change and nondeposition rather than erosion. The interpretation seems reasonable because both Las Cruces and Rancheria strata are basinal, relatively deep-water deposits. In a generally subsiding basin, subaerial ero-

sion produced by either uplift or a major fall in sea level seems unlikely. On the other hand, Laudon and Bowsher (1949) described the contact as "a conspicuous unconformity" and implied that uplift and subaerial erosion were involved. In my opinion, the contact is an unconformity that represents a relatively long interval of little or no deposition, with no accompanying erosion.

Throughout the northern part of the map, the Las Cruces Formation maintains a uniform thickness of 115-125 ft, but it thins abruptly to 69 ft on the northern slopes of Bear Canyon. Further depositional thinning to the north may be responsible for the reported absence of the Las Cruces in the southern San Andres Mountains (Bachman and Myers, 1969).

Lithology of the Las Cruces Formation is distinctive. Typically, the strata are very even, parallel-bedded, black micrite that weathers blue-gray in the northern part of the area and light gray at Bishop Cap. Beds are 0.5-1 ft thick. Much of the formation lacks chert, but some beds contain thin, black, pancake-shaped chert nodules or scattered irregular nodules. The strata greatly resemble the middle part of the overlying Rancheria Formation; in fact, they may be a facies of the Rancheria as suggested by Laudon and Bowsher (1949). Pray (1961) and Yurewicz (1973), in their studies of the Las Cruces and Rancheria, also pointed out similarities between the two formations in the Sacramento Mountains. Moreover, they suggested that the Las Cruces be redefined as a member of the Rancheria, because only a diastem separated them. However, I consider the contact to be an unconformity, and the distinctive, mappable rocks on either side to merit formational status.

Other than local skeletal grains, no fossils were found in the Las Cruces Formation. An Osagian and Meramecian (late middle Mississippian) age is based on the studies of Laudon and Bowsher (1949) and Lane (1974). Lane also suggested that the Las Cruces represented a basin facies that is correlative with the shelf limestones of the Doña Ana Member of the Lake Valley Formation. From my work, however, the Las Cruces appears to overlap the Lake Valley completely and to be separated from it by a major erosion surface. At Bear Canyon, Las Cruces beds unconformably overlie massive, crinoidal, cherty limestone which may be the Doña Ana Member. If so, the two units could not be laterally correlative facies.

Rancheria Formation

In the southern San Andres-northern Organ Mountains, the Rancheria Formation disconformably overlies the Las Cruces Formation and disconformably underlies the Lead Camp Limestone (Pennsylvanian). From a distance, the brown-weathering, ragged cliffs of the Rancheria are easy to recognize (fig. 27). By contrast, Lead Camp and Las Cruces strata weather medium or light gray and usually form ledgy slopes.

The contact between the Rancheria and the basal Lead Camp is not always obvious. Uppermost Rancheria strata can usually be identified by their abundant laminae of fine sand and locally by massive crinoidal limestone. Basal Lead Camp strata contain no sand or crinoidal beds, but they do have several shale breaks, and locally green or maroon shale directly overlies the Rancheria.

The Rancheria Formation thins northward from 370 ft in the Franklin Mountains (Harbour, 1972) to its pinchout 10 mi north of Bear Canyon. From Bishop Cap to Bear Canyon the formation is thinner than in the Franklins, but maintains a nearly uniform thickness of 200-250 ft. North of Bear Canyon the thinning continues, but at a greater rate, to the pinchout noted above. Apparently complete but thin stratigraphic sections are locally present, as at the Merrimac mine (table 1). Here the formation has been metamorphosed to marble and calc-silicate rocks, and thinning by ductile flow may have occurred. Other formations in the same area, however, have normal thicknesses; therefore, local depositional thinning of the Rancheria may be indicated.

Thinning of the Rancheria northward from the Franklin Mountains is entirely through depositional processes. This aspect is illustrated by the fact that the same set of sandy, laminated limestone beds, some crinoidal, form the upper part of the Rancheria everywhere. The pre-Lead Camp erosion surface at the top

TABLE 1—SUMMARY OF THICKNESSES (IN FEET) OF PALEOZOIC AND CRETACEOUS STRATA, ORGAN AND SOUTHERN SAN ANDRES MOUNTAINS.

	Bear Canyon N	Bear Canyon S	Black Mountain S side	Loman Canyon	Hardscrabble Hill	Merrimac mine	Hilltop mine	Bishop Cap	Rattlesnake Ridge	Love Ranch area	west-central Organ Mountains
Mancos equivalent										1000 ±	
Dakota Sandstone											
Sarten Sandstone										165	
Yeso-San Andres										95	
Abo-Yeso										550 ±	
Hueco Limestone					1675					435 ±	
Panther Seep Formation					2037						1874 +
Lead Camp Limestone			654			869-872					
Berino Formation											
La Tuna Formation								516			
Helms Formation								259			
Rancheria Formation	214		247	264		168		132			
Las Cruces Formation	69	155(?)	125	116		121		222			
Lake Valley Formation	153	34-73	34-58	147		97		0-13			
Caballero Formation	7	6	19			7	29	15-181			
Percha Shale		61-70	171-141				84	28			
Canutillo Formation								140			
Fusselman Dolomite		110	160				149	44			
Montoya Group		368					405	310			
Cutter		102					153	470			
Aleman		171					152	155			
Upham		79					85	198			
Cable Canyon		16					15	117			
El Paso Group	780						876	810 +	950-1000		
Bliss Sandstone	125						144				

of the Rancheria in the southern San Andres Mountains plainly is neither deep nor irregular.

Lithologically, the Rancheria Formation is distinguished by 1) abundant chert, up to 70 percent in some parts of the formation; 2) interlayered black micrite or microsparite; 3) generally brown-weathering rocks; and 4) a thin-bedded appearance. Many of the strata are also sandy and siliceous without necessarily carrying chert. Near the middle of the formation is approximately 50 ft of gray-weathering micrite with scattered black chert nodules and lenses; it is similar to the Las Cruces Formation. From the Franklin Mountains to Bear Canyon, this unit forms a distinct gray band amid the otherwise brownish Rancheria strata. Sandy, laminated limestone and massive beds of crinoidal limestone with disc-shaped lenses of chert 3–4 ft long and 1 ft thick distinguish the upper third of the formation.

The Rancheria Formation is poorly fossiliferous, except for the crinoids in the uppermost strata. On the basis of conodont studies, Lane (1974) confirmed Laudon and Bowsher's earlier (1949) assignment of the Rancheria to the Meramecian and Chesterian (late middle to Late Mississippian).

Relatively deep-marine, quiescent, restricted conditions of deposition are indicated by the dark micritic rocks, the thin bedding, the lack of an abundant fauna (other than conodonts), and the fine comminuted skeletal debris. Shallowing conditions in late Meramec and Chester time are suggested by the well-sorted crinoidal grains, prolific normal-marine fauna, terrigenous clastic material, and scattered oolite beds in the upper parts of the Rancheria and throughout the Helms Formation.

Helms Formation

The shallow-water, largely clastic strata of the Helms Formation interfinger with upper Rancheria beds at Bishop Cap, on Rattlesnake Ridge, and farther south. Approximately 130 ft thick at Bishop Cap, the Helms thins rapidly northward and is absent in the northern Organ Mountains. As with the Rancheria, most of the thinning is depositional, though part may be a result of pre-Pennsylvanian erosional truncation. At Bishop Cap there is a sharply disconformable contact between the Helms and the La Tuna Formation (Pennsylvanian), but there is no hint of truncation. In the Franklin Mountains, Harbour (1972) reports apparent intertonguing of Helms and La Tuna strata. Because the formation consists mostly of soft, shaley strata, it weathers to slopes and saddles between the cliff- or steep-slope-forming limestones above and below.

The Helms consists mostly of interbedded shale, soft, nodular limestone, and massive limestone ledges that contain a profusion of fossils. Near the top of the formation are thin but extensive oolite beds. Crinoidal beds are common, and some limestones contain a rich fauna of unbroken bryozoans, brachiopods, corals, trilobites, snails, and other mollusks. These fossils, as well as the conodonts recovered by Lane (1974), indicate a Chesterian (Late Mississippian) age and a shallow-marine environment for the Helms.

Pennsylvanian and Permian rocks

Pennsylvanian and Permian strata nearly 4,400 ft thick are exposed in the Organ and southern San Andres Mountains. Lacking major unconformities, the sequence indicates nearly continuous deposition in south-central New Mexico for 55 m.y. The Lead Camp Limestone and La Tuna and Berino Formations are normal-marine, stable-shelf deposits, but these grade up into the thick, largely clastic beds of the Panther Seep Formation which filled the Orogrande Basin in Late Pennsylvanian time (Pray, 1959). A return to stable-shelf conditions is indicated by the Hueco Limestone of Early Permian age. Gradually, however, the edge of the Hueco sea was forced to the southern limits of New Mexico by the red clastic wedge of Abo Sandstone, derived from highlands in Colorado. Lagoonal rocks of the Yeso Formation and the marine Yeso–San Andres Limestone overlie the Abo and record the gradual spread of seas again across south-central New Mexico. Younger Permian strata have not been found in the map area.

A noteworthy feature of the Pennsylvanian and Hueco strata is their cyclicity. Individual lithologies or groups of lithologies are repeated many times as one walks across outcrops of these rocks. Clearly the recurrences reflect cyclical changes in environments of deposition, most likely related to changing water depths (Wilson, 1967). These cycles, which are also a distinctive feature of strata of late Paleozoic age throughout the United States, are interpreted as resulting from sea-level changes caused by episodic glaciation in the southern hemisphere during the late Paleozoic (Ross, 1979).

Lead Camp Limestone

Lower and Middle Pennsylvanian rocks, named Lead Camp Limestone by Bachman and Myers (1969), disconformably overlie the Rancheria Formation in the northern Organ and southern San Andres Mountains. The formation is distinguished by the massive, gray limestone or dolomite cliffs or steep, ledgy slopes to which it weathers. Basal beds in some places are massive, gray limestone or dolomite lying on the Rancheria, but elsewhere grayish-green shale forms the basal strata. Uppermost beds, transitional into the Panther Seep Formation, consist of approximately 130 ft of orange- to olive-gray-weathering dolomitic and gypsiferous limestone and shale, which contrast greatly with the grays of the rest of the formation. Intertonguing of Lead Camp carbonate and Panther Seep shale renders choosing a boundary between the two arbitrary. In this study the base of the Panther Seep was selected at the lowest thick (30 ft), persistent shale bed.

In the map area the Lead Camp Limestone varies in thickness from 650 to 870 ft. At Bishop Cap and Rattlesnake Ridge, strata correlative with the lower and middle part of the Lead Camp are 775 ft thick. The formation appears to thin irregularly northward. Five mi north of Bear Canyon, Bachman and Myers (1969) measured only 320 ft. South of Bishop Cap, rocks correlative with the Lead Camp thicken to at least 1,500 ft in the Franklin Mountains (Harbour, 1972).

Excellent unmetamorphosed sections of Lead Camp Limestone crop out in Loman and Bear Canyons and on Black Mountain. At the latter locality, a typical section of massive to medium-bedded dolomite and cherty limestone is cyclically interbedded with thin shale units that are poorly exposed. Within the carbonates are repeti-

tions of cherty, fossiliferous, silty, intraclastic, and micritic constituents. Locally dolomite predominates, but elsewhere the section is mostly limestone. Between 130 and 250 ft above the base of the Lead Camp at Black Mountain and elsewhere, a distinctive section of porcelanite, black shale, sandstone, crossbedded quartzite, and conglomerate, all interbedded with limestone, is seen. The clastic units are discontinuous, however, and in many other outcrops of the Lead Camp the clastic units are either thin or absent. A similar clastic sequence, described by Kottlowski and others (1956), at Ash Canyon 10 mi north of Black Mountain, contains the Derryan–Desmoinesian boundary.

Fusulines from the Lead Camp have been studied by Kottlowski and others (1956) and Bachman and Myers (1969). These fusulines show that the Lead Camp was deposited during Early to Middle Pennsylvanian time (Morrowan(?), Atokan (Derryan), Desmoinesian, and Missourian). Fusulines collected during the present study 425 ft above the base of the Lead Camp on Black Mountain are highly evolved *Beedina* of latest Desmoinesian age (W. E. King, personal communication, 1976). On the columnar section (plate 3, in pocket), the Desmoinesian–Missourian boundary was placed just above these fusulines.

La Tuna Formation

In the Franklin Mountains, rocks of Pennsylvanian age were assigned to the Magdalena Formation and divided into four members by Harbour (1972). From oldest to youngest these are the La Tuna Member, Berino Member, Bishop Cap Member, and an unnamed upper member. Because the Magdalena is generally accorded group status in New Mexico (Gordon, 1907; Kelley and Silver, 1952), these members are regarded as formations in this report. The lower three formations are approximately correlative with the Lead Camp Limestone; the lithologies they contain indicate similar environments of deposition. The upper formation is correlative with most of the Panther Seep Formation. At Bishop Cap and on Rattlesnake Ridge, the La Tuna and Berino Formations have been recognized (fig. 26). Part of the Bishop Cap may be present in one faulted, somewhat metamorphosed outcrop on Rattlesnake Ridge. Beyond the Franklin, Organ, and other nearby ranges none of these formations can be recognized on the basis of their lithologies, hence detailed correlation with the Lead Camp or other Pennsylvanian formations usually depends on biostratigraphic studies with fusulines or other significant fossils.

The La Tuna Formation forms massive cliffs of gray limestone above the Helms shale. The limestone, approximately 260 ft thick, contains a great deal of rust-weathering chert that forms conspicuous bands on the gray cliffs. Bedding thicknesses decrease progressively from 8-10 ft in the basal part of the formation to 1-2 ft in the upper part. The limestone is mostly micrite, but locally contains abundant fine- to medium-grained skeletal debris. A brown quartzite bed near the middle of the unit is 1-10 ft thick and contains *Lepidodendron*. Medium-bedded, light-gray dolomite is interbedded with the limestone at the top. Authigenic quartz crystals are abundant in most La Tuna outcrops. Excellent specimens of silicified rugose corals are common, but brachiopods, bryozoans, and local lenses of crinoidal debris are rarer. Atokan (Derryan) fusulinids were identified from basal Berino beds, so it seems likely that upper parts of the La Tuna also are of Atokan age.

Lane (1974) states that the La Tuna is of earliest Morrowan age and Harbour (1972) reports *Millerella* sp. of Morrowan age from the lower part of the La Tuna.

Berino Formation

The Berino Formation overlies La Tuna limestones conformably; the base was chosen at the base of the first thick (10-15 ft) shale bed. At Bishop Cap, uppermost beds of the Berino Formation form Bishop Cap Peak (fig. 26); younger strata (Bishop Cap Formation) have been eroded, but they may be present beneath Quaternary gravels west of Bishop Cap. On Rattlesnake Ridge an erosion surface cut into the Berino in Laramide (early Tertiary) time is overlain by lower Tertiary conglomerate and volcanic rocks.

The Berino Formation includes a variety of gray-, yellow-gray-, orange-, or pink-weathering shale, limestone, and soft, marly strata that crop out in ledgy slopes. Cyclical repetition of biomicrite, intrasparrudite, crinoidal biosparrudite, and interbedded shale is especially characteristic. Although most of the limestone is medium bedded, thick, massive beds of crinoidal limestone form imposing cliffs, and thick, cherty limestone at the top of the Berino forms the peak at Bishop Cap. Much of the limestone is sandy, and chert nodules are common. There is a profusion of fossils in most strata, including accumulations of broken shell debris and beds of whole fossils. Petrified wood has been reported in some shale beds.

Fusulines collected 25 ft above the base of the Berino are of Atokan age according to W. E. King (personal communication, 1979). In the Franklin Mountains, Harbour (1972) reported fusulines of Desmoinesian age from the upper part of the formation.

Panther Seep Formation

Rocks of the Panther Seep Formation are conformable between the Lead Camp Limestone and the overlying Hueco Limestone in the northern and western Organ and southern San Andres Mountains. In the central and southern areas of the Organ Mountains, however, Panther Seep beds were eroded from the summit and flanks of a broad Laramide uplift, and lower Tertiary conglomerate or volcanic rocks lie upon older rocks.

The Panther Seep Formation is well exposed in Bear Canyon, in the graben east of Quartzite Mountain, along the west-central edge of the Organ Mountains, and northwest of the Merrimac mine. The formation generally is 2,000 ft thick in these areas and consists mostly of fine- to medium-grained, siliceous, brown to gray, terrigenous, clastic rocks that were deposited in the Orogrande Basin during Late Pennsylvanian–Early Permian time (Virgilian to Wolfcampian) (Kottlowski, 1960; Pray, 1961). Being soft and easily eroded, the formation weathers to low, rounded hills or strike valleys, and the shaley beds are seldom exposed except in the banks of arroyos. At Hardscrabble Hill and vicinity, the formation can be divided into four units whose lithol-

ogies are representative of the Panther Seep throughout the map area.

The lower 425 ft of the Panther Seep is black to gray shale and laminated, platy micrite. The arbitrary base was chosen at the base of a thick (15-20 ft) persistent shale bed lying above orange- or olive-weathering Lead Camp dolomite. Numerous ledges of micrite are interbedded, but few exceed 1-2 ft in thickness. Thin porcelanite and siliceous sandstone layers become more numerous toward the top. Several massive gypsum beds, up to 10 ft thick each, are present between 200 and 400 ft above the base of the formation. Along strike, the thicker gypsum units locally merge, forming beds 50-75 ft thick. Many micrite and shale beds near the base of the formation also are dolomitic and gypsiferous.

The second unit, 550 ft thick, is mostly calcareous porcelanite, siliceous siltstone, cross-laminated sandstone, hard and dense, siliceous micrite, and silty and platy micrite. Many of the rocks weather to shades of brown to olive gray. The unit is resistant and forms the high hill near the center of sec. 19, T. 21 S., R. 4 E. Gray to blue-gray, nonsiliceous micrite beds, rarely more than 1 or 2 ft thick, are scattered through the sequence; thin stromatolitic algal beds are common in the upper third of the unit. All the strata are laminated and the coarser grained sandstone beds are of channel form and exhibit cross-lamination in sets as much as 1 ft thick. Ripple marks and mudcracks are common in some sandstone, siltstone, and silty micrite beds.

The third unit of the Panther Seep Formation, approximately 560 ft thick, is distinguished by an abundance of dark-gray, platy, laminated micrite, and silty, laminated, platy, brown-weathering micrite. Intercalated are thin beds of more massive micrite or, less commonly, biomicrite. Stromatolitic algal beds, 0.5-1 ft thick, appear cyclically through the sequence. Many of the sandier micrite beds exhibit ripple marks and mudcracks. The unit readily erodes and forms low, rounded hills.

The upper 400 ft of the Panther Seep Formation is transitional into the overlying Hueco Formation. Upward in the unit strata become thicker bedded and less laminated and contain more chert, phylloid algal debris, and skeletal grains. Ledgy beds of cross-laminated sandstone, sandy limestone, and biomicrite are separated by shale breaks 1-2 ft thick. At least two caliche layers and two gypsum beds occur between 200 and 320 ft below the top of the formation.

The abundance and cyclical repetition of such features as stromatolitic algae, mud cracks, and ripple marks, as well as gypsum, caliche, and gypsiferous dolomite, indicate that intertidal to supratidal deposition was prevalent during most of Panther Seep time, as pointed out by Kottlowski and others (1956). According to Wilson (1967), the laminated micrite, silty micrite, and porcelanitic rocks represent deposition during periods of relatively deeper water in the Orogrande Basin.

No fusulines were found in the Panther Seep Formation in the map area. Kottlowski and others (1956) report *Triticites* and *Dunbarinella,* both of Virgilian age, from the Panther Seep Formation farther north. It is generally agreed that most of the Panther Seep Formation is Virgilian, but an unknown thickness of the basal part probably is Missourian in age and upper beds probably are Wolfcampian. Panther Seep beds grade upward into basal Hueco strata containing *Pseudoschwagerina morsei* Needham (W. E. King, personal communication, 1976). These Hueco beds definitely are Wolfcampian, and because the base of the Hueco was arbitrarily picked at a distinctive limestone ledge, there is reason to presume that underlying beds also are Wolfcampian. Probably 200-400 ft of uppermost Panther Seep strata are Wolfcampian; lithologically these strata are transitional between typical Hueco and typical Panther Seep.

Hueco Limestone

Complete sections of Hueco Limestone are preserved above the Panther Seep in downfolded regions north of the Bear Peak thrust and fold zone. South of that zone, however, on the Laramide uplift discussed in the previous section, Hueco and older formations were variably eroded in early Tertiary time. Along the western edge of the Organ Mountains, on what was probably the flank of the Laramide uplift, erosion cut into upper Hueco beds. In several places west of the Modoc mine, the unconformity, overlain by lower Tertiary volcanic rocks and conglomerate, is exposed.

Hueco limestone and shale units intertongue both vertically and laterally with the Abo Formation. This intertonguing probably accounts for the northward thinning of the Hueco along the western edge of the range. In Bear Canyon and on Hardscrabble Hill, the Hueco (including some thin marine Abo tongues) is 1,425 ft thick. Farther south, in the central Organ Mountains near the Modoc mine, the Hueco (including a few Abo tongues) is nearly 1,900 ft thick (fig. 29; sheet 3, in pocket).

While the Orogrande Basin apparently persisted as a subsiding feature throughout the Early Permian, the character of deposition changed. In contrast to the unstable shelf and restricted environment of the Panther Seep, the Hueco records a return to almost normal marine conditions, except locally as in the Doña Ana Mountains (Kottlowski and others, 1975). The repetitions of shaly and sandy strata interbedded with limestone in the Hueco of the San Andres–Organ area record cyclic changes in sea level or influxes of terrigenous clastics or both. Sedimentologic studies are needed to determine whether regression of the shoreline, shallowing of the sea bottom, relative fall of sea level, or combinations of these, were associated with these influxes.

As elsewhere in southern New Mexico, the Hueco of the Organ and southern San Andres Mountains can be subdivided into three informal members based on lithologies and specific marker beds. The lower and middle members contain distinctive lithologic associations that are separated by a zone containing one to three orange-weathering marker beds. These two members have been identified in the Robledo and in the western Doña Ana Mountains. The upper part of the Hueco in the Organ–southern San Andres Mountains is defined as that part above the middle member that contains thin marine tongues of Abo sandstone or siltstone, or gray shale and porcelanite beds believed to represent the distal portions of Abo tongues.

The lower member of the Hueco appears to be conformable with underlying Panther Seep beds. The basal

part is marked by a widespread, conspicuous, cherty limestone ledge 10-20 ft thick. A unit of alternating platy and shaly limestone approximately 125 ft thick forms a slope above; this is followed by 100 ft of massive cliff-forming micrite. The rest of the lower member consists of 285 ft of interbedded sandy limestone, shale, algal and oolitic limestone, chert-pebble conglomerate, and biomicrite; these rocks weather to shades of brown, olive, yellow, and orange and form a ledgy slope. The top of the lower member is marked by the highest of two or three bright-orange micrite beds, apparently the same distinctive beds that occur at the same stratigraphic position in the Robledo and Doña Ana Mountains.

The middle member is approximately 500 ft thick and consists of ledgy, dark-gray, sandy biomicrite with a profusion of planispiral gastropods, echinoid spines, phylloid algal fragments, and lesser amounts of ostracods, brachiopods, and skeletal grains (figs. 30 and 31). These biomicrites are interbedded with shale or with shaly nodular micrite. A few thin beds of porcelanite or fine-grained siltstone probably are tongues of the Abo. The top of this member was placed at the base of the lowest shale-siltstone unit of the Abo that is at least 10-20 ft thick.

Above the middle member, thin siltstone beds of the Abo and comparatively thick porcelanitic shale units are abundant within the upper Hueco. This part of the section was mapped separately as "intertonguing Abo–Hueco" (Pah on the geologic map, sheet 1, in pocket). This unit actually consists mostly of limestone that is similar to but sandier than that of the middle member. Grayish-green to white porcelanite units constitute 10-35 percent of this Abo–Hueco unit and range in thickness up to 50 ft. They usually contain medial, thin, tan, cross-laminated Abo siltstone beds. Red beds are present locally only near the top. The ratios of limestone to porcelanite, and of porcelanite to siltstone, increase southward; at southernmost exposures near the Modoc mine, sandy limestone and porcelanitic shale dominate the Abo–Hueco section. The Abo–Hueco also thickens southward from 425 ft in Bear Canyon to over 1,000 ft near the Modoc mine. The thickening of this transition zone is a result of the southward transformation of the main body of Abo red beds, which overlies the Hueco from Bear Canyon northward, into the marine shale, porcelanite, and limestone of the Hueco (fig. 32).

Fusulinids reported here and by Kottlowski and others (1956), Bachman and Myers (1969), and Harbour (1972) confirm an Early Permian (Wolfcampian) age for the Hueco Limestone.

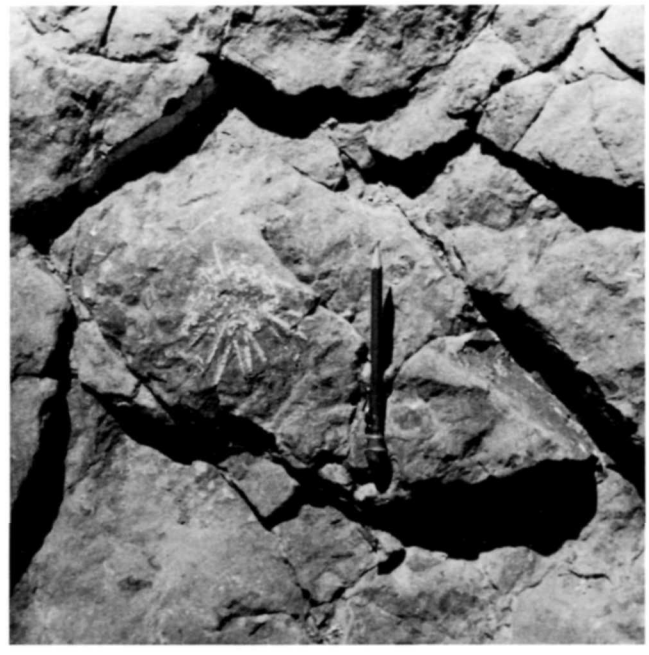


FIGURE 31—ECHINOID IN HUECO LIMESTONE; radial spines that bristled from the animal's body have collapsed but were otherwise undisturbed when the animal was buried.

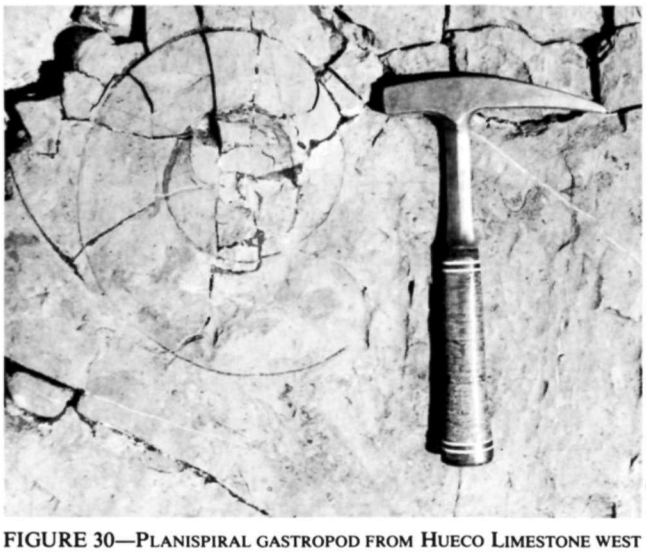


FIGURE 30—PLANISPIRAL GASTROPOD FROM HUECO LIMESTONE WEST OF MODOC MINE; geologic hammer is approximately 1 ft long.

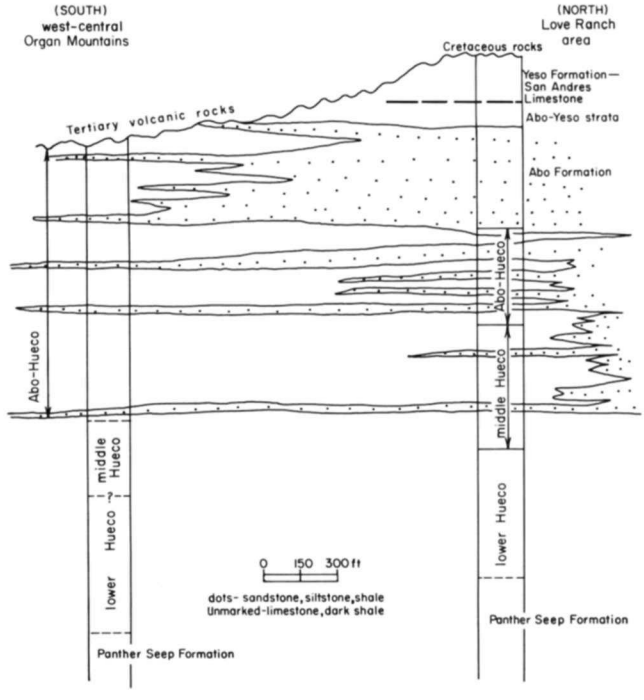


FIGURE 32—DIAGRAMMATIC SECTIONS OF PERMIAN ROCKS IN SOUTHERN SAN ANDRES AND ORGAN MOUNTAINS showing interfingering of clastic and limestone units.

Abo and Yeso Formations

In addition to the thin tongues of Abo that occur within the main body of the Hueco, a conspicuous sequence of Abo red beds overlies the Hueco near Love Ranch (fig. 3) and northward. Bachman and Myers (1969) mapped these red beds as an upper tongue of the Abo, stating that the lower tongue changed facies into the Hueco much farther north in the San Andres Mountains. South of the Bear Canyon fold and thrust zone, the upper tongue of the Abo is also missing, owing partly to Laramide erosion and partly to a facies change into porcelanite, shale, and siltstone of the Abo–Hueco unit (fig. 31).

Kottlowski and others (1956) believed that this red-bed unit contains both Abo and Yeso strata, and they mapped overlying limestone beds containing a "typical San Andres fauna" as San Andres Limestone. Definite Abo strata make up at least the lower 325 ft of the red-bed section at Love Ranch. The strata consist of dusky red to reddish-brown sandstone, siltstone, and shale, and interbedded gray or greenish shale. Overlying beds, which may be Yeso, include 100-150 ft of soft, orange-, brick-red-, or yellow-weathering siltstone and sandstone; no gypsum was seen.

Bachman and Myers (1969), on the other hand, assigned the whole red-bed sequence to the Abo. They state that definite Yeso limestone beds in the northern part of the San Andres Mountains can be traced southward into the limestone above the red-bed unit at Love Ranch. Fossils they collected from the limestone apparently are diagnostic of neither Yeso nor San Andres. During the present study no conclusions were reached regarding this stratigraphic problem. The red-bed unit was mapped as Abo–Yeso undifferentiated (Pay), and the overlying limestone as Yeso–San Andres (Pys) undifferentiated. The Wolfcampian age for the lower or Abo part of the unit is indicated by its intertonguing with Hueco Limestone.

Yeso and San Andres Formations

The 550 ft of limestone capping the Paleozoic sequence near Love Ranch is either San Andres Limestone or a limestone unit in the Yeso Formation, as discussed above. The limestone appears to overlie Yeso(?) or Abo(?) strata conformably. Quartzite and sandstone of Cretaceous age are unconformable on the limestone. The limestone caps cuestas or, where beds are vertical or overturned, forms strike ridges.

Light- to medium-gray, medium-bedded, fetid limestone is typical of the Yeso and San Andres. Alternating light and dark bands or laminae also are distinctive. A few Yeso-type beds of yellow-weathering, fine-grained sandstone are interbedded with the limestone. Some limestone beds contain abundant skeletal debris, but most of the limestone is micritic. Both Yeso and San Andres Formations are Leonardian in age (lower middle Permian), according to Kottlowski and others (1956).

Cretaceous rocks

Cretaceous rocks, approximately 1,250 ft thick, in the Love Ranch area include the Sarten and Dakota Sandstones and strata correlative with the Mancos Shale and Gallup Sandstone of central and northwest New Mexico (S. C. Hook, personal communication, 1978) (plate 3, in pocket). Within the Mancos, Hook also has recognized a medial sandstone unit thought to be correlative with the Tres Hermanos Sandstone Member in the Carthage area of Socorro County. According to Kottlowski and others (1956), a slight angular unconformity is present between the Yeso–San Andres and the overlying Sarten–Dakota in the Love Ranch area. A somewhat greater angular discordance is present, but not obvious at any one outcrop, between the Mancos or Gallup strata and overlying fanglomerate of the Love Ranch Formation (lower Tertiary). South of the Bear Peak fold and thrust zone, Cretaceous strata were completely eroded from the map area in early Tertiary time. The closest outcrops to the south are those in the El Paso area.

Sarten–Dakota Sandstone

No attempt was made to distinguish between Sarten Sandstone and Dakota Sandstone on the geologic map (sheet 1, in pocket). Near Love Ranch, the two formations together are approximately 260 ft thick, probably mostly Sarten according to S. C. Hook (personal communication, 1978). A group of gray, resistant, crossbedded quartzite beds near the middle of the section conveniently divides it into upper and lower parts. Below the quartzite, 95 ft of soft, brown, yellow, or gray sandstone and interbedded black shale is exposed. At the base of the unit, a discontinuous chert-pebble conglomerate overlies the Yeso–San Andres, and 15-20 ft above this base a coquina contains pelecypods of Albian age (S. C. Hook, personal communication, 1978). Above the resistant quartzites are approximately 100 ft of poorly exposed, soft, platy, nodular sandstone with interbedded, ledge-forming sandstone. The uppermost of these yellow-, light-gray-, and greenish-gray-weathering strata may be Dakota beds. No contact with shaly beds of the overlying Mancos Shale was seen, but the general impression is one of conformity; however, Kottlowski and others (1956) report a disconformable contact between the Dakota and the Mancos.

The Dakota Sandstone is of early Late Cretaceous age whereas Sarten strata are of late Early Cretaceous (Albian) and early Late Cretaceous (Cenomanian) age according to recent detailed regional studies by S. C. Hook (personal communication, 1978), based on fossils recovered from correlative beds in the Silver City–Deming region.

Strata correlative with Mancos Shale and Gallup Sandstone

Approximately 1,000 ft of greenish or gray shale, olive-brown sandstone, and massive tan crossbedded sandstone overlie the Dakota near Love Ranch. The lower 700 ft of the section is correlative with the Mancos Shale, though the strata here appear to be sandier than the well-known Mancos shales farther north. Near the middle of the Mancos, approximately 300 ft of olive-gray to olive-brown, medium-bedded sandstone splits the Mancos into lower and upper shale units. The sandstone, which contains abundant concretions and (locally) petrified wood, has been correlated with the Tres

Hermanos Sandstone Member of the Mancos by S. C. Hook (personal communication, 1978). The upper tongue of the Mancos, above the Tres Hermanos, contains locally abundant pelecypods and ammonites; collections made by Bachman and Myers (1969) and identified by W. Cobban (personal communication, 1960) indicate an early Late Cretaceous (late Turonian) age for the upper Mancos.

The upper tongue of the Mancos grades up into approximately 270 ft of massive, well-sorted, parallel-bedded or crossbedded, tan sandstone and interbedded shale that clearly represent a regressive beach or shallow offshore deposit. The sandstones probably are correlative with the regressive Gallup Sandstone of northwest and central New Mexico according to Hook (personal communication, 1978), but it is not certain whether 100 ft of green shale at the top of the unit is an intra-Gallup shale or another Mancos tongue. The top of the Cretaceous sequence is limited by a major erosion surface on which Love Ranch fanglomerates were deposited in early Tertiary time.

Summary of Precambrian, Paleozoic, and Mesozoic history

Detailed interpretation of geologic events during the Precambrian is impossible because of the depth of erosion, the degree of metamorphism, and the extent to which the metamorphic rocks are intruded by huge batholiths (see Condie and Budding, 1979, for best discussion of regional Precambrian geology in south-central New Mexico). Nevertheless, it is clear that the granitic and metamorphic rocks in the Organ–southern San Andres area represent the deeply eroded roots of an ancient mountain or rift system, formed 1.3-1.4 b.y. ago (Condie and Budding, 1979). The gneisses and schists, seen now as roof pendants in the Precambrian batholith, probably originated as sedimentary rocks formed in some arc-related basin or rift, perhaps hundreds of millions of years before they were metamorphosed and intruded by granitic batholiths as part of the mountain-building process. Much later in the Precambrian the region underwent extension in a southeast-northwest direction and swarms of diorite-diabase dikes were intruded into the resulting northeast-trending fractures. The last few tens or hundreds of millions of years of Precambrian time saw erosion of the rifts or mountain ranges down to their roots and the formation of a broad erosion surface with remarkably little relief. Across this extensive flat surface the early Paleozoic seas spread for the first time.

Late Cambrian and Early Ordovician seas transgressed eastward or northeastward across the Organ–San Andres area. Nearshore and shallow offshore deposits at the eastern edge of the sea are represented by the Bliss Sandstone, which becomes younger eastward. As the shorelines shifted beyond the south-central New Mexico area, tidal to shallow-water shelf carbonates accumulated transitionally on top of the Bliss to form the El Paso Group. Most of these strata were completely dolomitized, probably before overlying Montoya beds were deposited.

In Middle Ordovician time, southern New Mexico was gently uplifted and El Paso and Bliss strata were tilted south perhaps 10 ft per mi (Bachman and Myers, 1969). Erosion beveled the edges of El Paso strata, resulting in a regional thinning from south to north. Across this beveled surface, shallow seas spread again in Middle to Late Ordovician time to deposit the Cable Canyon Sandstone in advance of the rest of the Montoya carbonates. Dolomitization probably accompanied deposition of the carbonates, suggesting a very warm, shallow, saline marine environment, perhaps in an arid climate. Again the region was uplifted and gently tilted southward, so that Montoya strata were truncated by erosion in a manner similar to the earlier beveling of El Paso beds. The land lay above sea level until Middle Silurian time, when the Fusselman Dolomite was deposited in shallow-marine waters on eroded Montoya beds. Like the previous formations, the Fusselman was quickly dolomitized. Southward tilting and erosion were repeated once again during the Late Silurian and Early Devonian, this time producing a widespread, flat erosion surface across south-central New Mexico that truncated successively older strata from south to north across the region.

The return of a marine environment to south-central New Mexico in Middle and Late Devonian time was accompanied by a major change in the character of sedimentation. Unlike earlier Paleozoic deposits, those of the Devonian are silty or clayey and appear to have formed in shallow seas where marine water was restricted in its movement. Consequently most of the Devonian strata—the Percha Shale—are black and nonfossiliferous and contain pyrite, the product of anaerobic bottom conditions. Less restricted conditions from time to time are recorded by a few limestone beds containing fossil debris, as in parts of the Canutillo and basal Percha sequence.

In most places in the Organ–San Andres area, Devonian shale appears to grade into limestone of Mississippian age, and the fossiliferous Caballero limestones generally record that transition. At any rate, by Early Mississippian time the disagreeable Devonian seas were gradually replaced by shallow, warm, marine waters that teemed with life. Much of the Lake Valley Formation from Bishop Cap northward contains rocks interpreted to be well-winnowed accumulations of crinoid debris, perhaps banks, submarine dunes, or mounds, separated by stretches of calcareous mud, in and on which hosts of brachiopods, bryozoans, corals, crinoids, and other organisms lived and died. South of Bishop Cap, the Lake Valley Formation is missing, perhaps because of deepening of the Lake Valley seas into a broad basin, in which little or no sediment accumulated (Wilson, 1975). This basin may have been a precursor to the deep, starved basin that developed in middle and Late Mississippian time as far north as the southern San Andres Mountains and in which the deep-marine deposits of black calcareous mud of the Las Cruces and Rancheria strata accumulated. From Bishop Cap northward, these basinal deposits buried a most irregular karst and channeled surface formed on the Lake Valley carbonates. Gradual withdrawal of the Rancheria seas southward in latest Mississippian time and shallowing of the water are recorded by the nearshore terrigenous clastic rocks, oolitic limestone, and abundantly fossiliferous rocks of the Helms Formation.

As the seas regressed southward in Late Mississippian time, previously deposited Mississippian strata were exposed and eroded so that Early Pennsylvanian beds formed by the next northward advance of the sea buried the erosion surface. This surface is evident as far south as Bishop Cap; however, near El Paso, which apparently marks the southernmost retreat of the Mississippian seas, the unconformity has not been recognized. In that region continuous deposition from Mississippian into Pennsylvanian time has been reported (Harbour, 1972). In the Caballo Mountain region, local uplift and erosion between Lake Valley and Pennsylvanian time has been documented by Kelley and Silver (1952).

From the El Paso area and from other regions, the Pennsylvanian seas spread across almost all of the New Mexico area, inundating the state and much of the continent. Marine conditions prevailed in the Las Cruces area for the next 55 m.y., at least into the middle Permian. Some important variations in sedimentation during that time are linked to local tectonic activity and to glaciation in the southern hemisphere.

Early and Middle Pennsylvanian rocks of the Lead Camp Limestone and La Tuna and Berino Formations indicate shallow, warm, normal marine conditions. The cyclical nature of the deposits probably reflects changes in sea level brought about by recurrent glaciation in the southern hemisphere. Occasional influxes of coarse arkosic sand, pebbles, and clay were derived from early stages of uplift of the Pedernal region almost 100 mi to the east (Kottlowski, 1965; Meyer, 1966). Late Pennsylvanian time saw the maturing of a broad, relatively rapidly subsiding basin, the Orogrande Basin, formed by downwarping of a large oval-shaped region to the west of the Pedernal uplift. The thick, cyclical, mostly clastic deposits of the Panther Seep Formation accumulated in the basin, with the infilling process approximately keeping pace with subsidence. Intertidal to supratidal conditions were common as indicated by mud cracks, ripple marks, stromatolites, local caliche and gypsum beds, and dolomitized limestone. Fluctuating water level again seems to explain the cyclical repetition of rock types, with coarser clastics forming during periods of low water and fine-grained clastics or laminated carbonate mud during higher stands of sea level (Wilson, 1957). An almost complete lack of marine fauna suggests that waters were either sediment laden and murky or restricted in circulation, or both.

Near the beginning of the Permian, the character of the Orogrande Basin changed. Subsidence apparently continued, judging from the relatively thick accumulation of Lower Permian sediment, but normal marine waters gradually returned and abundant faunas flourished, especially algae, fusulines, gastropods, and echinoids. Carbonate mud, some of it still very sandy or pebbly, formed over vast areas of southern New Mexico, later to be lithified into the Hueco Formation. Cyclical repetition of carbonate and terrigenous clastics reflected continuing glacial control of sea level in the southern hemisphere.

Uplift in northern New Mexico, southern Colorado, and southeastern Utah in Early Permian time produced a huge apron of sand, gravel, silt, and mud that was distributed southward across central New Mexico by innumerable streams. The flood of clastics—the Abo Formation—gradually pushed the edge of the Hueco sea southward, but the shoreline fluctuated back and forth across the southern San Andres area many times before it was finally displaced to a position somewhere near the southern end of the Organ Mountains. The shifting shoreline is revealed by the intertonguing of Abo red beds and Hueco Limestone in the northern Organ, San Andres, and Robledo Mountains. In middle Permian times the sea prevailed once again and marine waters spread across the state. Gypsiferous sand and silt, deposited in lagoons or in shallow, restricted basins in front of the advancing sea, formed the Yeso Formation, only to be buried by carbonate muds of the Yeso and the San Andres Formation that precipitated from the shallow, normal marine seas that followed.

If any Late Permian seas covered the south-central New Mexico area, their rock record is gone, eroded away during the vast amount of time between latest Permian and Early Cretaceous time. The same can be said for deposits of Triassic and Jurassic age, although marine Jurassic rocks have been reported from a deep drill hole 25 mi southwest of Las Cruces (Thompson and Bieberman, 1975). In general, most of the Las Cruces area appears to have been uplifted and to have undergone erosion throughout the Mesozoic until the latest part of Early Cretaceous time when shallow-marine seas spread across the Las Cruces area in two stages to deposit basal Cretaceous sandstones.

The Sarten and Dakota Sandstones are interpreted as beach and near-shore deposits associated with these marine transgressions whereas the overlying Mancos mudstone and shale represent the offshore facies that followed as the sea edge moved farther inland. The basal part of the Tres Hermanos Sandstone Member records a brief regression of the Mancos seas; upper Tres Hermanos and overlying marine Mancos beds reflect a second transgression. In detail, the shoreline shifted back and forth through the Love Ranch area several times. A major regression in Late Cretaceous time is indicated by the beach deposits of the Gallup Sandstone. Higher Cretaceous strata were eroded during the Laramide orogeny, a period of mountain building which ushered in the Tertiary Period.

The abundant sand, silt, and mud deposited in the Late Cretaceous seas in the Organ–San Andres area hint at the tectonic instability developing in areas to the west or southwest. The stability that characterized south-central New Mexico during the Paleozoic and Mesozoic ended abruptly after deposition of the Upper Cretaceous strata as the Laramide orogeny gained momentum in latest Cretaceous time and culminated in the early Tertiary. This orogeny is documented by fanglomerate beds of the Love Ranch Formation that were deposited both concurrently with and following the uplift and deep erosion of Laramide mountains. The orogeny also produced one of the major structural features of the San Andres–Organ–Franklin chain, the Bear Peak fold and thrust belt.

Laramide orogeny

Laramide tectonic setting

Most of south-central New Mexico lies adjacent to the Cordilleran orogenic belt of Drewes (1978; fig. 33), the New Mexico portion of which was described by Corbitt and Woodward (1973). In New Mexico and adjacent parts of Mexico the belt is distinguished by northwest-trending thrust faults and associated asymmetric or overturned folds of Laramide age, interpreted to be of regional extent. Many of these structures involve strata, particularly Cretaceous strata, of geosynclinal proportions deposited in extensive northwest-trending, back-arc basins at the southern edge of the continental craton. Along the northern margin of the orogenic belt in southwest New Mexico, Precambrian crystalline rocks were involved in the thrusting, at least locally; throughout the rest of the New Mexico–Chihuahua segment of the orogenic belt, thin-skinned deformation prevailed. Indeed, in much of Chihuahua, décollement on evaporite layers has been postulated (Gries and Haenggi, 1970). In contrast, the region to the north of the orogenic belt, including the Franklin–Organ–San Andres area, was part of the continental platform during the Cretaceous as well as during the rest of the Mesozoic and Paleozoic and was covered by a relatively thin veneer of sedimentary rocks. During the Laramide phase of the Cordilleran orogeny this region failed, together with the rest of the Cordilleran foreland from Wyoming southward, in a distinctive manner—by the formation of broad, basement-cored block uplifts flanked by monoclines or steeply dipping faults.

Fig. 34 shows the major known or inferred structural features that formed during the Laramide on the foreland region of south-central New Mexico. In most instances the full extent and geometry of the structures is unknown because of the masking effect of younger rocks and deformation. However, basement-cored uplifts, similar to those of the Colorado Plateau or to the lesser members of the central and southern Rockies, have been reconstructed in the area (Seager, 1975). These uplifts are associated with marginal, high-angle faults, monoclinal flexures, and local cascade folds (Kelley and Silver, 1952). Trends of the larger uplifts are hard to establish because large parts of them lie buried in grabens. The trends of small structures or short segments of large structures preserved in modern ranges may be indicative of the trends of major uplifts and basins in the area. Using these clues it appears that some west-northwest-trending, basement-cored uplifts and basins formed parallel to the Cordilleran orogenic belt on the southern part of the Cordilleran foreland. From fig. 34 it also is apparent that major north-trending uplifts and basins are interspersed with the more northwest-trending structures. In this respect, the region

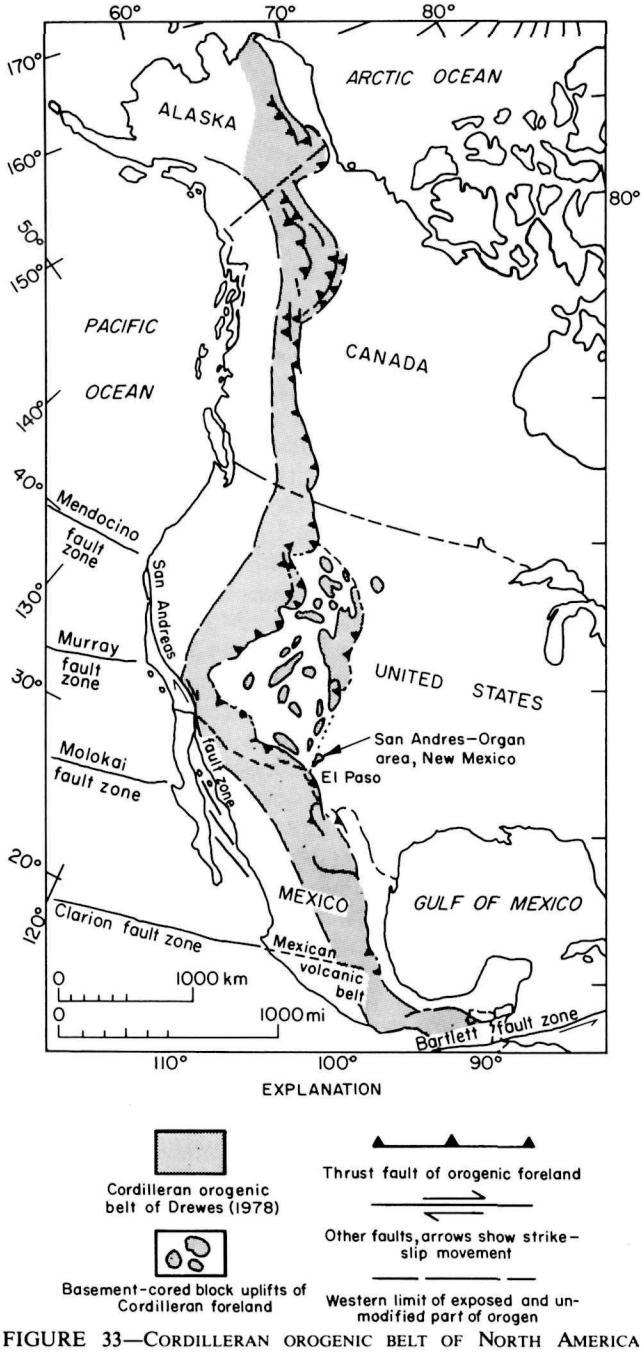


FIGURE 33—CORDILLERAN OROGENIC BELT OF NORTH AMERICA SHOWING RELATION WITH CORDILLERAN FORELAND AND SAN ANDRES–ORGAN AREA (after Drewes, 1978).

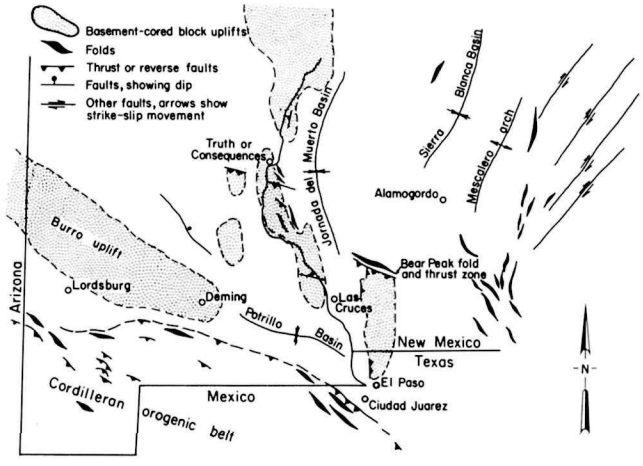
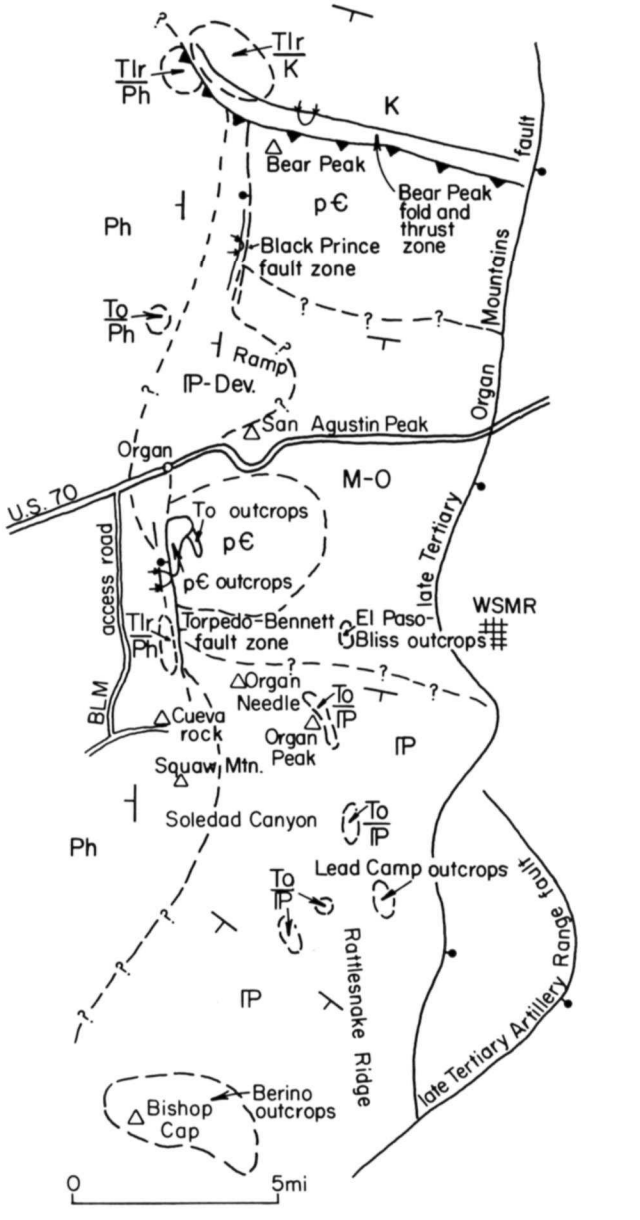


FIGURE 34—MAJOR LARAMIDE STRUCTURAL FEATURES OF SOUTH-CENTRAL NEW MEXICO.

appears to represent a tectonic transitional zone between the predominantly north-trending Laramide structures of northern New Mexico and Colorado and the northwest-trending structures of the Cordilleran orogenic belt. Laramide structures in the Organ and southern San Andres Mountains illustrate the blend of west-northwest- and north-trending structures especially well (fig. 34).



To — Orejon Andesite
Tlr — Love Ranch Formation
K — Cretaceous rocks
Ph — Hueco Formation
IP — Pennsylvanian rocks
M-O — Mississippian through Ordovician rocks
IP-D — Pennsylvanian through Devonian rocks
p€ Precambrian rocks
Tlr/Ph — indicates Love Ranch Formation overlies Hueco Formation

FIGURE 35—INTERPRETIVE GEOLOGIC MAP OF THE LARAMIDE UPLIFT IN THE ORGAN MOUNTAINS AREA just before its burial by andesitic rocks in late Eocene time; most contacts are highly speculative and the whole map is based on only nine outcrops of the pre-late Eocene unconformity, and on a few other key outcrops.

Structural features

The main structural features associated with a large Laramide block uplift in the Organ–southern San Andres area are the Bear Peak thrust and fold belt and the Torpedo–Bennett fault zone. The Black Prince fault zone may also have been initiated in Laramide time, but this is far from certain; the fault zone could be entirely of late Tertiary age (see discussion of Black Prince fault zone). These structures, together with structural ramps between them, form the northern and western boundaries of the Laramide uplift. The eastern side of the uplift now lies buried in the Tularosa Basin, having been cut off and dropped down by movement on the Organ Mountains fault in late Tertiary time. The southern flank appears to have been formed by middle Paleozoic rocks which probably dipped gently south and westward in early Tertiary time. The top of the uplift has been so modified by erosion and intrusion that its character is hard to define, but a few xenoliths or roof pendants of Paleozoic, Precambrian, and lower Tertiary rocks in the Organ batholith can be used to estimate the general depth of erosion across the summit of the uplift in Laramide time. A very speculative geologic map showing the Laramide uplift just before burial by upper Eocene andesite is shown in fig. 35.

Bear Peak thrust and fold belt

The Bear Peak thrust and fold belt, approximately 1 mi wide, trends west-northwest obliquely across the southern San Andres Mountains, turning northwest at its westernmost exposure west of Love Ranch. The zone is the major feature along which the Laramide uplift was raised. Cross sections 1–8 on sheet 3 (in pocket) illustrate the general structure of the zone (figs. 36 and 37). The structure is relatively simple, consisting of a large block of Precambrian and Paleozoic rock, raised by movement along a zone of west-northwest-trending reverse faults. The major reverse fault in this zone, which places Precambrian rocks against rocks as young as the Hueco Limestone, dips approximately 60 degrees south in surface exposures. Minimum stratigraphic separation is nearly 5,000 ft. At Bear Peak the dip separation is calculated from cross section 4 (sheet 3, in pocket) to be 11,000 ft.

The downthrown block, on the north side of the

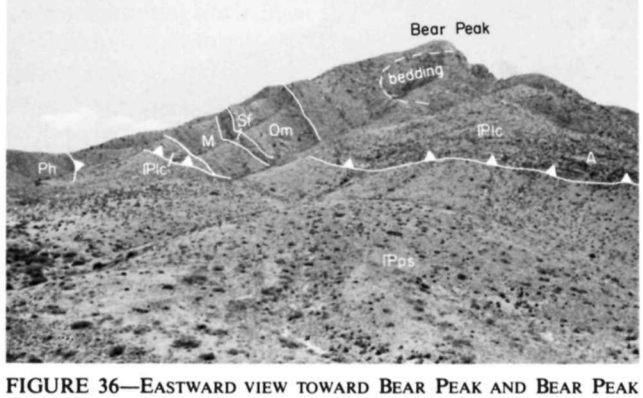


FIGURE 36—EASTWARD VIEW TOWARD BEAR PEAK AND BEAR PEAK FOLD AND THRUST ZONE. **Oe**—El Paso Group; **Om**—Montoya Group; **Sf**—Fusselman Dolomite; **M**—Mississippian formations and Percha Shale; **IPlc**—Lead Camp Limestone; **IPps**—Panther Seep Formation; **Ph**—Hueco-Abo beds.

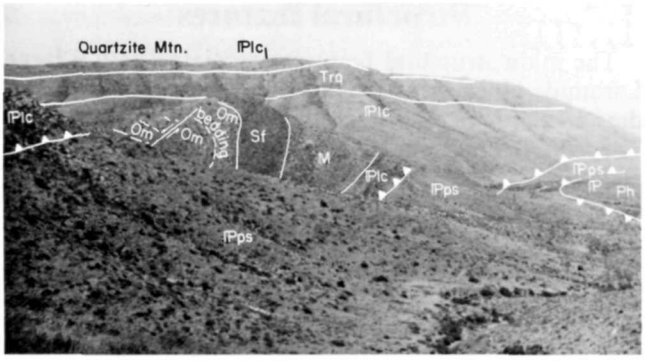


FIGURE 37—WESTWARD VIEW (FROM NEAR POINT A IN FIG. 36) LOOKING ALONG BEAR PEAK FOLD AND THRUST ZONE TOWARD QUARTZITE MOUNTAIN. **Om**—Montoya Dolomite; **M**—Mississippian formations and Percha Shale; **PPlc**—Lead Camp Limestone; **PPps**—Panther Seep Formation; **Trq**—rhyolite of Quartzite Mountain; **Ph**—Hueco-Abo beds.

thrust and fold zone, consists of a sharply overturned syncline whose axial trace parallels the main reverse fault zone (fig. 38). The average dip of overturned beds is 60-70 degrees south, but locally beds dip only 15 degrees south, having been rotated through 165 degrees. Thrust faults have tectonically thinned formations in the overturned limb, especially incompetent formations such as the Panther Seep and the Percha Shale. Some of the thrusts are associated with relatively minor tear faults that offset the overturned limb, such as those south of Love Ranch. Thrust faulting is also locally present in the upright limb of the fold at Black Mountain, resulting in repetition of Paleozoic strata there (cross sections 5 and 8, sheet 2, in pocket). All of these thrust faults appear to terminate at the main, steeper-dipping reverse fault at the Precambrian contact. Thus, the thrust faults seem to be a product of squeezing of the syncline by the uplifted block of Precambrian granite.

High- and low-angle normal faults of late Tertiary age, which trend northerly, intersect the Bear Peak fold and thrust zone between Bear Peak and the eastern edge of the range. The faults break the Laramide structure

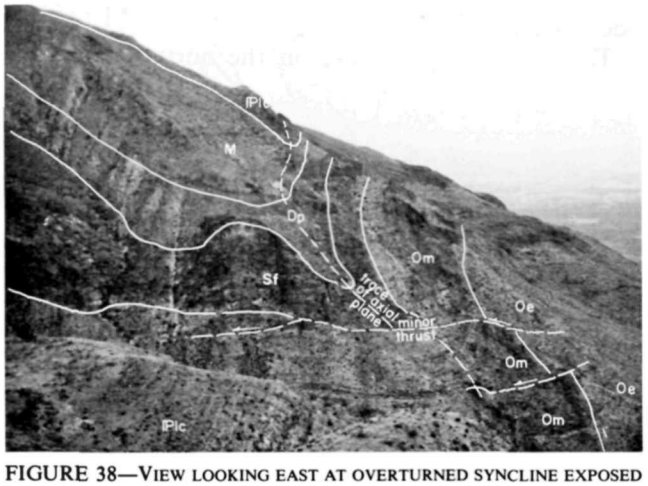


FIGURE 38—VIEW LOOKING EAST AT OVERTURNED SYNCLINE EXPOSED ON SOUTHERN SLOPES OF BLACK MOUNTAIN. **Oe**—El Paso Group; **Om**—Montoya Group; **Sf**—Fusselman Dolomite; **Dp**—Percha Shale; **M**—Mississippian rocks; **PPlc**—Lead Camp Limestone; Precambrian is thrust against El Paso Group just off picture to the right.

into segments, thereby adding complexity to an otherwise comparatively simple structure. Right-slip separation of approximately 3,500 ft was measured across the Deer fault, with lesser but substantial offset across the Rock House, Black Mountain, and other late Tertiary faults. Fold axes, as well as faults and bedding in the Laramide zone, are offset.

From Bear Peak to the eastern edge of the range Paleozoic strata have been completely removed from the uplifted Precambrian block. The attitude of the Paleozoic cover rocks on the summit of the uplift is therefore speculative. However, a gentle south or southwest dip of the whole uplift is suggested by the fact that at the southern end of the Organs, erosion had only proceeded into Pennsylvanian strata by late Eocene; in the northern part of the range, evidence presented in the next section suggests erosion into the Precambrian.

West of Bear Peak, Paleozoic rocks are still preserved on the upthrown side of the fold and thrust zone, but they have been so disturbed by late Tertiary block faulting and possible rotation that their Laramide attitude is hard to interpret. However, near the boundary reverse fault, the Paleozoic strata on the upthrown side of the fault bend down abruptly and become overturned as they cross and are offset by faults in the zone (fig. 37; section 4, sheet 2, in pocket). The overturned anticlinal axis is parallel to the reverse fault zone and clearly is related to it (cross section 4, sheet 2, in pocket). However, there is little evidence that the deformed zone represents an overturned, thrust-faulted anticline in which the basement participated during folding. Rather, the common overturned limb of the anticline in the upthrown block and the syncline in the downthrown block is interpreted to be the product of passive draping of strata across the faulted edge of the Precambrian block. We will return to this analysis in the section on mechanics of Laramide folding.

Torpedo-Bennett fault zone

The Torpedo-Bennett fault zone is a north-trending zone of high-angle normal and reverse faults exposed from north of Organ to south of Baylor Canyon along the western edge of the Organ Mountains. Evidence cited below indicates that the fault zone is older than middle Tertiary. On the basis of its geometric similarity with the Bear Peak fold and thrust zone, the fault zone is thought to have formed in a similar manner and is presumed to be of Laramide age. As shown in fig. 35, the fault zone is interpreted as marking part of the western edge of the Laramide uplift.

Between Baylor and Blair Canyons, the fault zone separates a raised block of Precambrian rocks on the east from vertical to overturned Paleozoic strata as young as the Hueco Formation, inferred to have been draped over the edge of the Precambrian block (cross section G-G′, sheet 2, in pocket). Maximum stratigraphic separation across the fault zone is approximately 6,000 ft, and the dip separation is approximately 8,000 ft near the Stevenson-Bennett mine. Closely spaced, anastomosing and branching faults, some dipping east and others west, compose the zone.

Unlike the Bear Peak fold and thrust zone, the Torpedo-Bennett fault zone is mineralized and intruded

by the Organ batholith. In fact, from north of the Memphis mine southward to Blair Canyon and from Baylor Canyon southward, the western edge of the batholith closely follows the fault zone, apparently being localized by it. Between Blair and Baylor Canyons the batholith contact makes an important eastward embayment and, as noted above, it is in this area that Precambrian rocks form the eastern side of the fault zone. The roughly linear batholith contact, some 4.5 mi long, was regarded by Dunham (1935) and Glover (1975) as a postbatholith fault. Although brecciation of the monzonite near the Torpedo mine may indicate some late-stage movement of the batholith, details of the batholith contact and drilling on the Torpedo property (described under mineral deposits) prove that the contact is intrusive along its whole length. At the same time, however, it is clear that the edge of the intrusive occupies a preexisting fault zone.

Evidence confirming the intrusive nature of the batholith contact with the Torpedo–Bennett fault zone can be seen just north of Baylor Canyon. Precambrian rocks form the hanging wall of the fault zone in this area. At one locality an apophyse of the batholith cuts successively across Precambrian granite, a major reverse fault in the fault zone, and folded Lead Camp Limestone west of the fault zone. The batholith has not been deformed by the fault zone. Besides showing the intrusive nature of the contact, these relations indicate that the faulting is older than the batholith (32.8 m.y.) and mostly likely is related to Laramide uplift.

Except for the block between Baylor and Blair Canyons, most of the Precambrian core of the Laramide uplift that is adjacent to the Torpedo–Bennett fault zone was assimilated or displaced by the Organ batholith. Several small xenoliths or roof pendants remain, however, and some contain lower Paleozoic as well as Precambrian rocks. A few larger remnants of upper Eocene andesite also are roof pendants or xenoliths, but no remnants of middle to upper Paleozoic strata have been found east of the Torpedo–Bennett fault. These facts are interpreted to mean that upper Eocene rocks were deposited on Precambrian and lower Paleozoic strata in the core area of the Laramide uplift, and that these rocks, together with volcanics related to the batholith, subsequently formed the roof of the Organ batholith.

Black Prince fault zone

The Black Prince fault zone (cross sections B–E, sheet 1, in pocket; fig. 35) forms the western edge of the large raised block of Precambrian granite between Bear Peak and the Black Prince mine. This fault zone trends northerly, parallel with the Laramide Torpedo–Bennett fault, but it also parallels many late Tertiary faults in the area. At Bear Canyon the fault zone intersects but does not appear to offset the Bear Peak fold and thrust belt. The fault zone's continuation north of the Bear Peak fold and thrust belt has not been identified with certainty; it may be one of several simple faults, none of which have displacements nor complexity comparable to the Black Prince fault zone. At its southern end, the fault zone terminates where it intersects the Quartzite Mountain fault, which is downthrown to the east, opposite the Black Prince fault. The north-trending graben between these faults is a major structural feature between Bear Canyon and the Hilltop mine, whose origin is considered in the section on late Tertiary deformation.

Among the faults of the region, the Black Prince fault zone is unusual in its degree of complexity. It comprises an intricate network of fault slices locally ⅓ mi wide, which contrasts with the relative simplicity of late Tertiary faults. At its southern end near the Black Prince mine, the zone comprises reverse faults, dipping approximately 70 degrees east beneath Precambrian granite. In this area, Paleozoic strata within as well as adjacent to the fault zone are vertical or overturned, and some have been offset by low-angle, east-dipping thrusts, which also are part of the fault zone. Northward, however, the fault zone passes into a zone of steep normal faults; this is accompanied by a decrease in dip of adjacent Paleozoic strata. There is no evidence for strike-slip movement. Maximum stratigraphic separation along the faults is approximately 5,000 ft.

The fault zone cannot be dated directly. It displaced rhyolite of Quartzite Mountain which, though undated, is presumably of middle Tertiary age and related to the Organ batholith. On the other hand, the fault zone is geometrically similar to the Laramide Torpedo–Bennett fault zone; because of its complexity, steepness of dip, and local evidence of compression, the Black Prince fault zone is dissimilar to late Tertiary faults in the region. From these facts it seems possible that the fault zone was initially formed in Laramide time along the western margin of the major uplift previously described (fig. 35). Subsequent movement in late Tertiary time may account for offset of the rhyolite of Quartzite Mountain, the unusual complexity of the fault zone, and the fact that possible continuations of the fault zone north of the Bear Peak fold and thrust belt are simple fractures with reduced throw.

Mechanics of Laramide uplift

Structures in the Bear Peak fold and thrust zone, the Torpedo–Bennett fault zone, and probably the Black Prince fault zone, together with unconformities, may be interpreted to indicate that Laramide deformation in the region involved mostly vertical uplift and relatively minor crustal shortening within a regional compressive stress field. There is evidence neither for strike-slip motion along the faults bounding the uplifted block of Precambrian granite nor for flattening of faults in the Bear Peak zone with depth; either or both would indicate substantial horizontal slip. Consequently, an interpretation of dominantly vertical movement and only minor crustal shortening seems warranted. Because the major fault in the Bear Peak zone is reverse, some crustal shortening clearly was involved; this may have been responsible for squeezing of the syncline on the northern side of the fault and for the generation of low-angle thrusts in its limbs. For the most part, however, the sedimentary cover rocks are viewed as having folded passively by draping over the faulted edges of the uplifted block or by forming structural ramps between faults (figs. 35 and 39). The draped strata were subsequently compressed and thrust-faulted as uplift continued.

Large folds whose shape and trend are governed by the shape and trend of an uplifted, perhaps tilted, block of basement belong to a class of folds termed forced

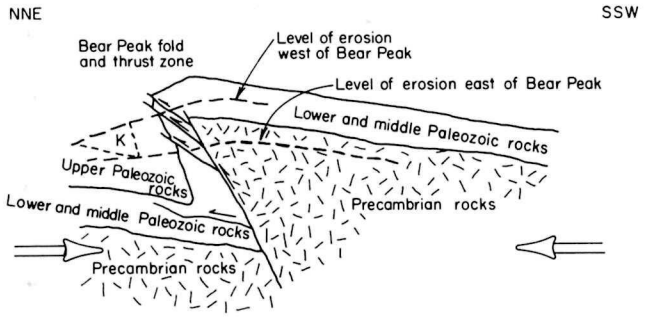


FIGURE 39—DIAGRAMMATIC CROSS SECTION THROUGH THE LARAMIDE BLOCK UPLIFT IN THE SOUTHERN SAN ANDRES–ORGAN MOUNTAIN AREA showing draping of Paleozoic cover rocks over the faulted edge of uplifted Precambrian rock. Note lesser thrusts in draped beds; horizontal arrows show inferred compression that raised the block of Precambrian rock.

folds (Stearns, 1971, 1978). Such folds appear to characterize most of the Laramide uplifts in the Colorado–Wyoming region and on the Colorado Plateau (Stearns, 1978; Davis, 1978). The Laramide uplift in the Organ area is of a similar style, although by virtue of its asymmetry, it perhaps exhibits more evidence of a compressional origin than most uplifts, and it has been greatly modified by younger events.

Origin

Uplift of the Organ–San Andres Laramide structure appears to have resulted from compression from the south-southwest. This is based on the fact that the Bear Peak fold and thrust zone, which forms the most important structural boundary of the uplift, trends west-northwest and is strongly asymmetrical to the north-northeast (fig. 39; sections 1-7, plate 3, in pocket). All the structures in the fold and fault zone indicate a component of motion to the north-northeast, although vertical movement on the Precambrian block was apparently dominant. Drape folds and vertically uplifted blocks similar to the Bear Peak structure have been produced by compression in model experiments (Davis, 1978; Logan and others, 1978).

Fig. 34 illustrates that the Bear Peak fold and thrust belt is parallel to the Cordilleran orogenic belt of southwest New Mexico. Structures in the two zones are coeval (Corbitt and Woodward, 1973) and both indicate compression directed north-northeast, so it seems likely that both were formed in the same stress field. In fact, all the Laramide structures on the southern New Mexico foreland, including the more northerly trending ones, are coeval with those of the orogenic belt and must somehow be related. Trends, asymmetry, and structural styles of deformed rocks both on the foreland and in the orogenic belt seem consistent with the idea that both are products of northeast- to north-northeast-directed compression generated by subduction of the Farallon plate as reconstructed by Coney (1976, 1978) and Dickinson and Snyder (1978) and supported in Arizona by the study of Rehrig and Heidrick (1976). In this hypothesis, thick, back-arc basinal deposits (mostly Cretaceous in age) in southwest New Mexico and Chihuahua could be deformed in a thin-skinned style, related in part to evaporites. More rigid platform rocks to the north and northeast might yield simultaneously by uplift of fault-bounded, basement-cored uplifts, some trending north-northwest and some more nearly north. As pointed out for the monoclines of the Colorado Plateau by Davis (1978), such uplifts are a natural consequence of shortening of the crust by small amounts by persistent compression.

Love Ranch Formation

Throughout south-central New Mexico, Laramide structures were buried by deposits ranging in age from latest Cretaceous to Eocene. The angular unconformity between the deformed rocks and the strata that buried them is striking in many places and has long been known (Kelley and Silver, 1952). Locally, as in the central parts of the Jornada del Muerto Basin or Potrillo Basin (Uphoff, 1978), great thicknesses of lower Tertiary strata, derived from erosion of adjacent Laramide uplifts, are preserved (fig. 34). One of the best exposed and most instructive of these deposits is preserved in the downwarped region adjacent to the Bear Peak fold and thrust zone.

A thickness of more than 2,000 ft of boulder conglomerate and interbedded red sandstone, siltstone, and mudstone overlies Cretaceous and Permian beds on a pronounced unconformity in the Love Ranch area (fig. 3). These rocks, named Love Ranch Formation by Kottlowski and others (1956), were formed through erosion of the broad Laramide uplift described above. The formation represents a complex of alluvial-fan deposits whose clasts record erosional unroofing of the Paleozoic cover from the fault block as it rose, and whose internal unconformities and structures document several stages of uplift of the block. Much thinner deposits of the Love Ranch Formation along the western and southern edges of the Organ Mountains are interpreted as pediment veneers on the flanks of the Laramide uplift. These deposits' clast content and the Paleozoic rocks on which they were deposited provide evidence for the depth of erosion, and hence amount of uplift in those areas.

The Love Ranch Formation was informally divided into upper and lower parts in the area near Love Ranch. Both parts are almost identical lithologically, but along the southern edge of the hill west of Love Ranch (sec. 25) a major angular unconformity separates them. The lower member is folded into a sharply overturned syncline (part of the Bear Peak fold and thrust zone) whereas the upper member overlaps the eroded overturned limb of the fold, a major thrust fault, and overturned Abo–Hueco beds in the upthrust block. The upper member has also been gently folded about an axis parallel to the fold and fault belt. Within a short distance north of the unconformity, bedding in upper and lower members is parallel and the two units appear to be conformable. Each member is at least 1,000 ft thick (sections A-A′ and 1, sheets 2 and 3, in pocket).

Approximately equal amounts of coarse conglomerate and reddish-brown sandstone and siltstone or mudstone compose the lower member. Kottlowski and others (1956) report a thin lens of andesite-tuff breccia, but it is not clear which part of the section contains it. The conglomerate beds are most conspicuous because they form resistant ledges. Boulders as large as 3 ft in

diameter are common near the base of the unit, but clast size appears to decrease irregularly upward. Pebbles, cobbles, and boulders are generally subrounded to well rounded. They are in a matrix of poorly sorted hematitic sand and are cemented by calcite. The sand comprises at least as much calcite as quartz, rock fragments, and chert. All the clasts were derived from Cretaceous through lower Permian (lower Hueco) beds, but the lower member of the Love Ranch overlies only Cretaceous strata ranging from Gallup Sandstone well down into Mancos Shale.

Lithology of the upper member is virtually the same as that of the lower member with two notable differences. First, the size of clasts in the upper member does not change noticeably from lower to upper parts of the member. Largest clasts in uppermost exposures are as large as those at the base, 1 ft or more in diameter. Secondly, conspicuous beds of fresh-water limestone up to 100 ft thick are interbedded in the upper member. These beds, previously mapped as landslide blocks of Hueco Limestone, are largely burrowed gray micrite, in many places containing pisolites, algal filaments, and spongy-textured travertine. No marine invertebrates are present and there is no brecciation of the limestone, even at the base where it lies undisturbed on conglomerate beds. Furthermore, some of the limestone fills cracks and cements pebbles in the underlying conglomerate. The limestones are interpreted to be the deposits of warm springs and associated small lakes. Similar deposits have been found within Love Ranch beds at San Diego Mountain (Seager and others, 1971).

Greenish-gray, calcareous, arkosic sandstone, approximately 30 ft thick, overlies the Love Ranch Formation west of Love Ranch. The base appears to be an important disconformity judging from the drastic lithologic change from bouldery Love Ranch to the fine- to medium-grained sandstone. The top of the unit is limited by an intrusive of monzonite porphyry. Poorly sorted, angular clasts of feldspar, quartz, and siliceous rock fragments compose the sandstone. It resembles many of the beds in the McRae Formation (Kelley and Silver, 1952; Bushnell, 1953, 1955), but the correlation is very tenuous and the inferred early Tertiary age of the sandstone is uncertain. The sandstone's significance lies in the interpretation that it documents exposure of the Precambrian granitic core of the Laramide uplift, erosion of which provided the granitic minerals found in the rock.

In the western and southern parts of the Organ Mountains, the Love Ranch Formation is thin and discontinuous, probably because it was deposited on the flanks of the Laramide uplift rather than in downwarped areas. Between the Stevenson-Bennett and Modoc mines, Love Ranch conglomerate only a few feet thick is angularly unconformable above Hueco and Abo beds. Clasts are mostly rounded Abo and Hueco boulders and cobbles, but there are a few fragments of lower Paleozoic rocks. Basal beds of the overlying Orejon Andesite contain scattered pieces of gneiss, schist, and granite as well, but whether they were derived from erosion of exposed Precambrian rocks or brought up by explosive volcanism is uncertain. Beds correlative with the Love Ranch overlie Middle Pennsylvanian rocks in Boulder Canyon at the south end of the Organ Range. Angular clasts, here mostly cobble size, consist largely of Pennsylvanian rocks.

Age and correlation

The Love Ranch Formation is probably Eocene and Paleocene in age. The formation has not been directly dated by radiometric techniques or by fossils, but current studies show that in the central parts of Laramide basins, such as the Jornada del Muerto Basin, the Love Ranch intertongues with middle and upper parts of the McRae Formation and with lower parts of the Palm Park Formation. Basal beds of the McRae are latest Cretaceous in age (Kelley and Silver, 1952; Bushnell, 1953), and the Palm Park Formation is mostly of late Eocene age (Kottlowski and others, 1969; Seager and others, 1975). Thus, it seems likely that near the centers of subsiding Laramide basins, such as the central Jornada del Muerto, the interfingering Love Ranch and McRae and Palm Park strata record nearly continuous deposition throughout the Paleocene and through most of the Eocene. Along Laramide uplift margins, however, only uppermost Love Ranch beds have been found. These deposits are usually thin and interfinger with the basal part of the Palm Park Formation that overlies eroded pre-Tertiary rocks. They are among the youngest Love Ranch beds in the region (late Eocene in age) and are interpreted as deposits—mostly veneers on pediments—that overlapped the edges of local Laramide uplifts.

In the southern San Andres Mountains, the thick Love Ranch fanglomerates were deposited in a locally downwarped basin but, relative to the center of the Jornada del Muerto, in a regionally uplifted area. Consequently, Love Ranch deposition seems to have started earlier near the center of the Jornada del Muerto than at Love Ranch; basal Love Ranch conglomerates near Love Ranch probably are not the oldest in the region, but they are probably considerably older than any of the thin, discontinuous Love Ranch conglomerates exposed on eroded Laramide uplifts elsewhere in south-central New Mexico. The lower part of the Love Ranch in the map area probably is Paleocene to early Eocene in age, while upper parts may range into the late Eocene.

Interpretation of Laramide history

The diagrams in fig. 40 illustrate a possible sequential development of the Laramide uplift and downwarp, and the relation of these to the Love Ranch Formation. Initial uplift of the southern San Andres–Organ region caused erosion of the upper parts of the Cretaceous section and deposition of detritus in the Jornada del Muerto Basin to form oldest Love Ranch fans (fig. 40a). As uplift accelerated and became localized along the Bear Peak fold and thrust zone, Love Ranch fans gradually buried eroded Cretaceous beds on the downwarped side of the structure (fig. 40b). Uplift continued and the Love Ranch fans were sharply folded, thus becoming part of the fold and thrust belt (fig. 40c). Continuing erosion produced still more Love Ranch fan material, which sequentially buried the deformed older fan deposits, a major upthrust, and at least part of the upthrust block. Spring activity on the fan surface accompanied deposition of gravels during this stage (fig. 40c). Finally, the Love Ranch beds were again gently folded by

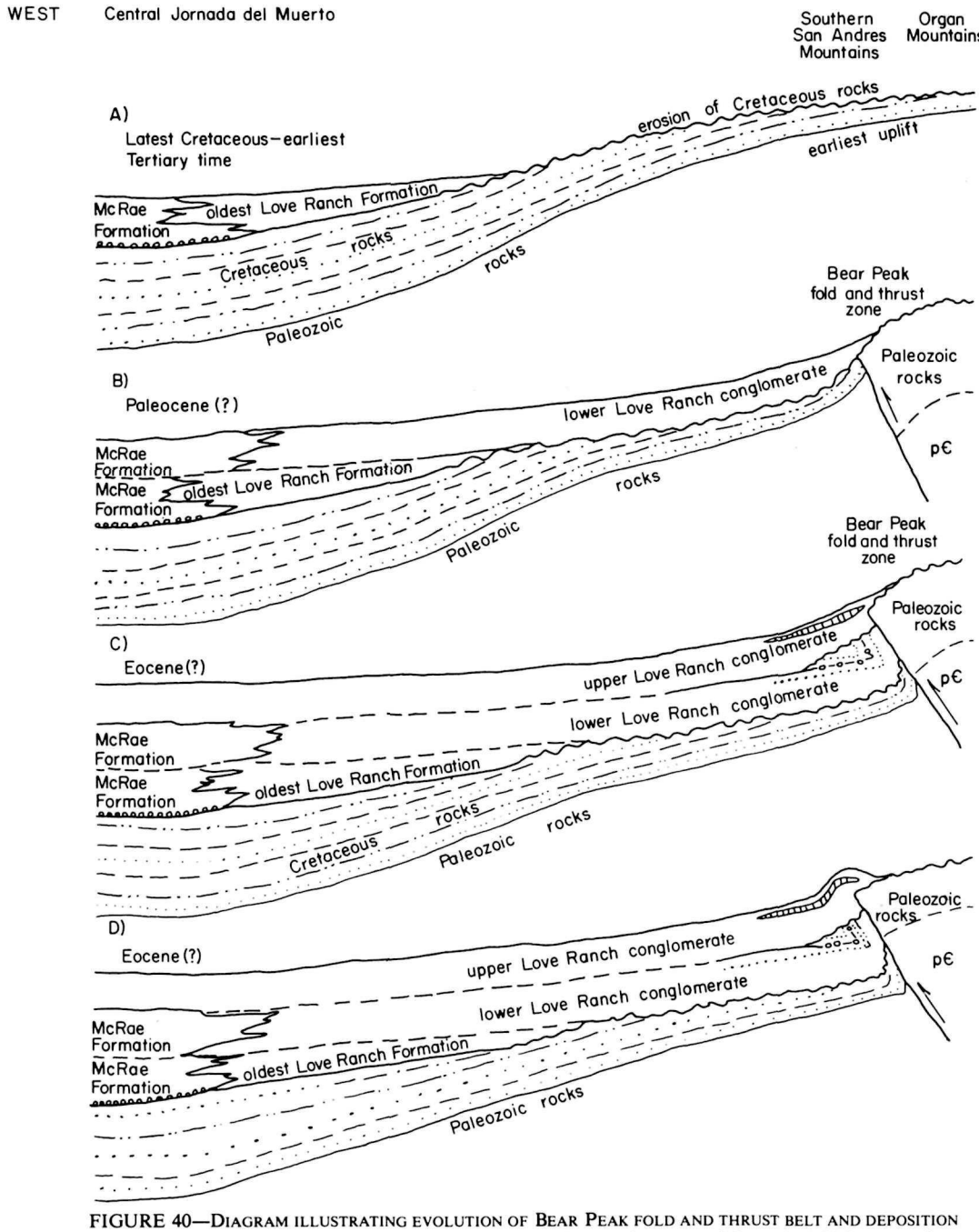


FIGURE 40—Diagram illustrating evolution of Bear Peak fold and thrust belt and deposition of Love Ranch–McRae Formations in the southern San Andres–central Jornada del Muerto region; see text for explantion.

relatively minor uplift along the Bear Peak thrust zone (fig. 40d).

During most of this history Abo–Hueco beds were being eroded from the summit of the uplift. Eventual exposure of the Precambrian is suggested by the arkosic sandstone that unconformably overlies the Love Ranch, and by the fact that a few miles south, near the Stevenson–Bennett mine and Baylor Canyon, upper Eocene andesitic rocks appear to have been deposited on lower Paleozoic and Precambrian rocks. However, no deposit records erosion of the thousands of feet of lower and middle Paleozoic strata, except for occasional pebbles in Love Ranch near the Modoc mine. Much, if not all, of the deeply and irregularly eroded uplift was buried by andesitic flows and volcaniclastic rocks of the Orejon Andesite during the late Eocene.

Eocene or Oligocene andesitic volcanism

A great volume and thickness of lava flows and tuffs eventually buried the Laramide deposits and structures of the Organ Mountains area. The Organ batholith, the source of most of the volcanic rocks, subsequently intruded its own volcanic covering. These igneous rocks document a long period during the middle Tertiary when volcanism rather than uplift, faulting, or folding shaped the landscape of the Organ area as well as the rest of south-central New Mexico. The period of volcanic activity lasted from late Eocene to Miocene time and peaked in the Oligocene. Except perhaps for the Miocene volcanic activity, the igneous activity was a product of continued subduction of the Farallon plate beneath the southwestern states (Lipman and others, 1972; Coney and Reynolds, 1977; Dickinson and Snyder, 1978).

In parts of the Organ Mountains, the middle Tertiary volcanic rocks exceed 2 mi in thickness. They were emplaced in two stages, one in the late Eocene or early Oligocene and one, 4-10 m.y. later, during the middle of the Oligocene. The upper 9,000 ft of the volcanic section are mostly rhyolitic; they were erupted during the Oligocene stage. They are comagmatic with the Organ batholith and accumulated in a major caldera—the Organ caldera. These rocks and structures are the topic of the next section of this book. The lower 2,000 ft of volcanic rocks are mostly andesitic to dacitic. They buried the Laramide structures and deposits and formed the roof rock for most of the Organ batholith. This lower part of the volcanic section was named Orejon Andesite by Dunham (1935).

From the Modoc mine southeastward to Boulder Canyon, a distance of approximately 6 mi, the Orejon crops out as a comparatively narrow band above the Organ batholith (geologic map, sheet 1, in pocket). The intrusive contact between them, while steep owing to the forceful rise of the batholith or subsidence of the volcanics, is concordant for the most part. Plainly, the Orejon formed the lower part of the roof above this segment of the batholith, the upper part being composed of Oligocene ash-flow tuffs. Roof pendants of Orejon also are preserved on top of the batholith in several places farther east and north. Most notable of these is the pendant that forms most of the high divide west of Granite Peak. Several hundred feet of Orejon are exposed, and the triangular-shaped pendant covers approximately 1 sq mi.

North of the Modoc mine, Paleozoic rocks overlie the batholith and the Orejon is discontinuously exposed above the Paleozoics or Love Ranch Formation on the pediment at the western edge of the range. Drilling north of Organ shows that the Orejon underlies parts of the pediment there, and a water well at the Hopkins Ranch, 0.5 mi west of the Stevenson-Bennett mine, also penetrated the Orejon beneath a few feet of pediment gravel (J. Hawley, personal communication, 1976). The contact between Paleozoic rocks and Orejon Andesite is an angular unconformity, the discordance generally being 10-20 degrees.

Notable at the base of the Orejon in several places is 100-200 ft of massive to poorly bedded siliceous tuff containing angular fragments of siliceous or andesitic rock, scattered pieces of granite, schist, and gneiss, and locally abundant rounded limestone cobbles. Dunham (1935) considered this basal tuff to be unrelated to the Orejon and mapped it separately. However, it appears to grade into the Orejon and probably represents initial explosive activity that heralded the main outpouring of Orejon lavas.

The Orejon lavas include lahar breccia as well as aphyric and porphyritic andesite and dacite flows (fig. 41). Two chemical analyses are presented in appendix B, and chemical classification after Irvine and Baragar (1971) is shown in fig. 42. The flows are mostly dark colored, ranging from dark gray to purplish, bluish, or reddish gray. Most outcrops have a greenish tint imparted to them by epidote and chlorite that occur in patches and clots or as pervasive alteration of mafic minerals and matrix. In fact, alteration is so extensive in these rocks that thin sections reveal limited information about the primary mineralogy. Phenocrysts are altered plagioclase and hornblende with minor sanidine and quartz. Plagioclase in one section is andesine (An_{40}). Much of the hornblende is either altered to the calc-silicate minerals noted above or to finely divided, opaque minerals, mostly hematite. In some flows phenocrysts are aligned and produce flow banding; in others, a vague flow banding is formed by zones of light and dark aphanitic material. Many flows exhibit little or no foliation.

The flows are interbedded with coarse-grained, poorly sorted breccias interpreted to be the deposits of volcanic mudflows. The breccias are massive lenticular bodies, dark colored like the flows and with similar alteration. Clasts range up to several feet in diameter, embedded in a matrix of pebbles, sand, and crystals, or in mudstone. Some lahars contain many varieties of andesite or dacite porphyry clasts while others are monolithologic. Rarely, the breccias are associated with thin deposits of sandstone or laminated mudstone laid down by streams that preceded or followed the mudflows.

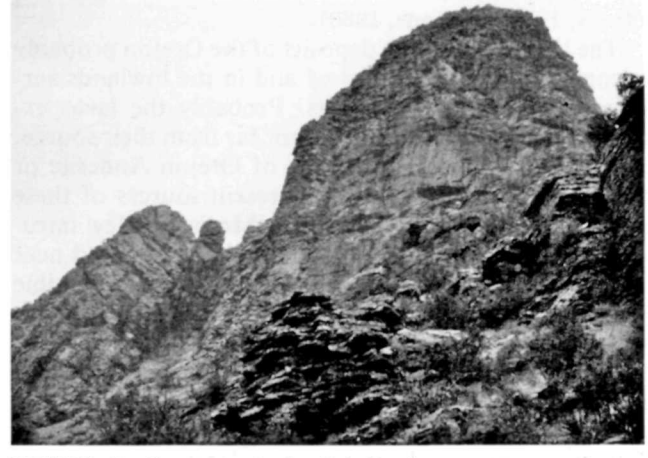


FIGURE 41—Steeply dipping Orejon Andesite lava flows in "The Narrows," Fillmore Canyon; flows have been deformed by intrusion of Needles quartz monzonite phase of Organ batholith or by subsidence of volcanic section in Organ cauldron; view to west.

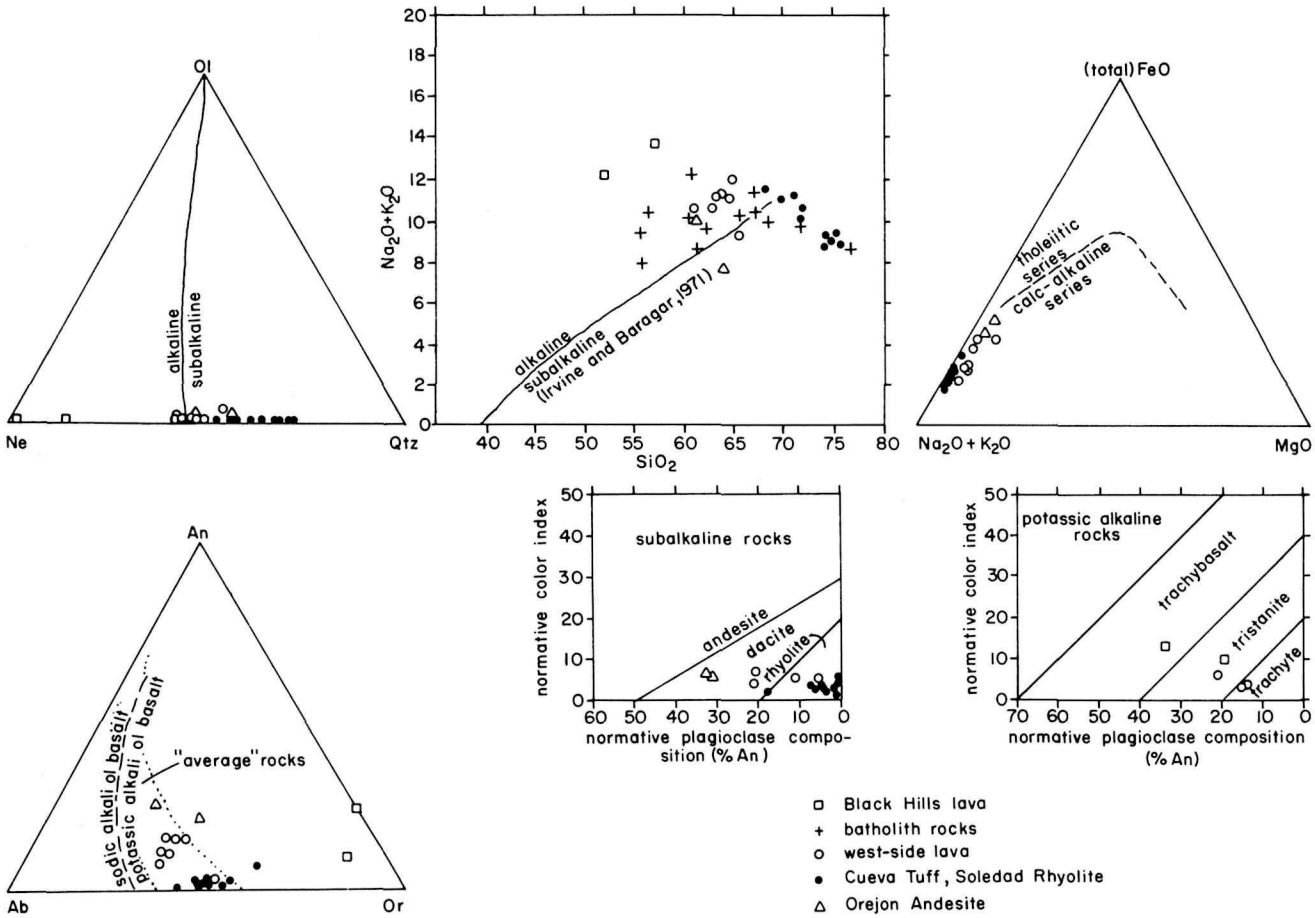


FIGURE 42—CHEMICAL CLASSIFICATION OF ORGAN MOUNTAIN IGNEOUS ROCKS AFTER IRVINE AND BARAGAR (1971). The Q-Ol-Ne ternary diagram was used to determine alkalinity, the AMF diagram to distinguish tholeiitic from calc-alkaline rocks, and the Ab-An-Or diagram to determine whether rocks belong to the potassic or sodic series.

The Orejon Andesite has not been dated radiometrically, and probably cannot reliably be so dated because of the alteration. Its late Eocene or early Oligocene age is based on physical correlation with the Palm Park and Rubio Peak Formations of south-central New Mexico, which contain similar rock types and occupy a similar stratigraphic position. The Palm Park and Rubio Peak Formations have yielded K/Ar dates ranging from 51 to 37.6 m.y. (Kottlowski and others, 1969; Seager and others, 1975; Clemons, 1980).

The lavas and laharic deposits of the Orejon probably accumulated on the flanks of and in the lowlands surrounding andesitic volcanoes. Probably the lavas exposed today in the Organs are not far from their source. However, few intrusive masses of Orejon Andesite or correlative rocks that might represent sources of these lavas are known in southern New Mexico. A few intrusive porphyries of Eocene age have been reported near El Paso (Hoffer, 1970; Lovejoy, 1976), and one possible intrusive has been mapped in the Doña Ana Mountains (Seager and others, 1976). A few thin aphyric andesite dikes cut the Orejon in Fillmore Canyon, and the thick andesite porphyry sill near the Ruby mine may be intrusive Orejon. The outcrop of Orejon at Hardscrabble Hill also appears to be intrusive, at least in its northern part where it is in contact with the Hueco Limestone. The massive porphyritic rock here is lithologically similar to the intrusive Cleofas Andesite of the Doña Ana Mountains (Seager and others, 1976). Still, no remnants of andesitic volcanoes have been mapped in the region, so the vents for the Orejon and correlative lavas remain unknown.

In the San Juan Mountains, early, intermediate-composition lavas (30-35 m.y. old) have been interpreted to represent early stages in development of a high-level batholith from which silicic differentiates were later (30-26 m.y.) erupted as ash-flow tuffs (Steven and Lipman, 1976). The Orejon Andesite may be similarly related to the middle Oligocene pyroclastic rocks and to the Organ batholith. Perhaps an early, nonfractionated body of intermediate-composition magma, which erupted to form the Orejon sequence in late Eocene or early Oligocene time, subsequently rose to a high level, fractionated extensively, and then vented the silicic, pyroclastic sequence about 33-34 m.y. ago. All or part of the remaining magma was then emplaced as the Organ batholith. The scheme assumes that the Orejon Andesite, younger silicic lavas and pyroclastics, and the Organ batholith are comagmatic. Certainly the more mafic phases of the batholith, as well as some of the middle Oligocene lavas, overlap the Orejon in composition (fig. 43). However, if all the rocks are cogenetic, the long hiatus between the end of andesitic volcanism and the onset of silicic volcanism seems odd, particularly if the Orejon proves to be late Eocene in age (44-40 m.y.). In the San Juan field, no lengthy hiatus appears

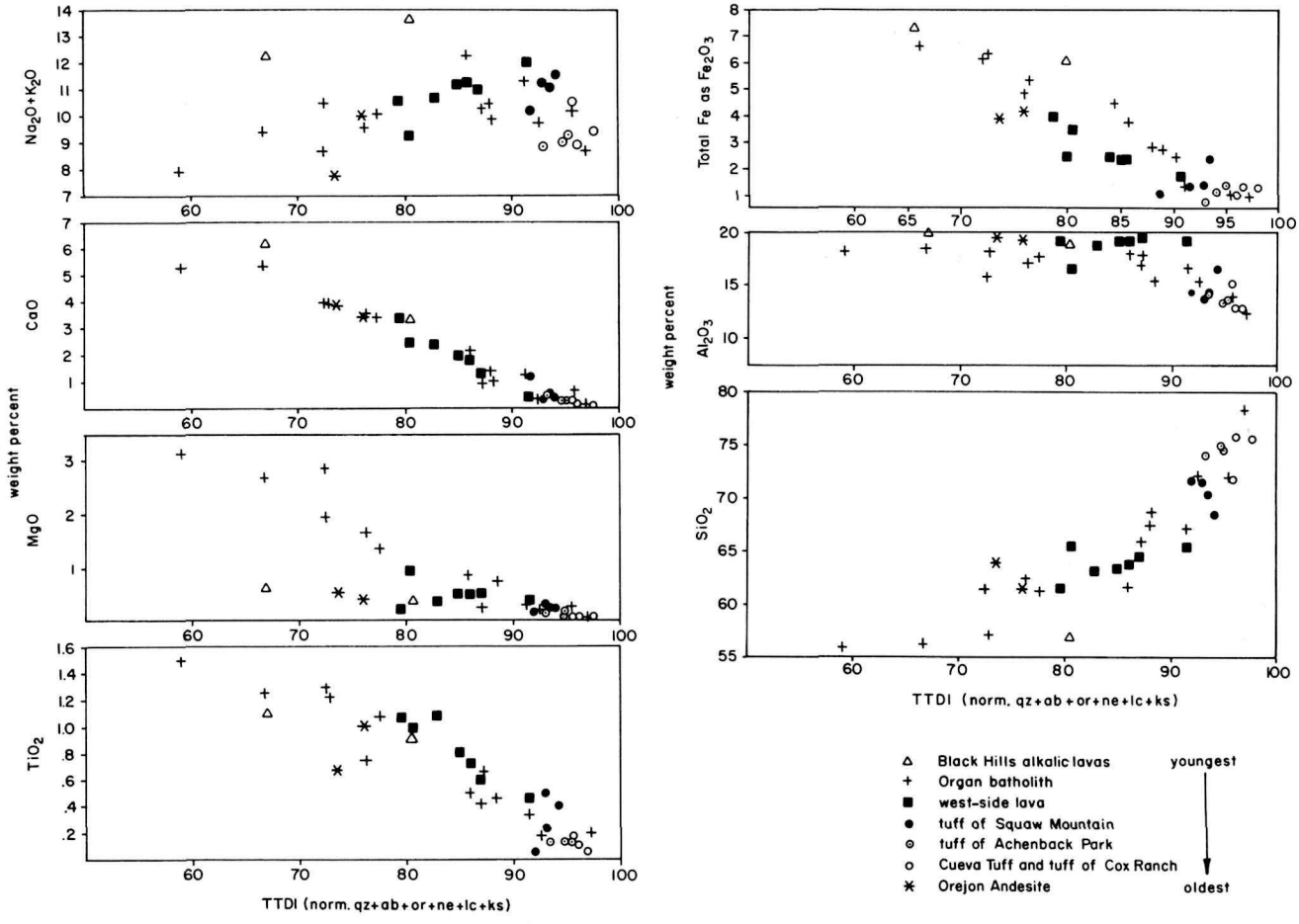


FIGURE 43—VARIATION DIAGRAM FOR OREJON ANDESITE, MIDDLE OLIGOCENE VOLCANIC AND PLUTONIC ROCKS, AND MIOCENE (?) LAVAS FROM THE ORGAN MOUNTAINS. Oxides were recalculated to 100 percent without H_2O or CO_2. TTDI is Thornton-Tuttle (1960) differentiation index.

between the end of intermediate-composition volcanism and the onset of silicic volcanism (Steven and Lipman, 1976). If the Orejon is only 36-37 m.y. old, the likelihood of a genetic relationship with the younger rocks by fractionation seems possible; however, if the Orejon is fully 8-10 m.y. older, the likelihood is much diminished.

Middle Tertiary silicic magmatism and volcano-tectonics

From a geologic viewpoint, the Organ Mountains are probably best known for the Organ batholith, one of the larger granitic bodies of Tertiary age exposed in New Mexico. The shallowly eroded batholith forms the fluted, serrated backbone of the range, as well as its eastern slopes. Northerly trending in outcrop (geologic map, sheet 1, in pocket), the batholith has steep, discordant sides, but a semi-concordant roof composed largely of thick volcanic rocks (mostly ash-flow tuff). Similar ages of the volcanics (33.0-33.7 m.y.) and the batholith (32.5-34.4 m.y.; table 2) as well as their overlapping chemical compositions support the general conclusion that they are comagmatic. The cycle of igneous activity in the Organs is one familiar to students of silicic volcanism the world over—eruption of voluminous, silicic ash-flow tuffs and lavas and cauldron collapse of the volcanics into the partially emptied magma chamber. On the other hand, little evidence of resurgent doming exists. What makes the Organ Mountains rocks notable is that: 1) three ash-flow sequences were erupted, each of which probably was voluminous enough to produce cauldron collapse, 2) compositional zoning through the whole tuff and lava section documents a compositional layering in the erupted magma volume at the top of the magma chamber, and 3) exposures of part of the remains of the magma chamber are represented by the Organ batholith.

Keep in mind that the Organ Mountains fault block of late Tertiary age is superimposed across the older volcano-plutonic complex. On the one hand this was fortunate because a cross section of part of an ash-flow tuff cauldron and its underlying plutonic roots resulted, together with exposures of its mineral wealth. On the other hand, tilting and erosion that accompanied the late Tertiary uplift drastically changed the configuration of the cauldron and obscured many of its details, particularly its margins. Parts of the cauldron complex are either buried or completely eroded away; only a fragment of the complex is exposed in the Organ Mountains. One important problem is the origin of the moderate (35-40 degree) west dip of the ash-flow tuff sequence. Is this west dip wholly a result of rotation on late Tertiary faults, or partly, at least, a product of volcano-tectonic subsidence or forceful intrusion of the batholith? In spite of the uncertainties, a partial picture of the complex can be reconstructed from the present study and from the pioneering work of K. C. Dunham, who made many important contributions toward understanding the igneous rocks of the Organ Mountains.

Dunham's (1935) study involved both mapping of and detailed petrographic work with the igneous rocks. He named the Soledad Rhyolite and Cueva Tuff, two major components of the ash-flow tuff sequence, and recognized their great thickness, though he interpreted the Soledad as lava flows rather than as pyroclastic deposits. He also recognized a basinal structure defined by dips of foliation in the flows and inferred that the source of the flows was beneath the basin. He suggested that subsidence caused the basin and that its formation was consequent on eruption of the lavas, a view used by Seager and Brown (1978) to support their cauldron picture. With regard to the batholith and its metamorphic halo, Dunham's detailed petrographic studies are invaluable. He also documented the role that piecemeal stoping played during emplacement of the batholith, and he showed that the batholith invaded the volcanic sequence. However, Dunham (1935, p. 57-58) argued that the "lavas cannot be regarded as a surface manifestation of the Tertiary batholith . . . since it differs both in composition and in age from the intrusive body." Of course, Dunham worked without benefit of the radiometric dates, chemical data, and detailed maps that are available now and that support the view that the intrusive and extrusive rocks are comagmatic.

Volcanic sequence

An impressive pile of rhyolitic ash-flow tuffs and rhyolitic to trachytic lava flows, compositionally zoned as a unit and approximately 10,000 ft thick (geologic map, sheet 1, in pocket), forms much of the southern Organ Mountains. These rocks unconformably overlie the Orejon Andesite that predates them by 3-10 m.y. but, as noted in the previous chapter, might be cogenetic with them. The whole volcanic section, together with thin strips of Paleozoic rocks, formed an insulating blanket below which the batholith crystallized. Radiometric dates of 33.0 m.y. and 33.7 m.y. from the base and top of the silicic volcanic sequence, respectively,

TABLE 2—SUMMARY OF RADIOMETRIC DATES OF ROCKS ASSOCIATED WITH ORGAN BATHOLITH.

Name	Location	Age	Reference
1—Hornblende monzonite-latite porphyry dike	0.6 mi NE of Organ	32.1 ± 1.1 m.y. (hornblende) 32.9 ± 1.2 m.y. (biotite)	Loring and Loring, 1980
2—Sericitized quartz-monzonite porphyry sill	1.2 mi N or Organ	34.4 ± 1.1 m.y. (sericite)	Loring and Loring, 1980
3—Sugarloaf Peak quartz-monzonite porphyry	San Agustin Pass	32.8 ± 0.5 m.y. (biotite)	Loring and Loring, 1980
4—West-side lavas (middle part)	2 mi WSW of summit of Squaw Mountain	33.7 ± 0.7 m.y. (biotite)	new date (this report)
5—Peña Blanca tuff	SW side of Peña Blanca	33.0 ± 1.4 m.y. (sanidine)	new date (this report)

and the lack of significant unconformities show the tuffs and lavas were emplaced quickly. The Organ batholith, 32.8 m.y. old, intrudes high into the volcanic section along subsidence fractures, at once confirming the age of the volcanic rocks and the contemporaneity of the batholith.

Beyond the southern Organs, only two small exposures of the volcanic sequence are known, one in the Black Hills and one on the pediment east of the Ruby mine. Presumably, extensive outflow-tuff sheets spread from the Organ cauldron early in its eruption history. If so, the sheets are covered by broad areas of gravel. No outflow tuffs that might be correlative with the Organ sequence have been recognized on the basis of general lithology or petrographic or chemical characteristics in other exposures of middle Tertiary volcanic sequences in the region. However, thick cauldron-fill tuffs (Doña Ana cauldron) in the Doña Ana Mountains, located 15 mi northwest of the Organ Mountains (fig. 1), are lithologically and chemically similar to the Organ sequence and are approximately the same age (Seager and others, 1976). In view of the similarities, the two cauldrons may have formed above a common batholith source or may even be parts of the same cauldron.

Three major sequences of ash-flow tuff have been recognized in the Organ cauldron complex (fig. 44). Each is separated by a few feet of sandstone or conglomerate, which mark minor disconformities. The lower tuff sequence, approximately 2,000 ft thick, is composed of the Cueva Tuff of Dunham (1935) and tuff of Cox Ranch (new name), which overlies the Cueva Tuff gradationally. Both units consist of comparatively thin ash-flow tuff sheets and interbedded pyroclastic and epiclastic strata, interpreted as recording eruptions preliminary to the major caldera-forming events. Above the tuff of Cox Ranch, the upper two tuff sequences are remarkable for their degree of welding and collective thickness (as much as 7,700 ft). The eruption of each must have been a caldera-forming event, and they probably accumulated as a cauldron-facies tuff within the caldera. The lower of the two, named tuff of Achenback Park (new name), is approximately 3,100 ft thick near the presumed center of the cauldron. The upper tuff, at least 4,600 ft thick, is called tuff of Squaw Mountain (new name). The two thick tuffs, together with the tuff of Cox Ranch, compose Dunham's (1935) Soledad Rhyolite.

Capping the volcanic section is a series of porphyritic lavas ranging in composition from rhyolite to trachyte. Their top is buried by gravel but they are at least 1,000 ft thick. The flows are separated from the underlying tuffs by an erosion surface that does not appear to represent a great deal of time. The lavas, being only slightly younger than the tuffs, are certainly comagmatic with them. The lavas may represent residual, defluidized magma left in the magma chamber after eruption of the higher, volatile-rich portion as ash-flow tuff. The lavas also extend most of the chemical and mineralogic variation trends established in the tuffs.

The whole volcanic sequence is compositionally zoned, both mineralogically and chemically (fig. 45). The zonation is relatively simple in the tuff section and more complex in the lavas but, in general, duplicates the familiar zoning pattern recognized in many silicic ash-flow tuff sequences (Williams, 1942; Lipman, 1967; Ratté and Steven, 1964; Lipman and others, 1966; Smith and Bailey, 1966; Giles, 1967; Hildreth, 1979). Crystal-poor, high-silica (77 percent SiO_2) rhyolite predominates in the lower part of the tuffs, changing to crystal-rich (alkali feldspar) low-silica (68 percent SiO_2) rhyolite or quartz latite at the top. Overlying lavas also are crystal-rich (plagioclase) and contain 61-66 percent SiO_2. Alkalis, alumina, magnesia, calcium, titanium, and iron increase upward through the whole section—the increase in TiO_2 and Mg_2O being notably regular. Clearly, such a zonation reflects compositional zoning in the magma chamber from which the volcanics were erupted (Lipman and others, 1966); some aspects of this zoning will be discussed in a later section.

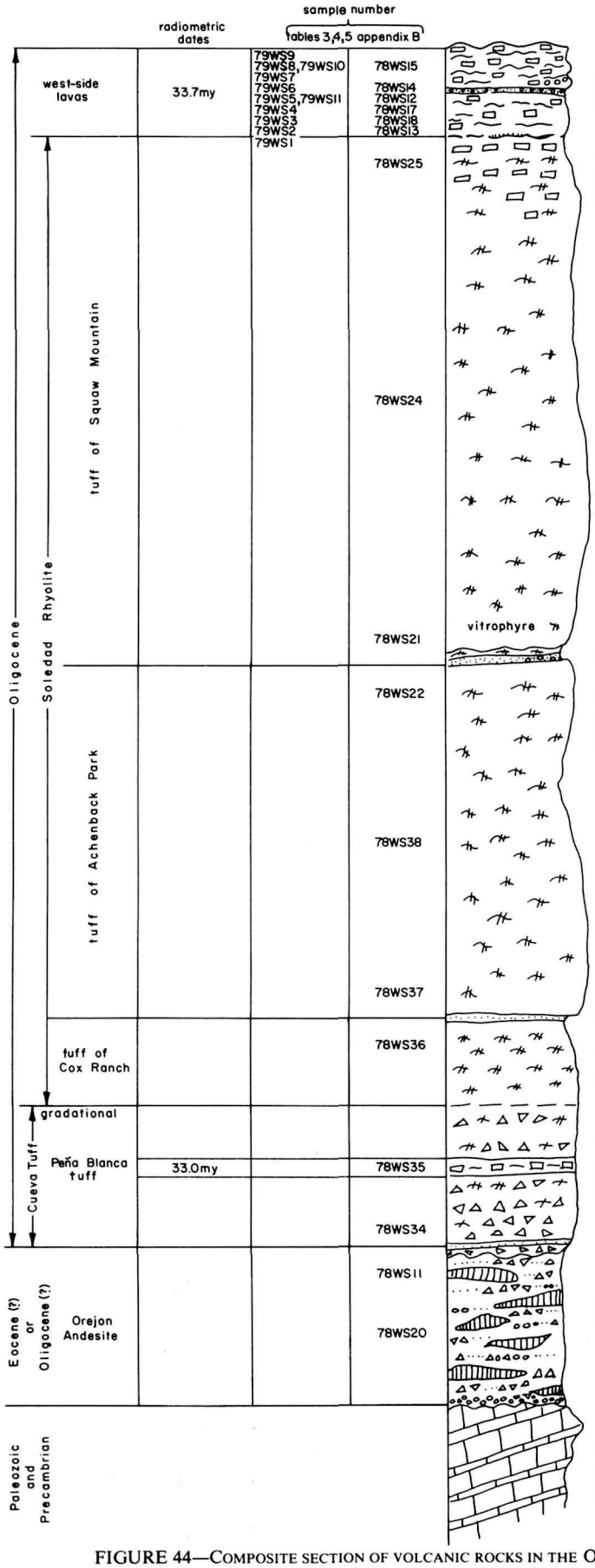
Descriptions of the volcanic rocks are presented in the following sections. Classification of the rocks shown in fig. 42 is after Irvine and Baragar (1971), and the chemical data on which classifications are based can be found in appendix B. Raw analyses were recalculated to 100 percent after removing H_2O and CO_2 and adjusting Fe_2O_3/FeO so that percent Fe_2O_3 = percent $TiO_2 + 1.5$.

Cueva Tuff

The Cueva Tuff was named for exposures at Cueva rock at the mouth of Fillmore Canyon (fig. 46). The formation's varied rock types are best displayed, however, on the western slopes of Boulder Canyon and at Peña Blanca (fig. 47). A section compiled from the latter locality is shown in fig. 48. Ash-flow tuffs, both compound and simple cooling units, are interbedded with epiclastic beds. Except for two thin, crystal-rich tuff sheets near the middle of the formation (described below), the Cueva is distinguished by the following features: 1) light color—light gray, pink, yellow, tan, cream; 2) abundant uncollapsed pumice; 3) notable lithic fragments, especially at the base, consisting of rhyolite, andesite, granite, and gneiss; 4) sparse phenocrysts; and 5) high SiO_2 content. The silica data are based on three analyses, two of which came from a comparatively xenolith-free part of the upper Cueva and yielded values of 77 percent and 79 percent. However, the latter value was not reported in appendix B nor in fig. 45 because total oxides in the analyses were not considered close enough to 100 percent. The third silica value (72 percent) was obtained from the xenolith-rich basal part of the Cueva. The number is somewhat in doubt because of possible contamination of the sample by small andesitic xenoliths. Thickness of the Cueva Tuff decreases northward from a maximum of 1,350 ft at Peña Blanca to a few hundred feet at Fillmore Canyon, largely by thinning and pinching out of the lower and middle tuff units. At Fillmore Canyon and Cueva rock only the uppermost tuff sheet remains.

An additional lithology, not reported in fig. 48, is contained in basal and upper parts of the Cueva Tuff in the Soledad Canyon area. Masses of flow-banded, spherulitic rhyolite, tens of feet thick and hundreds of feet long, appear to be gradational with pumiceous units. How the rhyolite, which is not merely densely welded or flow-laminated tuff, came to be mixed with pumiceous ash-flow tuff remains an unresolved problem.

The two crystal-rich tuff sheets near the center of the



Porphyritic rhyolite, dacite, and trachyte flows; vitrophyre near middle; brown to purplish-gray to medium-gray. About 1,000 ft exposed.

Vitric ash-flow tuff, sanidine-rich at top; gray, brown, pink; vitrophyre locally at base; densely welded; compound cooling unit. Maximum thickness about 4,600 ft.

Epiclastic rocks and air-fall tuff. Thin ash-flow tuff.

Vitric ash-flow tuff, uniformly crystal poor; gray to pink; densely welded in lower half, less so in upper half; massive; compound cooling unit. Maximum thickness about 3,100 ft.

Epiclastic rocks.

Vitric ash-flow tuff, gray, pink, brick-red, brown; platy foliation; moderately welded; compound cooling unit; gradational with Cueva Tuff. Maximum thickness about 850 ft.

Vitric highly pumiceous ash-flow tuff becoming lithic rich in lower part; yellow, tan, pink-gray; generally poorly welded; crystal-rich, welded Peña Blanca tuff member locally near middle, and epiclastic beds are interbedded. 300–1,300 ft thick.

Andesite and dacite porphyry flows, laharic breccia and volcaniclastic rocks; purple, gray, greenish, maroon; epidote alteration; about 1,500–2,000 ft thick.

Limestone, dolomite, shale; lesser sandstone, siltstone; Precambrian rocks are red and brown granite plutons, diorite-diabase dike swarms, pegmatites, minor metamorphic rocks.

FIGURE 44—COMPOSITE SECTION OF VOLCANIC ROCKS IN THE ORGAN MOUNTAINS; locations of samples described in tables 3, 4, and 5 are shown as well as units dated radiometrically.

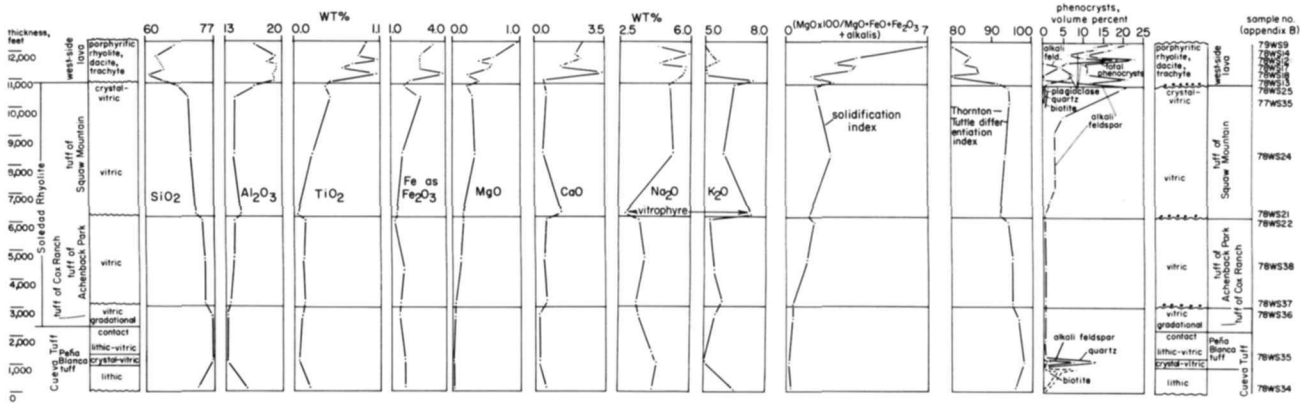


FIGURE 45—CHEMICAL AND MINERALOGIC VARIATIONS WITH AGE IN CUEVA TUFF, SOLEDAD RHYOLITE, AND WEST-SIDE LAVAS; oxides were recalculated to a volatile-free basis.

Cueva—the Peña Blanca tuff and an unnamed unit beneath it (Tc)—may be stray tuffs unrelated to the Organ cauldron. This is suggested mostly by their thinness (less than 250 ft each) and by their high crystal content (15-20 percent) which contrasts with the virtually aphyric character of all except the youngest part of the rest of the 9,000 ft of ash-flow tuff (fig. 45). Chemical variations, on the other hand, seem consistent with those of the rest of the tuff sequence, and the two tuffs follow other units in the Cueva by thinning and pinching out northward.

Regardless of whether they are related to the cauldron or not, the two tuffs—especially the Peña Blanca tuff—are important units. Sanidine from the Peña Blanca tuff yielded a K/Ar age of 33.0 m.y., a date nearly indistinguishable from the 33.7 m.y. value obtained from lavas nearly 10,000 ft higher in the section. Because of distinctive lithologies, both tuff sheets are also useful in helping to reveal the complex faulting in the southern Organ range.

Normally gray and moderately to densely welded, the Peña Blanca tuff also exhibits a red facies in Soledad Canyon caused by hematite dust that clouds the rock's matrix. Both matrix shards and scattered pumice lumps have devitrified, the former to a fine-grained mosaic of quartz and feldspar and the latter to somewhat coarser, lens-shaped mosaics of the same minerals, often with euhedral vapor-phase crystals of quartz and alkali feldspar partly filling central cavities. The rock is composed of 15-20 percent subhedral phenocrysts, mostly broken quartz and slightly perthitic sanidine with lesser albite or oligoclase and biotite. The other crystal-rich tuff in the Cueva is similar to the Peña Blanca but is redder, less welded, and restricted to the Peña Blanca–Boulder Canyon area.

Gradationally overlying the light-colored uppermost unit of the Cueva Tuff is a densely welded, reddish-brown to dark-gray ash-flow tuff sequence named tuff of Cox Ranch. There is no doubt that the tuff of Cox Ranch is a continuation of the upper cooling unit of the Cueva Tuff, but the striking differences in color and welding are easily mappable. Dunham (1935) used this color boundary to separate Cueva Tuff from his Soledad Rhyolite. Thus, in this report, the tuff of Cox Ranch is the lowest member of the Soledad Rhyolite, but genetically most of the unit is simply the welded part of the upper cooling unit of the Cueva Tuff. (After the geologic map was published it became clear that the upper unit of the Cueva Tuff and most of the tuff of Cox Ranch were one cooling unit which deserved only one name. To avoid confusion in correlating map with text, I have chosen only to acknowledge this problem rather than to attempt a nomenclature revision in the text that would not appear on the map.)

Tuff of Cox Ranch

Tuff of Cox Ranch, named for exposures on the ridge just southwest of the Cox Ranch headquarters near

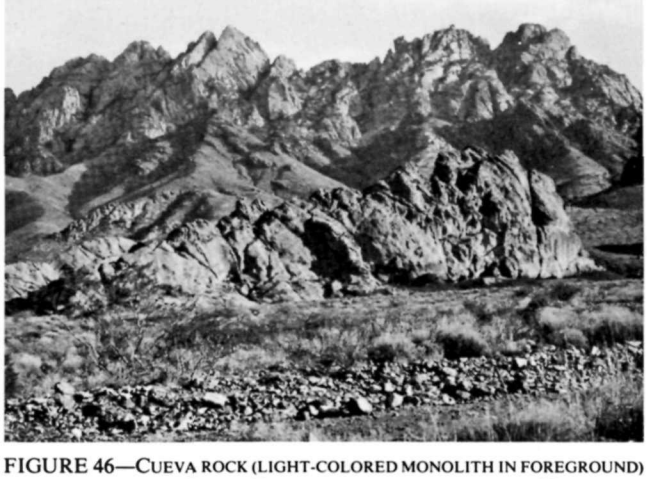


FIGURE 46—CUEVA ROCK (LIGHT-COLORED MONOLITH IN FOREGROUND) IS COMPOSED OF CUEVA TUFF DIPPING APPROXIMATELY 50 DEGREES SOUTHWEST (TO RIGHT); Organ Needles in background; view looks northeast.



FIGURE 47—LOWER 1,100 FT OF CUEVA TUFF EXPOSED ON EASTERN SIDE OF PEÑA BLANCA RIDGE; **Tcp**—Peña Blanca tuff member, 33.0 m.y. old.

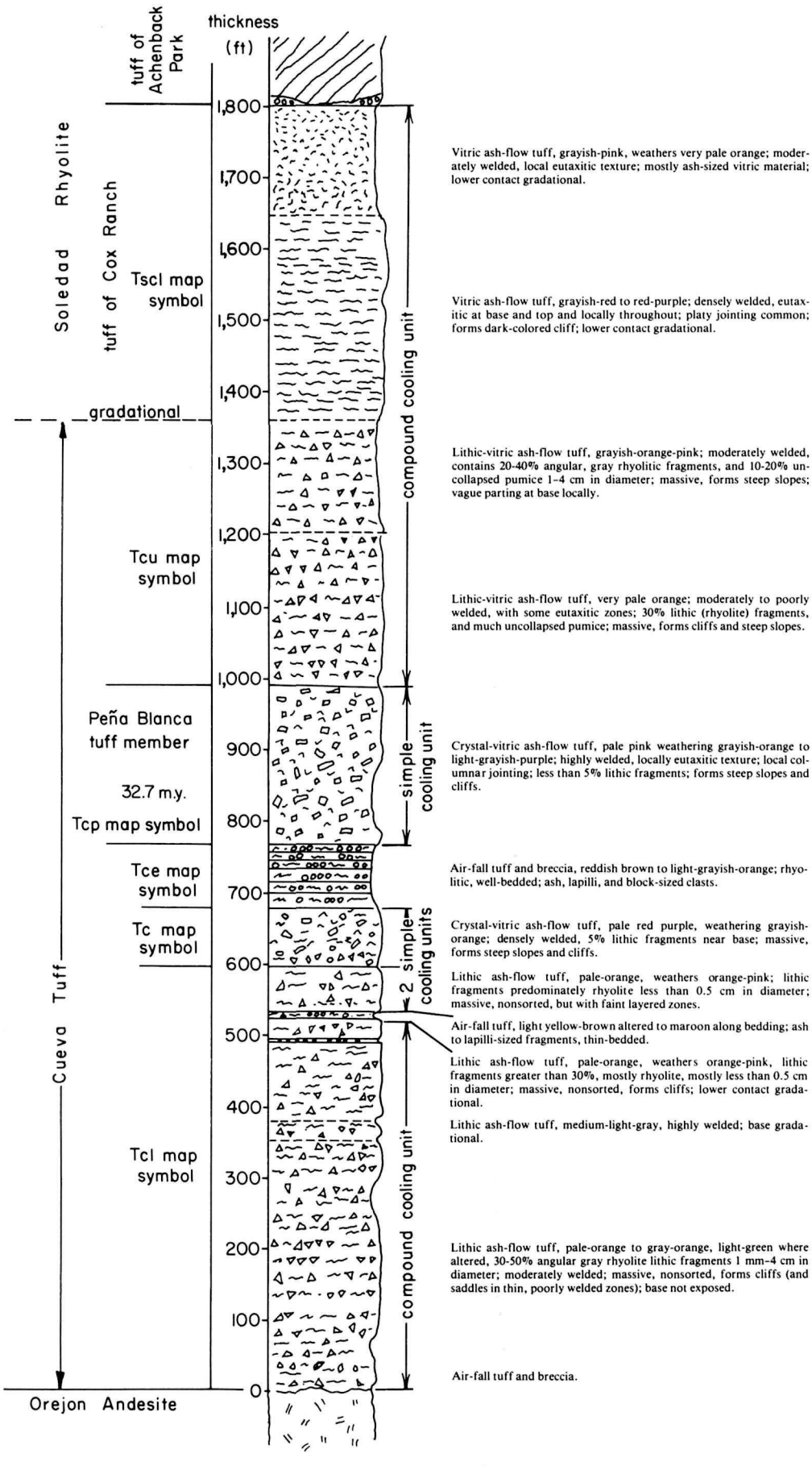


FIGURE 48—COLUMNAR SECTION OF CUEVA TUFF AND TUFF OF COX RANCH AT PEÑA BLANCA.

Cueva rock, includes two rhyolitic ash-flow tuff cooling units, locally separated by a few feet of air-fall tuff. Throughout most of the southern Organ Mountains (as at Peña Blanca, fig. 48), only the lower unit is present and it is gradational downward into the Cueva Tuff. Both units are crystal-poor, pumiceous tuffs, locally so densely welded and compacted that the flattened pumice in cross section gives the appearance of flow banding. Where the welding is less extreme, the tuffs have a distinctive platy fracture and they weather to myriads of small, angular, platy fragments. Near the top of each of the two cooling units the tuff is gray, massive, and only moderately welded, but underlying welded zones are reddish brown to purplish brown, the color typical of most of the Soledad Rhyolite. The pumice and shard matrix of the rock is largely devitrified, and the minerals and textures described for the Peña Blanca tuff matrix apply equally well to the tuff of Cox Ranch. The common reddish-brown color is the result of hematite dust in the matrix and the very few rounded sanidine fragments are the only phenocrysts. Thickness of the tuff of Cox Ranch varies between 500 and 1,300 ft, depending on the presence of the upper tuff unit.

Discontinuous deposits of sandstone and conglomerate up to 10 ft thick overlie the tuff of Cox Ranch, separating it from the tuff of Achenback Park, the lowest cauldron-facies tuff in the Soledad Rhyolite. Although the volcaniclastic strata clearly represent a break in the eruption sequence, it is thought to be a minor one because the overlying tuffs are nearly identical to those beneath, and they continue the same chemical trends (fig. 45).

Tuff of Achenback Park

The tuff of Achenback Park, one of the two exceptionally thick tuff units that compose most of the Soledad Rhyolite, is named for exposures in Achenback Park, the amphitheaterlike drainage basin at the head of Achenback Canyon (fig. 49). The tuff is a good example



FIGURE 50—TUFF OF SQUAW MOUNTAIN **(Tss)**, TUFF OF ACHENBACK PARK **(Tsa)**, AND TUFF OF COX RANCH **(Tsc)** EXPOSED JUST SOUTH OF CUEVA ROCK; compare thickness of tuff of Achenback Park here near inferred cauldron margin (650 ft) with fig. 49 taken 3 mi south near the inferred center of the cauldron; view to south.

of a cauldron-facies tuff—one whose eruption was accompanied by subsidence of a caldera in which the tuff accumulated to an unusually great thickness. It is approximately 3,100 ft thick at Achenback Park along the southwest edge of the range but thins rapidly northward to only 650 ft thick near Cueva rock (fig. 50) and eastward to 1,000 to 1,650 ft thick at North and Boulder Canyons. Thickness estimates at the southern end of the range are unreliable, but the variations cited above indicate that the tuff filled a subsiding basin whose northern and eastern margins approximately correspond to the present outcrop of the Organ batholith. The geologic map (sheet 1, in pocket) and fig. 51 best show the geometry of the tuff sheet.

Many individual ash flows make up the tuff of Achenback Park; some are thin and some thick, but all are gradational with each other. Different flows are recognizable only by the crude layering outlined by sets of columnar joints. No sharp contact between flows or evidence of an unconformity exists throughout the se-

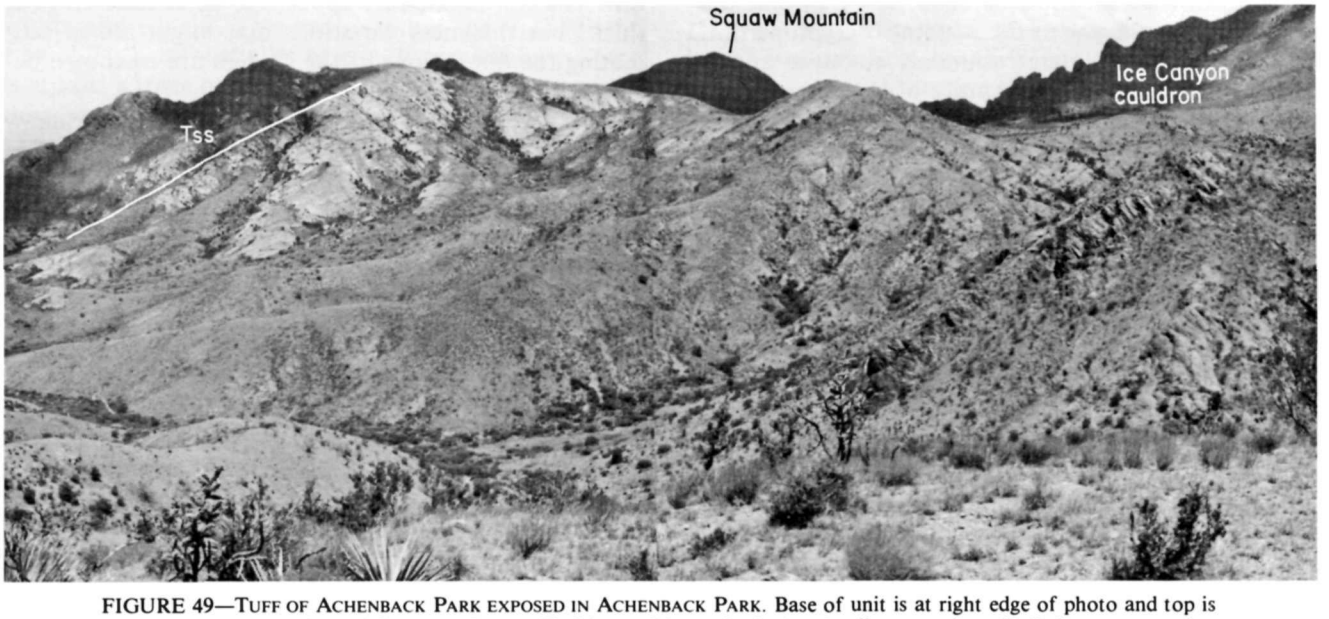


FIGURE 49—TUFF OF ACHENBACK PARK EXPOSED IN ACHENBACK PARK. Base of unit is at right edge of photo and top is marked by contact line at left center; **Tss**—tuff of Squaw Mountain; both units dip approximately 40 degrees west; view looks north.

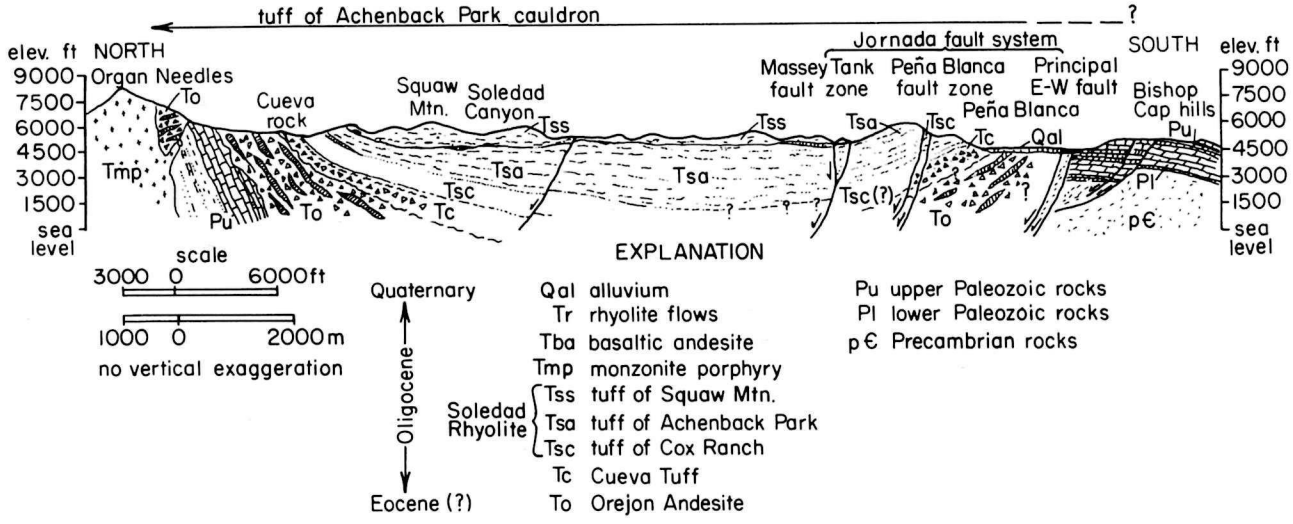


FIGURE 51—NORTH-SOUTH CROSS SECTION ALONG SOUTHWEST EDGE OF ORGAN MOUNTAINS SHOWING THICKNESS VARIATIONS IN TUFF OF ACHENBACK PARK.

quence. Apparently the flows were emplaced so rapidly that, while most cooled enough to develop a set of joints, they were plastic enough to weld to the next younger deposit. The tuffs are uniformly crystal poor and range in color from dark reddish brown in the lower half to pinkish gray or light tan in the upper half. Welding is extreme throughout the sequence; pumice is totally collapsed and much of the formation has eutaxitic foliation that could be mistaken for flow banding. The dark-brown lower half of the formation is especially dense and weathers to a steep, ledgy slope or series of impressive cliffs, while the pink or light-gray upper half forms barren, rounded topography and strangely shaped hills. According to the 1971 chemical classification of Irvine and Baragar (fig. 42), the tuff of Achenback Park is rhyolite from top to bottom.

Thin sections reveal devitrified pumice and groundmass textures and mineralogy similar to those already described. Sanidine and lesser quartz are phenocryst phases, but together these compose less than one percent of the rock. Some of the sanidine is cryptoperthitic and edges of crystals are commonly embayed and intruded by matrix material. A trace of biotite and zircon was noted. Magnetite is relatively common; the matrix of the redder and dark-brown tuffs is clouded, as usual, with hematite.

Above the tuff of Achenback Park, a few feet or tens of feet of purple, brick-red, and brown sandstone, conglomerate, and discontinuous, thin tuffs mark a comparatively minor hiatus in the volcanic succession. Culmination of the eruption cycle followed, however, with emplacement of the tuff of Squaw Mountain, thickest of the succession of ash-flow tuffs deposited in the Organ cauldron complex.

Tuff of Squaw Mountain

The tuff of Squaw Mountain was named for Squaw Mountain, located on the northern side of the western segment of Soledad Canyon. Squaw Mountain and the high peaks to the east and south are composed almost entirely of this tuff, as is much of the rock pediment that lies to the west. The base of the tuff is exposed on the eastern slope of Squaw Mountain, and the top can be seen in outlying hills on the pediment about 2 mi to the southwest. An outcrop of Soledad Rhyolite in the Black Hills, east of the Organ Mountains frontal fault zone, may also be tuff of Squaw Mountain or possibly one of the older tuff units.

Eruption of the tuff of Squaw Mountain was probably the last caldera-forming event. The tuff is thicker and more voluminous than any of its predecessors, reaching a thickness of approximately 4,600 ft near Squaw Mountain and perhaps even greater thickness in the huge subsided block labeled Ice Canyon cauldron on the geologic map (sheet 1, in pocket) and on section J-J′ (sheet 2, in pocket). As with the tuff of Achenback Park, however, the tuff of Squaw Mountain thins abruptly northward so that within 1.5 mi of Squaw Mountain the tuff is only 1,800 ft thick. Again, the thinning suggests a caldera margin not far north of the Fillmore Canyon drainage in the vicinity of the batholith. The rest of the tuff appears to be at least 1,000 ft thick, but thickness variations that might aid in estimating the dimensions of the caldera are unknown because the top is eroded.

Like the tuff of Achenback Park, the tuff of Squaw Mountain is a compound cooling unit. Many tiers of columnar-jointed flows form whole mountains (fig. 52), with individual flows ranging from a few to hundreds of feet thick. Again, contacts between flows are entirely gradational, and no epiclastic or air-fall beds are visible in the sequence. A discontinuous black vitrophyre, up to 10 ft thick, marks the base of the tuff in many places. The tuff units are mostly reddish brown, pinkish gray, purplish gray, and medium gray; they are densely welded throughout, except for the top few hundred feet. Pumice fragments range from totally to partially collapsed and they impart a pronounced foliation to the flows that locally can be mistaken for flow banding. Between Achenback Canyon and Squaw Mountain, lineation formed by elongated pumice is locally conspicuous on the foliation. The lineation focuses on the central part of the Organ batholith.

Most of the tuff of Squaw Mountain is calc-alkaline

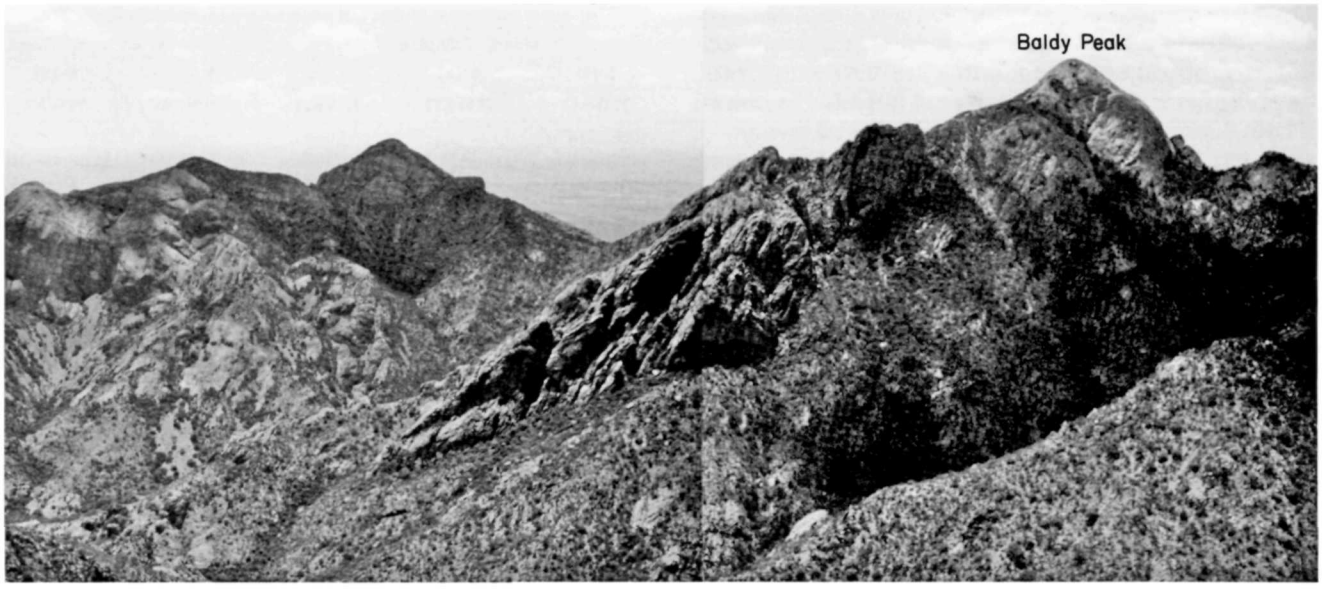


FIGURE 52—TUFF OF SQUAW MOUNTAIN EXPOSED IN WEST WALL OF NORTH CANYON. Tuff here is within Ice Canyon cauldron; nearly vertical foliation beneath Baldy Peak has been turned up by Organ batholith; dips in left part of picture are 40-50 degrees; view looks west.

rhyolite (fig. 42), but samples from the middle and upper parts of the unit contain 2-4 percent normative acmite, indicating local peralkalinity (Irvine and Baragar, 1971). Silica content ranges from 72 percent at the base to 68 percent in the crystal-rich upper part of the tuff.

Phenocryst phases, while more abundant than in underlying tuffs, still compose less than 5 percent of most of the tuff of Squaw Mountain. However, crystal content increases rapidly in the upper few hundred feet to approximately 20 percent (fig. 45). Phenocryst phases from this enriched zone are mostly blocky, perthitic sanidine with much less quartz, plagioclase, and biotite. The euhedral to subhedral sanidine is glassy and relatively unaltered. Most crystals are 2-5 mm in length and display sharp contacts with surrounding matrix whereas a few are embayed or intruded by veinlets of groundmass. In some crystals, especially those lower in the tuff, kaolinization has extended along cleavage or within albite blebs. This kaolinization accounts for the crystals' generally chalky or cloudy appearance. There is at least a trace of fresh biotite and zircon in most sections, and relative to tuffs beneath the Squaw Mountain, biotite is notably more abundant in the Squaw Mountain rocks. Devitrification products and textures are similar to those already described.

Scattered throughout the tuff of Squaw Mountain are zones of abundant, euhedral, pink orthoclase crystals. These are thought to be a product of postdepositional potash metasomatism in the tuffs. Such rocks were not collected for chemical analyses in order to avoid altered K_2O/Na_2O ratios. Nevertheless, some of the irregularity in the Na_2O and K_2O variation diagrams (fig. 45) may indicate altered alkali ratios. Especially suspect is the high normative Or and low normative Ab values for the basal vitrophyre of the tuff of Squaw Mountain (fig. 65). These values fall well off the general compositional trend of the diagram. This should not be surprising, however, because most secondarily hydrated glasses have lost Na and gained or lost K (Noble, 1968), at least in the case of peralkaline rhyolites.

The tuff of Squaw Mountain is overlain by at least 1,000 ft of lava flows. Although an unconformity separates the two sequences, radiometric dating reveals the lavas to be indistinguishable in age from all the underlying ash-flow tuffs.

West-side lavas

The lavas above the tuff of Squaw Mountain are exposed in a group of small hills on the pediment west of Squaw Mountain, and in three small gully-bottom outcrops 1 or 2 mi farther north. The top of the lava section is covered by gravel; graphic measurements indicate that a thickness of approximately 1,000 ft is exposed. The base also is covered, but scattered silicified boulders and other ground clutter appear to be weathering from a buried conglomerate; therefore, a minor disconformity is presumed to mark the base. Individual flows range from a few to one hundred feet thick or more. Almost all are porphyritic types, and dark gray and reddish brown are usual colors. Only one or two of the flows near the base of the section are vesicular and gas cavities are filled with calcite. Some flows are flow banded, consisting of alternating thin layers of reddish-brown and black aphanitic material or glass. Others are massive, and some have closely spaced, platy joints. A few feet of discontinuous, tan, conglomeratic sandstone near the middle of the section probably marks a minor disconformity. A black vitrophyre overlies the sandstone and forms the base of the upper half of the section. A biotite-rich, devitrified dacite immediately above the vitrophyre yielded a K/Ar date of 33.7 m.y.

In composition the lavas range from trachyte to dacite to rhyolite. On Q-Ne-Ol plots the lavas cluster about the alkaline-subalkaline boundary, but on alkalis versus silica diagrams they are clearly alkalic (fig. 42). In choosing rock names, I used the Q-Ne-Ol plot to determine alkalinity. Of six samples analyzed (whole-rock analyses), three are calc-alkaline rhyolite or dacite, two are trachyte, and one is tristanite (fig. 42). The latter rock type reflects the unusually high CaO in the whole-

TABLE 3—ELECTRON-MICROPROBE ANALYSES OF GLASSES IN WEST-SIDE LAVAS; number in parentheses is number of analyses averaged (data by N. Stoll).

	1 (1)	2 (2)	3 (4)	4 (3)	5 (1)	6 (5)	7 (3)	8 (3)	9 (3)
Sample number	**79WS2**	**79WS5**	**79WS5**	**79WS11**	**79WS11**	**79WS11**	**79WS11**	**79WS9**	**79WS9**
Description	inclusion in plagioclase	inclusion in plagioclase	groundmass glass	inclusion in plagioclase	inclusion in plagioclase; groundmass glass	groundmass glass, mottled	groundmass glass, brown-red	groundmass glass, mottled	groundmass glass, red
SiO_2	57.28	71.52	67.54	67.89	68.47	68.30	67.87	67.14	67.12
Na_2O	3.90	2.86	5.01	6.04	4.76	4.47	4.50	4.89	5.55
Al_2O_3	15.98	13.48	15.79	15.89	15.79	15.84	15.93	15.77	15.33
K_2O	7.99	7.96	6.01	4.13	6.74	6.73	6.92	6.23	5.16
CaO	.96	.31	1.16	1.60	1.07	.84	1.07	1.30	1.23
$FeO_{Total\ Fe}$	4.72	1.58	1.52	2.19	1.55	1.88	1.76	1.83	1.76
MgO	.59	.18	.28	.24	.12	.10	.04	.25	.11
TiO_2	2.61	.20	.59	.63	.61	.64	.61	.54	.66
total	94.03	98.09	97.90	98.61	99.11	98.80	98.70	97.95	96.92

rock analysis. Microprobe analyses of glass and plagioclase phenocrysts in the rock do not confirm high CaO. With a lower CaO, and lower normative An, the rock would probably fall in the trachyte field. Whole-rock silica in the lava suite varies between 61 and 65 percent (fig. 45). Groundmass glass, on the other hand, is relatively constant at 67-68 percent SiO_2 as indicated by microprobe analysis of four specimens from different parts of the sequence (table 3). The difference between the groundmass and whole-rock chemistries must be accounted for by the phenocryst variations in the lava sequence.

Fig. 45 and table 4 show crystal variations within the lava sequence. Although all of the flows are comparatively rich in crystals, ranging from 10-22 percent, the crystal-poorer rocks are found in the lower half of the lava section and the crystal-richer rocks in the upper half. Moreover, there is an irregular but steady increase in crystals, mostly plagioclase, upward in the section, especially in the upper part. This increase, together with chemical variations, suggests a continuation of most of the chemical and mineral variation trends established in the underlying tuffs—with two notable differences. The first is that the variations in the lava sequence are much less regular than those in the tuff and, secondly, that the lava-sequence crystals are predominantly plagioclase rather than sanidine.

Sanidine was found in only two flows near the base of the lava section. The anhedral to subhedral crystals, 1-1.3 mm long, are corroded and embayed; they were plainly out of equilibrium with the surrounding melt.

Plagioclase phenocrysts, on the other hand, include 1) clear, euhedral laths; 2) almost completely resorbed, equant, anhedral grains; and 3) resorbed crystals with poorly developed overgrowth rims. Normal zoning is common in both overgrowths and on clear, euhedral laths. Oscillatory zoning is far less frequent and is confined to euhedral laths. In composition, the plagioclase phenocryst population varies from oligoclase to sodic labradorite as determined by both microprobe and thin-section studies (N. Stoll, unpublished data; table 5). Resorbed crystals might be slightly more calcic (An_{40}-An_{60}) than the clear, euhedral variety (An_{40}-An_{49}), but this is far from certain.

The resorbed calcic plagioclase crystals and those with overgrowths have reacted with the surrounding melt; therefore, they are disequilibrium crystals. The clear, euhedral, normally zoned plagioclase laths, on the other hand, are in equilibrium with their surroundings and probably represent crystals growing in the melt at the time of eruption. The disequilibrium plagioclase crystals compose approximately 50 percent of the total plagioclase phenocryst population (table 4).

Mafic phenocryst minerals compose less than 5 per-

TABLE 4—MODAL ANALYSES OF WEST-SIDE LAVAS (data by N. Stoll; point count = 500 points).

			Plagioclase[a]			Total					
Description	**Sample number**	**Sanidine**	**resorbed**	**clear**	**matrix**	**phenocrysts**	**Biotite**	**Hornblende**	**Pyroxene**	**Magnetite**	**Matrix**
base of	79WS1	8.2				1.6	0.8	—	—	0.8	88.6
lavas	79WS2	—	5.2	0.4	13.2	5.6	—	—	0.6	1.4	79.2
	79WS3	—	4.4	3.2	—	7.6	—	1.2[b]	0.8	1.6	88.8
	79WS4	3.8	2.4	2.2		4.6	0.2	—	0.6	1.4	89.4
	78WS50	—				5.8	0.4	2.4	0.4	0.4	90.6
	79WS5	—	11.6	7.2		18.8	1.0	0.2	0.8	1.4	77.8
	79WS11	—	6.6	3.6		10.2	2.2	0.6	0.2	0.4	86.4
	79WS6	—				7.2	1.4	1.0[c]	0.4	0.8	89.2
	79WS7	—	4.8	6.0		10.8	2.6	1.6[c]	0.2	0.6	84.2
	79WS8	—	4.4	8.8		13.2	1.8	1.2	0.2	0.8	82.8
	79WS10	—				12.8	1.6	1.6	0.2	2.0	81.8
top of lava section	79WS9	—	4.6	12.4		17.0	1.6	1.4	tr	1.2	78.8

a) distinctions were made between resorbed and nonresorbed (clear) crystals and, in some instances, groundmass laths if they were abundant and large
b) uralite after pyroxene
c) oxyhornblende

TABLE 5—ELECTRON-MICROPROBE ANALYSES OF PLAGIOCLASE PHENOCRYSTS IN WEST-SIDE LAVAS; number in parentheses is number of analyses averaged; (data by N. Stoll).

	Base					West-side lavas									Top
	1 (3)	2 (2)	3 (3)	4 (3)	5 (4)	6 (3)	7 (4)	8 (3)	9 (3)	10 (1)	11 (1)	12 (1)	13 (3)	14 (5)	15 (3)	16 (4)
Sample number	79WS2	79WS2	79WS2	79WS2	79WS2	79WS5	79WS11	79WS11	79WS11	79WS11	79WS11	79WS11	79WS11	79WS9	79WS9	79WS9
Description	phenocryst, clear	phenocryst, clear	resorbed phenocryst, core	resorbed phenocryst, rim	groundmass laths	phenocryst, clear, normally zoned	resorbed phenocryst	resorbed phenocryst	resorbed phenocryst, core	resorbed phenocryst, inner rim	resorbed phenocryst, middle rim	resorbed phenocryst, outer rim	resorbed phenocryst, rim (average)	resorbed phenocryst	phenocryst, clear	phenocryst, normally zoned
SiO_2	54.79	56.44	56.23	53.09	58.28	56.05	56.18	58.21	55.47	53.89	53.05	57.37	55.12	57.37	57.49	57.27
Na_2O	5.77	6.42	6.19	5.91	6.07	5.63	5.76	6.55	5.38	4.70	4.67	6.29	5.30	6.52	6.46	6.52
Al_2O_3	25.74	24.54	24.39	25.62	24.77	26.19	26.61	24.89	27.31	28.73	27.59	26.04	27.38	25.05	25.41	24.89
K_2O	.86	1.16	.97	.67	.88	.48	.48	.66	.40	.35	.32	.61	.41	.62	.54	.70
CaO	10.09	8.62	9.03	10.19	9.55	10.25	10.01	8.57	11.59	13.34	13.16	10.14	11.90	8.29	8.66	8.61
$FeO_{Total\ Fe}$	.63	.66	.42	.68	.64	.36	.48	.46	.47	.50	.53	.48	.48	.43	.42	.39
MgO	.05	.05	.02	.06	.00	.00	.00	.00	.00	.00	.00	.00	.00	.00	.00	.00
TiO_2	.03	.13	.04	.02	.11	.05	.07	.09	.07	.12	.13	.18	.10	.09	.10	.08
total	97.96	98.02	97.29	96.24	100.30	99.01	99.59	99.43	100.69	101.63	99.45	101.11	100.69	98.37	99.08	98.46
total percent An	An_{47}	An_{40}	An_{42}	An_{47}	An_{44}	An_{49}	An_{48}	An_{40}	An_{53}	An_{60}	An_{60}	An_{46}	An_{54}	An_{49}	An_{41}	An_{40}

cent of the flows (table 4). Biotite is present in most flows, occurring as splinters or bent plates 0.7-2 mm long; some are fresh and some show reaction rims. Subhedral to euhedral hornblende up to 0.5 mm in diameter composes less than two percent of most rocks. Unzoned brown and greenish-brown hornblende and red-brown oxyhornblende were noted in different flows. Less than one percent unzoned pyroxene is present in the lavas. Some of the unzoned pyroxene is pale green and fibrous (hypersthene?) and is interstitial between plagioclase and other mafics; in other flows, pale-green, subhedral to euhedral, nonpleochroic pyroxene fragments up to 0.5 mm across can be found. The pyroxene in some sections is replaced by uralite. In at least one flow aegirine-augite was identified, confirming the alkaline tendencies of the lava sequence. Small, equant, irregular grains of magnetite compose up to two percent of each thin section.

The matrix of the lava flows consists generally of devitrified glass, opaque minerals, and in most flows, abundant flow-aligned microlites of plagioclase. The composition of the microlites, determined by petrographic techniques for one flow, is An_{39}-An_{50} (N. Stoll, unpublished data). For another flow, microprobe analysis indicates groundmass plagioclase is An_{44}. Thus, the compositions of clear, euhedral, phenocryst plagioclase and groundmass plagioclase appear to be essentially the same. Alternating bands of black and red-brown glass make up the matrix of at least two flows. In each case the composition of the two glasses is identical, removing the likelihood that they represent different magmas that mixed. Tables 3 and 5 indicate that most of the alkalis in these rocks, particularly K_2O, are concentrated in the groundmass. This concentration is supported by the lack of potassium-bearing phenocryst minerals.

Organ batholith

Age and relation to volcanic rocks

The composite Organ batholith crops out over an area of 40-50 sq mi and forms the lofty, rugged peaks of the central Organ Mountains (fig. 53) as well as some of the lower ground east of San Agustin Pass. The batholith was emplaced beneath and into the volcanic rocks of the Organ cauldron, and its northern part also intruded the Precambrian rock core of a large Laramide uplift. The age of the batholith has been well established by radiometric dating. Loring and Loring (1980) report that one of the younger phases of the batholith is 32.8 m.y. old and that, allowing for the error margin, sericite alteration and dikes associated with this phase yield nearly indistinguishable ages of 34.4 and 32.5 m.y. While geologic relations indicate the batholith is relatively younger than the volcanic rocks, radiometric dates of volcanics and the batholith are virtually identical. Both were emplaced within a 1 m.y. span 32.8-33.7 m.y. ago.

Considering their close spatial and temporal relationship, a common parentage of batholith and volcanic rock suites seems only natural. Overlapping chemistries of volcanic and plutonic rocks shown on variation diagrams (fig. 43) also are suggestive of a cogenetic relationship, but certainly do not prove it. More convincing



FIGURE 53—EAST-CENTRAL PART OF ORGAN BATHOLITH AS VIEWED LOOKING WEST UP ASH CANYON. Granite Peak on far skyline near the middle of the picture is nearly 8,500 ft elevation and approximately 4,000 ft above the viewer; it is composed of granite of Granite Peak; closer monoliths are syenite facies of Organ Needle quartz monzonite.

is the plot of SiO_2–Al_2O_3–$Na_2O + K_2O$, shown in fig. 54 (Bailey and McDonald, 1969). The fact that batholith and volcanic rocks overlap in composition and lie in the same slightly curving surface indicate that they probably are comagmatic, possibly related at least partly by crystal fractionation of alkali feldspar and plagioclase (Bailey and MacDonald, 1969).

Fig. 43 shows that the Organ batholith, averaging 60-65 percent SiO_2, is more mafic in composition than most of the volcanic rocks. It is closest in composition to the west-side lavas—especially in SiO_2, CaO, TiO_2, and alkalis—although the lavas are somewhat lower in FeO and MgO. Mineral contents also are similar except that plagioclase in the batholith is oligoclase and in the lavas mostly andesine with lesser oligoclase. Although the problem of different plagioclase is a troublesome inconsistency, a tentative conclusion of this study is that 1) the batholith represents magma of intermediate composition left in the magma chamber after its silicic cap was erupted as ash-flow tuffs, 2) this magma was the source of the west-side lavas, and 3) the remains of the magma chamber solidified beneath its own volcanic roof as the composite Organ batholith.

Batholith geometry and emplacement

Interpretations of the shape of the batholith depend largely on how much the Organ range was tilted west-

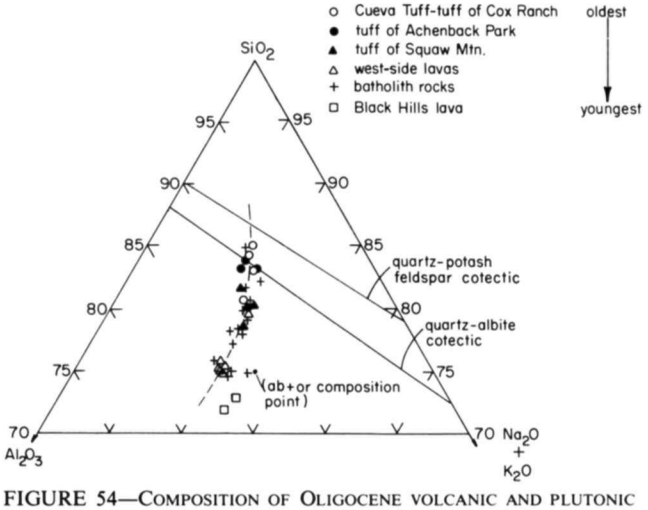


FIGURE 54—COMPOSITION OF OLIGOCENE VOLCANIC AND PLUTONIC ROCKS OF THE ORGAN MOUNTAINS IN THE SYSTEM SiO_2–Al_2O_3–($Na_2O + K_2O$), EXPRESSED AS MOL PERCENT. Cotectics are from Schairer and Bowen (1955, 1956); all compositions except the Black Hills lavas lie on the same somewhat curved surface, and the trend terminates near the quartz-K feldspar cotectic; also, the volcanic and batholithic rocks show a time progression toward lower SiO_2, the more fractionated (higher SiO_2) magmas having been emplaced first. These relationships argue for consanguinity between the various batholith and volcanic magmas; the diagram suggests that batholith and volcanic rocks may be related by fractionation of alkali feldspar and plagioclase. The compositional trend does not radiate exactly away from the alkali feldspar composition point (at 75 percent SiO_2, 12.5 percent AlO_3, 12.5 percent $K_2O + Na_2O$), indicating that besides alkali feldspar, fractionation of plagioclase was responsible for changing the magma composition. Fractionating plagioclase gives a curving liquid trajectory as the fractionating feldspar becomes more albite-rich. The west-side lavas and batholith rocks, whose compositions are largely responsible for the curving trajectory, contain abundant disequilibrium plagioclase or zoned plagioclase and perthite; however, there is little mineralogical evidence for feldspar fractionation in the section of ash-flow tuffs (see summary and discussion).

ward in late Tertiary time. Unfortunately this is not known for certain. If the tilting amounts to 40 degrees—the average dip of the youngest volcanic rocks—then the geologic map (when viewed from the east looking down-dip) becomes a geologic cross section and the batholith is revealed as a thick sill-like body with a floor of Precambrian rocks and a roof of volcanic rocks and Paleozoic limestone. However, at least three aspects of this interpretation are unsatisfactory. First, at least two plutons within the composite batholith are steep-sided, cylindrical bodies that do not appear to have been rotated more than 10-20 degrees since they were emplaced. Secondly, roof pendants dip only 10-20 degrees west (although Paleozoic strata within one of them, deformed during the Laramide, dip as much as 43 degrees). Finally, removal of 40 degrees of tilt leaves Laramide structures such as the Stevenson-Bennett, Black Prince, and Bear Peak fault and fold zones with unlikely Laramide geometries. For these reasons, I suspect that tilting of the range during the late Tertiary amounts to no more than approximately 20 degrees and that viewing the geologic map by the down-structure method would yield an unrealistic view of the shape of the batholith.

As is typical of many epizonal plutons, the Organ batholith lacks foliation or lineation (except locally near the margins), so these characteristics are of little help in establishing the geometry of the batholith. Contacts with wall rocks are useful, however, and they reveal that the batholith is steep sided with a steep to moderately dipping, semiconcordant roof. A similar picture was painted by Dunham (1935) and Lindgren and Graton (1906), the latter referring to the batholith as a "laccolithic stock." Northern and southern ends of the batholith are steep, transgressing Precambrian and Paleozoic rocks upward to the level of Pennsylvanian strata. The northern contact plunges northward and the batholith presumably underlies the Bear Canyon–Quartzite Mountain area, where it supplied sills and dikes found high in Paleozoic limestone there. Steep contacts with Precambrian granite are also exposed along the eastern side of the batholith from Texas to Johnson Canyons; the rest of the eastern contact is so poorly exposed as to offer little information. Roof contacts along the western edge of the batholith are more complicated.

Relationships of roof rock with the batholith vary along the length of the contact (geologic map, sheet 1, in pocket). Above the southern part of the batholith the roof is simple, consisting almost entirely of volcanic rocks, including two sizable roof pendants; contacts are concordant, dipping moderately to steeply west. Near the Modoc mine this simple relation changes as the batholith transgresses the Modoc fault, an arc-shaped fracture bordering the subsided Ice Canyon cauldron, into deformed Paleozoic strata. From there northward, the western edge of the batholith is steep and follows or transgresses the steep Laramide Torpedo–Bennett fault zone (and the folded strata adjacent to it) to the vicinity of the Memphis mine. As judged from roof pendants, part of the northern roof of the batholith east of the Torpedo–Bennett fault zone was Precambrian granite and lower Paleozoic rocks that earlier formed the core of the Laramide uplift. North of the Memphis mine, outcrops and drilling again demonstrate a moderate west-dipping, nearly concordant contact with Paleozoic strata; this relationship continues to the steep northern edge of the batholith. We have then a batholith whose eastern, northern, and southern sides are steep and crosscutting, and whose upper (roof) contact varies from moderately dipping and concordant to steep and discordant. The upper contact is concordant where the batholith underlies the west-dipping volcanic fill of the Organ cauldron, and it is steep and discordant where it follows or transgresses crosscutting Laramide structures. Removal of approximately 20 degrees of late Tertiary rotation leaves the batholith with an original cross-sectional shape that may approximate that shown in fig. 55.

Volcanic roof rocks steepen gradually in dip toward the batholith, locally becoming vertical or even overturned at its contact. This relationship can be explained in either of two ways. First, perhaps the batholith made room for itself by forcibly intruding and lifting its roof. Second, the steep dips may be entirely a result of subsidence of the volcanic rocks into the batholith. By this second hypothesis, the batholith would simply represent the outer, upper part of the magma chamber at the mar-

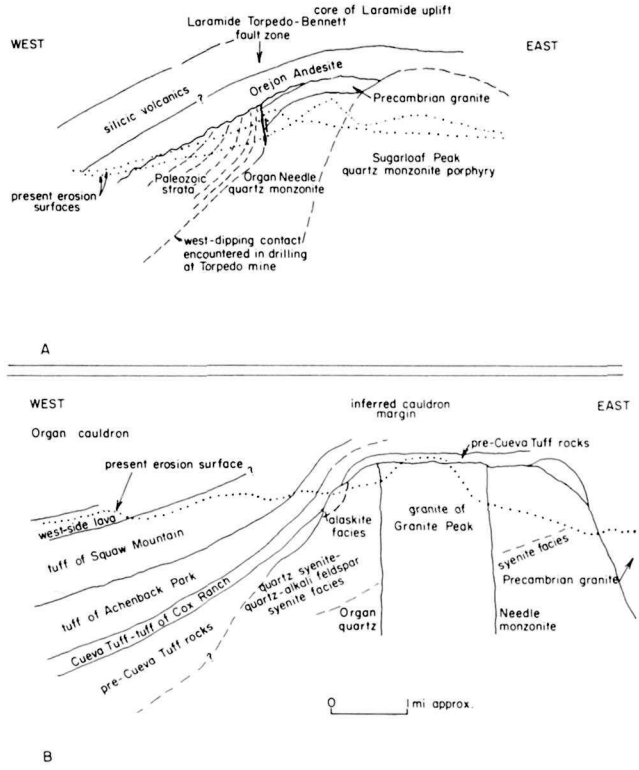


FIGURE 55—DIAGRAMMATIC SECTIONS THROUGH THE ORGAN BATHOLITH AND ADJACENT ROCKS AFTER REMOVAL OF 20 DEGREES OF LATE TERTIARY ROTATION. In **A**, approximately through the Stevenson-Bennett mine–Baylor Canyon area, the batholith is interpreted as intruding the Precambrian rock core of a Laramide uplift, whose western boundary is the Torpedo–Bennett fault zone; in **B**, approximately through Granite and Baldy Peaks (with the Ice Canyon cauldron omitted for clarity), the batholith is interpreted to be a ridgelike cupola above a broader batholith at depth. The cupola is visualized as occupying a hinged margin of the Organ cauldron, the location of the hinge being inferred mostly from thickness variations in the tuff of Achenback Park (see summary and discussion); compositional layering in the Organ Needle quartz monzonite is suggested by facies described in the text.

gin of the subsided block. The facts that tuff units thin toward the batholith and that relatively undeformed roof pendants of volcanic rock cap the ridgelike batholith favor the second idea. Furthermore, similar structural relationships between cauldron fill and adjacent plutons in major cauldrons like the Ossipee and certain Queensland cauldrons have been interpreted as due to subsidence (Branch, 1966; Kingsley, 1931). However, steep dips in Paleozoic rocks adjacent to both the batholith and the Stevenson-Bennett fault zone may be in part due to Laramide deformation.

Dunham (1935) pointed out that scattered xenoliths of wall rock constituted evidence that the magma chamber (and batholith) made room for itself by piecemeal stoping. The large blocks of limestone in the South Canyon area, which appear to have sunk 1,000 ft or more, are striking examples of this process. To some extent the batholith may have lifted its roof, but I believe the steep dips in roof rocks are more consistent with subsidence than with forceful intrusion.

Batholith rocks

The Organ batholith is composite, consisting of three main plutonic phases and two related hypabyssal phases, as well as pegmatite, aplite, rhyolite, and other kinds of dike rocks. Additional rock variety is provided by important compositional facies present in one of the three major plutons. A fourth plutonic phase, the oldest of all, is represented only by xenoliths and two or three small patches completely surrounded by younger phases.

Table 6 shows a modal analysis of rocks from the batholith and fig. 56 classifies them according to I.U.G.S. (International Union of Geological Sciences) recommendations. (I.U.G.S. rock names are somewhat different from the field terms appearing on the geologic map, because the map was printed before modal analysis of the rocks was complete.) Chemical compositions are presented in appendix B. Although rock types vary from granite to monzodiorite, the most abundant rocks are quartz syenite and quartz alkali-feldspar syenite; thus the batholith has alkaline tendencies. This alkaline tendency is also evident in a plot of alkalis versus silica (fig. 42). Table 7 summarizes the relative ages (so far as is known), major rock types, and silica contents of various phases of the batholith.

Mineralogic and chemical similarities among all the phases suggest that they are related to a common source and that they crystallized under generally similar conditions. Specifically, plagioclase in each phase is oligoclase (An_{15}), alkali feldspar is cryptoperthite, and at least some alkali feldspar crystals in each phase are zoned—oligoclase cores mantled with perthite. Furthermore, all except the final phase of the batholith were emplaced in rapid succession as indicated by 1) lack of chilling along contacts, 2) lack of dikes of one phase transecting others, and 3) mutually embayed contacts. Only the granite of Granite Peak stock contains ramifying dikes that extend into adjacent phases of the batholith, supporting the conclusion that the Granite Peak stock is the youngest component of the batholith.

In the following sections, phases of the batholith will be described in order of decreasing age as shown in table 7.

DIORITE AND DIORITE PORPHYRY—The diorite and diorite porphyry map unit includes mostly rocks ranging in composition from monzodiorite to monzonite, which occur in two ways: 1) as rounded xenoliths, or 2) as wispy, ragged, intruded patches. In both cases the rock is medium gray, exhibits a fine to medium equigranular texture, and locally contains scattered, euhedral, alkali-feldspar phenocrysts approximately 1 cm long that may be metasomatic in origin. Biotite is the most abundant mafic mineral, constituting 20-30 percent of the rock. The origin of the xenoliths is in doubt. They could be interpreted as cumulates, the product of fractional crys-

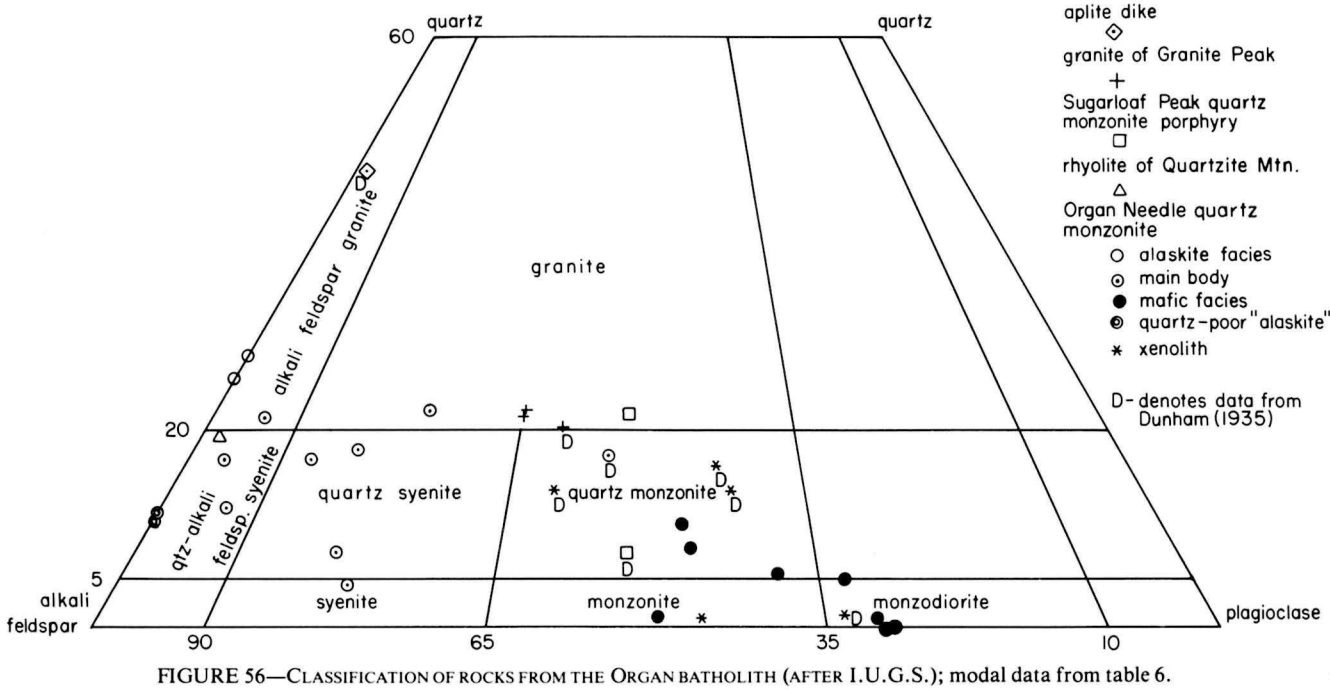


FIGURE 56—CLASSIFICATION OF ROCKS FROM THE ORGAN BATHOLITH (AFTER I.U.G.S.); modal data from table 6.

TABLE 6—MODAL ANALYSES OF THE ORGAN BATHOLITH AND RELATED ROCKS; asterisk * denotes amphibole unidentified and possibly sodic (data by D. Herrell; point count = 1,000 points).

Description	Sample number	Quartz	K-spar	Plagioclase	Biotite	Hornblende	Pyroxene	Opaques	Accessories
rhyolite (sill) of Quartzite Mountain	76WS1	18.8	77.2	1.4	1.3	0.1	—	1.2	—
rhyolite of Baylor Peak	76WS39	4.6	28.1	2.5	0.2	0.5	—	0.2	—
Sugarloaf Peak quartz-monzonite porphyry	75WS30	19.2	32.8	37.5	3.9	3.9	—	1.9	0.8
granite of Granite Peak	78WS43	20.5	48.6	25.7	3.6	—	—	0.6	1.0
granite of Granite Peak	77WS119	20.8	48.1	25.6	3.8	—	—	1.7	—
Organ Needle quartz monzonite-alaskite facies	77WS77	25.3	71.3	—	0.2	0.2*	—	2.4	0.6
Organ Needle quartz monzonite-alaskite facies	77WS87	27.4	70.5	—	0.3	0.3*	—	0.8	0.7
Organ Needle quartz monzonite-quartz-poor alaskite	76WS44	10.7	83.4	—	—	3.4	—	2.1	0.4
Organ Needle quartz monzonite-quartz-poor alaskite	76WS31	11.3	85.0	—	—	1.5	—	1.9	0.3
Organ Needle quartz monzonite-main body	77WS86	20.3	70.2	5.4	0.7	0.8	—	1.8	0.9
Organ Needle quartz monzonite-main body	76WS41	17.1	63.9	13.9	0.2	2.4	—	1.5	1.1
Organ Needle quartz monzonite-main body	77WS92	15.6	75.9	4.4	1.3	—	—	2.5	0.3
Organ Needle quartz monzonite-main body	78WS40	12.2	78.1	6.5	0.8	—	—	1.6	0.8
Organ Needle quartz monzonite-main body	77WS100	21.0	56.8	18.0	0.4	1.7	—	1.5	0.6
Organ Needle quartz monzonite-main body	78WS47	16.2	68.8	10.3	1.5	0.7	—	1.3	1.2
Organ Needle quartz monzonite-main body	77WS20	6.9	67.0	16.2	0.1	5.5	—	2.5	1.8
Organ Needle quartz monzonite-lowest part	78WS46	4.2	68.1	17.7	1.7	5.2	—	1.8	1.3
Organ Needle quartz monzonite-transitional to mafic facies	77WS129	5.2	32.5	51.2	2.4	5.1	—	1.7	1.9
Organ Needle quartz monzonite-transitional to mafic facies	77WS128	6.7	37.4	40.0	2.6	9.5	—	2.6	1.2
Organ Needle quartz monzonite-middle part, mafic facies	77WS127	1.0	39.5	39.7	2.7	5.0	6.7	3.5	1.9
Organ Needle quartz monzonite-lower part, mafic facies	77WS126	4.5	27.3	45.3	8.4	4.2	6.1	3.0	1.2
Organ Needle quartz monzonite-lower part, mafic facies	78WS44	8.0	21.7	50.4	5.9	4.6	10.1	4.5	1.0
Organ Needle quartz monzonite-mafic facies	77WS131	8.6	35.9	39.9	4.2	7.5	—	2.9	1.0
xenolith in Organ Needle quartz monzonite	77WS136	0.8	37.6	44.6	2.9	8.5	—	3.0	2.6
dike? cutting Organ Needle quartz monzonite	77WS101	14.2	44.8	30.2	3.9	3.6	—	1.9	1.4

TABLE 7—AGE RELATIONS, ROCK TYPES, AND SILICA CONTENT OF DIFFERENT PHASES OF THE ORGAN BATHOLITH (major phases are noted by *).

	Phases	Major rock types	SiO_2
youngest	granite of Granite Peak*	granite	67 percent
	Sugarloaf Peak quartz *monzonite porphyry**	granite and quartz *monzonite*	61-62 percent
age relations not known	rhyolite sill of Quartzite Mountain	quartz-alkali feldspar syenite	
	rhyolite porphyry of Baylor Mountain (may be pressure-quenched facies of Organ Needle quartz monzonite)	rhyolite porphyry	
	Organ Needle quartz monzonite*	compositional facies ranging from alaskite to quartz-alkali feldspar syenite to monzodiorite	56-77 percent
oldest	diorite and diorite porphyry	not studied in thin section	

tallization in the parent-magma chamber, or as representatives of an early stage in the development of the magma chamber before silicic differentiation had modified the intermediate-composition parent magma. The wispy, intruded patches might represent a mafic differentiate that was only partly crystallized when the Organ batholith was emplaced.

ORGAN NEEDLE QUARTZ MONZONITE—The Organ Needle quartz monzonite, the oldest major phase of the batholith, forms much of the high backbone and rugged central part of the Organ Mountains, including the Needles and Rabbit Ears (figs. 57 and 58). The pluton is exposed through a vertical distance of 4,500 ft. Contacts and geometry described for the batholith as a whole apply particularly to the Organ Needle pluton because this phase forms most of the central and southern part of the batholith (geologic map, sheet 1, in pocket). From Sugarloaf Peak northward, most of the Organ Needle pluton was intruded and displaced by the slightly younger Sugarloaf Peak quartz monzonite porphyry stock. From the unchilled and mutually embayed contacts it is clear that the Organ Needle and Sugarloaf Peak plutons, as well as the hypabyssal rhyolite porphyry of Baylor Mountain, were emplaced almost simultaneously, cooling as a single unit. That the Organ Needle is oldest, however, is indicated by 1) slight flow alignment of crystals in the younger rocks along contacts, and 2) by minor short apophyses and blurred veins of younger phases cutting Organ Needle rocks. Compositionally, the Organ Needle pluton is the most complex phase in the batholith.

As shown in fig. 56, composition of the Organ Needle quartz monzonite ranges from monzodiorite to quartz-alkali feldspar syenite to alaskite. However, the bulk of the pluton is medium-grained to porphyritic quartz syenite and quartz-alkali feldspar syenite, and this constitutes one of three important facies of the rock mass. A second facies, alaskite and related rocks, occurs in cupolas or immediately beneath the roof. The third facies, a dark-colored mafic rock ranging in composition from quartz monzonite to monzodiorite, is located in the central part of the pluton.

Alaskite occurs discontinuously just beneath the roof of the batholith or comprises small apophyses that pro-

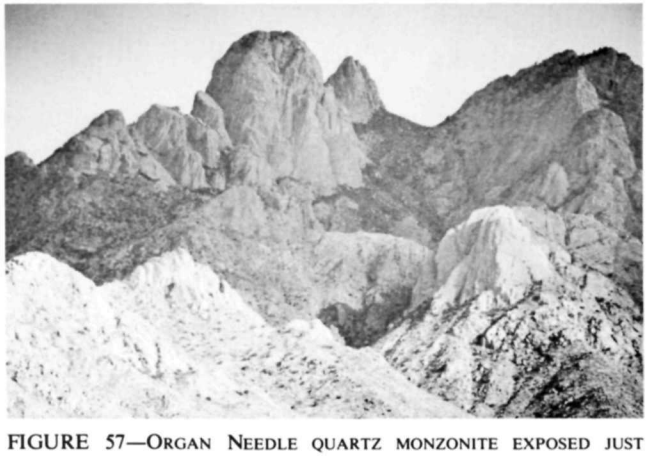


FIGURE 57—ORGAN NEEDLE QUARTZ MONZONITE EXPOSED JUST SOUTH OF BAYLOR CANYON in this view taken by Bob Sigmon (courtesy *Las Cruces Sun News*); view to east.

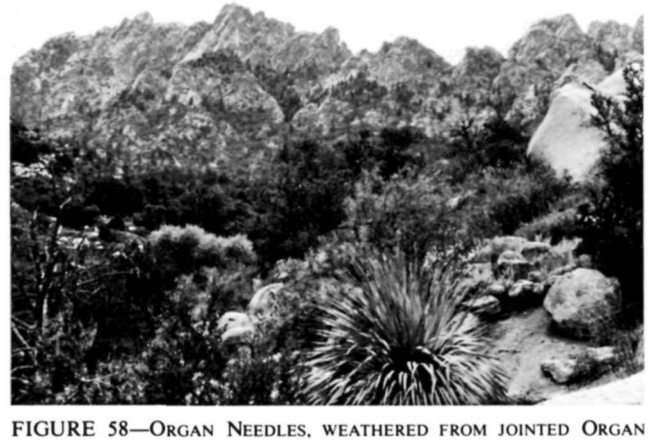


FIGURE 58—ORGAN NEEDLES, WEATHERED FROM JOINTED ORGAN NEEDLE QUARTZ MONZONITE, AS VIEWED FROM THE VICINITY OF AGUIRRE SPRING; view to southwest.

ject well up into the volcanic roof, as in Dorsey Canyon. The rock is fine to medium grained and ranges from light gray and slightly porphyritic in the apophyse noted above to pink and equigranular near the Stevenson–Bennett mine. The gray, porphyritic variety contains subhedral, prismatic perthite approximately 3 mm long set in a groundmass consisting mostly of quartz and perthite. It is also distinguished by approximately 77 percent SiO_2, 25 percent modal quartz, and less than 4 percent magnetite, accessory minerals, and mica. The pink variety consists of 85 percent perthite in subhedral to equant grains approximately 1 mm long, only 11 percent quartz, and 4 percent other minerals; it is referred to as quartz-poor alaskite in fig. 56. Both rocks grade abruptly into coarser grained rock representative of the main body of the Organ Needle quartz monzonite.

Quartz syenite–quartz-alkali feldspar syenite facies make up the bulk of the Organ Needle quartz monzonite. This facies is coarse grained, equigranular or slightly porphyritic, and ranges in color from brick red in the Soledad Canyon area to gray to buff elsewhere. Quartz syenite and quartz-alkali feldspar syenite are the most common rock types, but locally these grade to quartz monzonite or even granite, and outcrops along the eastern side of the batholith near Texas Canyon are syenite. Silica content ranges from 68 percent in the most silicic rocks sampled to 61 percent in the syenite. The most distinctive feature of this facies is the conspicuously zoned feldspar crystals that compose much of the rock. These crystals have lavender or gray oligoclase centers that are mantled with white to tan perthite. Differential weathering of the crystals, deepest in the cores, makes them easy to spot. Pale-tan aplite dikes are moderately common, and locally there are clusters of diorite or monzodiorite xenoliths.

Thin sections reveal textures varying from medium grained, seriate miarolitic to coarse grained, equigranular porphyritic. Coarser grained varieties, with feldspar grains averaging 7-8 mm, are typical of the syenitic rocks. Feldspar composes more than 70 percent of most samples studied; it is mostly perthite mantling oligoclase, as described above. Most oligoclase cores are equant, euhedral crystals, while overgrowth perthite may be phenocrystic, or consist of anhedral to subhedral grains filling open spaces. Interstices also commonly are filled with anhedral mosaics of perthite that are not overgrowths. Less than 2 percent each of biotite, hornblende, magnetite, sphene, and apatite is generally present, except in the syenitic rocks that contain approximately 5 percent hornblende. Quartz, difficult to see in hand specimens even with a lens, generally composes 10-15 percent of the more silicic parts of the facies, and occurs as interstitial grains or graphic intergrowths at the edges of perthite crystals. Less than 5 percent quartz is present in the syenite.

Compositional zoning in the Organ Needle pluton is suggested by the chemical and mineral data at hand (fig. 59). The most silica- and quartz-rich facies (alaskite) is found beneath the roof, while the most silica- and quartz-deficient part (syenite) forms the eastern margin (lowest exposed part) of the pluton. The syenite also appears to be enriched in hornblende and oligoclase relative to western (higher) parts of the pluton. This distribution of facies as well as the well-zoned alkali feldspar that distinguish the Organ Needle rocks could be accounted for by crystal fractionation. The zoning in alkali feldspar is a possible product of settling of those crystals; sinking of alkali feldspar and hornblende could also account for the upward enrichment of silica in the pluton. More thorough study of these rocks is necessary, however, to confirm this hypothesis.

Dunham (1935) interpreted the *mafic facies* to be a separate pluton (his Qm_1) and the oldest phase of the batholith. However, the mafic facies is entirely gradational (over 100-200 yds) with the main body of the Organ Needle quartz monzonite and thus is here regarded as a facies of that pluton. Nevertheless, there is a strong possibility that the facies was emplaced as a separate injection of unusually mafic magma that mixed with the surrounding Organ Needle magma to produce the gradational boundary. Now largely obliterated by younger intrusives, the mafic facies occurs mostly as septa between them. Its original form appears to have been a steep, cylindrical body located near the center of the exposed part of the batholith.

The mafic facies is conspicuously darker colored

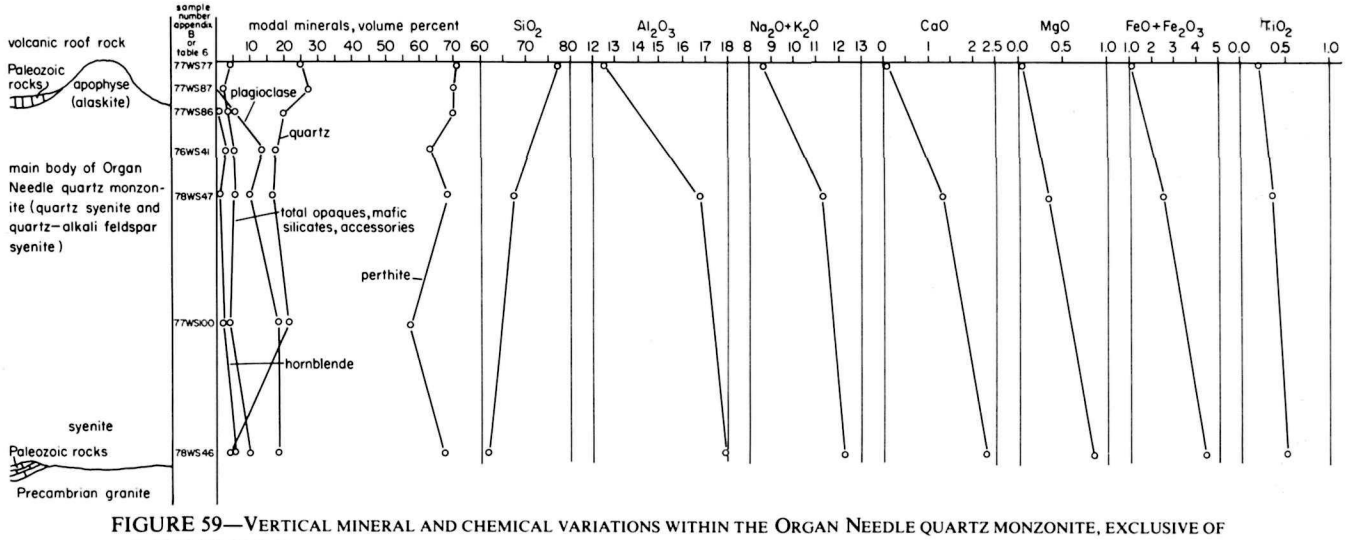


FIGURE 59—VERTICAL MINERAL AND CHEMICAL VARIATIONS WITHIN THE ORGAN NEEDLE QUARTZ MONZONITE, EXCLUSIVE OF THE MAFIC FACIES.

(C.I. = 10-25) than the rest of the Organ Needle rocks. It also is clearly zoned in composition, becoming relatively richer in plagioclase and mafic minerals (particularly pyroxene) and poorer in quartz and K-feldspar toward the interior of the facies. Quartz is virtually absent in the most mafic part of the facies. Mineral variations are accompanied by a concentric zonation of rock types from nepheline-normative monzodiorite in the interior of the facies, grading imperceptibly outward through monzonite and quartz monzonite, to the syenitic or quartz-syenitic rocks of the main body of the Organ Needle pluton. Chemical variations also parallel the mineral variations and both are shown on fig. 60.

Aside from being obviously richer in mafic minerals, particularly pyroxene, the mafic facies differs in other ways from the rest of the Organ Needle rocks. For one thing, it is finer grained (average grain size 2-4 mm) and equigranular. As in other facies of the Organ Needle pluton, oligoclase is the only plagioclase. In the mafic facies, however, oligoclase constitutes 40-50 percent of the rock in contrast to the 18 percent or less found in other facies of the Organ Needle pluton. Furthermore, unlike the rest of the Organ Needle rocks, the oligoclase lacks zoning and exhibits a rather indistinct albite twinning. Orthoclase rather than perthite is the dominant K-feldspar phase, although orthoclase perthite does occur. Much of the K-feldspar is interstitial, but some mantles oligoclase as it does in other facies and phases of the batholith. Pyroxene, absent in all other parts of the batholith, is the dominant mafic mineral in the mafic facies; however, there is nearly as much biotite and hornblende present. The pyroxene and hornblende form subhedral prismatic grains and the biotite forms anhedral, poikilitic patches or plates. Frequently, hornblende rims pyroxene and biotite replaces hornblende. Some of the biotite forms radiating tufts as an alteration of pyroxene and magnetite. This secondary biotite may document mineral reaction of the mafic facies to emplacement of the adjacent, more silicic granite of Granite Peak. From the foregoing discussion, it seems clear that the mafic facies is compositionally and texturally unlike other facies of the Organ Needle pluton. However, the differences are most distinct at the center of the mafic facies and become less distinct as the outlying, more silicic rocks of the Organ Needle pluton are approached.

The mafic facies probably represents a separate intrusion of magma, perhaps derived from a deeper level in the source-magma chamber than had previously been tapped in the course of volcanic eruptions. If so, emplacement of this magma coincided with emplacement of the rest of the Organ Needle pluton so that the two compositionally distinct magma bodies mixed at their contact boundary.

RHYOLITE PORPHYRY OF BAYLOR MOUNTAIN—The high ridge surmounted by Baylor Peak is capped by a sheet of rhyolite porphyry, herein called rhyolite porphyry of Baylor Mountain. On top of the mountain the sheet dips west approximately 30 degrees, but near the western base it steepens to nearly vertical. The rhyolite transects its host, the Organ Needle quartz monzonite; however, contacts between the two are mutually embayed and offer little evidence of chilling. Mineralogically, the rhyolite resembles the Organ Needle phase of the batholith, so it seems to be genetically as well as spatially related to it.

Besides the medium-gray color and fine-grained porphyritic texture, the most distinctive features of the rhyolite are: 1) abundant dark, angular xenoliths of volcanic rock, 2) conspicuous rounded quartz xenocrysts with embayed edges, and 3) tabular pink perthite phenocrysts up to 4 mm long. The perthite usually mantles oligoclase. The groundmass, which composes 45-65 percent of the sections studied, consists of mosaics of subhedral quartz and feldspar with an average grain size of 0.5 mm. The rounded quartz grains, together with an occasional quartzite or sandstone xenolith, are probably all of sedimentary origin; hence the 72 percent SiO_2 reported for the rock (appendix B) may not be an accurate measure of its magmatic silica content. Mafic minerals compose less than 4 percent of the rock and include anhedral patches of hornblende, biotite, and magnetite, usually associated with subhedral sphene.

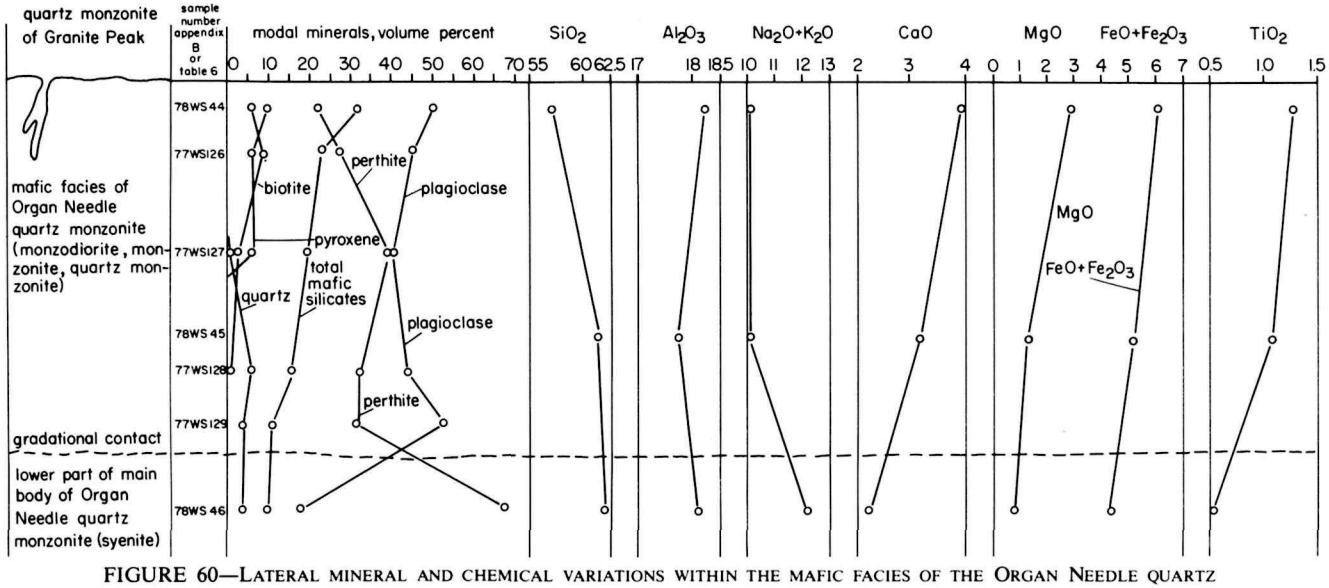


FIGURE 60—LATERAL MINERAL AND CHEMICAL VARIATIONS WITHIN THE MAFIC FACIES OF THE ORGAN NEEDLE QUARTZ MONZONITE.

In an interpretation of the origin of the rhyolite porphyry of Baylor Mountain, two relationships need to be explained: 1) the quenched, fine-grained texture typical of a subvolcanic pluton, and 2) its compositional similarities with and spatial association to the Organ Needle phase of the batholith. Perhaps the rhyolite porphyry represents part of the Organ Needle magma that became mobile and moved upward from lower parts of the chamber, perhaps even venting at the surface. While no evidence exists of temperature differences between the two magma fractions that might have caused quenching, a sufficient pressure drop and loss of volatiles could freeze the rhyolite as it passed through upper parts of the batholith or its roof (Jahns and Tuttle, 1963). In order to create sufficient pressure drop and loss of enough volatiles to freeze the magma, the intrusive probably had to vent to the surface.

RHYOLITE OF QUARTZITE MOUNTAIN—The rhyolite of Quartzite Mountain is exposed in a sill up to several hundred feet thick within Pennsylvanian limestone and shale beds in Quartzite Mountain and adjacent areas. At the surface it is actually connected to the batholith in only one small area near the Excelsior mine, where the rhyolite (in the form of a laccolith) has been invaded by Sugarloaf Peak quartz monzonite porphyry. The rhyolite is therefore older than the Sugarloaf Peak, but age relations with other phases of the batholith are unknown. The rhyolite sill in the Quartzite Mountain area is inferred to be connected with the batholith at depth.

The rhyolite ranges from light gray to buff to pale orange and has a fine, equigranular texture almost like aplite. Perthite and quartz compose most of the rock; plagioclase, biotite, a trace of hornblende, and magnetite are also present. Some perthite probably has plagioclase cores. Mineralogically, the rhyolite resembles alaskite found at the top of the Organ Needle pluton. Like the alaskite, the rhyolite may represent a differentiate, but unlike the alaskite, the latter was injected as sills into the roof of the batholith.

SUGARLOAF PEAK QUARTZ MONZONITE PORPHYRY—Most of the northern part of the batholith is composed of the Sugarloaf Peak quartz monzonite porphyry that nearly equals in volume the Organ Needle phase of the batholith. The porphyry is well exposed in Sugarloaf dome (fig. 10), at Aguirre Spring, at San Agustin Pass, and throughout the Organ mining district (fig. 18); it also underlies much of the pedimented lowland east of San Agustin Pass. At San Agustin Pass biotite from the Sugarloaf Peak indicated an age of 32.8 m.y. (Loring and Loring, 1980).

Roughly oval in plan and approximately 8 mi long, the Sugarloaf Peak stock invaded the northern part of the Organ Needle pluton. The southern edge of the Sugarloaf Peak stock cuts steeply across the mafic facies of the Organ Needle pluton, and a few short veinlike dikes with blurred edges extend into the mafic rocks. Eastern and western contacts of the stock offer little information, except that: 1) Sugarloaf Peak rocks have sharp but unchilled contacts where they transect the older pluton, and 2) north of Organ, concordant contacts with Paleozoic roof strata are exposed in several places. Along the northern edge of the pluton the contact with Paleozoic strata becomes cross cutting, but it generally dips only moderately northward. In contrast to the rest of the batholith, whose magma was relatively dry, the Sugarloaf Peak exhibits a variety of rocks and hydrothermal effects that indicate that the magma was relatively rich in volatiles when it was emplaced.

Several varieties of dikes cut the Sugarloaf Peak pluton, especially in the Organ–San Agustin Pass area. Of these, the most abundant are discontinuous aplites, locally in swarms. Pegmatite dikes and pods and quartz veins also are common, but far less abundant than the aplites. Some pegmatites are notable for their content of base and precious metals, and these are described further under mineral deposits. At least two kinds of rhyolite dikes, one flow banded and another nearly aplitic in texture, also transect the northern part of the Sugarloaf Peak. Finally, hornblende monzonite or latite porphyry dikes are present north of Organ. Dated 32.5 m.y. (average of two dates, 32.07 m.y. and 32.95 m.y.) by Loring and Loring (1980), the dikes are extensively altered and thought to be associated with mineralization in parts of the Organ district.

Metamorphism, metasomatism, and hydrothermal alteration are especially intense in the same general area as the dikes. Pervasive quartz-sericite or sericite alteration of the Sugarloaf Peak is present east and north of Organ; some sericite has been dated 34.4 m.y. (Loring and Loring, 1980). Chlorite-quartz alteration along shear zones in the quartz monzonite porphyry can also be found over a wide area. Marbleization, formation of calc-silicate minerals, and hydrothermal mineralization have modified most outcrops of limestone adjacent to the igneous rocks. These are described further under metamorphism and mineral deposits.

In hand specimens or outcrops, the Sugarloaf Peak is a gray to pinkish-gray, coarse-grained rock with a granitic appearance. Large pink perthite phenocrysts (1-2 cm square) weather to cream-colored square fragments, common in the soil. Most outcrops exhibit at least a few medium-gray, medium-grained, equigranular, rounded xenoliths; locally they occur in swarms, crowded together as closely as boulders, cobbles, and pebbles in a stream bed (fig. 61). Many of the xenoliths resemble the mafic facies of the Organ Needle pluton



FIGURE 61—SWARM OF "MAFIC" XENOLITHS—OR MORE LIKELY AUTOLITHS—IN SUGARLOAF PEAK QUARTZ MONZONITE PORPHYRY EXPOSED ALONG PINE TREE TRAIL; in composition, the rounded equigranular fragments range from monzonite to monzodiorite.

and are compositionally similar (fig. 56). Schlieren, formed by flow alignment of biotite and hornblende, is locally present at the margins of the pluton, especially in the Indian Springs Canyon area; however, in general, this phase of the batholith is structureless and apparently homogenous in composition. Uncommon miarolitic cavities up to several feet wide contain museum-quality aggregates of twinned orthoclase, albite, smoky quartz crystals (figs. 62 and 63), and gemmy apatite (V. C. Kelley, personal communication, 1979).

In thin section, the rock is coarse grained and seriate to porphyritic. Orthoclase perthite occurs both as well-formed crystals and as anhedral, interstitial grains. It mantles plagioclase only rarely. Plagioclase is oligoclase, generally in subhedral, tabular to euhedral prismatic, white crystals up to 1.1 cm long. Frequently the oligoclase is zoned, becoming more sodic outward. Biotite and pale green hornblende compose 10-12 percent of the volume of the rock. Quartz exists as interstitial grains and as myrmekitic intergrowths between perthite and plagioclase crystals. Quartz ranges from less than 10 to more than 20 percent in the samples studied; those with more than 20 percent quartz are granite porphyry (fig. 56).

GRANITE OF GRANITE PEAK—The high, rugged, east-central part of the Organ batholith is formed mostly of the granite of Granite Peak. Exposed through a vertical distance of 3,500 ft, the pluton appears to be a steep-sided, cylinder-shaped body approximately 2 mi wide and 3 mi long. It apparently represents the last batch of magma to rise into the batholith, and it is more silicic (67 percent SiO_2) than any of its predecessors except for the most silicic parts of the Organ Needle pluton. The relative age of the Granite Peak is based on the long dikes that extend from the Granite Peak stock across adjacent parts of the Organ Needle phase of the batholith. The dikes require that the Organ Needle pluton be essentially solidified when the Granite Peak stock was injected, a condition generally not true when other phases of the batholith were emplaced.

Massive, nearly homogeneous granite (fig. 56) is characteristic of the Granite Peak stock. Equigranular pink

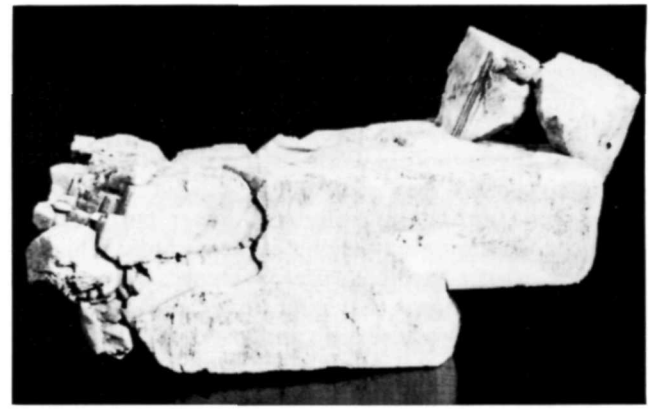


FIGURE 63—TWINNED ORTHOCLASE CRYSTALS FROM SAME LOCALITY THAT YIELDED SPECIMEN IN FIG. 62; such crystals often show Baveno and Carlsbad twins; specimen is 7 inches long.

alkali feldspar, shiny biotite, and abundant glassy quartz are conspicuous in the rock, which is distinctly more cream colored than the surrounding gray to tan Organ Needle rocks. Many short, narrow aplite dikes are associated with this phase, but there are no known pegmatites. Mafic, fine- to medium-grained xenoliths are common, though not abundant. A large part of the stock carries a sulfide system, mostly disseminated pyrite (up to 3 or 4 percent) and some chalcopyrite. The stock was not tested for molybdenum. Quartz-sericite alteration is pervasive and extensive along the contact with a large roof remnant of Orejon Andesite, which overlies the stock (fig. 64). Blue lazurite or lazulite is conspicuous in parts of the alteration aureoles.

Thin sections reveal that alkali feldspar, the most abundant mineral, is orthoclase perthite. It occurs as interstitial anhedral grains, as subhedral prismatic grains, and as phenocrysts up to 3 mm long. Some perthite mantles oligoclase. Most oligoclase, however, is present as subhedral to euhedral prismatic grains up to 6 mm long. Quartz, as interstitial grains or as fine graphic intergrowths with alkali feldspar, makes up more than 20 percent of the rock. Fresh biotite is the only mafic mineral present, other than a little magnetite.

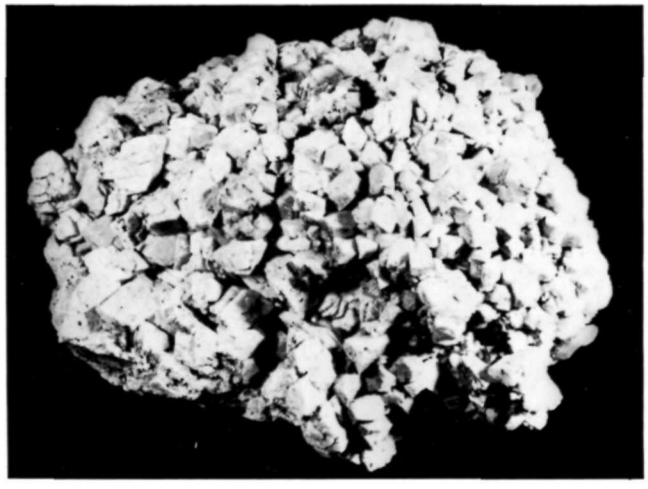


FIGURE 62—CLUSTER OF TWINNED ALBITE CRYSTALS FROM LARGE MIAROLITIC CAVITY IN SUGARLOAF PEAK QUARTZ MONZONITE PORPHYRY; largest crystals are nearly two inches across; specimen is approximately 10 inches across.

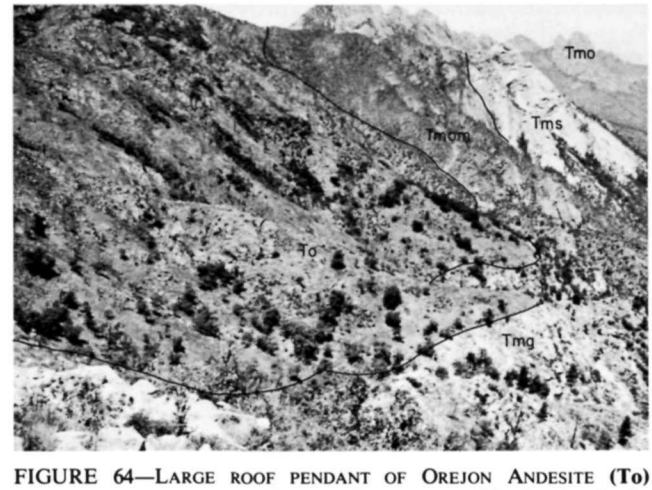


FIGURE 64—LARGE ROOF PENDANT OF OREJON ANDESITE **(To)** OVERLYING GRANITE OF GRANITE PEAK STOCK **(Tmg)**; view looks westward toward Sugarloaf and Organ Needles; **Tmom**—mafic facies; **Tmo**—quartz-alkali feldspar syenite facies; **Tms**—Sugarloaf Peak quartz monzonite porphyry.

Summary and discussion

Between 45 and 36 m.y. ago intermediate-composition volcanic activity in the Organ area may have represented an early stage in the rise and evolution of the Organ batholith, particularly if the volcanism proves to be of the younger age. By 33-33.7 m.y. ago silicic magma had accumulated in a shallow chamber and the upper part of the accumulation erupted as three large rhyolitic ash-flow tuff sequences. Each successive eruption was more voluminous than its predecessor. In all, a thickness of approximately 10,000 ft of pyroclastic material was ejected and accumulated in a large subsiding caldera. Outpouring of lavas followed. Rhyolitic to trachytic in composition and at least 1,000 ft thick, the lavas apparently were the final phase in the cycle of volcanic activity.

Zoning in the magma chamber

The chemistry and mineralogy of the ash-flow tuffs and lavas show that a compositionally zoned magma chamber was tapped at successively deeper levels by successive eruptions. The top of the magma chamber, represented by the earliest tuffs, consisted of high-silica (77 percent), crystal-poor rhyolite that graded downward into silica-poor (68 percent) sanidine-rich rhyolite. This part of the magma chamber erupted as the last of the tuff sequence. Following a short hiatus in volcanism, porphyritic rhyolite, dacite, and trachyte lava flows, whose chemical composition approaches that of much of the batholith (61-68 percent), erupted from the upper part of the remaining magma body. However, differences in chemical composition between the youngest tuffs and the lava sequence (fig. 45) suggest a compositional gap in the erupted magmas that corresponds to the hiatus between ash-flow and lava eruptions. The idea is supported by the fact that plagioclase phenocrysts rather than sanidine dominate the lavas, approximately half of the phenocrysts showing signs of disequilibrium. Perhaps significant chemical or mineral changes took place in the magma chamber during the brief hiatus, either through fractionation, addition of new magma into the chamber, or pressure-temperature re-equilibration following eruption of the tuffs.

Similarly zoned magma chambers inferred from chemical and mineral variations in ash-flow tuffs and lavas elsewhere have been described by Williams (1942), Ratté and Steven (1964), Lipman and others (1966), Smith and Bailey (1966), Giles (1967), and Hildreth (1979). Hypotheses to account for the zonation include crystal settling, assimilation, partial melting, magma mixing, volatile transfer, and convection-driven thermogravitational diffusion.

Not enough data is available yet to determine which of these processes might account for zoning of the Organ magma chamber, although some of the data is consistent with two of the processes noted above. The lack of disequilibrium crystals in upper parts of the tuff sequence suggests that crystal settling was not an important process in zoning of the magma volume erupted as tuffs. On the other hand, major-element chemical variations in the tuffs are similar to those in the Bishop tuff, from which Hildreth (1979) developed his thermogravitational diffusion hypothesis (Shaw and others, 1976). In the case of lower parts of the magma chamber, represented by the lavas, disequilibrium plagioclase phenocrysts might indicate that crystal fractionation was a zoning process in operation. (However, other processes could account equally well for the disequilibrium textures.)

Depth, water-vapor pressure, and temperature of the magma chamber

Because the normative-quartz (Qz), albite (Ab), and orthoclase (Or) compositions of the tuffs in the Organ cauldron complex approach 100 percent, the experimental system Qz-Ab-Or-H_2O (Tuttle and Bowen, 1958) can be used to make estimates of water-vapor pressure, temperature, and depth to the magma chamber that yielded the volcanic rocks (Lipman, 1966). The results of some of Tuttle and Bowen's studies are shown in fig. 65. The position of the thermal minimum and ternary eutectic are shown for $P_{H_2O} = 500$, 1,000, 2,000, and 3,000 bars. Each thermal minimum curve indicates the theoretical composition of the remaining magma, at the given water pressure, after ideal fractional crystallization of a rhyolitic magma has accompanied a drop in temperature to the thermal minimum value. Also shown are experimentally based fractionation curves extrapolated from Tuttle and Bowen's (1958) data by Lipman and others (1966). By fractional crystallization, a liquid with an initial composition in the Or-rich part of the feldspar field would, as the temperature dropped, change its composition continuously along one of the fractionation curves until it reached the appropriate thermal valley, at which point quartz and feldspar would crystallize simultaneously. Fractionation curves for $P_{H_2O} = 600$ bars were plotted because they fit most closely the normative Q-Ab-Or trend of the Organ Mountain rocks, shown by circles and plusses on the diagram.

Except for the lavas and vitrophyre, the data points define a reasonably linear trend that is parallel to the fractionation curves and that terminates at the thermal valley curve $P_{H_2O} = \sim 1{,}700$ bars (the normative Q + Ab + Or in the phenocryst-rich lavas ranges from 81 to 87; therefore, these rocks do not approach either magmatic liquids or Tuttle and Bowen's (1958) experimental system as closely as the phenocryst-free silica-rich rocks, and this may account for their deviation from the general linear trend—the anomalous data point given by the vitrophyre is thought to result from a change in the K:Na ratio due to alteration). Taken at face value, this indicates water pressures in the magma chamber were approximately 1,700 bars when the tuff erupted. However, a basic assumption here is that rocks with the highest silica content and Q:Ab:Or ratios were sampled, and this may not be the case. If $P_{H_2O} = 1{,}700$ bars is an accurate estimate of the water-pressure conditions at eruption, Tuttle and Bowen's (1958) fractionation curves for 1,000 bars or 2,000 bars curves should fit the compositional trend more closely than they do, and the 600 bar curves should not fit as closely as they do. Thus, the data are conflicting, and P_{H_2O} in the upper part of the erupted magma volume can be estimated no closer than 600 to 1,700 bars, perhaps nearer the former value. Assuming that water pressure was equal to lithostatic pressure, which seems likely but not provable by the data at hand, depth to the top of the magma cham-

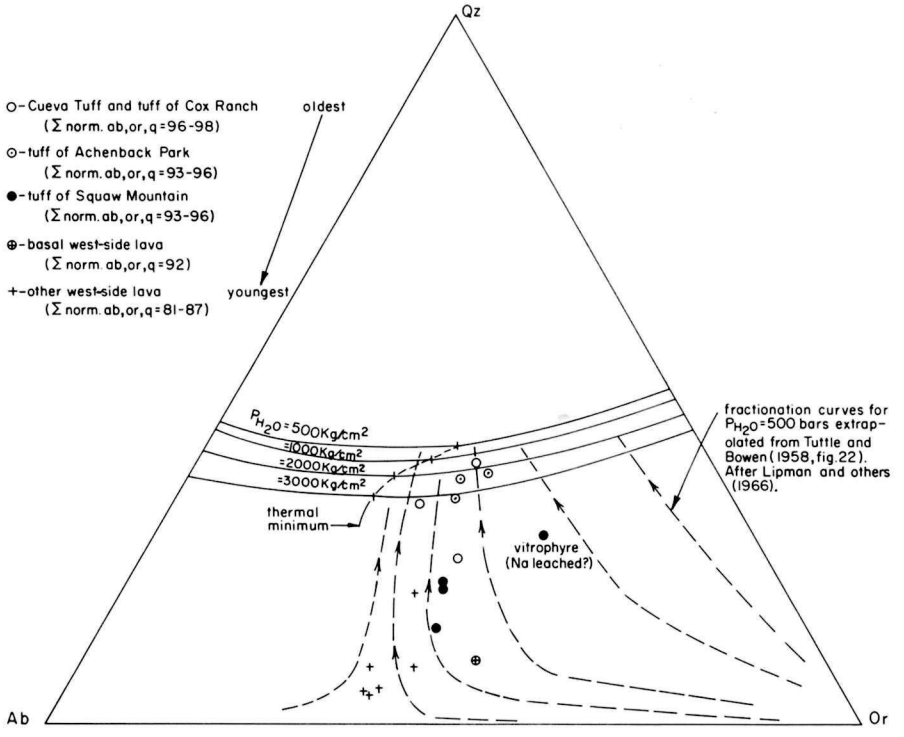


FIGURE 65—DIAGRAM SHOWING COMPOSITIONAL TREND OF OLIGOCENE ASH-FLOW TUFFS AND LAVAS IN THE SYSTEM Qz-Ab-Or; isobaric temperature minima and quartz-feldspar cotectics are after Tuttle and Bowen (1958). Fractionation curves are after Lipman and others (1966), who extrapolated them from Tuttle and Bowen.

ber was 1.4-3.7 mi, a value comparable with the 2-mi-thick roof of volcanic rocks observed above the batholith today. Finally, experimental data of Tuttle and Bowen (1958, p. 58) indicate a water content of 3-5.5 percent and temperature of 700° to 750°C in the top of the erupted magma volume.

Organ cauldron

Eruption of such an enormous volume of magma from such a shallow reservoir almost always results in formation of a sizable caldera, often of the resurgent type (Smith, 1960; Smith and Bailey, 1968; Ratté and Steven, 1967; Byers and others, 1975; Steven and Lipman, 1976; Rhodes, 1976). That eruption of at least two of the three major tuff units in the Organ Mountains also produced calderas whose subsiding floors allowed the tuffs to accumulate to such unusual thicknesses seems an inescapable conclusion.

Unfortunately, only a piece of the Organ cauldron complex is preserved within the Organ range. Much of the cauldron has been uplifted, tilted, intruded by the batholith, buried by widespread gravel deposits, or eroded away, so that its original limits and shape may never be known. The cauldron could be a very large, complex structure containing nested or overlapping cauldrons, each component formed by an outburst of tuff. Even the Doña Ana cauldron might be part of the complex, or the Organ cauldron might be separate from the Doña Ana cauldron but related to the same underlying pluton.

The only direct evidence that suggests the location and nature of a cauldron margin in the Organ range is the thickness variations in the tuffs of Achenback Park and Squaw Mountain. These tuffs are thickest between Soledad Canyon and Achenback Park along the western edge of the range. Both thin northward toward the batholith remarkably quickly, so that in the Cueva rock–Fillmore Canyon area they are only one-quarter to one-third their maximum thickness. The tuff of Achenback Park also thins eastward toward the batholith. In the North Canyon and Boulder Canyon area it is one-half to one-third as thick as it is along the western edge of the range. These variations are best seen on the geologic map, on the cross sections, and in fig. 51. Thinning of tuff units toward the batholith suggests that the batholith may now occupy the eastern margin of the Organ cauldron. Indeed, the steep dips of volcanic rocks adjacent to the batholith are best interpreted as resulting from subsidence at the edge of the cauldron. These steeply dipping rocks, together with comparatively undeformed roof pendants on top of the batholith, constitute a structure best described as a westfacing monocline cored by a ridge of the Organ batholith (fig. 55). The flexure appears to be a hinged margin of the Organ cauldron (fig. 66). The fact that tuff units thin toward this flexure (and the adjacent batholith) argue that emplacement and subsidence of the tuffs and formation of the hinged margin were processes operating together. By this hypothesis, the batholith represents the upper, outer part of the magma chamber into which the volcanic rocks subsided.

The location and nature of the rest of the cauldron boundary is more indefinite than the inferred hinged part. Seager and Brown (1978) suggested that the southern and western boundary of the cauldron might be formed by the major fault zone (Jornada fault) that extends from Rattlesnake Ridge westward past Bishop Cap hills and then northwestward past Tortugas Mountain (fig. 66). The idea was based on three main lines of evidence: 1) the fault zone is arc shaped; 2) the fault

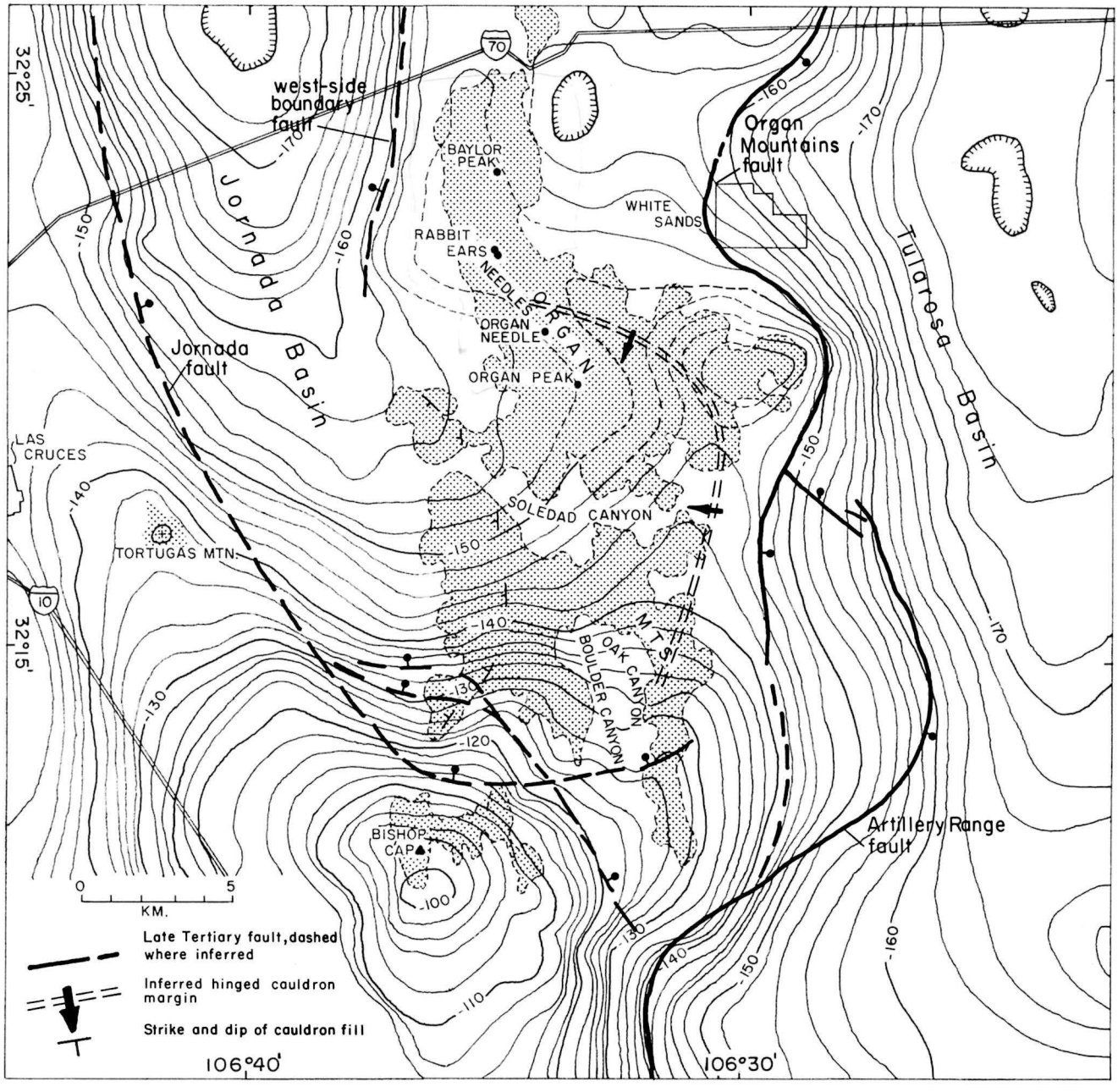


FIGURE 66—COMPLETE BOUGUER GRAVITY MAP OF ORGAN MOUNTAINS AREA BY L. BROWN; contours are in miligals; Late Tertiary faults are shown, together with an inferred hinged margin of the Organ cauldron.

zone separates thick cauldron-fill tuffs from structurally high precauldron rocks (at Bishop Cap and Tortugas Mountain) that might be interpreted as remnants of a cauldron wall, and 3) the Cueva Tuff is thickest and contains the most cooling units adjacent to the fault.

Such an interpretation is not without difficulties, however. For example, the Jornada fault is primarily a major late Tertiary structure that separates grabens from a series of uplifted blocks as far north as the Caballo Mountains. If the segment between Tortugas Mountain and Rattlesnake Ridge is also a cauldron boundary, the late Tertiary fault simply follows the older ring fracture through this part of its course. Unfortunately, no features that usually distinguish ring fracture zones, such as rhyolite intrusions or alteration, have been noted along the fault. Also, the decrease in stratigraphic separation between Rattlesnake Ridge (1,700 ft) and Bishop Cap (8,000 ft, including the offset on the Peña Blanca and Massey Tank faults) indicates that the Jornada fault zone probably branches southward between Rattlesnake Ridge and Bishop Cap, thus creating what would be an unusual embayment in a ring-fracture zone. Consequently, it seems at least equally plausible that the Jornada fault zone is randomly superimposed across the Organ cauldron complex. By this interpretation, part of the fill of the Organ cauldron complex was merely preserved on the downthrown (Organ Mountain) side of the fault, and the fill eroded away over wide areas on the upthrown (Bishop Cap–Tortugas Mountain) side. If this interpretation is correct, other parts of the cauldron should be buried beneath the Mesilla Basin west of the upthrown block. Exploratory geothermal

wells west of Tortugas Mountain may have penetrated an unknown thickness of Soledad Rhyolite (L. N. Chaturvedi, personal communication, 1979).

Organ batholith

The batholith probably represents part of the magma remaining in the chamber after the volcanic rocks were expelled. The fact that batholith and volcanics are virtually the same age and associated with one another is not the only support offered for this conclusion. Chemically, the batholith rocks appear to be consanguineous with the volcanics. This is suggested first by overlapping chemistries portrayed on variation diagrams (figs. 43 and 54) which, however, fall short of convincing proof. The chemical variations offer more compelling evidence when they are related to the time taken to complete the volcanic-plutonic cycle.

With few exceptions there is a steady decline in SiO_2 content of rocks emplaced first as ash-flow tuffs, then as lava flows, and finally as the major phases of the Organ batholith (fig. 67). The most straightforward interpretation of this relation is that the tuffs represent the gas-rich silicic cap of the magma chamber, the lavas a somewhat deeper less-silicic level, and the batholith represents magma that remained in the chamber after the volcanics were erupted.

However, we must remember that the batholith is a composite one, made of several intrusions of different chemical composition. Their chemistries seem related, nonetheless, and they were intruded, except for the final phase, in such rapid-fire progression that they must have been derived from a common magma chamber rather than from successive melting episodes at the base of the crust. Perhaps the various phases of the batholith originated in the following way (summarized in fig. 68):

The oldest, most voluminous phase of the batholith—the Organ Needle quartz monzonite—may represent the outer, upper part of the magma chamber that remained after the silicic tuffs were erupted. Because this part of the batholith has approximately the same range of chemical composition as the west-side lavas, it may also have been the direct source of the lavas. In fact, the pressure-quenched rhyolite porphyry of Baylor Mountain may represent the hypabyssal feeder zone for some

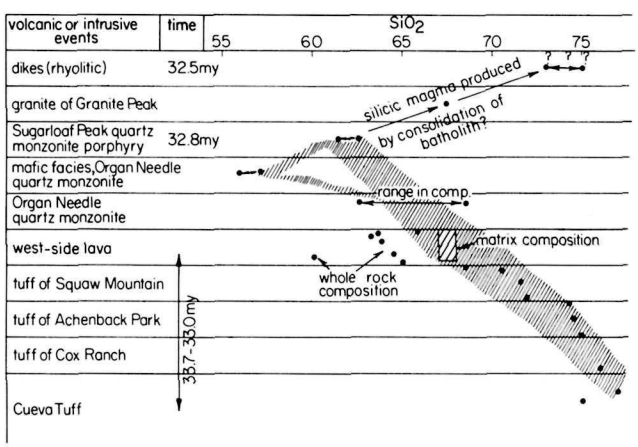


FIGURE 67—DIAGRAM ILLUSTRATING PROGRESSIVE DECLINE IN SiO_2 WITH DECREASING AGE OF VOLCANIC AND PLUTONIC ROCKS, except for the final phases of the batholith, which record increasing SiO_2; see text for discussion.

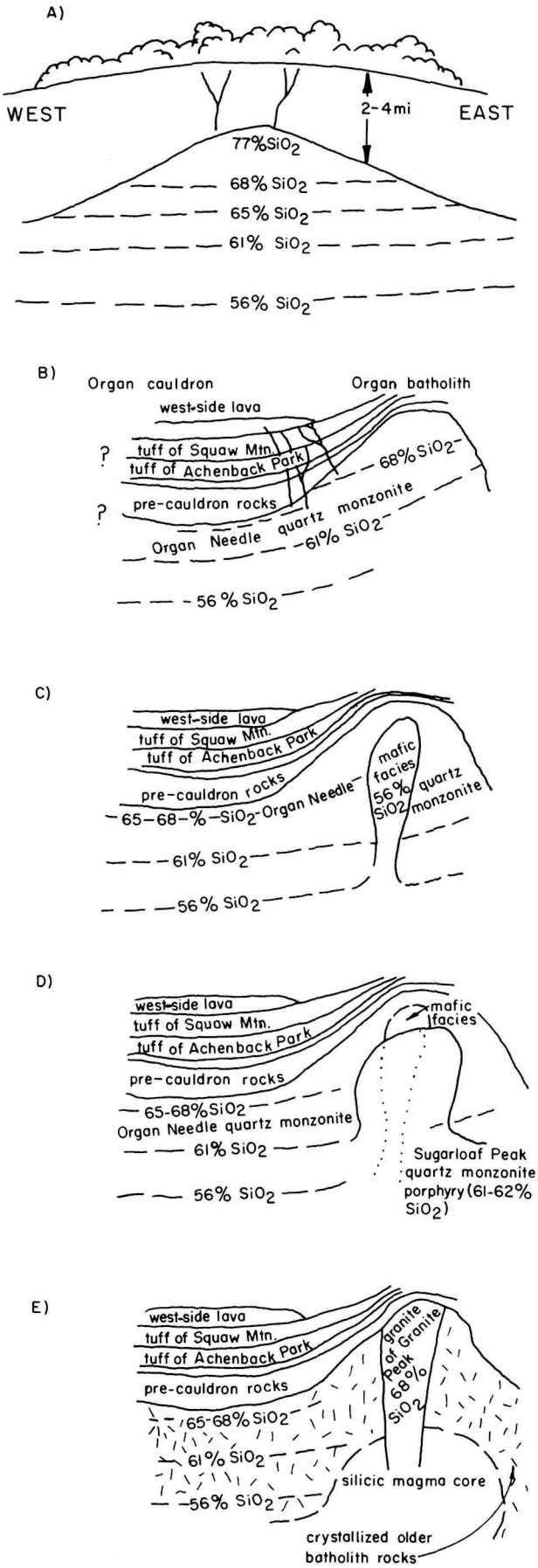


FIGURE 68—DIAGRAMS ILLUSTRATING ONE POSSIBLE EVOLUTIONARY SEQUENCE FOR THE ORGAN MOUNTAINS VOLCANIC-PLUTONIC CYCLE; see text for discussion.

of the lavas. That the Organ Needle magma chamber was compositionally zoned is suggested by chemical and mineral gradients between the roof of the chamber and its lowest exposures—silica (77-61 percent) and quartz (25-4 percent) illustrating the clearest gradients. The more mafic, but unexposed, levels of the Organ Needle pluton may then have been mobilized to supply the mafic facies of the Organ Needle pluton, as well as the other major component of the batholith, the Sugarloaf Peak quartz monzonite. All three of these intrusions cooled essentially as a single unit, judging from the nature of their contacts. Finally, the granite of Granite Peak stock was emplaced. More silicic than its immediate predecessors, this granite was emplaced after the rest of the batholith had crystallized and fractured. Perhaps the stock represents a silicic residual-magma core, the product of progressive crystallization of the magma chamber, that broke through its crystallized roof to be emplaced at a higher level as the final event in construction of the batholith (see Reesor, 1958, for a similar history of the White Creek batholith).

An essential feature of the hypothesis just described is that the Organ batholith is just the outer, upper part of a broader batholith at depth that is probably coextensive with the Organ cauldron. The Organ batholith is viewed as a somewhat ridgelike cupola isolated along the cauldron margin by subsidence of the volcanic section over the central part of the magma chamber (fig. 55). Besides general subsidence of the cauldron fill, huge blocks of the volcanic roof apparently foundered piecemeal into the batholith. The parabolic-shaped Modoc and Long Canyon fault zones enclose such blocks (for example, Ice Canyon cauldron). At least in the case of the Modoc fault, the fault zone was subsequently invaded by dikes and by an apophyse of the batholith itself (fig. 69).

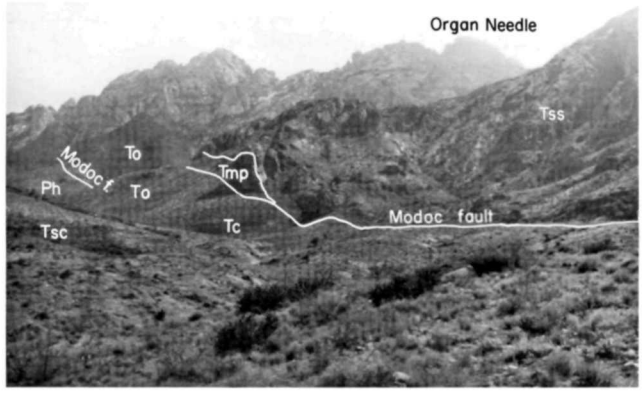


FIGURE 69—MODOC FAULT, BOUNDARY OF THE HUGE FOUNDERED BLOCK OF VOLCANIC ROCKS CALLED ICE CANYON CAULDRON. Tuff of Squaw Mountain (**Tss**) within subsided block on right; Hueco Limestone (**Ph**), Orejon Andesite (**To**), Cueva Tuff (**Tc**), and tuff of Cox Ranch (**Tsc**) to the left of the fault; monzonite porphyry dike (**Tmp**) partially fills fault zone; view to northeast.

Metamorphic effects

A metamorphic aureole 0.1-1 mi wide borders the northern and western margins of the Organ batholith. Paleozoic sedimentary rocks within the aureole are variably altered, especially adjacent to the Sugarloaf Peak quartz monzonite porphyry.

Except for a few areas, thermal metamorphism adequately accounts for most of the textural and mineral changes in the sedimentary rocks, the changes being primarily related to original lithology. Massive sandstone beds in the Bliss, Lead Camp, and Cable Canyon were merely converted to quartzite. Dolomite, dolomitic limestone, and limestone of the El Paso, Montoya, and Fusselman have been extensively recrystallized to massive marble, some of which contains tremolite, garnet, and, according to Dunham (1935), serpentine. Calcium-magnesium silicates are common in the vicinity of chert beds or nodules and near siliceous, laminated beds at the base of the El Paso. Shale in the Percha Shale and Lead Camp Limestone has been converted to hornfels that contains small quantities of fine-grained mica, diopside ($Ca,MgSi_2O_6$), and epidote. Impure sandy limestone and cherty limestone or dolomite produced the widest variety and most conspicuous mineral assemblages. Such beds in the Lead Camp, Rancheria, Las Cruces, and Lake Valley formations contain garnet, specularite, diopside, wollastonite ($CaSiO_3$), epidote, hematite, tremolite [$Ca_2Mg_5(Si_8O_{22})(OH)_2$], and idocrase (complex hydrated Ca,Mg,Fe,Al silicate) as secondary minerals within marble. In many places these minerals occur sparingly and probably formed by simple reaction between original constituents of the sedimentary rocks. In a few places, however, such as near the Modoc, Merrimac, Excelsior, and Memphis mines, huge masses of garnet and other calc-silicate minerals replaced whole limestone beds; this indicates that metasomatism was an important process acting in those areas. In areas beyond the influence of metasomatism but still within the metamorphic aureole, the purer limestone beds were converted to massive, coarse-grained, white to gray marble.

Dunham (1935) lists many other minerals found in the metamorphic aureole. His lists and account of the equilibrium assemblages should be referred to by those interested in details of the metamorphic geology of the area.

Late Tertiary deformation

The latest chapter in the geologic evolution of southern New Mexico, one that is not yet complete, is the development of the modern fault-block mountains and intervening valleys. These structures are the product of persistent east-west extension in the crust, which has pulled apart a relatively narrow, north-trending swath of land from Colorado to Mexico known as the Rio Grande rift (Bryan, 1938; Kelley, 1952; Chapin, 1971; Cordell, 1978; Decker and Smithson, 1975; Cook and others, 1979). According to Chapin and Seager (1975) and Chapin (1979), extension in the rift began 26-32 m.y. ago, following a long period during the middle Tertiary when volcano-tectonic structures, such as those in the Organ Mountains, formed in an essentially neutral stress field. These studies point out a complex evolution of the rift that includes local subsidence of broad, early rift basins in the early Miocene and late Oligocene, initial uplift of some ranges during the Miocene, culmination of rifting in the late Miocene and Pliocene, appearance of basaltic to rhyolitic volcanoes in the rift during and following the culmination, and continued tectonic and volcanic activity of the rift into the late Quaternary.

In this chapter, discussion is focused on the late Tertiary evolution of the northern Franklin–Organ–southern San Andres ranges and adjacent parts of the Tularosa and Jornada Basins. The rock record of this evolution is far from complete and absolute dates of events are unknown, with few exceptions. Nevertheless, geologic relationships between different structures, particularly faults, are sufficiently revealing that one can interpret how the basins and ranges might have evolved.

The first thing that becomes clear when late Tertiary structure in the ranges is examined is that the southern San Andres, Organ, and Bishop Cap–northern Franklin areas all are different. (For comparison, see sections B-B′, J-J′, and O-O′, sheet 2, in pocket.) Different structural styles in the three areas suggest that each responded differently to late Tertiary extension, at least during early stages of the rifting process. The second structural feature of interest is that both the San Andres and Bishop Cap–northern Franklin Mountains areas reveal systems of closely spaced faults, uplifted and preserved within the ranges, that apparently predate the range-boundary faults. These older faults are interpreted as having formed during early stages of uplift of the range. In the following paragraphs, discussion of the older fault systems will be followed by an account of the younger range-boundary faults.

Older fault systems

Southern San Andres Mountains

An older system of closely spaced late Tertiary normal faults is exposed in the Bear Peak–Bear Canyon area. Near the eastern mouth of Bear Canyon some of the faults within this system are truncated by the Organ Mountains fault, the principal break of the younger fault and the one on which the modern fault block was uplifted. Relative dating of the older and younger fault sets is based on this truncation and on the fact that the geometry of the older faults appears to reflect a distinctive style of deformation not seen in the younger. Unfortunately, exactly when the older faults were active cannot be closely determined because late Tertiary rocks are not involved. However, the faults consistently offset rocks and structures in the Laramide Bear Peak fold and thrust belt and also displace monzonite dikes that, though undated, are likely satellites of the Organ batholith (32.8 m.y.). Thus, the faults appear to be late Tertiary structures.

The older fault system in the Bear Canyon–Black Mountain area composes a complex array of north-trending, branching, and anastomosing faults that extends eastward from Quartzite Mountain to the eastern boundary of the range. Representative faults in the system are the Quartzite Mountain fault, Black Prince fault zone (a reactivated Laramide (?) structure), Rock House fault, Deer fault, and the Black Mountain and Goat Mountain fault zones (geologic map, sheet 1, in pocket; figs. 70, 71, and 72). Relative ages of faults within the system are hard to determine because faults do not appear to offset each other. Indeed, the whole branching and anastomosing pattern within which major fault zones appear to connect with each other sug-

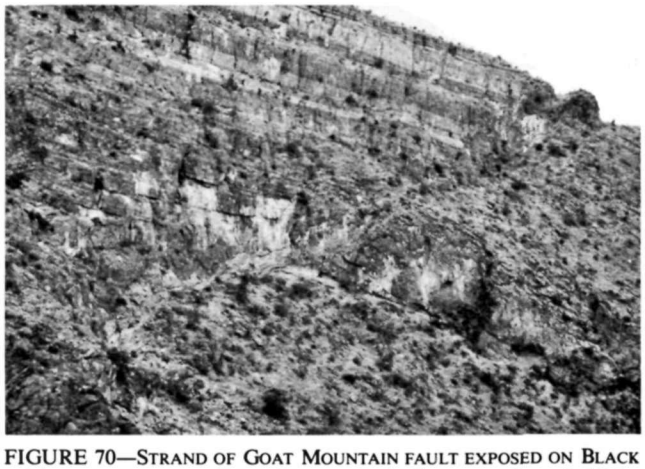


FIGURE 70—STRAND OF GOAT MOUNTAIN FAULT EXPOSED ON BLACK MOUNTAIN SOUTH OF BEAR CANYON; fault dips approximately 20 degrees west; Montoya Dolomite forms hanging wall, El Paso Group the footwall.

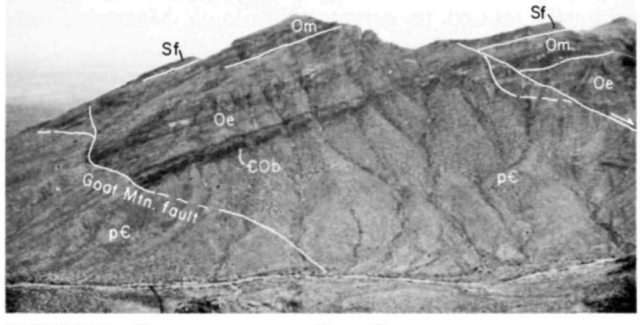


FIGURE 71—EASTERN MOUTH OF BEAR CANYON LOOKING SOUTH; note low-angle Goat Mountain fault on left and another major low-angle fault on right; **Sf**—Fusselman Dolomite; **Om**—Montoya Dolomite; **Oe**—El Paso Group; **€Ob**—Bliss Sandstone; **p€**—Precambrian rocks.



FIGURE 72—EASTERN MOUTH OF BEAR CANYON LOOKING NORTH; TULAROSA BASIN ON THE RIGHT; low-angle faults of the Goat Mountain fault zone and Black Mountain fault zone are marked; note reverse drag adjacent to some faults; symbols as in fig. 71; also **IPlc**—Lead Camp Limestone; **M**—Mississippian formations; **D**—Percha Shale.

gests that the system is roughly contemporaneous. Stratigraphic separation generally ranges from 1,000 to 3,000 ft on the major faults mentioned above, notably lesser on other faults in the system. Dip separation is on the same order of magnitude. Slickensides indicate that latest movement on several of the faults was essentially dip slip. Several faults in the system, notably the Goat Mountain fault zone and some of the strands of the Black Mountain zone, die out laterally by dividing, or splaying, into numerous, closely spaced, subparallel faults, each with a lesser amount of displacement relative to the master fault.

Dips of fault surfaces, measured on exposures in many instances, or calculated as three-point problems, range from steep to low angle (figs. 70, 71, and 72), and some of the faults on cross sections A-A′ through C″-C″′ are shown as gradually flattening downward. This downward flattening is based partly on reverse drag of strata on the downthrown side of some faults (section A-A′; fig. 72), but mostly on good exposures of the Black Mountain fault. This fault dips 55 degrees west at an altitude of 6,200 ft, but only 34 degrees west in an adjacent canyon bottom 1,000 ft lower. This represents a much more rapid rate of flattening of faults than reported elsewhere (Hamblin, 1965; Proffett, 1977) and cannot persist very far without the fault becoming horizontal. Presumably the rate of flattening diminishes with depth; that interpretation is used in the cross sections. Another important feature of the faults in the older system in the Black Mountain–Bear Canyon area is the progressive decrease in dip of the west-dipping faults as one approaches the eastern boundary of the range.

Except for the westernmost faults, which dip steeply east and separate west-tilted blocks, most of the faults in the older system dip west and separate blocks that are tilted eastward toward the Tularosa Basin. Thus, the overall structure of the southernmost part of the San Andres is a broad, highly faulted arch (sections A-A′–C-C′). In general, the easterly dipping blocks are progressively more steeply rotated downward and their boundary faults are progressively flatter eastward. This is most obvious within a mile or two of the eastern edge of the range where Paleozoic strata dip 50-60 degrees east and the associated normal faults dip only 10-15 degrees west (sections A-A′ to C″-C″′). Because the flattening of faults appears directly related to the progressive tilting of beds, it seems unlikely that the low-angle faults are just exposures of the flatter parts of downward-curving faults. Rather, both tilting of beds and flattening of faults seem to be related to downwarping along the range-basin margin. The large graben in the western part of the system, east of Quartzite Mountain, may be a pull-apart feature related to the downbending. Similar grabens and downbending and antithetic faults form the western edge of the Afar depression, although the deformation there is distributed over a wider area (Abbate and Sagri, 1969; Morton and Black, 1975).

Organ Mountains

A glance at the geologic map (sheet 1, in pocket) shows that the Organ Mountains lack the complex faulting that distinguishes the areas of Paleozoic rocks to the north and south. This may be partly due to the fact that faults are hard to identify where they cross homogeneous bodies of crystalline rocks. Certainly this is true for many of the major faults that extend from Black Mountain into Precambrian granite north of US-70, probably accounting for the discontinuous outcrops of the dikes there. The exact position of these faults was not determined, so they were not plotted on the map.

There appears to be little, if any, faulting in the Tertiary batholith, however. Contacts between separate plutons are not offset, nor are contacts between the batholith and its roof. In fact the only faults identified within the batholith or its thick volcanic roof are the parabolic Modoc and Long Canyon fault zones. As described in a previous chapter, these are interpreted to be subsidence faults, related to emplacement of the batholith. Moderately dipping now, they probably were originally steep fractures, rotated to lower angles when the Organ fault block was raised and tilted west. In general, during early stages of rifting, the batholith seems to have been too massive a block to fail in the same manner as the bedded limestone sequences farther north and south.

Bishop Cap–northern Franklin Mountains

Faulting in the Bishop Cap area is quite different from that in the southern San Andres Mountains. Most faults in the former dip east approximately 45-60 degrees, separating blocks of Paleozoic limestone tilted west at 20-45 degrees (cross section O-O′, sheet 2, in pocket). The faults are rather closely spaced and are roughly orthogonal to bedding. Presumably the field of tilted blocks exposed at Bishop Cap and Rattlesnake Ridge continues beneath the covered gap between the two localities.

Farther south, in the northern Franklin Mountains, west-dipping fault blocks also are separated by east-dipping, antithetic normal faults (fig. 73; Harbour, 1972). The situation is similar to that at Bishop Cap, except that faults are low angle (approximately 20 degrees) and the Paleozoic strata between the faults dip somewhat more steeply.

Dating of these faults and those at Bishop Cap cannot be done with precision. However, the faults are not spa-

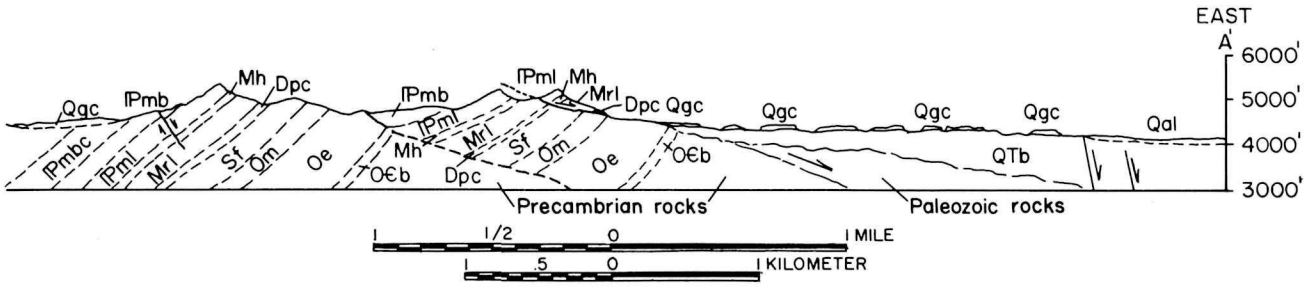


FIGURE 73—CROSS SECTION SHOWING LOW-ANGLE FAULTS IN THE NORTHERN FRANKLIN MOUNTAINS (after Harbour, 1972).

tially associated with the batholith, nor with obvious Laramide structures, so it is likely that they are late Tertiary features. However, they are not the youngest late Tertiary faults. Some are truncated by the Jornada fault system, one of the major range-boundary faults in the region, which passes along the northern edge of the Bishop Cap hills (fig. 66); some faults in the Franklin Mountains are cut by the more recent eastern boundary fault of the range (Lovejoy, 1975). The overall structure of the Bishop Cap–northern Franklin area resembles that described by Morton and Black (1975), Proffett (1977), and Chamberlin (1978), which they interpret as resulting from rotation of initially high-angle faults into low-angle positions as new, steep faults form and tilting of the mountain block progresses.

Younger faults

Organ Mountains and Artillery Range fault zones

The Organ Mountains fault and Artillery Range fault zone are part of the zone of faulting that extends from El Paso to Mockingbird Gap along the eastern base of the Franklin–Organ–San Andres mountain chain. These faults can easily be identified from either ground or air by nearly continuous scarplets of varying height in alluvial fans at the mountain base. Movement on these faults raised the modern fault-block range and downdropped the western part of the Tularosa and Hueco Basins. Because the Organ Mountains and Artillery Range faults truncate the older sets of faults in the range, the former are younger and are the latest set of faults to form in response to continuing extension in the Rio Grande rift.

In contrast to the broad system of closely spaced fractures typical of the older fault system, the modern range-front faults appear to be relatively widely spaced single fractures or narrow zones of faults, some of which have short en echelon segments. Their sinuous course suggests that the fault surfaces are wavy on a giant scale, resembling very large mullions. One exposure of the Organ Mountains fault at the interchange between US-70 and the WSMR access road shows that the fault dips east at 65-70 degrees. Throw on these boundary faults has not been determined exactly, but it is great. WSMR Test Well T-14, located approximately 4 mi nothwest of WSMR headquarters, penetrated approximately 6,000 ft of bolson fill without entering bedrock (Doty and Cooper, 1970). Modeling of gravity data in the same area suggests 7,000-10,000 ft of bolson fill and a total displacement on the fault of at least 12,000-15,000 ft (Seager and Brown, 1978).

Numerous short faults, related to the range-boundary faults, displace the surface of the western Tularosa and Hueco Basins (Seager, 1980). They make up a belt of scarps 3-15 mi wide that parallels the mountain front from El Paso to US-70 (fig. 74). The scarps, up to approximately 80 ft high, bound grabens and horsts (minor antithetic rifts), which are interpreted as resulting from stretching of downwarped basin fill on the downthrown side of the range-front faults. Cloos's

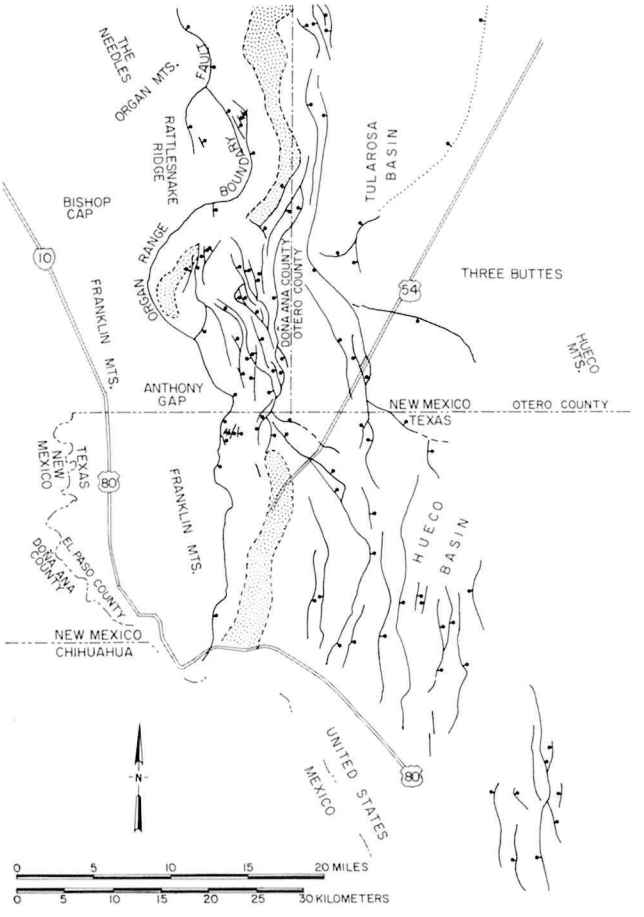


FIGURE 74—SYSTEM OF MINOR ANTITHETIC FAULTS AND RIFTS IN WESTERN TULAROSA AND HUECO BASINS. Shaded areas are topographically and structurally lowest parts of the basins; fault system is thought to result from downbending of bolson sediments to fill gap created by a pull-apart in horizontally extending upper crust; see also fig. 79.

(1968) experiments with clay cakes beautifully illustrate the development of such faults adjacent to major fault zones. This fault system, as well as the Organ Mountains and Artillery Range faults, has been active through much of the Quaternary.

The Organ Mountains fault appears to be one of the most recently active faults in New Mexico (Reiche, 1938). Soil studies by L. H. Gile of faulted fan surfaces near WSMR headquarters indicate approximately 30 ft of displacement in the last 4,000-5,000 years (L. H. Gile, personal communication, 1979). M. Machette's studies of fault height and fault scarp angle relationships have confirmed Gile's conclusion (personal communication, 1979). Gile's studies involve analysis of soils on the surfaces of the youngest fans displaced by the faults and on the oldest fan surfaces not displaced. Structure, composition, and maturity of the soils as well as geomorphic relations are studied to determine the relative age of the surfaces, and the soils are compared with others of similar character for which C-14 ages are available. In this manner the age of the soil and fan surfaces can be estimated and the latest fault movement bracketed.

(Absolute ages of different soils is one result of the nearby Desert Soil-Geomorphology Project. Carried out by L. Gile, J. W. Hawley and others, the project involved detailed studies of the ages, structure, composition, and geomorphic relations of a wide variety of soils in the Las Cruces area between 1957 and 1972. The results are currently in press. C. Tascheck, New Mexico State University Agronomy Department, currently is studying details of the soils along the Organ Mountains fault just west of WSMR.)

A history of repeated movement during the Quaternary along the Organ Mountains and Artillery Range faults is indicated by varying heights of scarps that cut at least five generations of fans. Scarps displacing the oldest fans (Qcru, Qcrc), inferred to be early Pleistocene or latest Pliocene in age, are 100-150 ft high or more; scarps truncating fan surfaces of middle Pleistocene age (Qcrp) are generally about 90 ft high (figs. 75 and 76); those cutting late Pleistocene surfaces (Qpo) are approximately 40 ft high; and Holocene scarps (cutting Qpy) range up to approximately 30 ft high. Clearly, the older, higher scarps are composite, the product of multiple scarp-producing events dating back at least to the early Pleistocene or late Pliocene.

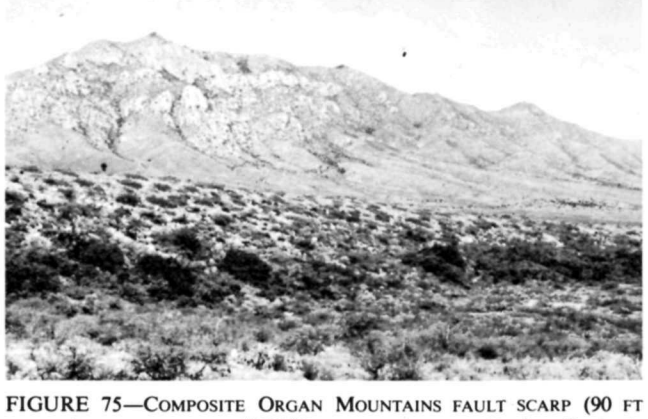


FIGURE 75—COMPOSITE ORGAN MOUNTAINS FAULT SCARP (90 FT HIGH) JUST EAST OF WSMR HEADQUARTERS; Baylor Peak in background; view to northwest.



FIGURE 76—COMPOSITE ORGAN MOUNTAINS SCARP DISPLACING **Qcrp** FAN; faulted Holocene fan crosses the scarp along left edge of picture; both fans are shown in the aerial view in fig. 77; view to south.

Because of the composite nature of most of the scarps, it is difficult to determine the length of the Holocene breaks. Where Holocene fans are displaced, the extent of the Holocene scarp across that fan can easily be seen (fig. 77), but the portion of a composite scarp produced by a Holocene event cannot readily be distinguished from older parts of the scarp. However, minimum length of the Holocene breaks is clearly several miles.

The several generations of fans found along the mountain fronts probably are related to repeated movement along the faults. That is, a scarp-producing event lowers the base level for streams draining the current fan, the streams begin to trench that fan, erode the scarp, and spread debris into a new fan below the scarp. The old fan is by-passed by sedimentational processes and abandoned. The cycle is repeated upon renewed movement along the fault.

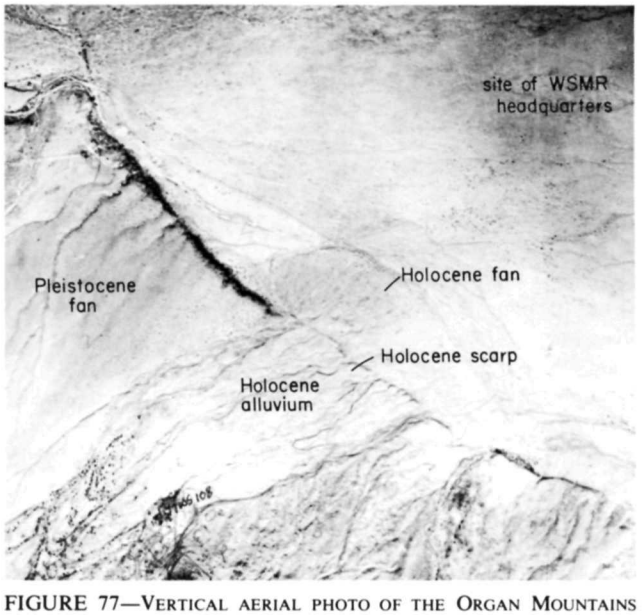


FIGURE 77—VERTICAL AERIAL PHOTO OF THE ORGAN MOUNTAINS FAULT SCARP 1 MI SOUTHWEST OF WSMR HEADQUARTERS. Prominent scarp, approximately 90 ft high, in upper part of picture is composite and cuts a fan of middle to early Pleistocene age; the scarp cutting the Holocene fan to the southeast is approximately 30 ft high.

West-side boundary fault

Evidence for a boundary fault on the western side of the Organ Mountains is based mainly on the gravity survey done in 1977 by L. Brown (figs. 66 and 78). The map shows a north-trending, steep gravity gradient 1-2 mi west of the mountain front, which extends northward from west of the Modoc mine to west of Hardscrabble Hill. The gradient is interpreted as indicating a relatively steep, westward-dipping, bedrock slope, presumably a fault scarp (fig. 78). Drilling northwest of the town of Organ apparently has also located the fault. While most holes drilled near Organ penetrated only 100-200 ft of alluvium above bedrock, one hole in sec. 34, just west of the map, penetrated 1,620 ft of gravel above bedrock. This probably means that the boundary fault (or zone) passes through the eastern half of sec. 34. No fault scarps are associated with this fault, but I believe that movement on this and the Organ Mountains fault raised the northern part of the Organ range as a horst, with greater and most recent uplift associated with the latter fault.

Jornada fault

The Jornada fault zone, previously discussed in relation to the Organ cauldron margin, is a major fault zone that extends from the Caballo Mountains southward to Tortugas Mountain where it arcs eastward and passes between the Bishop Cap hills and southern Organs. Regionally, the fault zone separates a series of uplifted blocks on the west and south (southern Caballo, San Diego, Doña Ana, and Tortugas Mountains and Bishop Cap hills) from grabens or half grabens on the east (Jornada Basin). Although some faults in the zone are exposed on Rattlesnake Ridge, in the Bishop Cap hills, and as the Peña Blanca and Massey Tank faults on Peña Blanca ridge, the fault zone is covered for the most part, but marked throughout its length by a steep gravity gradient (fig. 66) and by scattered outcrops of bedrock on the upthrown side. Displacement on the fault zone is nearly 8,000 ft along the edge of the southern Organs; gravity data suggest a similar amount at Tortugas Mountain (Seager and Brown, 1978). East of Bishop Cap hills the main part of the zone apparently turns south and, in so doing, accounts for the repetition of Paleozoic strata on Rattlesnake Ridge and Bishop Cap. However, the point worth strongest emphasis here is that on a regional scale the fault bounds the western and southern side of the west-dipping Organ–San Andres block. The downdip western part of the block is the southern part of the Jornada Basin; the updip eastern part is the Organ–San Andres Mountains (fig. 79).

Westward tilting of the ranges

The amount of westward tilting of the range during late Tertiary deformation is speculative. The average westward dip varies from 20 to 25 degrees in the northern part of the area where the range is a horst to as much as 40 degrees in the south where it is a simple west-tilted block. These dips represent the sum of several periods of deformation, including Laramide, volcano-tectonic deformation during the Oligocene, tilting associated with the older sets of late Tertiary faults, and finally, westward tilting along the modern range-boundary faults. In general, a 10-20 degree angular unconformity separates Tertiary units from rocks deformed during the Laramide, but locally the discordance is as much as 90 degrees. Steep dips of volcanic rocks near the batholith probably were caused by Oligocene subsidence of cauldron fill as indicated by the thickness variations described earlier. The problem is how to separate the deformation due to these older events from that due to younger tilting, when there are practically no rocks younger than Oligocene exposed in the range.

In the chapter on Middle Tertiary silicic magmatism and volcano-tectonics, I presented reasons for believing that late Tertiary westward rotation of the range amounts to approximately 20 degrees. In addition to those reasons, cross sections A-A′ and B-B′ (sheet 2, in

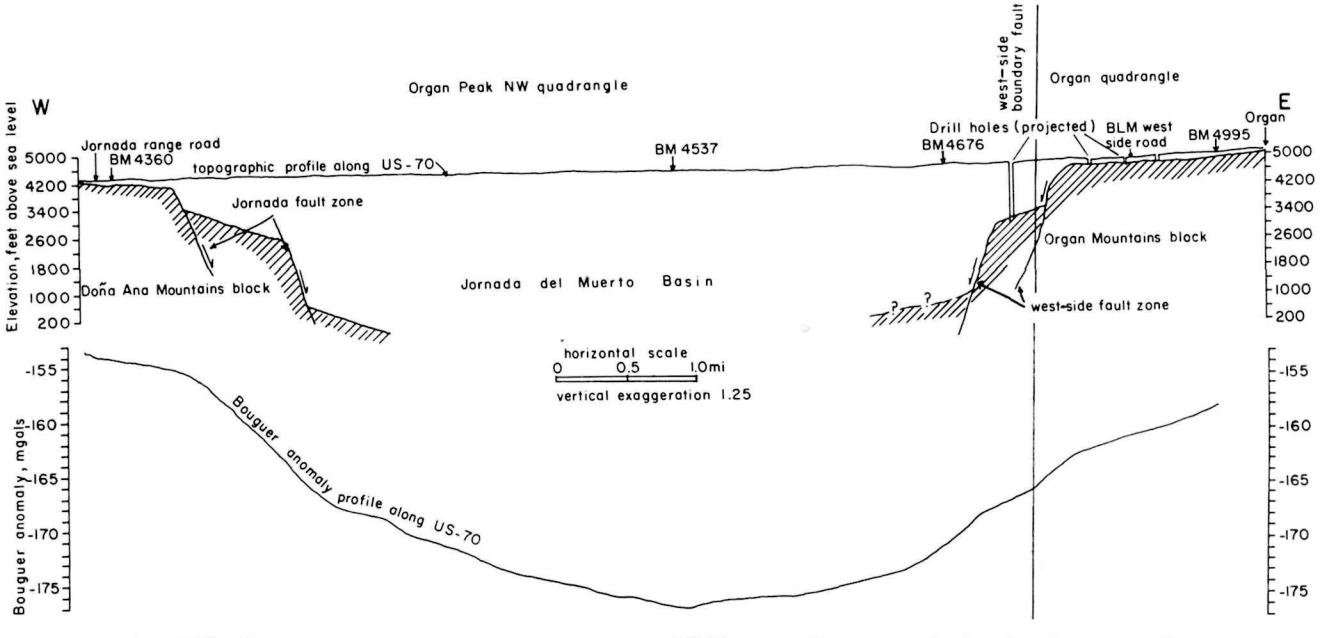


FIGURE 78—GRAVITY PROFILE AND GEOLOGIC SECTION ALONG US-70 WEST OF ORGAN; (gravity data from L. Brown, 1977).

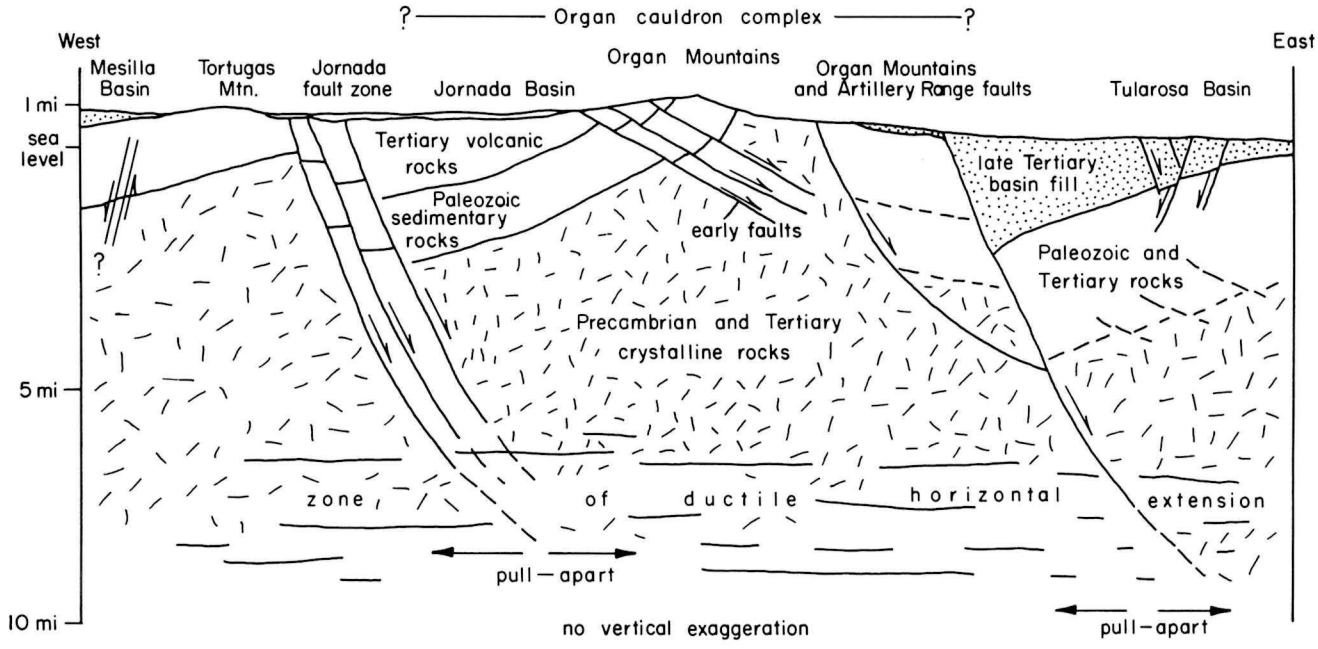


FIGURE 79—DIAGRAMMATIC EAST-WEST SECTION FROM WESTERN TULAROSA BASIN THROUGH THE ORGAN MOUNTAINS TO THE MESILLA BASIN. Major fault blocks, antithetic fault system and inferred downbending of bolson fill in western Tularosa Basin, and possible pull-apart zones at depth are shown; see discussion in text for further description of the diagram.

pocket) suggest in a very subjective way that westward tilting of the southern San Andres range by approximately 20 degrees accompanied uplift along the Organ Mountains fault. This is inferred from the fact that Precambrian rocks rise structurally eastward (at a dip of approximately 20 degrees) and are exposed over a wide area on the eastern side of the range in spite of the earlier eastward dip of the Paleozoic section toward the Tularosa Basin. The mountains have the appearance of a fault block whose westward tilt modified an older east-facing monocline; this hypothesis is considered further in the following section. Near the eastern mouth of Bear Canyon, lower Pleistocene or uppermost Pliocene fan gravels which originally sloped perhaps 1 degree toward the Tularosa Basin, now dip westward by the same amount, suggesting a rate of westward rotation of the mountain block of perhaps 2 degrees every 1-3 m.y.

Discussion

Fig. 80 illustrates one interpretation of the progressive evolution of the southern San Andres–Bishop Cap–northern Franklin Mountains area and adjacent parts of the Tularosa Basin in late Tertiary time. Because the southern San Andres and Bishop Cap–northern Franklin Mountains areas apparently responded differently to extensional stresses, at least during the earlier stages of rifting, each area is represented by its own block diagram. The southern San Andres is considered first.

The diagram suggests that initial differential movement between the Tularosa Basin and ancestral San Andres highlands formed a gentle, east-facing downwarp broken by moderately dipping antithetic normal faults. As seen on cross sections A-A′ to C-C″′ (sheet 2, in pocket), the faults cut bedding at angles of approximately 45 to 60 degrees. This immediately suggests that the faults are simply shear fractures related to extension in concentrically folded beds. Of the two possible orientations of shear fractures, only those antithetic to the downwarp and its general hinge are developed. The large graben illustrated in fig. 80 and shown on sections A-A′ to C-C″′ (sheet 2, in pocket) seems to be a natural consequence of extension in the hinge area.

The most distinctive feature of the west-dipping antithetic faults on the downwarp is the progressive flattening of successively more easterly faults in the system. These unusually low dip angles could be explained in either of two ways. First, the faults may have formed as relatively steep fractures at an early stage of downwarping (fig. 80) and then were rotated into low-angle positions as the downwarp evolved into a rather steep monoclinal flexure (fig. 80B and C). Cloos's (1968, p. 427-428) experiments show such flattening of closely spaced, antithetic faults with progressive down-bending of the downthrown block in half-grabens (fig. 81). The second possibility, illustrated in fig. 82 (Hobbs, 1971; Ramberg, 1963) is that no rotation of faults from high-angle to low-angle positions was involved, that all faults formed with their present attitudes, and that their attitudes were determined by the strain characteristics of various parts of the downwarped limb. This hypothesis would mean that low-angle faults such as the Goat Mountain and Black Mountain faults developed initially as low-angle faults and that most of the movement on them was horizontal. As pointed out by Morton and Black (1975), large horizontal movements on normal faults are nearly impossible to reconcile with regional extensional stresses. Consequently, from a mechanical viewpoint at least, the first possibility seems most likely. As initially steep faults were flattened by downwarping, displacement continued to accumulate until the faults became so flat that movement on them no longer could accommodate the extension. At this point they became inactive but continued to flatten, and the new, steep

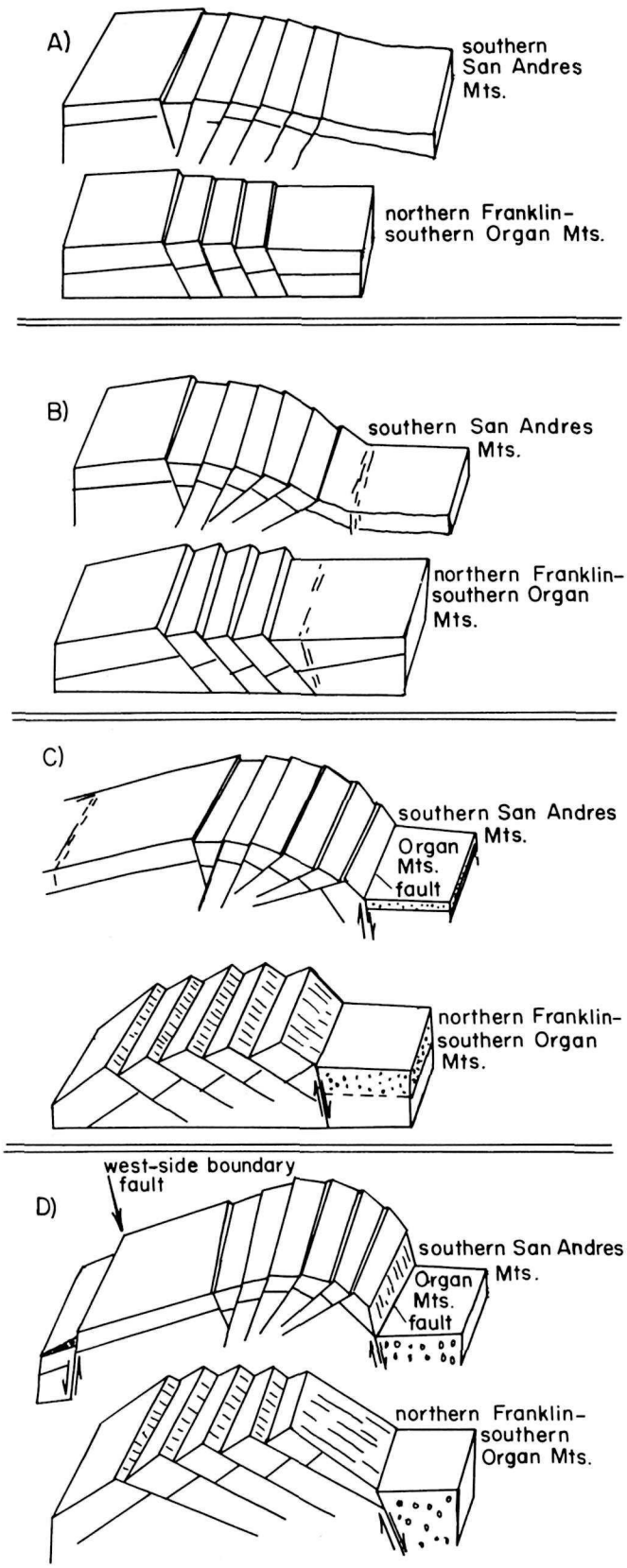


FIGURE 80—DIAGRAM SHOWING ONE INTERPRETATION OF THE SEQUENTIAL EVOLUTION OF THE SOUTHERN SAN ANDRES AND NORTHERN FRANKLIN MOUNTAINS-BISHOP CAP AREA IN LATE TERTIARY TIME. Earliest stage is represented by A; explicit in the diagram is rotation of early-formed high-angle faults into low-angle ones in both areas as tilting of strata progresses.

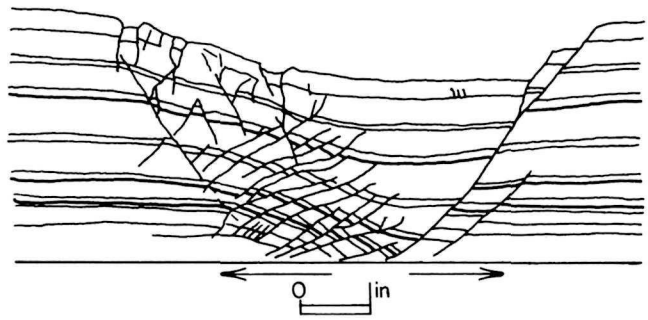


FIGURE 81—CLAY-MODEL EXPERIMENT OF E. CLOOS (1968). Clay cake was extended horizontally by pulling two overlapping steel plates on which the clay was resting; the closely spaced, low-angle faults in the lower two-thirds of the clay were initially high-angle faults that rotated to lower angle positions as extension and downbending of the clay progressed. The east-dipping rocks and antithetic low-angle faults in the southern San Andres Mountains are thought to be related in the same way. The major difference between the model and the southern San Andres structures is that downbending and closely spaced, low-angle faulting in the model is in the downthrown block, whereas in the southern San Andres Mountains it is in the upthrown block.

Organ Mountains fault formed in response to the continuing regional extension (fig. 80C and D). Subsequent uplift of the range or sinking of the basin was accomplished by movement on this fault and, to a lesser extent, the west-side boundary fault.

The preceding analysis is based on the interpretation that the closely spaced antithetic faults predate the Organ Mountains boundary fault and represent a brittle response of strata to an initial stage of downwarping of the Tularosa Basin. The possibility exists that uplift on the Organ Mountains boundary fault, arching of the Paleozoic strata on the upthrown block, and antithetic faulting were concurrently operating processes. Indeed, Lowell (1970) has shown that low-angle antithetic faults and downbending develop concurrently with marginal upthrusts along the edges of Laramide blocks, although the antithetic faults that he documents are invariably minor ones, whereas those in the San Andres are major fault systems. However, in view of the apparent age difference between the antithetic fault system and the range-boundary fault, I believe the two-stage uplift of the range modeled in fig. 80 best fits the available data.

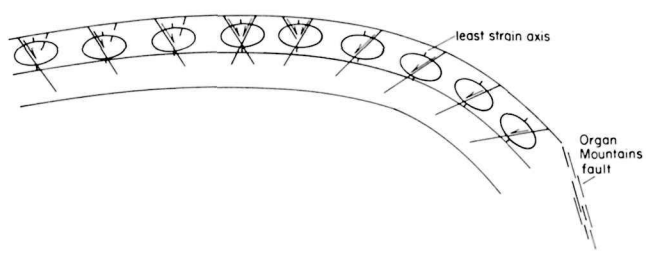


FIGURE 82—ORIENTATION OF SHEAR FRACTURES AND STRAIN ELLIPSOID ON CONCENTRICALLY FOLDED STRATA. Low-angle faults on right could form as either 1) high-angle faults subsequently rotated to low-angle positions as folding progressed, or 2) initially low-angle faults on the already-formed steeply dipping limb of a fold. The former possibility seems more likely in the case of the southern San Andres Mountains, as discussed in the text; compare the sketch with cross sections A-A′ through C″-C″′ (sheet 2, in pocket).

The second set of block diagrams in fig. 80 portrays the somewhat different evolution of the northern Franklin Mountains–Bishop Cap area. There it seems that block faulting and westward tilting rather than downwarping towards the Tularosa Basin were the response of the upper crust to extension from the beginning. As uplift and westward tilting progressed in this area, the earlier formed, steep east-dipping faults were rotated to angles sufficiently low that movement on them could no longer aid the extension (fig. 80C and D). A new fault formed—the eastern boundary fault of the Franklin range and its northern continuation, the Artillery Range fault zone. The latter intersects the Organ Mountains fault at a high angle and appears to be a separate fault zone. Uplift of the modern Franklin–southern Organ block took place through subsequent movement on this fault.

The general structure of the Bishop Cap–northern Franklin area is similar to that of the Yerington district, Nevada (Proffett, 1972), Socorro area (Chamberlin, 1978), and southern margin of Afar (Morton and Black, 1975). The closely spaced, rotated, early faults in these areas appear to be indicative of rapid attenuation, high geothermal gradients, and comparatively shallow, brittle behavior (Morton and Black, 1975; Chamberlin, 1978). Possibly those conditions also were prevalent in the Bishop Cap–northern Franklin area during early stages of rifting. Judging from the change in structural style, the latest stages in evolution of the San Andres–Organ–Franklin area involved extension of a thicker, more brittle crust.

The relatively simple horst-and-graben or tilted fault-block structure of the Tularosa Basin and adjacent ranges and the widely spaced, apparently uncomplicated boundary faults together suggest that a thicker, more brittle crust was involved in later stages of extension in this part of the Rio Grande rift. Boundary faults may extend deeper and the local geothermal gradient may be less than when the closely spaced earlier faults formed. Tilting of the ranges and grabens could have resulted from any of three possible mechanisms, or a combination of them. First, Taber (1927), DeSitter (1956), and Sales (1978) have emphasized the idea that tilting may result from the buoyant effect of uplifted blocks in which mass is unequally distributed. Secondly, if boundary faults are curved and concave upward, as suggested elsewhere in the Rio Grande rift by seismic reflection studies (L. Russell, Rio Grande rift symposium paper, 1978), then tilting of the fault blocks would be a natural consequence of sliding down these surfaces. Finally, Stewart (1971; 1978) maintains that rotation of fault blocks can be achieved through the development of complex, asymmetric grabens above pull-apart zones in a horizontally extending layer in the upper crust. The boundary faults may be either planar or curving, but the tilt is largely produced by downbending of the crust to fill the gap created by the pull-apart. Cloos's (1968) model illustrates the idea particularly well (fig. 81), and Seager (1980) applied it to explain asymmetry in the Tularosa and Hueco Basins. Fig. 79 also uses the idea to help explain the westward tilt of the Organ range, although the hypothetical downward-curving faults and buoyancy effects of the uplifted block could also contribute to the tilting.

Volcanic and sedimentary rocks probably related to early stages of rifting

In the Black Hills, east of Rattlesnake Ridge, a down-faulted series of mafic, ultra-potassic lava flows and associated conglomerate unconformably overlies the Soledad Rhyolite. Approximately 500 ft of lava flows, which dip eastward, crop out. The full thickness and extent of the flows and conglomerate are unknown because they are largely buried by Pleistocene sand and gravel. Aside from one other small outcrop in a canyon bottom just west of the Black Hills, no other exposures are known.

The conglomerate, a bouldery, well-lithified unit, is in fault contact with the lavas along the south side of the Black Hills. Relations along the fault show that the conglomerate is at least 100 ft thick and normally underlies or is interbedded with the flows. Clasts up to 2 ft in diameter were derived mostly from the mafic lavas and to a lesser extent from rhyolitic tuffs. The lack of granite, monzonite, or more than a trace of limestone suggests that either the present mountains had not yet been elevated when the conglomerate formed or, if the mountains were present, the Paleozoic, batholithic, and Precambrian rocks had yet to be exposed by erosion. The conglomerate resembles other fanglomerates in the region that are interstratified with mafic, calc-alkaline lavas of late Oligocene to early Miocene age. Such lavas have been interpreted by Chapin and Seager (1975) and other workers in the Rio Grande rift as accompanying early extension in the rift, and the conglomerates have been interpreted as fan deposits washed off the rising fault blocks. The same interpretation may be applicable to the lavas and conglomerate in the Black Hills. They may record an early stage of regional extension and uplift of the Organ or some other fault block in the area that exposed volcanic rocks.

The lava flows are mostly dark, vesicular, fine-grained types up to approximately 50 ft thick each. A few have been oxidized to red-brown and some have fairly abundant hornblende and/or feldspar phenocrysts. Superficially, they resemble a few of the lava flows that overlie the tuff of Squaw Mountain on the western side of the range. Chemically, texturally, and mineralogically the two lava suites are very different, however, and it seems most unlikely that they are co-magmatic.

Chemical analyses of two flows from the Black Hills are shown in appendix B. The flows' silica content, 49-55 percent, is 10 weight percent lower than the west side lavas, and this fact distinguishes the two suites immediately. There are notable differences among other oxides, best shown in the variation diagrams of fig. 43. The Black Hills lavas are most extraordinary, however, for their high K_2O values (9-10 percent), high total Fe (6-7 percent), and high Fe/Mg ratio. Taken at face value these high percentages make the rocks greatly undersaturated, nepheline-normative, highly alkaline rocks according to the classification of Irvine and Baragar (1971). Leucite is present in one of the norms and they plot as trachybasalt and tristanite (fig. 42). The high potash and K_2O/Na_2O values may be interpreted, how-

ever, in another way, which does not involve such an unusual magma.

The Black Hills lavas may have undergone considerable potash metasomatism, which may have added K_2O to the lavas or modified primary K_2O/Na_2O through alkali exchange (Orville, 1963). This possibility is suggested because the K_2O/Na_2O ratio is high (3), suggesting alkali exchange, and because no modal leucite is present in the rocks.

More than 95 percent of the rock is composed of elongated, flow-oriented feldspar microlites, hematite dust, and other opaque oxides. The composition of the microlites is uncertain. No albite twinning was observed. A few may be oligoclase and some of the larger are probably sanidine. Most must be potash feldspar, however, to account for the high K_2O. Phenocrysts are not abundant, and those present are corroded and embayed sanidine or oligoclase surrounded by reaction rims. They appear to be xenocrysts (accidental crystals) genetically unrelated to the rest of the rock.

On the geologic map (sheet 1, in pocket), the Black Hills lavas are shown as basaltic andesites rather than trachybasalt or tristanite. This interpretation was based largely on the high K_2O/Na_2O ratio as an indicator of metasomatism and on the absence of modal leucite, and was colored by the fact that ultrapotassic rocks have not been previously reported from the Rio Grande rift, except for those clearly of metasomatic origin (Chapin and others, 1978). The Black Hills lavas also may be potassic because of alkali metasomatism, but there is little evidence in thin section to support this, and matrix microlites appear to be unaltered, high-temperature sanidine rather than orthoclase or alteration products such as potash clays or sericite. Therefore, that the rocks represent true ultrapotassic magmas seems almost equally probable. Such rocks are fairly widespread in Arizona where they are interpreted as unaltered (Shafiqullah and others, 1976; M. Shafiqullah, personal communication, 1979).

Late Pliocene and Quaternary deposits

Quaternary deposits in the southern San Andres and Organ Mountains have been divided into three main subdivisions on the basis of age. The oldest unit, whose basal part ranges into the late Pliocene, is correlated with the Camp Rice Formation of the upper Santa Fe Group, described in the Rio Grande valley and adjacent areas by Strain (1966), Hawley and others (1969, 1976), Seager and Hawley (1973), and Seager and others (1971, 1975). This unit consists mostly of alluvial fan deposits and pediment gravels in the map area, but also includes a notable body of fluvial deposits exposed in the southeast foothills of the Organ Mountains. Youngest beds in the Camp Rice Formation are of middle Pleistocene age, perhaps as young as 350,000-250,000 yrs old (Hawley, 1975, 1978). An intermediate group of deposits includes several generations of alluvial fans of late Pleistocene age. The youngest unit, composed of modern arroyo-channel deposits and canyon fill as well as alluvial fans, is largely Holocene in age, but may include some sediment as old as 15,000 yrs.

The three groups of deposits can be distinguished from each other by the following features: 1) geomorphic position of the deposits and associated constructional and erosion surfaces, 2) degree of soil development, 3) drainage pattern on fan surfaces, 4) condition of weathered boulders in the deposits, and 5) degree of lithification of the deposits. Geomorphic relations among the three groups of fan deposits are diagrammatically illustrated in fig. 83.

Camp Rice Formation

Deposits of late Pliocene to middle Pleistocene age compose the Camp Rice Formation. West of the Organ–San Andres range, the Camp Rice marks final aggradation of the southern Jornada and Mesilla Basins prior to entrenchment of the Rio Grande into its modern valley. The Tularosa–Hueco Basins, east of the range, are still without drainage to the Rio Grande and consequently have continued to aggrade since Camp Rice time.

The Camp Rice deposits also mark the initial development of an ancestral Rio Grande fluvial system in southern New Mexico. The fluvial deposits in the Camp Rice show that the ancient river flowed down the axes of the Jornada and Mesilla Basins and for a time passed into the southern Tularosa and Hueco Basins through Fillmore Gap. Remnants of a huge fan-delta, constructed by the river as it entered the Tularosa Basin, are exposed in Camp Rice deposits on the southeastern piedmont slopes of the Organ Mountains. These fluvial beds are one of the facies of the Camp Rice (Qcrf). The other facies, mostly piedmont-slope deposits and the fill of mountain valleys, underlie (Qcrc), overlie (Qcrp), and intertongue with (Qcrp, Qcrc) the fluvial beds. Undifferentiated Camp Rice piedmont-slope deposits, generally consisting of basal fanglomerates overlain by less-consolidated piedmont-slope alluvium, were mapped locally as Qcru.

Basal piedmont-slope facies

Oldest beds of the Camp Rice Formation consist of a well-cemented series of pale yellowish-brown to tan conglomerate derived from adjacent mountain uplands. The unit is designated by the symbol Qcrc on the geologic map (sheet 1, in pocket). Maximum thickness is approximately 300 ft. Individual clasts in the conglomerate, though averaging cobble to small boulder size, range up to several feet in diameter. They are tight-

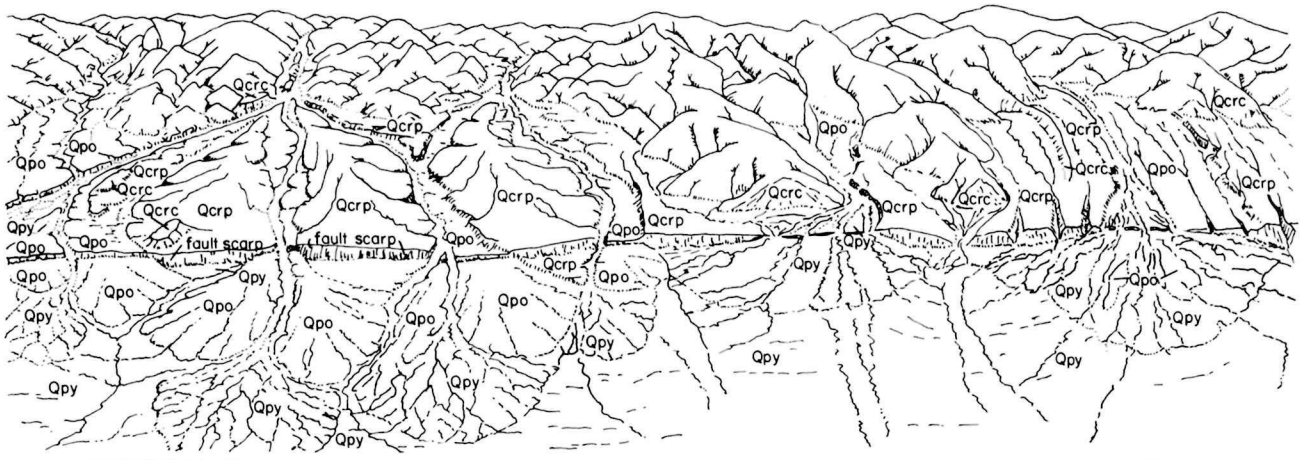


FIGURE 83—Diagram illustrating geomorphic relationships among fans on eastern piedmont slopes of Organ and southern San Andres Mountains. **Qcrc**—basal Camp Rice deposits; **Qcrp**—upper Camp Rice deposits (associated with Jornada I constructional and erosional surface); **Qvo**—late Pleistocene deposits (associated with Jornada II constructional and erosional surface); **Qpy**—latest Pleistocene and Holocene alluvium (associated with Isaacks' Ranch and Organ constructional and erosional surfaces).

ly cemented in a matrix of finer boulders, cobbles, pebbles, and sand by calcium carbonate that was probably precipitated from ground water at a time when the gravels were at least temporarily in the zone of saturation (J. Hawley, personal communication, 1979). Bedding in the deposits is generally weakly developed, but in some outcrops is obvious when viewed from a distance. In places along the Organ Mountains fault, crude bedding, which originally sloped eastward and parallel to the surface of basal Camp Rice fans, now dips westward toward the mountains as a result of Quaternary movement on the fault. Composite fault scarps cutting Qcrc fans are locally more than 150 ft high.

The basal conglomerate beds of the Camp Rice represent two kinds of depositional environments. Most are major alluvial-fan or coalescent-fan deposits formed at the mouths of drainages such as Bear, Ice, and Johnson Canyons. The fans are preserved as: 1) isolated, high-level remnants in rock-defended positions, especially near canyon mouths, 2) as more extensive, but deeply eroded, deposits farther down slope, or 3) as buried fans on piedmont toe slopes or beyond. Where extensive exposures remain, the deposits have been scored into narrow ridges and valleys by younger parallel drainage; seldom is the original shape or surface of these fans preserved.

Camp Rice fan deposits partly backfilled the lower reaches of Bear and Ice Canyons to depths of 200 ft or more. Clearly, those canyons were developed in much their present form in pre-Camp Rice time, perhaps during the late Pliocene. Following backfilling by the Camp Rice gravels, the canyons were exhumed nearly to their original depth by late Pleistocene and Holocene cycles of erosion.

The second type of basal Camp Rice conglomerate can be seen just north of the eastern mouth of Bear Canyon. Very coarse, angular boulder deposits of colluvium, talus, and landslide debris mantle triangular-shaped remnants of steep mountain slopes adjacent to the Organ Mountains fault. Composed of lower Paleozoic clasts, these deposits document the former existence of an adjacent steep, perhaps cliffy, mountain front below which aprons of coarse, angular blocks accumulated. Gently rolling low hills of Precambrian terrain surround the ancient slope deposits today, and the modern topographic range front lies 1 mi or more farther west.

Fluvial facies

On the structural bench between the Organ Mountains and Artillery Range faults, a broad expanse of Camp Rice fluvial deposits are exposed, sandwiched between basal and upper Camp Rice piedmont-slope gravels and conglomerate. The body of fluvial sediment is wedge shaped, tapering to a feather edge westward near the mountain front and thickening eastward toward the Tularosa Basin. Maximum exposed thickness is approximately 60 ft. Except for offset along the Artillery Range fault, the unit is undeformed.

The fluvial sediment consists largely of light-tan and gray sand and gravel formed in river channels, and light-brown to reddish-brown, sandy to clayey overbank deposits. The channel units are arkosic, moderately well sorted and locally crossbedded. Their most distinctive feature, however, and one most useful in establishing a fluvial origin, is their content of well-rounded pebbles of quartz, chert, quartzite, and other siliceous rock fragments. Identical clasts distinguish fluvial facies in the Camp Rice Formation elsewhere in the Rio Grande region. They clearly have been transported substantial distances, probably from sources far north of Las Cruces. Locally derived volcanic, granitic, and carbonate clasts also compose part of the fluvial deposits.

The fluvial deposits are interpreted to be part of a huge fan-delta constructed on the nearly flat floor of the Tularosa Basin by the ancestral Rio Grande after it flowed into the basin through Fillmore Gap (fig. 84). The deposit extends at least as far north as Soledad Canyon and to an unknown distance east. Southward, fluvial deposits have been encountered in the subsurface of the Tularosa and Hueco Basins as far as El Paso, and south of there the deposits are again exposed in the walls of the Rio Grande valley for many miles. Thus, the river, after passing through Fillmore Gap and constructing the fan-delta, flowed southward, perhaps emptying into lakes at the southern end of the Hueco bolson and

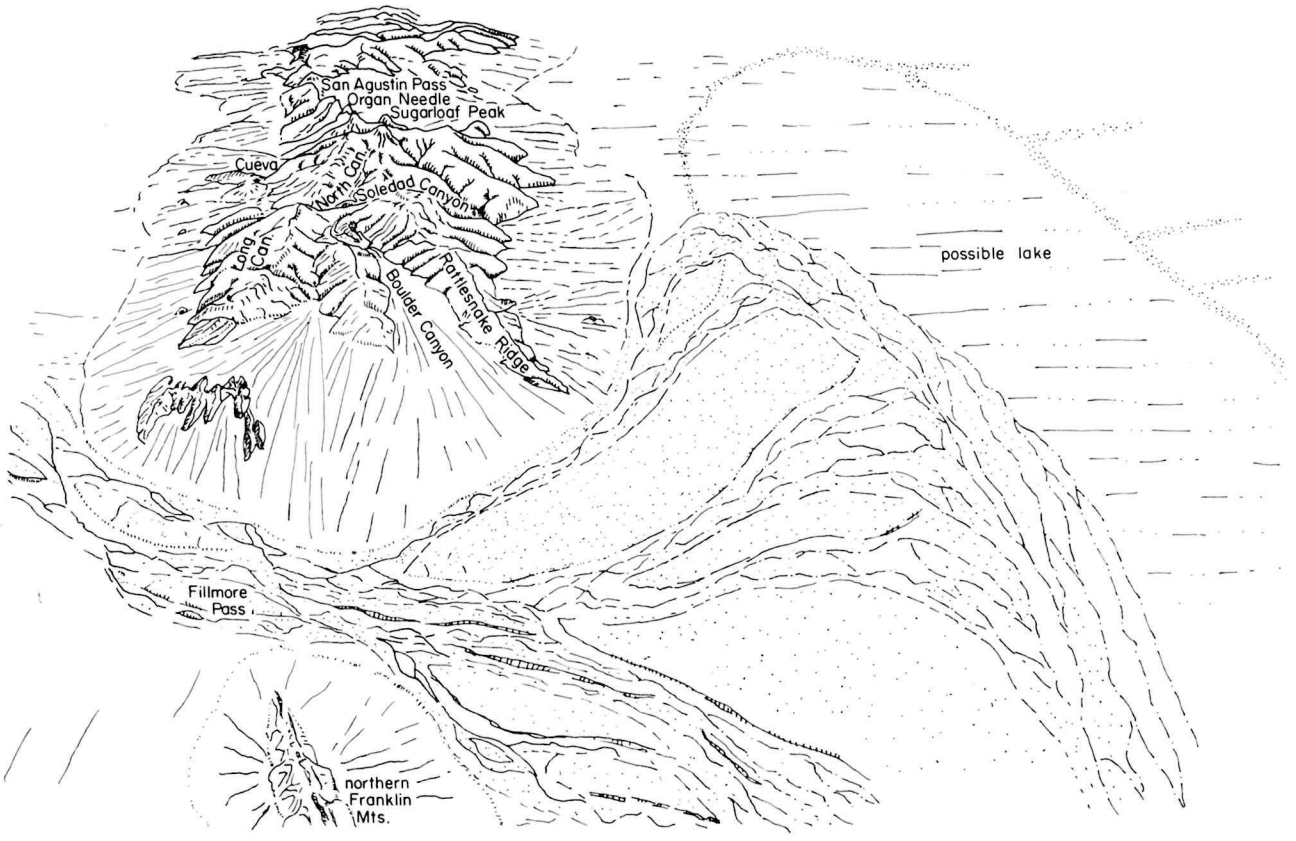


FIGURE 84—DIAGRAM ILLUSTRATING CAMP RICE FAN DELTA CONSTRUCTED BY ANCESTRAL RIO GRANDE AFTER FLOWING THROUGH FILLMORE GAP INTO WESTERN TULAROSA BASIN; view looks north toward Organ Mountains.

adjacent parts of Chihuahua (Hawley, 1975). Eventually, the river abandoned its course through Fillmore Gap. Perhaps it finally was forced westward into the Mesilla Basin by continuing uplift of the eastern side of the Organ–Franklin chain.

Upper piedmont-slope facies

Uppermost Camp Rice beds adjacent to the Organ and southern San Andres Mountains include extensive but relatively thin alluvial-fan deposits as well as gravel veneers on pediment surfaces. The latter generally are mountainward continuations of fan-construction surfaces (Jornada I surface). The deposits and erosion surfaces are inset below remnants of older Camp Rice fans in many places, especially near canyon mouths; downslope, the fans overlap older fan deposits. This situation is true not only for Camp Rice fans, but also for each succeeding generation of fans. The trenching of old fans by younger ones could be attributed either to periodic uplift of the mountain block by movement on the border faults or to normal downcutting on the fans and in bedrock canyons, or to both. In either case, the building up of base level at the foot of the fans results, so that at some point downslope the younger fans overlap the older ones. All this generally results in shallower gradients for successively younger fans (fig. 85).

Several features distinguish upper Camp Rice deposits. First, in spite of extensive gullying by deeply incised parallel drainage, their fan form is generally preserved together with broad areas of the original constructional or erosional surfaces associated with the fans (Jornada I surfaces). These surfaces form the highest, extensively preserved surfaces on upper and middle piedmont slopes in the range. Secondly, the upper Camp Rice deposits are generally thin, less than 50 ft thick, and are weakly consolidated, except for their upper part that usually displays strong cementation by soil carbonates or clay. Soil carbonate (calcrete) predominates where carbonate rocks are found in the watershed; reddish-brown clay forms the bulk of the B-horizon where fans drain volcanic or granitic terrain. B-horizons on upper Camp Rice deposits average 1-3 ft thick. Thirdly, granite boulders on the fan surfaces, as well as within the deposits, are in advanced stages of spheroidal weather-

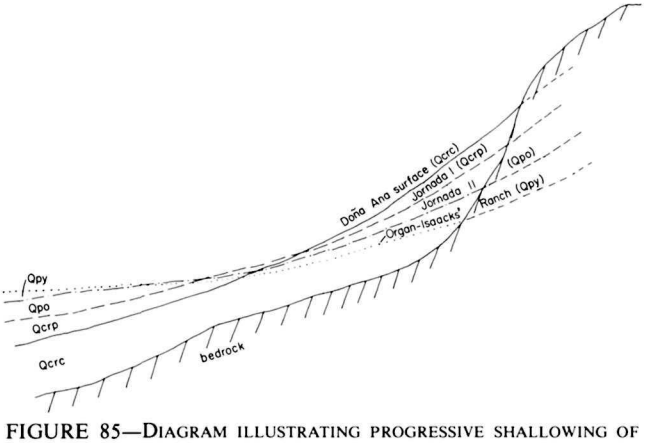


FIGURE 85—DIAGRAM ILLUSTRATING PROGRESSIVE SHALLOWING OF SUCCESSIVELY YOUNGER FAN GRADIENTS; note erosion of older fans on upper piedmont slope and burial of the fans downslope; note also progressive basinward shift of successively younger fan deposits.

ing and granular disintegration (fig. 86). However, they are generally not as thoroughly decomposed as boulders in the basal Camp Rice fanglomerates, which can usually be broken up manually or with a knife.

Upper Camp Rice fans that drain deep canyons heading in higher reaches of the mountains consist largely of huge boulders—up to 20 ft across—in a matrix of smaller boulders, coarse sand, and mud. Such fans appear to have formed almost exclusively by deposition from mudflows, because fluids of lesser viscosity would seem incapable of transporting such clasts, even when discharges and velocities were high. C. B. Hunt (personal communication, 1975) suggests that the mudflow deposits are indicative of periglacial conditions in the higher parts of the Organs during the Pleistocene. This is probably true. However, Holocene fan deposits also partly consist of equally coarse, mudflow-transported material. These may have been deposited under climatic conditions not far different from the present. Apparently, impressive mudflows, capable of transporting thousands of car-sized or larger boulders, need not be an exclusive byproduct of periglacial conditions.

Age of the Camp Rice Formation

While no dating of the Camp Rice Formation in the Organ–San Andres area has been possible yet, the general age of the formation throughout the region has been established by a few dated outcrops in the Rio Grande valley. At the type locality of the formation in Hudspeth County, Texas, Strain (1966) found vertebrates of Blancan age (latest Pliocene–earliest Pleistocene) in the lower part, suggesting that deposition started more than 2.0 m.y. ago. Pearlette type-B ash, approximately 2.0 m.y. old, also occurs in the lower part of the formation at its type area (J. W. Hawley, personal communication, 1978). Bachman and Mehnert (1978) report a basalt flow, 2.9 m.y. old, interbedded with fluvial Camp Rice strata near Truth or Consequences and pre–Camp Rice basalts 4.5 m.y. old near San Acacia. Along the east-central slopes of the Caballo Mountains, basalts interbedded just above the base of cemented Camp Rice fanglomerates are 3.12 m.y. old.



FIGURE 86—SPHEROIDALLY WEATHERED BOULDERS ON JORNADA I SURFACE (TOP OF **Qcrp** FAN) ALONG EAST SIDE OF ORGAN RANGE NORTH OF AGUIRRE SPRING; note jointing also in Organ Needle quartz monzonite that forms Baylor Mountain in background.

Thus, the oldest parts of the Camp Rice range back into middle Pliocene time.

Youngest Camp Rice beds are of middle Pleistocene age. This is based partly on the presence of an Irvingtonian (early to middle Pleistocene) vertebrate fauna collected from upper parts of the formation near Las Cruces (Seager and others, 1975), but mostly on correlation of volcanic ashes locally interbedded in upper parts of the formation (Hawley and others, 1976; Hawley, 1978). The ashes have been identified as air-fall deposits associated with eruptions at Bishop, California, and Yellowstone, 0.7 and 0.6 m.y. ago (Reynolds and Larson, 1972; Hawley, 1978). Post-Camp Rice basalt flows near Las Cruces, which flowed into the Rio Grande valley about 200,000 yrs ago, help bracket the upper limit of the Camp Rice. (Some of these flows have recently been redated by R. Marvin, U.S. Geological Survey, at about 0.5 m.y. [letter from R. Marvin to J. Hawley, April, 1979]. If the date becomes generally accepted, then Camp Rice deposition ended in southern New Mexico and the river became entrenched in the present valley prior to that time.) Based on these dates, Hawley (1978) suggests that Camp Rice deposition ended in closed basins of southern New Mexico approximately 250,000-300,000 yrs ago. In the Organ–southern San Andres Mountains, basal Camp Rice conglomerate (Qcrc) is considered in this report to be late Pliocene–early Pleistocene in age. The fluvial facies (Qcrf) is considered to be early to middle Pleistocene and the youngest piedmont-slope deposits to be middle Pleistocene. Undifferentiated Camp Rice piedmont-slope deposits (Qcru) range from late Pliocene to middle Pleistocene, but most were formed during the earlier parts of that time span.

Late Pleistocene deposits

Late Pleistocene alluvium includes as many as three generations of alluvial-fan and pediment deposits exposed largely on middle to lower piedmont slopes. These deposits, together with associated constructional and erosional surfaces, compose the Jornada II morphostratigraphic unit of Gile and others (1970). On middle and upper piedmont slopes, this group of deposits is very thin and overlies erosion surfaces cut on older fans and on bedrock. In general, these are inset below the ancient, high Camp Rice fans (Jornada I surface), but are several to many tens of feet above the Holocene deposits. Downslope, these fans, as well as all younger fans, overlap and bury the older deposits. Drainage on the late Pleistocene, as on older fans, is parallel.

While the late Pleistocene deposits can often be recognized by their intermediate geomorphic position, a study of the lithologic character of the deposits together with their soils is usually necessary for reliable identification. The deposits probably do not exceed 25 ft in thickness on piedmont slopes above the boundary faults. They are generally gravelly or sandy and locally consist of crowds of mudflow-transported boulders many feet in diameter. Induration is lacking except for strong cementation by soil carbonate or reddish clay beneath the surfaces of the older and, to a lesser extent, the younger deposits. Boulders on or within the late Pleistocene fans are notably less decomposed relative to

those on Camp Rice fans, but outer rinds may still be disaggregated with the help of a knife or other tool.

The late Pleistocene piedmont-slope deposits adjacent to the Organ and southern San Andres Mountains are correlated with the Picacho and Tortugas morphostratigraphic units of the Rio Grande valley near Las Cruces (Gile and others, 1970; Hawley, 1978). The Picacho and Tortugas units range from more than 22,000 yrs old to approximately 350,000 yrs old, based on snail faunas, K/Ar dates on basalts, and on C-14 activities of secondary carbonates in soils (Seager and Hawley, 1973; Hawley, 1975; Hawley, 1978).

Latest Pleistocene and Holocene deposits

The youngest group of alluvium on the piedmont slopes of the Organ and southern San Andres Mountains is correlated with the Organ and Isaacks' Ranch morphostratigraphic units of Gile and Hawley (1968) and Hawley and Kottlowski (1969). Radiocarbon dates from charcoal within the Organ alluvium range from approximately 6,500 to 1,100 yrs (Gile and others, 1970), and Hawley (1975) indicates that much of the Organ alluvium was deposited 6,500-3,900 yrs ago. Isaacks' Ranch alluvium has not been dated but it forms deposits and surfaces intermediate between Organ and Jornada II; it probably is no older than approximately 15,000 yrs (J. W. Hawley, personal communication, 1979).

Isaacks' Ranch and Organ alluvium form the fills of broad drainageways crossing older fans as well as locally sizable alluvial-fan deposits at the mouths of modern and ancient arroyo systems. Mountainward, the constructional surface of these deposits commonly passes into erosional surfaces cut on older fans or on bedrock. Near fan apexes, these surfaces or deposits are inset below all older deposits or surfaces and are graded very close to the level of modern gully or arroyo floors. As with older deposits, the Organ and Isaacks' Ranch alluvium overlaps older fans downslope, and it is on the piedmont toe slopes or middle slopes where the alluvium forms broad fan deposits, generally less than 25 ft thick. On the eastern side of the range, the largest Holocene fans are on the downthrown side of the Organ Mountains fault, the bulk of the alluvium having bypassed the piedmont slopes above the fans. In these fans, Holocene alluvium may be nearly 100 ft thick. In contrast to older fans which display parallel drainage, an intricate braided-channel pattern distinguishes the latest Pleistocene and Holocene fan surfaces.

Organ and Isaacks' Ranch alluvium is texturally and compositionally similar to late Pleistocene deposits. Extensive boulder accumulations, interpreted to be transported by mudflows or debris flows, are common on fans draining higher parts of the mountains, while pebbly or sandy deposits compose fans adjacent to lower, more rounded, deeply weathered hills. Virtually all of the deposits are poorly sorted, consisting of boulder- to sand-size materials. The deposits are completely nonindurated and soils are weakly developed. Caliche occurs as threads, small nodules, or veins and, in some soils, organic material and a slight development of clay may dominate over soil carbonate. Soils on the faulted Holocene fans near WSMR headquarters exhibit little more than an accumulation of organic matter and minor clay buildup in the B horizon according to L. Gile (personal communication, 1979). These fan surfaces are probably approximately 4,000 yrs old. Except for those reworked from older fans, boulders in the latest Pleistocene and Holocene deposits are not deeply weathered. However, most have acquired a rounded form through spheroidal weathering.

Mineral deposits

Discovery of the Stevenson orebody in 1846 ushered in mining in the Organ district. Earlier mining may have been done, however, as legend has it that a lost gold mine exists in the Organ Mountains, perhaps in the Mineral Hill area, and that Padre La Rue, a Franciscan missionary, developed the mine about 1800 (Kottlowski, 1966; Kelly, 1975). Although many have looked for it, and shortly before his mysterious disappearance Colonel A. J. Fountain claimed to have found it, the whereabouts of the mine and rich gold vein remain unknown (Dunham, 1935).

Mining activity peaked in the district in the late 1800's and early 1900's, particularly 1900-1909, then gradually dwindled until about 1935 when mining essentially ceased. A second flurry of exploration and development accompanied the first two or three years of World War II, but did not last. In 1945, large parts of the northeast Organ Mountains and adjacent San Andres range, including many gold, silver, zinc, copper, and lead prospects or mines, were removed from further development by withdrawal of land into White Sands Proving Ground. Intermittent drilling in the Organ area and along the Torpedo–Bennett fault zone has continued from the early 1950's to the present. The barite-fluorite prospects in the west-central and southern parts of the range likewise attract occasional attention and have recently produced small amounts of ore.

Up to 1942, mines in the Organ district yielded, in order or decreasing value of base and precious metal, 2,263 tons of copper, 7,219 tons of lead, 780,000 oz of silver, 375-500 tons of zinc, and $123,000 worth of gold (Dunham, 1935; Albritton and Nelson, 1943). Total value of these ores produced over the last 125 years or so is more than $2,500,000 at 1935 prices; approximately half of this represents production from the Stevenson–Bennett mine. The Ruby mine and Bishop Cap area have produced approximately 500 tons of fluorite since the early 1900's (McAnulty, 1978).

None of the mines or prospects in the Organ district were operational or in development in 1979. Indeed, most of the workings were in such a bad state of repair that examination of them was risky at best. Consequently, during the present study only the surficial geology of the mine areas was examined. Readers interested in details of mine history, production, geology, and mineralogy are referred to the particularly informative and detailed accounts given by Dunham (1935), Albritton and Nelson (1943), and McAnulty (1978). Other good discussions can be found in Lindgren and others (1910), Soulé (1951), Kramer (1970), Glover (1975), and Macer (1978), the latter three of which concentrated on fluorspar mineralization.

Much of what follows is a synthesis of the observations of Dunham (1935) and Albritton and Nelson (1943) regarding the mineral deposits in the Organ Mountains, modified where appropriate by the results of my mapping, other recent studies, and recent drilling. The main purpose of the discussion is to acquaint the reader with the general character of the ore deposits and their past history of production, with special emphasis on the diverse types of structural and lithologic controls.

Most of the base- and precious-metal deposits and some of the fluorspar in the Organ district are of Oligocene age, related to emplacement of the Organ batholith. Recently, however, Macer (1978) has shown that most of the fluorspar deposits in the west-central and southern part of the range are related to the Rio Grande rift, emplaced by cool, dilute, meteoric waters within the last 26 m.y.

Mineral deposits related to Organ batholith

Most of the mineral deposits in the Organ district are associated with the Sugarloaf Peak quartz monzonite porphyry stock, the most volatile-rich and one of the latest phases of the Organ batholith. Mineralized veins cutting the stock and ore replacement of calc-silicate minerals in the metamorphic aureole around the stock indicate that the ores were emplaced after consolidation of at least an outer shell of the stock, following silicate metamorphism of the country rock.

Dunham (1935) convincingly documented a zoning of sulfide mineralization in the quartz monzonite porphyry centered east of Organ. The overall pattern appears relatively simple (fig. 87). A zone of disseminated and vein pyrite is concentrated in the quartz monzonite porphyry near San Agustin Pass. This and the surrounding region of weaker pyrite mineralization may represent a pyritic core at the center of the zoning pattern. Minor chalcopyrite and molybdenite also are disseminated in the core region. Copper values are high immediately east of Organ, at the Torpedo and Memphis properties. A few hundred feet northwest of the Memphis mine, zinc becomes important; farther northwest, in the Homestake mine area, argentiferous galena is domi-

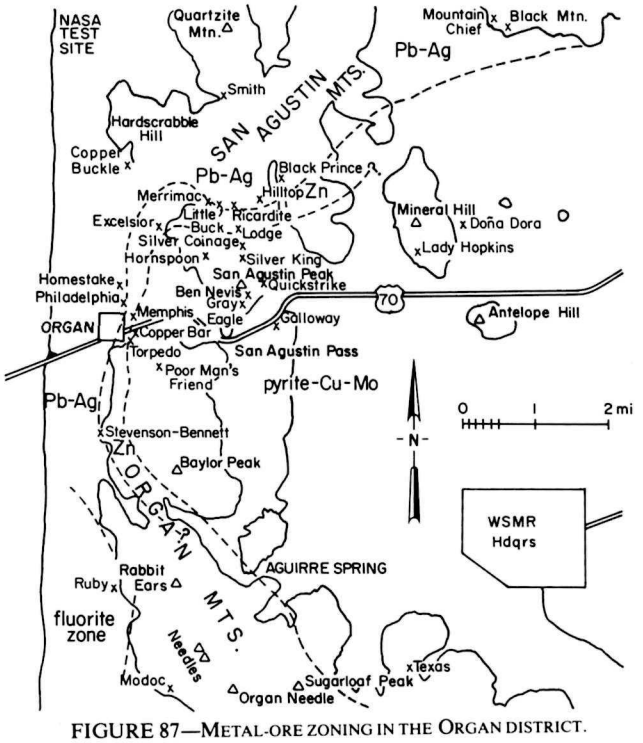


FIGURE 87—METAL-ORE ZONING IN THE ORGAN DISTRICT.

nant. The transition from copper to zinc can also be inferred near the Excelsior mine, located 2 mi north of Organ. One mile farther north, the Merrimac mine is definitely in the zinc zone. Deposits along the Percha–Fusselman contact north of the batholith and east of the Merrimac mine show a zinc to lead transition, and the Hilltop and Black Prince mines are on argentiferous galena deposits. North and east of these mines, silver values decrease and substantial barite appears. South of Organ, zinc occurs at depth in the Stevenson–Bennett mine while lead appears at shallower levels; a little fluorite occurs near the surface. Fluorspar, probably of late Tertiary age, predominates farther south, except at the Modoc mine where lead mineralization does not fit the zoning scheme. According to Dunham (1935), the copper veins at Texas Canyon, southeast of San Agustin Pass, probably belong to the copper zone, as do the copper-gold veins in Precambrian rocks in and around Mineral Hill. To the north of the latter veins, at Black Mountain and near the eastern mouth of Bear Canyon, small barite-galena deposits appear to indicate an eastward extension from the Hilltop–Black Prince area of the outer lead zone.

While the zoning pattern is portrayed as being relatively simple overall, it is complex in detail. Mineralization within the various zones is spotty, controlled by the interplay of impervious strata, soluble or reactive rocks, and structural features. For example, in the copper zone, copper values in nonreactive crystalline rocks are low, mineralization being confined to narrow vein fillings. In calcitic rocks along the igneous contact, however, copper values may be high, and the ores locally are massive replacement types. In the lead zone north of the batholith, mineralization is beneath impermeable Percha Shale in the upper parts of the Fusselman Dolomite. The ores cannot be found everywhere along this contact, however, having formed preferentially in the fractured crests of small anticlines (Albritton and Nelson, 1943). Even disseminated pyrite in the presumed core of the zoned system is lithologically or structurally controlled, veining being common in areas of fractured rock, while replacement of mafic minerals by pyrite appears elsewhere. Controls such as these can be seen for most of the deposits in the Organ district, leading to a simple classification into four main types: 1) segregations in pegmatites, 2) veins in crystalline rocks, 3) replacement deposits in limestone and dolomite, and 4) disseminations and microveining in quartz monzonite. Of these, the veins, and to a far lesser extent the pegmatites, have been important for their precious-metal content. Most production from the district, however, was won from base-metal replacement bodies.

Segregations in pegmatites

Lenticular pegmatitic masses, mostly a few tens of feet long and up to 10 ft across, but ranging to 600 ft long and 100 ft across, trend northwesterly through the San Agustin Peak and Sugarloaf Peak areas. Some of the pegmatites are simple, containing only albite, quartz, and orthoclase, and resembling those in the Precambrian batholith. Others are distinguished by a variety of minerals, notably diopside and other pyroxenes, sphalerite, chalcopyrite, tetradymite, galena, and argentite. All lack tourmaline, lithium mica, beryl, and other lithium or boron minerals typical of pegmatite dikes elsewhere. Silver has been the only metal produced from the pegmatites, mostly from the Gray Eagle, Quickstrike, and Ben Nevis mines, all located on the southeast slopes of San Agustin Peak. Total production was in the range of $30,000-$50,000 (Dunham, 1935). The pegmatites were not tested for uranium or thorium.

Veins in Precambrian rocks

Veins cutting Precambrian rocks are common in the Mineral Hill area. They generally strike east-west, dip steeply, and seldom exceed 2 ft in width. According to Dunham (1935), many veins follow dikes of Precambrian diorite, thus accounting for the observation made during this study that nearly every mine or prospect in the Precambrian terrain is on the edge of a diorite dike. Quartz, pyrite, and chalcopyrite are the most common minerals in the veins, although galena occurs locally. The veins were primarily valuable for their gold content, however, which occurs as grains in pyrite and probably chalcopyrite (Dunham, 1935). Most of the gold production in the Organ district ($123,000) came from 10 mines on Mineral Hill and from a group of mines on and adjacent to Rattlesnake Ridge, located approximately 2 mi northeast of Mineral Hill (Dunham, 1935; Kelly, 1975).

Dunham (1935) presents evidence that the veins in Precambrian rocks are of Tertiary age and related to the batholith. Apparently both shear zones along the edges of the diorite dikes, as well as the diorite itself, controlled deposition of the gold and copper. Locally on Mineral Hill, the mineralized veins are said to cut rhyolite dikes that represent the latest igneous activity associated with solidification of the batholith.

Mineralized veins and dikes in the Organ batholith

The Sugarloaf Peak quartz monzonite porphyry contains many mineralized veins and some mineralized dikes, located mostly between Aguirre Spring and the northern edge of the batholith. The veins, mostly quartz, are steep and compose both easterly and northwesterly trending groups. The mineralized dikes also trend northwesterly and have been mapped on the pediment west of San Agustin Peak. Most veins are a few inches wide, although those in Texas Canyon locally approach 10 ft in width. Lengths vary from a few tens of feet to perhaps several hundred feet, but groups of veins may persist for a thousand feet or more. The veins can usually be recognized by their limonitic, gossany cappings. Many have been prospected, but dozens showing good limonitic cappings remain unexplored, especially around the north and east sides of Baylor Mountain.

Both sets of veins were important for their silver values. Galena, freibergite [$(Cu, Fe, Zn, Ag)_{12}Sb_4S_{13}$], and argentite are the silver minerals, the latter two accounting for the richest ores. Reported oxidized silver minerals are cerargyrite (AgCl) and native silver. Published assays ran as high as 1,200 oz silver per ton, and shipments worth $55 per ton were made in 1934 from the Silver Coinage mine (Dunham, 1935). Thirty-five thousand dollars in oxidized silver ore was reported taken from one small vein at the Galloway property, 1 mi east of San Agustin Pass, in 1869. Other primary vein minerals are pyrite, chalcopyrite, sphalerite, en-

argite (Cu_3AsS_4), and tetradymite [$Bi_2(Te_1S)_3$]. Gold is generally present in trace amounts. Gangue is quartz, often stained green by chloritic alteration of wall rock. Notable workings that developed or at least explored the silver veins include Poor Mans Friend, Galloway, Silver King, Silver Coinage, and Hornspoon Group, the latter being 1 mi east-southeast of Isaacks' Ranch.

An east-trending vein in Texas Canyon cuts a mafic facies of the Organ Needle quartz monzonite. The vein is as notable for its values in copper as for its gold and silver potential. The vein, reported to be approximately 4,000 ft long and up to 10 ft wide by Albritton and Nelson (1943), has been explored by four drifts. Pyrite, chalcopyrite, a little barite, and minor tetradymite are the observable minerals; argentite also was found by Dunham. Dunham (1935) believed the vein to hold considerable potential in gold, but Albritton and Nelson (1943) indicated that only 6,000-7,000 tons of ore carrying 2 percent copper, 0.24 oz/ton gold, and 3 oz/ton silver could be expected from the vein.

On the pediment northeast of Organ several hornblende monzonite porphyry dikes, which appear to have invaded some of the northwest-trending shear zones in the Sugarloaf Peak quartz monzonite porphyry, are exposed. West of the graded road through sec. 36, the dikes are thoroughly sericitized, locally flooded with quartz, and contain abundant limonite derived from disseminated sulfides. The dikes, together with large tracts of the adjacent Sugarloaf Peak quartz monzonite porphyry, have been intensely altered by hydrothermal fluids and both are host to a sizable sulfide system. The dikes appear to have introduced the fluids. The mineralization in this area has resulted in considerable recent exploration effort that will be discussed under the section on recent drilling and future potential of the Organ district.

Replacement deposits

Almost all the larger base-metal deposits in the Organ district involve replacement of limestone or dolomite at or above the contact with the Sugarloaf Peak quartz monzonite porphyry. From Organ southward the contact is steep, following closely the dip of the Torpedo–Bennett fault zone. North of Organ, however, the contact is prevailingly concordant or gently crosscutting and dips west to north at about 60-30 degrees. Relatively extensive downdip mining of replaced strata was permitted where dips were shallow. The replacement deposits can be divided into 1) those associated with the Torpedo–Bennett fault zone, 2) those associated with porphyry contacts north of Organ, 3) those at the Percha–Fusselman contact, and 4) others.

REPLACEMENT DEPOSITS IN THE TORPEDO–BENNETT FAULT ZONE—Structure of the Torpedo–Bennett fault zone has been summarized under Laramide structure. The three major mines within the zone are the Stevenson–Bennett, Torpedo, and Memphis. Each deposit is different.

Three orebodies, important as lead, zinc, and silver producers, have been mined at the Stevenson–Bennett mine. All are tabular manto-type replacement deposits in steeply dipping Fusselman and Montoya Dolomite that lies between two major strands of the fault zone. Quartz monzonite porphyry dikes cut the dolomite and mineralization locally follows the dike contacts. At the surface the dikes are not connected with the batholith, being separated by a septa of Precambrian granite, 0.5 mi wide. Dunham interprets the deposits to be related to steep shear zones that he implies cut bedding. At the surface, however, these zones are parallel to near-vertical bedding; at least some of the massive "quartz veins" that he suggests are the surface expression of shear zones or the upper leached parts of orebodies may also be interpreted as massive chert beds in the Aleman Formation. Clearly there has been substantial shearing in the dolomite, but much of this appears to be bedding-plane slip.

The Stevenson orebody, easternmost of the three, appears to be within the Aleman Formation, which dips steeply eastward and is overturned. The orebody follows sheared chert beds to a depth of 50 ft where it flattens and follows the base of a west-dipping monzonite dike. Farther west, the Bennett orebody lies beneath the Percha Shale in Fusselman Dolomite which dips steeply westward. The orebody is tabular, 500 ft long and up to 20 ft thick, and has been followed down the dip for 600 ft. Upper parts of the deposit are oxidized while lower parts contain hypogene ore. The lead-to-zinc ratio increases upward. Between the Stevenson and Bennett deposits, the Page orebody, which is similar to the Bennett but smaller, replaces Cutter beds on the south (upthrown) side of a cross fault which contains the monzonite dike (mentioned above) that controls part of the Stevenson orebody.

Hypogene mineralization in all three orebodies is mainly sphalerite and argentiferous galena with minor chalcopyrite. Cerussite ($PbCO_3$), smithsonite ($ZnCO_3$), hemimorphite [$Zn_4(Si_2O_7)(OH)_2H_2O$], wulfenite ($PbMoO_4$), anglesite ($PbSO_4$), and limonite are the main oxidation products, although silver salts were important locally. The mine is well known to local and regional mineral enthusiasts for its variety of collectable minerals, especially the fine wulfenite specimens (fig. 88). Underground workings, however, are unsafe and the mine is on private property. Production from the Stevenson–Bennett probably totals more than $1,200,000 (Albritton and Nelson, 1943). In 1935, Dunham estimated reserves of approximately 35,000 tons of ore between the 250-ft and 450-ft levels in the



FIGURE 88—WULFENITE FROM STEVENSON–BENNETT MINE; crystals are approximately 1.25 inches long.

mine averaging 10-11 percent lead, 13 percent zinc, and 2.9 oz per ton of silver.

At the Torpedo mine, just east of Organ, as much as $800,000 worth of copper was produced, mostly before 1921. The geology and ore deposits of this mine are quite different from those at the Stevenson-Bennett property. Host to the orebody is silicified, kaolinized, and brecciated porphyry along the steep, east-dipping contact of Sugarloaf Peak quartz monzonite porphyry and metamorphosed Panther Seep beds. The deposit is tabular, 800 ft long and up to 150 ft wide, and has been explored to a depth of 500 ft down the contact. According to Dunham (1935), the Torpedo deposit and associated altered, brecciated rock is enclosed by two faults up to 200 ft apart, one of which separates ore and crushed porphyry from fresh porphyry, the other of which separates ore and crushed monzonite from limestone. South of the prominent dump on the property, the two faults and intervening altered zones converge to form a few feet of siliceous rock that continues south as a conspicuous rib or wall across the hills.

Primary minerals in the Torpedo deposit are pyrite and chalcopyrite that fill tiny stockwork fractures in the altered monzonite porphyry. Oxidation of the deposit has been complete to a depth of at least 300 ft, and the main orebody was a mass of chrysocolla, kaolin, and native copper containing minor silver values. Chalcocite was reported below 300 ft. Total production has been approximately 3.5 million pounds of copper (Soulé, 1951).

Earlier it was shown that the Torpedo-Bennett fault zone predates the Organ batholith by a substantial amount of time, and the interpretation was made that the fault zone localized part of the western edge of the batholith and guided ore fluids into reactive Paleozoic strata. Near the Torpedo mine, however, brecciated monzonite and the relatively straight trace and steep inclination of the monzonite-limestone contact have been interpreted by nearly all workers as a postbatholith fault that localized late-stage hydrothermal fluids. The problem with this conclusion is that elsewhere along the Torpedo-Bennett fault zone there is no evidence of postbatholith movement. Indeed, within short distances north and south of the Torpedo property, large and small apophyses of the batholith cut across the fault zone with no evidence of disturbance of the apophyses. One prospect, 0.5 mi north of the Memphis mine, exposes the contact between porphyry and sedimentary rocks with no evidence of faulting. Slanted drill holes, designed to test the mineralized contact deep beneath the Torpedo property, penetrated only fresh quartz monzonite porphyry at depths where the east-dipping fault contact was expected (Soulé, 1951; Albritton and Nelson, 1943). In the deepest parts of the holes monzonite was found to underlie and truncate bedding in Paleozoic rocks. Either the east-dipping fault contact suddenly becomes shallowly west dipping or the drill hole penetrated an apophyse of the quartz monzonite porphyry that intruded westward into the limestone. The latter possibility is consistent with the interpretation that the contact is intrusive and that the quartz monzonite porphyry invaded a preexisting fault zone.

But what about all the brecciated quartz monzonite porphyry? Perhaps minor adjustments occurred along the contact in the Torpedo area following emplacement of the batholith. Another possibility is that brecciation might be an effect of intense hydrothermal alteration (Sawkins, 1969). A third alternative, perhaps most likely of all, is that the breccia body is a tabular breccia pipe produced by fluidization along the edge of the batholith (Reynolds, 1954). In any case, the breccia body and the quartz monzonite-sedimentary rock contact clearly were responsible for locating the Torpedo orebody.

Approximately 0.25 mi north of the Torpedo workings is the Memphis property. The ground is credited with $200,000-$400,000 worth of copper, zinc, and silver (Albritton and Nelson, 1943). The deposits are replacements of west-dipping strata of Lead Camp Limestone adjacent to the Sugarloaf Peak quartz monzonite porphyry. The intrusive contact is essentially concordant, but near the north end of the property, it cuts westward across Lead Camp beds and becomes concordant again at a stratigraphically higher level. Lead Camp beds contained ore at four different horizons separated by barren calc-silicate rock (mostly garnetite) or marble. The tabular deposits dip west at 40-70 degrees and have been explored by open cuts, shafts, and drifts to depths of 200 ft. Chalcopyrite and sphalerite were the primary minerals, and malachite, azurite, chrysocolla, and hemimorphite formed in the oxidized zone that extends almost to the bottom of the workings. A large body of chalcocite also was found at shallow depths in the easternmost ore horizon. Gangue is mostly quartz, pyrite, hematite, and especially garnet. Small quantities of galena and tetradymite (Bi_2Te_2S) were reported by Dunham (1935). West of the Memphis property, Panther Seep beds crop out. These contain no evidence of ore mineralization and may be in fault contact with the Lead Camp.

REPLACEMENT DEPOSITS ALONG THE PORPHYRY CONTACT NORTH OF ORGAN—From the Memphis mine northward for 2-3 mi several notable replacement orebodies have been mined along intrusive contacts between rhyolite or quartz monzonite porphyry and metamorphosed sedimentary rocks. According to Dunham (1935) the orebodies are in the marbleized beds, mineralization having avoided the heavily calc-silicated rocks. While this may be generally true, a great deal of sulfide is in garnet skarn, as at the Merrimac mine and elsewhere. Dunham's thin-section studies show that ore sulfides generally replace the metamorphic silicates, indicating two stages of metamorphic processes. From south to north, the most notable workings are Homestake, Excelsior, and Merrimac mines, and the Lodge prospect.

At the Homestake mine, ¾ mi north of Organ, Panther Seep shaly beds dip westward beneath quartz monzonite porphyry. The porphyry is intensely altered to a mass of quartz and sericite, and drilling to the west indicates that its basic form is a sill above the Panther Seep beds. Deposits containing limonite, cerussite, argentojarosite, pyrite, and silver-bearing galena were mined along this contact in replaced Panther Seep beds.

One and a half miles farther northeast, the Excelsior mine area covers the intrusive contact between quartz monzonite porphyry of the batholith and west-dipping limestone beds of the Lead Camp and Panther Seep Formation. Lead Camp beds contain several tabular,

west-dipping orebodies that are reported to be irregular mantos of pyrite, chalcopyrite, sphalerite, and minor galena. Some of the ore shoots are also fracture controlled. Substantial oxidized ore as malachite also was present in upper parts of the workings.

Just east of the Excelsior workings a rhyolite laccolith has invaded the lower part of the Lead Camp Limestone. Extensive garnetization occurred along the floor of the laccolith with local shows of oxidized zinc and copper minerals, explored by small prospects.

Mineralization at the Merrimac mine, approximately 1 mi east-northeast of the Excelsior workings, was largely sphalerite and pyrite with lesser chalcopyrite and galena and their oxidation products. Payments for silver have also been made. A salient of the quartz monzonite porphyry extends to within a few feet of the mine, forming a semiconcordant tongue within the Percha Shale near the base of the Caballero–Lake Valley sequence. The ores are concentrated in limestone near the base of the Lake Valley Formation and above a series of garnetized sandy rocks that may be basal Lake Valley or Caballero. The orebodies appear to be localized along the crests of minor folds plunging northwest parallel to the dip of country rock (Albritton and Nelson, 1943). The longest fold, which passes through the Foy workings and apparently localized the orebody there, was traced at the surface by Albritton and Nelson for 400 ft. Three separate ore shoots were reported by Dunham, each approximately 20-40 ft wide and 2 ft thick. Two of the shoots in the main workings have been followed down a 36-degree plunge in the crests of anticlines for 200 ft. Sphalerite remains at the bottom of the stopes, which represent the mined-out, oxidized part of the orebody. Albritton and Nelson (1943) estimate that 4,000 tons of 10-15 percent Zn remain on the property.

Southeast of the Merrimac mine along the contact of the batholith with marbleized El Paso dolomites, a series of small prospects reveals sulfide replacement in El Paso beds not far above the Bliss contact. One mineralized shoot on the Lodge prospect dips northwest parallel to bedding and is approximately 6 ft wide and 4 ft thick. Mineralization is pyrite and sphalerite with minor galena, chalcopyrite, and pyrolusite (Albritton and Nelson, 1943). The shoot has been followed by stopes only a few feet downdip.

REPLACEMENT DEPOSITS AT THE PERCHA–FUSSELMAN CONTACT—Discontinuous zinc-lead-silver mineralization at the top of the Fusselman Dolomite characterizes the Percha–Fusselman contact at Black Mountain and from the Merrimac mine area eastward around the northern edge of the batholith to the Black Prince mine. The shale apparently presented a barrier to the movement of ore fluids so that mineral precipitation took place in reactive beds beneath the barrier. The ore deposits were further localized, according to Albritton and Nelson (1943), in the fractured crests of small anticlines whose trend is essentially down the dip of bedding that dips northwest at 30-35 degrees. Thus, the orebodies are elongated, northwest-plunging shoots. Maximum thickness of the shoots is 4-6 ft, and their greatest longitudinal dimension is not more than 60-80 ft.

North of the batholith, many small prospects have explored the contact with notable mineralization being found at the Little Buck, Rickardite, and Hilltop properties, and lesser ore at the Black Prince mine. Lead-zinc ratios vary progressively along the Percha–Fusselman contact between the Little Buck and Hilltop mines (Albritton and Nelson, 1943); this is part of the zoning pattern previously described. Zinc predominates at the Little Buck; lead is still subordinate, but relatively more abundant at the Rickardite, and at the Hilltop, lead exceeds zinc in abundance (Albritton and Nelson, 1943).

Much of the mineralization is present as massive replacement bodies or veins of coarsely crystalline galena-sphalerite, mostly localized in the fractured crests of small anticlines. Individual sulfide bodies, however, are most irregular, discontinuous, and relatively thin (up to 6 ft wide for the largest), judging from the size of mined-out stopes (Dunham, 1935). Thickest bodies left in the workings are on the order of 1 ft thick. A second, low-grade type of mineralization occurs as disseminations, mostly of pyrite but including galena and sphalerite, in dolomite. Substantial silver (in galena) and native gold were mined from the Hilltop and Little Buck mines. In fact, these metals accounted for most of the Hilltop's and the Little Buck's production. Altaite (PbTe) and rickardite (Cu_4Te_3) have also been reported, and native tellurium was fairly common in the Hilltop workings (Dunham, 1935). The Little Buck and Hilltop properties each produced $50,000-$60,000 worth of argentiferous galena and gold, the Rickardite more than $2,000 worth of zinc and lead ore, and the Black Prince mine yielded approximately $1,000 worth of argentiferous galena.

OTHER REPLACEMENT DEPOSITS—In the mountains both north and south of the eastern part of Bear Canyon, small deposits of barite and galena crop out at the Percha–Fusselman contact in several places. Some have been explored by small prospects, others have not. None appear to be sizable and barite predominates in all. Dunham (1935) reports that the galena is nonargentiferous.

Somewhat more significant deposits of galena and barite have been mined north of the eastern mouth of Bear Canyon just west of the edge of the mountain range. The deposits are located within and adjacent to a normal fault that separates Precambrian granite from El Paso Limestone. Mineralization is very irregular, filling fault breccia as well as replacing parts of the limestone beds. Besides the ores mentioned above, fluorite, cerussite, wulfenite, and vanadinite have been reported, the latter as museum-quality specimens according to Dunham (1935). Small amounts of galena and barite have been shipped from some of the workings.

Another notable deposit is the property known as the Smith mine located on the western strand of the Quartzite Mountain fault zone 0.5 mi south of Loman Canyon. Oxidized silver ore worth approximately $30,000 was produced from irregular orebodies within silicified Lead Camp Limestone adjacent to the fault. This is the only ore deposit associated with the Quartzite Mountain fault zone, and it suggests that the fault existed prior to emplacement of the mineralizing fluids.

Albritton and Nelson (1943) point out potential ore-bearing ground at the Copper Buckle prospect located at the fault contact between Hueco Limestone and Orejon Andesite just south of Hardscrabble Hill. A body of almost solid pyrite at least 15 ft across has been exposed

in prospects; its lateral and downward extent are unknown. Similar massive pyrite deposits at the Merrimac and Little Buck mines border zones of substantial lead and zinc mineralization (Albritton and Nelson, 1943).

Most notable of the deposits included as "other replacements" is that at the Modoc mine, located on the Modoc fault in the west-central part of the Organ range. Dunham states that as much as $200,000 worth of lead ore may have been produced, although the figure is in doubt. The deposit is an irregular replacement in Hueco Limestone that is in fault contact with Orejon Andesite. The fault is of volcano-tectonic origin, part of an arcuate fracture, movement on which allowed subsidence of a large block of ash-flow tuff and underlying rocks into the Organ batholith.

Although mineralization in the area of the Modoc mine is strong, it is also spotty and discontinuous. High-grade ore was confined to a mass 7 ft wide and 50 ft long that extended down the dip of the fault for 100 ft or more. The ore has been stoped out. Minerals, besides galena, included garnet, hematite, and epidote. The galena is reported to be low in silver. Several limestone beds near the mine have been converted to skarn or tactite; some are adjacent to thin monzonite porphyry sills, and some, such as that at the Orejon mine just south of the Modoc property, contained bodies of copper, lead, and zinc ore.

Finally, several areas within the Organ range contain noteworthy disseminated pyrite deposits. One, forming the core of the zoned sulfide system in the Organ district, has already been mentioned. An equally large or larger body of disseminated pyrite is present in the northern half of the granite of Granite Peak. The sulfide system is especially well developed in Maple and Rock Canyons and on adjacent ridges, where 1-4 percent pyrite is present. The quartz monzonite is stained red to brown over most of this area by shallow oxidation; fresh pyrite appears in most of the ravine bottoms. A single analysis of the quartz monzonite from this area gave 75 ppm Cu and 20 ppm Zn. Overlying the quartz monzonite is a roof pendant of Orejon Andesite. While the contact is intensely altered and veined with quartz and large areas of the roof pendant have been converted to quartz and sericite, three analyses of the altered rock gave no unusual values in base metals. The former presence of considerable pyrite in these rocks is, however, indicated by abundant limonite. Blue lazulite, at first mistaken for azurite, is conspicuous on outcrops of rocks altered to quartz and sericite. Sizable areas of disseminated and vein pyrite were mapped elsewhere in the range—in Orejon Andesite on the ridge south of Orejon Peak, in Organ Needle quartz monzonite on the divide between Fillmore and Indian Hollow Canyons, and in the rhyolite intrusive between Baldy Peak and Orejon Peak.

Mineral deposits probably related to late Tertiary rifting

Notable deposits of barite and fluorite are present in the west-central and southern parts of the Organ Mountains, at Tortugas Mountain near Las Cruces, and at Bishop Cap. The deposits have not yet proven to be major ones, and only approximately 400 tons of fluorite have been shipped from the Organ Mountains–Bishop Cap mines to date. Described in detail by McAnulty (1978), the fluorspar deposits are largely open-space fillings and minor replacements in fault blocks of lower and middle Paleozoic limestone or dolomite. Because the fluorspar appears to be adjacent to or within the Organ cauldron, it is tempting to assign the deposits a magmatic origin related to the middle Tertiary volcano-tectonic cycle. Clearly, the fluorite of the Stevenson-Bennett mine and Bear Canyon area can be so regarded. However, recent studies indicate that much of the barite-fluorite may be of late Tertiary age, related to the Rio Grande rift.

Studies of fluid inclusions in fluorite from the Ruby mine, Tortugas Mountain, and Bishop Cap deposits by Macer (1978) indicate that the fluorspar at these localities was emplaced by very dilute fluids at temperatures below 210°C. He interprets the fluorite as being deposited by connate-meteoric waters heated by high geothermal gradients beneath the Rio Grande rift, rather than by hydrothermal fluids related to the Organ cauldron. The conclusion is consistent with the fact that elsewhere near Las Cruces, barite-fluorite veins cut rift-bolson deposits dated 26-9 m.y. old (Seager and Hawley, 1973). Further, some fluorite veins at Bishop Cap formed in north-trending normal faults, interpreted in this report to be products of an early phase of extension in the rift (see section on late Tertiary deformation). Therefore, barite and fluorspar of late Tertiary as well as middle Tertiary age probably formed in the Organ Mountain area, with the larger, better-known deposits constituting the former.

Fluorspar (with barite) has been found in modest quantities at the Ruby mine, Bishop Cap area, and Devil's Canyon area. The interested reader should refer to the descriptions of Kramer (1970), Glover (1975), Macer (1978), and McAnulty (1978) for details of all but the last of these areas. The following summaries are intended to convey only the general character of the deposits.

Ruby mine (Hayner mine)

Approximately 400 tons of fluorspar have been mined from the Ruby property, located midway between Baylor and Fillmore Canyons on the western edge of the Organ range. The ore occurs as open-space fillings and lesser replacements of marble in several minor, north-trending, east-dipping faults that cut west-dipping marbleized Lead Camp Limestone. Within the marble, and exposed just east of the workings, is an andesite porphyry sill, some 500 ft thick; it too is reported to contain a little fluorite (Glover, 1975). Quartz and calcite are gangue minerals, and minor barite is present.

Bishop Cap area

At Bishop Cap the mineralization is of two kinds: 1) open-space filling with minor replacements in or near faults and 2) replacement of favorable beds within the Paleozoic sequence. The former type is by far the most dominant, and barite-fluorite deposits of this kind are widely scattered over the Bishop Cap hills. The most important deposits, however, are concentrated along three

faults and at their mutual intersection. Two of the faults are the westernmost of the north-trending group that breaks the Bishop Cap hills into five blocks; the other mineralized fault is strongly arcuate and has a general east trend, bisecting the hills almost down the middle. The latter fault, named Blue Star fault by Kramer (1970), contains the Blue Star prospect that has produced almost all the 120 tons of fluorspar shipped from the Bishop Cap area.

Most of the fluorspar in the Bishop Cap hills occurs where faults transect the Fusselman Dolomite. Lesser mineralization has been found beneath shale beds, such as the Helms, Percha, and several in the Berino Formation; the shales apparently blocked movement of fluids. The fluorspar is in the form of massive crystalline pods. Locally barite is abundant, but in the larger deposits it is subordinate to fluorite. Calcite is a common gangue. Trace amounts of pyrite, galena, chalcopyrite, azurite, malachite, hematite, and uranium minerals have been reported (McAnulty, 1978). Alteration is in the form of massive bodies of jasperoid, both along faults and other fractures and as replacement of beds. The fluorspar is always associated with the cryptocrystalline quartz, but many bodies of jasperoid contain little or no barite or fluorite.

Devil's Canyon area

Substantial barite deposits are exposed in the upper reaches of Boulder Canyon, especially near its intersection with Devil's Canyon. The Devil's Canyon mine, located at the mouth of the canyon with the same name, has exposed a sizable body of barite in marbleized El Paso Limestone. According to Dunham (1935) the deposit is approximately 100 ft long and 20 ft wide and has been explored to a depth of 25 ft. Small amounts of fluorite also are present. Considerable unprospected barite also crops out to the west of the mine in Lead Camp Limestone. Somewhat discontinuous bodies up to 200 ft long were noted along faults and replacing limestone beds in the southwest quarter of sec. 33. Other barite showings are common in marbles at the south end of the batholith east of the Devil's Canyon mine. Unfortunately, all of Boulder Canyon is an impact area for the Ft. Bliss artillery range.

Recent drilling and future potential of the Organ district

In the last two decades exploration in the Organ district has been directed toward discovery of porphyry-type copper deposits, disseminated or vein molybdenum, or massive replacement orebodies. Exploration has been encouraged by Dunham's (1935) concept of mineral zonation in the district; by the recognition that large areas of the Sugarloaf Peak quartz monzonite porphyry contain disseminated pyrite, molybdenite, and chalcopyrite; and by the fact that intense, pervasive quartz-sericite alteration of quartz monzonite porphyry occurs in secs. 25, 26, 35, and 36 north of Organ. Ample room for exploration, and for a sizable buried deposit, was found when drill holes proved that a shallowly buried pediment extended at least 1.5 mi west of the westernmost outcrops of the altered porphyry and over a wide area to the north and south. Recent radiometric dates of approximately 33 m.y. for the quartz monzonite porphyry probably dampened the enthusiasm of those only interested in Laramide stocks; the lack of abundant quartz veining in the altered rock may have discouraged others. Drilling, nevertheless, has continued so that now more than 40 holes have explored the pediment north of Organ in secs. 22, 25, 26, 27, 35, and 36. The generalized stratigraphy encountered in 6 of these holes is shown in table 8, and the distribution of rock types beneath the pediment penetrated by all of the holes is shown on the geologic map (sheet 1, in pocket). Drill-hole locations, mineralization, and alteration data are confidential at this time. However, from outcrops on or near the pediment, disseminated pyrite, molybdenite, and chalcopyrite seem clearly to be associated with a sizable body of quartz monzonite porphyry that has strong quartz-sericite alteration. The porphyry appears to be in the form of one or more moderately thick sills that dip west and underlie a large area of the pediment.

Hornblende monzonite porphyry dikes, also altered and containing disseminated sulfides, can be seen cutting the quartz monzonite porphyry along the eastern edge of the pediment. Hydrothermal alteration and mineralization appear to be related to the dike system. If so, replacement bodies of base metals may be expected where these dikes cut reactive beds, such as those in the Lead Camp Limestone or Lake Valley Formation, in the subsurface. Both formations have been located by drilling between sills of quartz monzonite porphyry beneath the pediment. Another worthy exploration target in view of its importance in localizing minerals elsewhere in the district is the upper part of the Fusselman Dolomite; however, it will generally be deeper than 4,000 ft beneath the surface.

South of Organ, outcrops and gravity data show the pediment is at least 1 mi wide, expanding to 2 or 3 mi wide west of the Organ Needles. Exploration along this part of the pediment has not been done with the same vigor as farther north, probably because few outcrops

TABLE 8—REPRESENTATIVE DRILL-HOLE DATA IN THE ORGAN AREA (reported depths and lithologies with depths reported in feet). Locations of holes, mineralization, and alteration is confidential information.

1	0-200, alluvium; 200-1380, monzonite and volcanics; 1380-T.D. calc-silicate rocks and marble; upper gypsum beds of Panther Seep Formation in bottom of hole
2	0-60, alluvium; 60-720, monzonite porphyry; 720-870, calc-silicate rocks; 870-1130, monzonite porphyry; 1130-T.D., calc-silicate rock with minor monzonite
3	0-45, alluvium; 45-360, monzonite porphyry; 360-590, calc-silicate rock; 590-870, monzonite porphyry; 870-2595, calc-silicate rock and marble with minor monzonite sills; 2595-T.D., monzonite porphyry; top of Lead Camp at 2150
4	0-125, alluvium; 125-415, monzonite porphyry; 415-565, andesite; 565-T.D. monzonite porphyry
5	0-100, alluvium; 100-910, monzonite porphyry and andesite; 910-T.D., calc-silicate rock and marble; top of Lead Camp 2600, top of Rancheria 3450, top of Las Cruces–Lake Valley sequence 3800; single sills in Lake Valley, Rancheria, and Panther Seep
6	0-30, alluvium; 30-2225, calc-silicate rock and marble; 2225-T.D., monzonite; top of Lead Camp at 1400

of altered igneous rock are present. Drilling on the Torpedo property shows, however, that apophyses of the batholith extend westward in the subsurface from the main batholith mass. Surface mapping has also revealed scattered porphyry dikes on the pediment almost as far south as Soledad Canyon. Calc-silicate metamorphism of Paleozoic rocks, intense near the batholith contact, weakens generally with distance from the contact, but locally persists on the pediment up to 1 mi from the contact.

Much of the pediment south of Organ is cut on Panther Seep strata, a unit notably nonsusceptible to mineralization even in the heart of the Organ district. This may account for the lack of mineral shows south of Organ. Where reactive rocks are exposed, such as near the Modoc and Ruby mines, mineral deposits have been found. Of course, Lead Camp Limestone, Lake Valley Formation, Fusselman Dolomite, and Montoya Dolomite can be expected in the subsurface beneath the Panther Seep where they may be host to replacement base-metal or fluorite deposits. These units may be especially favorable targets adjacent to the Modoc fault from a point 0.5 mi north of the Modoc mine to just south of Fillmore Canyon, south of which they are probably too deep. Hueco Limestone, which contains the Modoc orebody, is a relatively shallow target along and west of the Modoc fault to a point approximately 0.5 mi south of Fillmore Canyon.

With regard to the future mineral potential of the western pediment of the Organ Mountains, two conclusions based on current and past studies seem inescapable. First, probably all the major orebodies exposed at the surface have been found and further production of the known deposits cannot take place under present economic and land-status conditions, except on a very small scale. A possible exception to this is the potential for future discovery of precious metals in some of the unprospected fissure veins located between San Agustin Pass, Aguirre Spring, and Sugarloaf Peak. Also, potential uranium, thorium, and related metals in Sugarloaf Peak quartz monzonite pegmatites have not been tested. The second conclusion, one most important in formulating future land-use policies for the area, is that, except for the area north of Organ, essentially nothing is known regarding the subsurface potential of the pediment area.

Considering the value of metals won from deposits located within a few hundred feet of the present level of erosion, to suppose that no other deposits lie at other depths seems shortsighted. To assume that all the mineral deposits in the area happened to have formed at the present level of erosion is unrealistic. Deposits of equal or greater value than those dug from the shallow workings in the Organ district almost certainly lie hidden at other depths beneath the western slopes of the range. To be sure, enrichment has made deposits near the present surface richer and even brought some deposits up to ore grade, but many primary sulfide deposits in the Organ district constituted ore without benefit of enrichment. The potential for orebodies beneath the pediment from Soledad Canyon to north of Organ simply cannot be denied. Molybdenum and lead-zinc replacements appear to be especially promising targets there, while precious metals and possibly uranium-thorium or related mineralization is still prospective over much of the batholith.

References

Abbate, E., and Sagri, M., 1969, Dati e considerazioni sul margine orientale dell' altiplano etiopico nelle province del Tigrai e del Wollo: Societá Geologica Italiana, Boll., v. 88, p. 489-497

Albritton, C. C., and Nelson, V. E., 1943, Lead, zinc, and copper deposits of the Organ district, New Mexico (with a supplement on the occurrence of bismuth): U.S. Geological Survey, Open-file Rept. 43, 39 p.

Ames, C., 1892, Ascent of the Organ Mountains, New Mexico: Appalachia, v. 6, part 4, p. 289-302

Antisell, Thomas, 1856, Geological report; Parke's surveys in California and near the 32nd parallel, U.S. Pacific railroad exploration: 33rd Congress of the United States, 2nd session, Senate Exec. Doc. 78 and House Exec. Doc. 91, vol. 7, pt. 2, p. 161-162

Bachman, G. O., and Mehnert, H. H., 1978, New K-Ar dates and the late Pliocene to Holocene geomorphic history of the central Rio Grande region, New Mexico: Geological Society of America, Bull., v. 89, no. 2, p. 283-292

Bachman, G. O., and Myers, D. A., 1969, Geology of the Bear Peak area, Doña Ana County, New Mexico: U.S. Geological Survey, Bull. 1271-C, 46 p.

Bailey, D. K., and MacDonald, R., 1969, Alkali-feldspar fractionation trends and the derivation of peralkaline liquids: American Journal of Science, v. 267, p. 242-248

Bartlett, J. R., 1854, Personal narrative of exploration and incidents in Texas, New Mexico, California, Sonora, and Chihuahua 1850-1853: Chicago, The Rio Grande Press, Inc., p. 392-394

Branch, C. D., 1966, The volcanic cauldrons, ring complexes, and associated granites of the Georgetown Inlier, Queensland: Bureau Mineral Resources of Australia, Bull. 76

Brown, L. F., 1977, A gravity survey of central Doña Ana County, New Mexico: M.S. thesis, New Mexico State University, 56 p.

Bryan, Kirk, 1938, Geology and ground-water conditions of the Rio Grande depression in Colorado and New Mexico, *in* Rio Grande joint investigtions in the upper Rio Grande basin in Colorado, New Mexico, and Texas: Washington, D.C., National Resources Commission, Regional Planning, pt. 6, p. 196-225

Budding, A. J., and Condie, K. C., 1975, Precambrian rocks of the Sierra Oscura and northern San Andres Mountains, south-central New Mexico: New Mexico Geological Society, Guidebook 26th field conference, p. 89-93

Bushnell, H. P., 1953, Geology of the McRae Canyon area, Sierra County, New Mexico: M.S. thesis, University of New Mexico, 106 p.

———, 1955, Stratigraphy of the McRae formation, Sierra County, New Mexico: Compass, v. 33, p. 9-17

Byers, F. M., Jr., Carr, W. J., Orkild, P. P., Quinlivan, W. D., and Sargent, K. A., 1975, Volcanic suites and related cauldrons of Timber Mountain-Oasis Valley caldera complex, southwestern Nevada: U.S. Geological Survey, Prof. Paper 919, 70 p.

Chamberlin, R. M., 1978, Structural development of the Lemitar Mountains, an intrarift tilted fault-block uplift, central New Mexico (abs.): International Symposium of the Rio Grande Rift, Abstracts with Programs, p. 22-24

Chapin, C. E., 1971, The Rio Grande rift, part I: modifications and additions: New Mexico Geological Society, Guidebook 22nd field conference, p. 191

———, 1979, Evolution of the Rio Grande rift—a summary, *in* Rio Grande rift—tectonics and magmatism, R. Riecker, ed.: American Geophysical Union, Monograph, p. 1-5

Chapin, C. E., and Seager, W. R., 1975, Evolution of the Rio Grande rift in the Socorro and Las Cruces areas: New Mexico Geological Society, Guidebook 26th field conference, p. 297

Chapin, C. E., Chamberlin, R. M., Osburn, G. R., Sanford, A. R., and White, D. W., 1978, Exploration framework of the Socorro geothermal area, New Mexico, *in* Field guide to selected cauldrons and mining districts of the Datil-Mogollon volcanic field, New Mexico: New Mexico Geological Society, Spec. Pub. 7, p. 115-130

Clemons, R. E., in press, Geology of Massacre Peak quadrangle, Luna County, New Mexico: New Mexico Bureau of Mines and Mineral Resources, Geol. Map 51, scale 1:24,000

Cloos, E., 1968, Experimental analysis of Gulf Coast fracture patterns: American Association of Petroleum Geologists, Bull., v. 52, no. 3, p. 420-444

Condie, K. C., and Budding, A. J., 1979, Geology and geochemistry of Precambrian rocks, central and south-central New Mexico: New Mexico Bureau of Mines and Mineral Resources, Mem. 35, 58 p.

Coney, P. J., 1976, Plate tectonics and the Laramide orogeny, *in* Tectonics and mineral resources of southwestern North America: New Mexico Geological Society, Spec. Pub. 6, p. 5-10

———, 1978, Mesozoic-Cenozoic Cordilleran plate tectonics, *in* Cenozoic tectonics and regional geophysics of western Cordillera, R. B. Smith and G. P. Eaton, eds.: Geological Society of America, Mem. 152, p. 33-50

Coney, P. J., and Reynolds, S. J., 1977, Cordilleran Benioff zones: Nature, v. 270, p. 403-406

Cook, F. A., McCullar, D. B., Decker, E. R., and Smithson, S. B., 1979, Crustal structure and evolution of the southern Rio Grande rift, *in* Rio Grande rift—tectonics and magmatism, R. Riecker, ed.: American Geophysical Union, Monograph, p. 195-208

Corbitt, L. L., and Woodward, L. A., 1973, Tectonic framework of Cordilleran foldbelt in southwestern New Mexico: American Association of Petroleum Geologists, Bull., v. 57, no. 11, p. 2207-2216

Cordell, L. E., 1978, Regional geophysical setting of the Rio Grande rift: Geological Society of America, Bull., v. 89, p. 1073-1090

Darton, N. H., 1928, "Red Beds" and associated formations in New Mexico, with an outline of the geology of the state: U.S. Geological Survey, Bull. 794, 356 p.

Davis, G. H., 1978, Monocline fold pattern of the Colorado Plateau: Geological Society of America, Mem. 151, p. 215-234

Decker, E. R., and Smithson, S. B., 1975, Heat flow and gravity interpretation across the Rio Grande rift in southern New Mexico and west Texas: Journal of Geophysical Research, v. 80, no. 17, p. 2542-2552

DeSitter, L. U., 1956, Structural geology: New York, McGraw Hill, p. 144

Dickinson, W. R., and Snyder, W. S., 1978, Plate tectonics of the Laramide orogeny: Geological Society of America, Mem. 151, p. 355-365

Doty, G. C., and Cooper, J. B., 1970, Stratigraphic test well T-14, Post area, White Sands Missile Range, New Mexico: U.S. Geological Survey, Open-file Rept., 34 p.

Drewes, H., 1978, The Cordilleran orogenic belt between Nevada and Chihuahua: Geological Society of America, Bull., v. 89, p. 641-657

Dunham, K. C., 1935, The geology of the Organ Mountains: New Mexico Bureau of Mines and Mineral Resources, Bull. 11, 272 p.

Entwistle, L. P., 1944, Manganiferous iron-ore deposits near Silver City, New Mexico: New Mexico Bureau of Mines and Mineral Resources, Bull. 19, 70 p.

Flih, B., 1976, Osagian bioherms at the Bishop Cap hills, Doña Ana County, New Mexico: M.S. thesis, University of Texas (El Paso), 106 p.

Flower, R. H., 1953, Paleozoic sedimentary rocks of southwestern New Mexico: New Mexico Geological Society, Guidebook 4th field conference, p. 106-112

———, 1969, Early Paleozoic of New Mexico and the El Paso region: El Paso Geological Society, Guidebook 3rd field conference, p. 31-101

Gile, L. H., and Hawley, J. W., 1968, Age and comparative development of desert soils at the Gardner Spring radio-carbon site, New Mexico: Soil Science Society of America, Proceedings, v. 32, no. 5, p. 709-719

Gile, L. H., Hawley, J. W., and Grossman, R. B., 1970, Distribution and genesis of soils and geomorphic surfaces in a desert region of southern New Mexico: Soil Science Society of America, Guidebook geomorphology field conference, 156 p.

Giles, D. L., 1967, A petrochemical study of compositionally zoned ash-flow tuffs: Ph.D. thesis, University of New Mexico, 176 p.

Glover, T. J., 1975, Geology and ore deposits of the northwestern Organ Mountains, Doña Ana County, New Mexico: M.S. thesis, University of Texas (El Paso), 93 p.

Gordon, C. H., 1907, Notes on the Pennsylvanian formations in the Rio Grande valley, New Mexico: Journal of Geology, v. 15, p. 805-816

Greenwood, E., Kottlowski, F. E., and Thompson, Sam III, 1977, Petroleum potential and stratigraphy of Pedregosa Basin—

comparison with Permian and Orogrande basins: American Association of Petroleum Geologists, Bull., v. 61, no. 9, p. 1448-1469

Gries, J. C., and Haenggi, W. T., 1970, Structural evolution of the eastern Chihuahua tectonic belt, *in* The geologic framework of the Chihuahua tectonic belt, K. Seewald and D. Sundeen, eds.: University of Texas (Austin), West Texas Geological Society, p. 119-138

Hamblin, W. K., 1965, Origin of "reverse drag" on the downthrown side of normal faults: Geological Society of America, Bull., v. 76, p. 1145-1164

Harbour, R. L., 1972, Geology of the northern Franklin Mountains: U.S. Geological Survey, Bull. 1298, 129 p.

Hawley, J. W., 1975, Quaternary history of Doña Ana County region, south-central New Mexico: New Mexico Geological Society, Guidebook 26th field conference, p. 139-150

———, compiler, 1978, Guidebook to the Rio Grande rift in New Mexico and Colorado: New Mexico Bureau of Mines and Mineral Resources, Circ. 163, 239 p.

Hawley, J. W., and Kottlowski, F. E., 1969, Quaternary geology of the south-central New Mexico border region, *in* Border stratigraphy symposium: New Mexico Bureau of Mines and Mineral Resources, Circ. 104, p. 89-115

Hawley, J. W., Kottlowski, F. E., Seager, W. R., King, W. E., Strain, W. S., and LeMone, D. V., 1969, The Santa Fe Group in the south-central New Mexico border region, *in* Border stratigraphy symposium: New Mexico Bureau of Mines and Mineral Resources, Circ. 104, p. 52-76

Hawley, J. W., Bachman, G. O., and Manley, Kim, 1976, Quaternary stratigraphy in the Basin and Range and Great Plains provinces, New Mexico and western Texas, *in* Quaternary stratigraphy of North America: Stroudsburg, Pennsylvania, Dowden, Hutchinson, and Ross, Inc., p. 235-274

Hayes, P. T., 1975, Cambrian and Ordovician rocks of southern Arizona and New Mexico and westernmost Texas: U.S. Geological Survey, Prof. Paper 873, 98 p.

Hildreth, W., 1979, The Bishop Tuff—evidence for the origin of compositional zoning in silicic magma chambers, *in* Ash-flow tuffs, C. E. Chapin and W. E. Elston, eds.: Geological Society of America, Spec. Paper 180, p. 43-75

Hobbs, B. E., 1971, The analysis of strain in folded layers: Tectonophysics, v. 2, no. 5, p. 329-375

Hoffer, J. M., 1970, Petrology and mineralogy of the Campus Andesite pluton, El Paso, Texas: Geological Society of America, Bull., v. 81, p. 2129-2135

Hunt, C. B., 1975, Transverse valleys—comment by C. B. Hunt: New Mexico Geological Society, Guidebook 26th field conference, p. 6

Ingraham, R. L., 1979, A climbing guide to the Organ Mountains: New Mexico State University, Department of Physics, 104 p.

Irvine, T. N., and Baragar, W. R. A., 1971, A guide to the chemical classification of the common volcanic rocks: Canadian Journal of Earth Sciences, v. 8, p. 523-548

Jahns, R. H., and Tuttle, O. F., 1963, Layered pegmatite-aplite intrusions, *in* Symposium on layered intrusions: Mineralogical Society of America, Spec. Paper 1, p. 78-92

Johnston, W. D., Jr., 1928, Fluorspar in New Mexico: New Mexico Bureau of Mines and Mineral Resources, Bull. 4, p. 61-88

Jones, F. A., 1904, New Mexico mines and minerals: Santa Fe, The New Mexico Printing Co., p. 73-80

Kelley, V. C., 1952, Tectonics of the Rio Grande depression of central New Mexico: New Mexico Geological Society, Guidebook 3rd field conference, p. 93-105

Kelley, V. C. and Silver, C., 1952, Geology of the Caballo Mountains: University of New Mexico, Publications in Geology, no. 4, 286 p.

Kelly, T. E., 1975, The Lost Padre Mine and the Organ mining district: New Mexico Geological Society, Guidebook 26th field conference, p. 163-165

Keyes, C. R., 1905, Geology and underground water conditions of the Jornada del Muerto, New Mexico: U.S. Geological Survey, Water Supply Paper 123, 42 p.

Kingsley, L., 1931, Cauldron subsidence of the Ossipee Mountains: American Journal of Science, 5th ser., v. 22, p. 139-168

Kottlowski, F. E., 1957, High-purity dolomite deposits of south-central New Mexico: New Mexico Bureau of Mines and Mineral Resources, Circ. 47, 43 p.

———, 1960, Summary of Pennsylvanian sections in southwest New Mexico and southeast Arizona: New Mexico Bureau of Mines and Mineral Resources, Bull. 66, 187 p.

———, 1963, Paleozoic and Mesozoic strata of southwest and south-central New Mexico: New Mexico Bureau of Mines and Mineral Resources, Bull. 79, 100 p.

———, 1965, Sedimentary basins of south-central and southwestern New Mexico: American Association of Petroleum Geologists, Bull., v. 49, no. 11, p. 2120-2139

———, 1966, The Lost Padre mine: New Mexico Magazine, October, p. 22-23, 34, 36

Kottlowski, F. E., Flower, R. H., Thompson, M. L., and Foster, R. W., 1956, Stratigraphic studies of the San Andres Mountains, New Mexico: New Mexico Bureau of Mines and Mineral Resources, Mem. 1, 132 p.

Kottlowski, F. E., Weber, R. H., and Willard, M. E., 1969, Tertiary intrusive-volcanic mineralization episodes in the New Mexico region (abs.): Geological Society of America, Abstracts with Programs, pt. 7, p. 278

Kottlowski, F. E., LeMone, D. V., and Seager, W. R., 1975, Marginal marine and continental facies of the Lower Permian in central New Mexico, *in* Permian exploration, boundaries, and stratigraphy: West Texas Geological Society and Permian Basin Section, Society of Economic Paleontologists and Mineralogists, symposium volume, p. 119-124

Kramer, W. V., 1970, Geology of the Bishop Cap hills, Doña Ana County, New Mexico: M.S. thesis, University of Texas (El Paso), 76 p.

Lane, H. R., 1974, The Mississippian of southeastern New Mexico and west Texas—a wedge-on-wedge relation: American Association of Petroleum Geologists, Bull., v. 58, no. 2, p. 269-282

Laudon, L. R., and Bowsher, A. L., 1949, Mississippian formations of southwestern New Mexico: Geological Society of America, Bull., v. 60, p. 1-87

LeMone, D. V., 1969, Lower Paleozoic rocks in the El Paso area: New Mexico Geological Society, Guidebook 20th field conference, p. 68-79

Lindgren, W., and Graton, L. C., 1906, A reconnaissance of the mineral deposits of New Mexico: U.S. Geological Survey, Bull. 285, p. 74-86

Lindgren, W., Graton, L. C., and Gordon, C. H., 1910, The ore deposits of New Mexico: U.S. Geological Survey, Prof. Paper 68, p. 205-213

Lipman, P. W., 1966, Water pressures during differentiation and crystallization of some ash-flow magmas from southern Nevada: American Journal of Science, v. 264, p. 810-826

———, 1967, Mineral and chemical variations within an ash-flow sheet from Aso caldera, southwestern Japan: Contributions to Mineralogy and Petrology, v. 16, p. 300-327

Lipman, P. W., Christiansen, R. L., and O'Connor, J. T., 1966, A compositionally zoned ash-flow tuff sheet in southern Nevada: U.S. Geological Survey, Prof. Paper 524-F, 47 p.

Lipman, P. W., Prostka, H. J., and Christiansen, R. L., 1972, Cenozoic volcanism and plate tectonic evolution of the western United States, part I: Early and Middle Cenozoic: Royal Society of London, Philosophical Transactions, v. 271, p. 217-248

Logan, J. M., Friedman, M., and Stearns, M. T., 1978, Experimental folding of rocks under confining pressure, part VI: Further studies of faulted drape folds: Geological Society of America, Mem. 151, p. 79-100

Loring, A. K., and Loring, R. B., 1980, K/Ar ages of middle Tertiary igneous rocks from southern New Mexico: New Mexico Bureau of Mines and Mineral Resources, Isochron/West, no. 28, p. 17-19

Lovejoy, E. M. P., 1975, An interpretation of the structural geology of the Franklin Mountains, Texas: New Mexico Geological Society, Guidebook 26th field conference, p. 261-268

———, 1976, Geology of Cerro de Cristo Rey uplift, Chihuahua and New Mexico: New Mexico Bureau of Mines and Mineral Resources, Mem. 31, 84 p.

Lowell, J. D., 1970, Antithetic faults in upthrusting: American Association of Petroleum Geologists, Bull., v. 54, no. 10, p. 1,946

Macer, R. J., 1978, Fluid inclusion studies of fluorite around the Organ cauldron, Doña Ana County, New Mexico: M.S. thesis, University of Texas (El Paso), 107 p.

Marcy, R. B., 1850, Report on a route from Fort Smith to Santa Fe: 31st Congress of the United States, Senate Exec. Doc. 64, p. 197-198

McAnulty, W. N., 1978, Fluorspar in New Mexico: New Mexico Bureau of Mines and Mineral Resources, Mem. 34, 61 p.

Meyer, R. F., 1966, Geology of Pennsylvanian and Wolfcampian

rocks in southeast New Mexico: New Mexico Bureau of Mines and Mineral Resources, Mem. 17, 123 p.
Morton, W. H., and Black, R., 1975, Crustal attenuation in Afar, *in* Afar depression of Ethiopia: Inter-Union Commission on Geodynamics, Sci. Rept. 14, p. 55-65
Muehlberger, W. R., Hedge, C. E., Denison, R. E., and Marvin, R. R., 1966, Geochronology of the mid-continent region, United States, part 3: Southern areas: Journal of Geophysical Research, v. 71, p. 5409-5426
Nelson, L. A., 1940, Paleozoic stratigraphy of Franklin Mountains, west Texas: American Association of Petroleum Geologists, Bull., v. 24, no. 1, p. 157-172
Noble, D. C., 1968, Systematic variation of major elements in comendite and pantellerite glasses: Earth and Planetary Science Letters, v. 4, p. 167-172
Orville, P. M., 1963, Alkali ion exchange between vapor and feldspar phases: American Journal of Science, v. 261, p. 201-237
Pray, L. C., 1959, Stratigraphic and structural features of the Sacramento Mountain escarpment, New Mexico: Roswell Geological Society, Guidebook 12, p. 87-130
———, 1961, Geology of the Sacramento Mountains escarpment: New Mexico Bureau of Mines and Mineral Resources, Bull. 35, 144 p.
Proffett, J. M., 1972, Nature, age, and origin of Cenozoic faulting and volcanism in the Basin and Range province (with special reference to the Yerington district, Nevada): Ph.D. thesis, University of California (Berkeley), 77 p.
———, 1977, Cenozoic geology of the Yerington district, Nevada, and implications on the nature and origin of Basin and Range faulting: Geological Society of America, Bull., v. 88, p. 247-266
Ramberg, H., 1963, Strain distribution and geometry of folds: Geological Institutions of the University of Uppsala, Bull., v. 42, p. 3-20
Ratté, J. C., and Steven, T. A., 1964, Magmatic differentiation in a volcanic sequence related to the Creede caldera, Colorado, *in* Short papers in geology and hydrology: U.S. Geological Survey, Prof. Paper 475-D, p. D49-D53
———, 1967, Ash flows and related volcanic rocks associated with the Creede caldera, San Juan Mountains, Colorado: U.S. Geological Survey, Prof. Paper 524-H, 58 p.
Rehrig, W. A., and Heidrick, T. L., 1976, Regional tectonic stress during the Laramide and later Tertiary intrusive periods, Basin and Range province, Arizona: Arizona Geological Society, Digest, v. 10, p. 205-228
Reiche, P., 1938, Recent fault scarps, Organ Mountain district, New Mexico: American Journal of Science, Ser. 5, v. 36, no. 216, p. 440-444
Reesor, J. E., 1958, Dewar map area with special emphasis on the White Creek batholith, British Columbia: Geological Survey of Canada, Mem. 292, 78 p.
Reynolds, D. L., 1954, Fluidization as a geological process and its bearing on the problem of intrusive granites: American Journal of Science, v. 252, p. 577-614
Reynolds, R. L., and Larson, E. E., 1972, Paleomagnetism of Pearlette-like airfall ash in the midwestern and western United States—a means of correlating Pleistocene deposits (abs.): Geological Society of America, Abstracts with Programs, p. 405
Rhodes, R. C., 1976, Petrologic framework of the Mogollon Plateau volcanic ring complex, New Mexico—surface expression of a major batholith, *in* Cenozoic volcanism in southwestern New Mexico: New Mexico Geological Society, Spec. Pub. 5, p. 103-112
Ross, C. A., 1979, Late Paleozoic collision of North and South America: Geology, v. 7, no. 1, p. 41-44
Sales, J. K., 1978, Model studies of continental rifting related to the Rio Grande rift (abs.): International Symposium on the Rio Grande Rift, Abstracts with Programs, p. 80-82
Sawkins, R. J., 1969, Chemical brecciation, an unrecognized mechanism for breccia formation?: Economic Geology, v. 64, no. 6, p. 613
Schairer, J. F., and Bowen, N. L., 1955, The system K_2O-Al_2O_3-SiO_2: American Journal of Science, v. 253, p. 681-746
———, 1956, The system Na_2O-Al_2O_3-SiO_2: American Journal of Science, v. 254, p. 129-195
Seager, W. R., 1975, Cenozoic tectonic evolution of the Las Cruces area: New Mexico Geological Society, Guidebook 26th field conference, p. 241-250
———, 1980, Quaternary-age fault system in the Tularosa and Hueco Basins, southern New Mexico and west Texas: New Mexico Geological Society, Guidebook 32nd field conference
Seager, W. R., Hawley, J. W, and Clemons, R. E., 1971, Geology of San Diego Mountain area, Doña Ana County, New Mexico: New Mexico Bureau of Mines and Mineral Resources, Bull. 97, 38 p.
Seager, W. R., and Hawley, J. W., 1973, Geology of Rincon quadrangle, New Mexico: New Mexico Bureau of Mines and Mineral Resources, Bull. 101, 42 p.
Seager, W. R., Clemons, R. E., and Hawley, J. W., 1975, Geology of Sierra Alta quadrangle, Doña Ana County, New Mexico: New Mexico Bureau of Mines and Mineral Resources, Bull. 102, 56 p.
Seager, W. R., Kottlowski, F. E., and Hawley, J. W., 1976, Geology of Doña Ana Mountains, New Mexico: New Mexico Bureau of Mines and Mineral Resources, Circ. 147, 36 p.
Seager, W. R., and Brown, L. F., 1978, The Organ caldera, *in* Field guide to selected cauldrons and mining districts of the Datil-Mogollon volcanic field, New Mexico, C. E. Chapin and W. E. Elston, eds.: New Mexico Geological Society, Spec. Pub. 7, p. 139-149
Setra, A., 1976, Stratigraphy and microfacies analysis of the Mississippian Las Cruces Formation (Osage-Meramec), Vinton Canyon, El Paso County, Texas: M.S. thesis, University of Texas (El Paso), 87 p.
Shafiqullah, M., Lynch, D. J., Damon, P. E., and Pierce, H. W., 1976, Geology, geochronology, and geochemistry of the Picacho Peak area, Pinal County, Arizona, *in* Tectonic digest: Arizona Geological Society Digest, v. 10, p. 305-324
Shaw, H. R., Smith, R. L., and Hildreth, W., 1976, Thermogravitational mechanisms for chemical variations in zoned magma chambers (abs.): Geological Society of America, Abstracts with Programs, v. 8, p. 1102
Smith, R. L., 1960, Ash flows—a review: Geological Society of America, Bull., v. 71, p. 795-842
Smith, R. L., and Bailey, R. A., 1966, The Bandelier Tuff—A study of ash-flow eruption cycles from zoned magma chambers: Bulletin Volcanologique, v. 29, p. 83-104
———, 1968, Resurgent cauldrons: Geological Society of America, Mem. 116, p. 613-662
Soulé, J. H., 1951, Investigation of the Torpedo copper deposits—Organ mining district, Doña Ana County, New Mexico: U.S. Bureau of Mines, Invest. Rept. 4791, 10 p.
Stearns, D. W., 1971, Mechamisms of drape folding in the Wyoming province: Wyoming Geological Association, Guidebook 23rd field conference, p. 125-143
———, 1978, Faulting and forced folding in the Rocky Mountains foreland: Geological Society of America, Mem. 151, p. 1-37
Steven, T. A., and Lipman, P. W., 1976, Calderas of the San Juan volcanic field, southwestern Colorado: U.S. Geological Survey, Prof. Paper 958, 35 p.
Stevenson, F. V., 1945, Devonian of New Mexico: Journal of Geology, v. 53, p. 217-245
Stewart, J. H., 1971, Basin and Range structure: a system of horsts and grabens produced by deep-seated extension: Geological Society of America, Bull., v. 82, p. 1019-1044
———, 1978, Basin-range structure in western North America; a review, *in* Cenozoic tectonics and regional geophysics of the western cordillera, R. B. Smith and G. P. Eaton, eds.: Geological Society of America, Mem. 152, p. 1-31
Strain, W. S., 1966, Blancan mammalian fauna and Pleistocene formations, Hudspeth County, Texas: University of Texas (Austin), Texas Memorial Museum, Bull. 10, 55 p.
Taber, S. 1927, Fault troughs: Journal of Geology, v. 35, p. 557-606
Thompson, Sam III, and Bieberman, R. A., 1975, Oil and gas exploration wells in Doña Ana County: New Mexico Geological Society, Guidebook 26th field conference, p. 171-174
Thornton, C. P., and Tuttle, O. F., 1960, Chemistry of igneous rocks, part I: Differentiation index: American Journal of Science, v. 258, p. 664-684
Tuttle, O. F., and Bowen, N. L., 1958, Origin of granite in the light of experimental studies in the system $NaAlSi_3O_8$-$KAlSi_3O_8$-SiO_2-H_2O: Geological Society of America, Mem. 74, 153 p.
Uphoff, T. L., 1978, Subsurface stratigraphy and structure of the Mesilla and Hueco Bolsons, El Paso region, Texas and New Mexico: M.S. thesis, University of Texas (El Paso)
Welsh, N. J., 1914, The Organ mining district: Engineering and Mining Journal, v. 98, p. 331-334
Wheeler, G. M., 1879, Annual report upon the geographical surveys

of the Territory of the United States west of the 100th meridian: Washington, D.C., Government Printing Office, p. 224-227

Williams, H., 1942, The geology of Crater Lake National Park, Oregon, with reconnaissance of the Cascade Range southward to Mount Shasta: Carnegie Institution of Washington, Pub. 540, 162 p.

Wilson, J. L., 1967, Cyclic and reciprocal sedimentation in Virgilian strata of southern New Mexico: Geological Society of America, Bull., v. 78, p. 805-818

———, 1975, Regional Mississippian facies and thickness in southern New Mexico and Chihuahua, *in* Mississippian shelf edge and basin facies carbonates, Sacramento Mountains and southern New Mexico region: Dallas Geological Society, Guidebook, p. 124-128

Yurewicz, D. A., 1973, Genesis of the Rancheria and Las Cruces(?) Formations (Mississippian) of south-central New Mexico and west Texas: M.S. thesis, University of Wisconsin (Madison), 249 p.

Index

Abo Formation, 31, 33, 35, 38, 41
Abo Sandstone, 29
Abo tongues, 31
Achenback Canyon, 51, 52
Achenback Park, 13, 51, 66
Achenback Park tuff, 17, 47, 51, 52, 57, 66
Afar depression, 71, 77
Aguirre Spring, 13, 60, 63, 81, 84, 90
albite, 64
algae, 35
alluvial fan, 75, 77, 78, 82
  drainage pattern, 78, 80, 82
  geomorphic relations, 78, 79
  soil development, 78, 80, 82
altaite, 87
alteration, 67, 85
  jasperoid, 89
ammonites, 34
amphibolite, 21
anglesite, 85
Antelope Hill, 21
apatite, 64
aplite, 21, 58, 61, 63
argentiferous galena, 84, 85, 86, 87
argentite, 84, 85
argenojarosite, 86
Ash Canyon, 30, 56
ash-flow tuffs, 43, 46, 47, 51, 65
  chemical and mineralogic variation, 47, 48
  compositional trend, 66
  subsidence, 51, 66, 69, 74
autoliths, 21, 63
azurite, 86, 89

back-arc basins, 36, 40
Baldy peak, 15, 53, 57, 88
barite, 23, 84, 85, 87, 88, 89
basement-cored uplifts, 40
Baylor Canyon, 38, 39, 42, 57, 60
Baylor Mountain, 13, 81, 84, 88
  rhyolite porphyry, 60, 62, 63, 68
Baylor Pass, 13
Baylor Peak, 62, 73
Ben Nevis mine, 84
Bear Canyon, 13, 18, 20, 21, 22, 23, 24, 25, 27, 28, 29, 30, 31, 32, 39, 57, 70, 71, 75, 79, 84, 87
Bear Canyon fold and thrust zone, 33
Bear Peak, 20, 27, 39, 70
Bear Peak fold and thrust zone, 18, 20, 24, 31, 33, 35, 37, 38, 39, 40, 41, 42, 57, 70
Berino Formation, 25, 29, 30, 35, 89
Bishop, California, eruption, 81
Bishop Cap, 13, 20, 22, 23, 24, 25, 27, 28, 29, 30, 34, 35, 66, 67, 70, 71, 72, 74, 75, 76, 77, 83, 88, 89
Bishop Cap Formation, 30
Bishop tuff, 65
Black Hills, 47, 52, 77
Black Mountain, 20, 23, 24, 27, 29, 30, 38, 70, 71, 84, 87
Black Prince Canyon, 18
Black Prince mine, 39, 84, 87
Blair Canyon, 38, 39
Bliss Sandstone, 20, 21, 22, 24, 69, 70, 87
block uplifts, 36
Blue Star mine, 89
Boulder Canyon, 15, 16, 41, 47, 49, 51, 66, 89
brachiopods, 25, 29, 30, 32, 34
breccia pipe, 86
bryozoans, 29, 30, 34

Caballero Formation, 24, 25, 27, 34, 87
Caballo Mountains, 21, 22, 35, 67, 74
caldera, 66
Camp Rice Formation, 78, 79, 80, 81
  age, 81
  basalt, 81
  fan-delta, fluvial deposits, 78, 79, 80, 81
  mountain-valley fill, 78
  piedmont-slope deposits, 78, 79, 80
  volcanic ash, 81
Canutillo Formation, 24, 25, 34
cerargyrite, 84
cerussite, 85, 86, 87
chalcocite, 86
chalcopyrite, 64, 83, 84, 85, 86, 87, 89
Chihuahua, 80
chlorite-quartz alteration, 63
chloritic alteration, 85
chrysocolla, 86
Cleofas Andesite, 44
Colonel A. J. Fountain, 83
Colorado Plateau, 36, 40
conodonts, 29
copper, 21, 83, 84, 86, 87, 88, 89
Copper Buckle mine, 87
corals, 29, 30, 34
Cordilleran foreland, 36
Cordilleran orogenic belt, 36, 40
Cox Ranch, 13
Cox Ranch tuff, 47, 49, 50, 51
crinoids, 29, 34
Cueva rock, 17, 47, 49, 50, 66
Cueva Tuff, 16, 46, 47, 49, 50, 51, 67

Dakota Sandstone, 33, 35
debris flows, 82
Deming, 33
Derryan-Desmoinesian boundary, 30
Derryan Series, 25
Desert-Soil-Geomorphology Project, 73
Devil's Canyon, 88, 89
Devil's Canyon mine, 89
dikes, 63, 69, 70, 71, 84, 85, 89
diopside, 69
diorite and diorite porphyry, 58, 60
Doña Ana cauldron, 47, 66
Doña Ana Mountains, 31, 32, 44, 47, 74
Dorsey Canyon, 61
Dripping Springs resort, 15, 16

echinoids, 32, 35
El Paso, 22, 35, 44, 72, 79, 87
El Paso Group, 21, 22, 34, 38, 69, 70
  El Paso Limestone, 89
  Sierrite Limestone, 22
enargite, 84, 85
epidote, 69, 88
Excelsior mine, 63, 69, 84, 86, 87
exfoliation dome, 14, 15, 18

fan gravels, 75
Farallon plate, 40, 43
faults
  antithetic, 71, 72, 75, 76
  Artillery Range zone, 72, 73, 76, 79
  bedding-plane, 24
  Black Mountain zone, 38, 70, 71, 75
  Black Prince zone, 37, 39, 57, 70
  Blue Star, 89
  décollement, 37
  Deer, 38, 70
  downward flattening, 71
  en echelon, 72
  fault blocks, 70, 75, 77
  general, 20, 36, 43, 46, 70, 71, 72, 73, 74, 77, 85, 88
  Goat Mountain zone, 70, 71, 75
  graben, 39, 72, 74, 75, 77
  Holocene fan, 73
  horst, 72, 74, 77
  high- and low-angle normal, 38, 70, 71, 72, 75, 76
  Jornada, 66, 67, 72, 74
  late Tertiary, 39
  Long Canyon, 15, 69, 71
  Massey Tank, 67, 74
  Modoc, 17, 57, 69, 71, 88, 90
  normal, 38, 39, 70, 75, 87
  Organ fault block, 71
  Organ Mountains, 37, 52, 70, 72, 73, 74, 75, 76, 77, 79
  Peña Blanca, 67, 74
  Quartzite Mountain, 39, 70, 87
  range-boundary faults, 70, 74
  recently active, 73
  reverse, 37, 38, 39
  Rock House, 38, 78
  rotation, 76
  scarps, 72, 73, 79
  shear fractures, 75, 76, 85
  soil studies, 73
  Stevenson-Bennett zone, 57
  strike slip, 39
  subsidence fractures, 47, 71
  tear, 38
  thin-skinned, 40
  thrust, 24, 36, 38, 39
  Torpedo-Bennett zone, 37, 38, 39, 57, 83, 85, 86
  upthrust, 41, 76
  west-side boundary, 74
Fillmore Canyon, 13, 14, 15, 17, 43, 44, 47, 52, 66, 88, 90
Fillmore Gap, 78, 79, 80
Finlay Canyon, 13, 15, 16
flow-banded rhyolite, 47
fluid inclusions, 88
fluorite, 23, 83, 84, 87, 88, 89, 90
folds
  anticlinal axis, 38
  arch, 71
  cascade, 36
  drape, 40
  forced, 39, 40
  general, 43
  Laramide, 38, 39, 40
  mechanics, 38, 39
  monocline, 36, 40, 66, 75
  syncline, 38, 39, 40
  thrust-faulted anticline, 38
Fort Bliss, 13, 89
Foy mine, 87
Franklin Mountains, 13, 21, 23, 24, 27, 28, 29, 30, 70, 71, 72, 75, 76, 77
freibergite, 84
fresh-water limestone, 41
Fusselman Dolomite, 22, 23, 24, 25, 34, 38, 69, 70, 84, 85, 87, 89, 90
fusulines, 30, 35
  Beedina, 30
  Dunbarinella, 31
  Pseudoschwagerina morsei, 31
  Triticites, 31
fusulinids, 30, 32
  Millerella, 30

galena, 83, 84, 85, 86, 87, 88, 89
Galloway mine, 84, 85
Gallup Sandstone, 33, 34, 35, 41
garnet, 69, 86, 88

gastropods, 32, 35
geothermal wells, 67, 68
Glendale Canyon, 14
gold, 21, 83, 84, 85, 87
gossan, 84
graben, 71
Granite Peak, 14, 43, 56, 57, 58
Granite Peak granite, 56, 58, 60, 62, 64, 69
gravity survey, 74, 89
Gray Eagle mine, 84
gypsum, 31, 35

Hardscrabble Hill, 18, 30, 31, 44, 74, 87
Hayner mine, 88
Helms Formation, 25, 29, 34, 89
Helms shale, 25, 30
hematite, 69, 86, 88, 89
hemimorphite, 85, 86
Hilltop mine, 21, 22, 27, 39, 84, 87
Holocene deposits, 82
Homestake mine, 83, 86
Hopkins Ranch, 43
hornfels, 69
Hornspoon Group mine, 85
Hudspeth County, Texas, 81
Hueco Basin, 72, 77, 78, 79, 87
Hueco Formation, 31, 35, 38, 40
Hueco Limestone, 29, 30, 31, 32, 33, 35, 40, 44, 88, 90
hydrothermal alteration, 63, 85, 86, 89

Ice Canyon, 13, 15, 16, 79
Ice Canyon cauldron, 52, 53, 57, 69
idocrase, 69
Indian Springs Canyon, 64
Indian Hollow Canyon, 88
Issacks' Ranch, 85
Isaacks' Ranch alluvium, 82
Issacks' Ranch morphostratigraphic unit, 79, 82

Johnson Canyon, 57, 79
Jornada Basin, 70, 74, 78
Jornada (I,II) morphostratigraphic unit, 79, 80, 81, 82
Jornada del Muerto Basin, 14, 40, 41, 42

kaolin, 86
karst surface, 34

laccolith, 87
La Cueva, 13
Lake Valley Formation, 22, 25, 27, 34, 35, 69, 87, 89, 90
  Alamogordo Member, 27
  Andrecito Member, 27
  Arcente Member, 27
  bioherms, 27
  Doña Ana Member, 27, 28
  Nunn Member, 27
  Tierra Blanca Member, 27
Lake Valley Limestone, 24
Laramide orogeny, 35, 36
Laramide uplift, 20, 30, 31, 37, 38, 39, 40, 41, 55, 57
Laramide structures, 37
Las Cruces, 35, 73, 81, 82, 88
Las Cruces Formation, 22, 25, 27, 28, 29, 34, 69
Late Pleistocene deposits, 81, 82
La Tuna Formation, 25, 29, 30, 35
lava flows, 46, 47, 65, 77
lazurite and lazulite, 64, 88
lead, 83, 84, 85, 86, 87, 88, 90
Lead Camp Limestone, 22, 28, 30, 35, 38, 69, 71, 86, 87, 89, 90
Lepidodendron, 30
limonite, 85, 86
linguloid brachiopods, 25
Little Buck mine, 87, 88
Lodge prospect, 86, 87
Loman Canyon, 17, 29, 87
Long Canyon, 13, 15, 16
Love Ranch, 33, 37, 38, 40, 41
Love Ranch Formation, 33, 35, 40, 41, 42, 43
  fanglomerates, 34

Magdalena Formation, 30
Magdalena Group, 30
magma chamber, 46, 47, 65, 66, 68
  compositional zoning, 46, 47, 57, 65, 68, 69
  depth, 65
  temperature, 65, 66
  water-vapor pressure, 65, 66
malachite, 86, 87, 89
Mancos Shale, 33, 35, 40
  Tres Hermanos Sandstone Member, 33, 34, 35
  upper tongue, 34
Maple Canyon, 88
marble, 69, 88
marbleization, 63
McRae Formation, 40, 42
Memphis mine, 39, 57, 69, 83, 85, 86
Merrimac mine, 28, 30, 69, 84, 86, 87, 88
Mesilla Basin, 67, 75, 78, 80
metamorphism, 63, 69, 83
metasomatism, 63, 69, 78
mineral deposits, 63, 83
Mineral Hill, 83, 84
mineral zoning, 83, 84, 89
Mockingbird Gap, 72
Modoc mine, 31, 32, 41, 42, 43, 57, 69, 74, 84, 88, 90
molybdenum, 64, 83, 89, 90
Montoya Group, 21, 22, 34, 69, 90
  Aleman Dolomite, 23, 85
  Cable Canyon Sandstone, 23, 34, 69
  Cutter Dolomite, 23, 85
  Montoya Dolomite, 38, 70, 85
  Upham Dolomite, 23
mudflows, 81, 82

New Mexico foreland, 40
North Canyon, 15, 17, 51, 53, 66
northern New Mexico, 35

Orejon Andesite, 16, 41, 42, 43, 44, 45, 46, 64, 87, 88
  breccia, 43
  lahar, 44
  lava, 43, 44
  siliceous tuff, 43
  source, 44
Orejon mine, 88
Orejon Peak, 17, 88
Organ, 13, 43, 74, 83, 84, 85, 86, 89, 90
Organ alluvium, 82
Organ batholith, 18, 19, 20, 37, 39, 43, 44, 46, 47, 51, 53, 55, 56, 60, 64, 65, 66, 68, 69, 70, 72, 83, 84, 86, 88
  age relations, 60
  contacts, 57
  evolutionary sequence, 68
  floor, 57
  foliation, 57
  geometry and emplacement, 56, 57
  lineation, 57
  modal analysis, 58, 59
  piecemeal stoping, 46, 58
  radiometric dating, 55
  rock types, 58, 60
  roof pendents, 37, 39, 43, 57, 58, 88
  roof rock, 43, 46, 56, 57, 58, 60, 61, 63, 64, 66, 69, 71
  schlieren, 64
  septa, 61
  silica content, 60
  xenoliths, 37, 39, 58, 61, 63, 64
Organ cauldron, 19, 43, 47, 49, 52, 55, 57, 66, 67, 69, 88
  ash-flow tuff, 47
  cauldron wall, 67
  evolutionary sequence, 68
  limits and shape, 66
  margin, 51, 52, 66, 74
  ring fractures, 67
  subsidence, 88
Organ mining district, 19, 63, 83, 84, 85, 89, 90
Organ morphostratigraphic unit, 79, 82
Organ Mountains, 13, 14, 15, 17, 19, 20, 21, 23, 24, 25, 27, 29, 30, 31, 35, 37, 38, 40, 41, 43, 45, 46, 47, 48, 51, 52, 55, 56, 60, 66, 70, 71, 72, 74, 75, 78, 80, 81, 82, 83, 88, 90
  tilt, 56, 57, 74, 75
Organ Mountains fault block, 46
Organ Needles, 13, 14, 15, 17, 49, 60, 64, 89
Organ Needles quartz monzonite, 13, 16, 57, 60, 61, 63, 64, 68, 81, 88
  alaskite, 60, 61, 63
  compositional zoning, 61
  mafic facies, 60, 61, 62, 63, 85
  mineral and chemical variations, 61, 62
  quartz-alkali feldspar syenite, 60, 61
  syenite facies, 56, 60, 61
Orogrande Basin, 29, 30, 31, 35
orthoclase, 64
Oscura Mountains, 21, 22, 23
Ossipee cauldron, 58
ostracods, 32
outflow-tuff sheets, 47

Padre La Rue, 83
Paleozoic glaciation, 29
Palm Park Formation, 41, 43
Panther Seep Formation, 29, 30, 31, 35, 38, 86, 90
pearlette ash, 81
pediment, 18, 85
pegmatite, 21, 58, 63, 64, 84
pelecypods, 33, 34
Peña Blanca, 13, 47, 49, 50, 51, 74
Peña Blanca tuff, 49, 51
Percha Shale, 22, 24, 25, 34, 38, 69, 71, 84, 85, 87, 89
  Contadero Formation, 24
  Oñate Formation, 24
  Sly Gap Formation, 24
Pedernal uplift, 35
periglacial conditions, 81
petrified wood, 30, 33
phosphatic brachiopods, 24
phylloid algal debris, 31, 32
Picacho morphostratigraphic unit, 82
Pine Tree trail, 63
Poor Mans Friend mine, 85
potash metasomatism, 78
Potrillo Basin, 40
Precambrian
  batholith, 20, 21
  granite, 21, 22
  rocks, 20
pyrite, 84, 85, 86, 87, 88, 89
pyrolusite, 87

quartz alkali-feldspar syenite, 58
Quartzite Mountain, 13, 30, 38, 57, 63, 70, 71
  rhyolite, 38, 39, 60, 63
quartz mineralization, 21
quartz sericite, 63, 89
quartz syenite, 58
quartz veins, 63

Quaternary deposits, 78
Queensland cauldron, 58
Quickstrike mine, 84

Rabbit Ears, 13, 15, 60
radiometric dates, 46
Rancheria Formation, 22, 25, 27, 28, 29, 34, 69
Rattlesnake Ridge, 15, 20, 21, 22, 23, 24, 25, 29, 30, 66, 67, 71, 74, 77, 84
replacement deposits, 84, 85, 87, 88, 89, 90
  manto-type, 85, 87
  ore shoots, 87
resurgent doming, 46
rhyolite, 58
rickardite, 87
Rickardite mine, 87
Rio Grande, 13, 78, 79, 81, 82
  ancestral, 78, 79, 80
Rio Grande rift, 70, 72, 77, 78, 83, 88
  evolution, 70
Robledo Mountains, 31, 32, 35
Rock Canyon, 88
Rubio Peak Formation, 44
Ruby mine, 44, 47, 83, 88, 89, 90
rugose corals, 30

Sacramento Mountains, 23, 28
San Agustin Mountains, 13, 17, 18
San Agustin Pass, 13, 17, 27, 55, 63, 83, 84, 90
San Agustin Peak, 14, 18, 84
San Andres Formation, 33, 35
San Andres Limestone, 29, 33
San Andres Mountains, 13, 18, 20, 21, 22, 23, 24, 25, 26, 27, 28, 29, 30, 33, 34, 37, 41, 42, 70, 71, 72, 74, 75, 76, 78, 80, 81, 82
San Diego Mountain, 21, 41, 74
San Juan Mountains, 44
Santa Fe Group, 78
Sarten Sandstone, 33, 35
Second Value Dolomite, 23
seismic reflection studies, 77
sericite, 63, 88, 89
serpentine, 69
silver, 83, 84, 85, 86, 87, 88
Silver City, 33
Silver Coinage mine, 84, 85
Silver King mine, 85
skarn, 88
Smith mine, 87
smithsonite, 85
smokey quartz, 64
Socorro, 77
Soledad Canyon, 14, 15, 16, 17, 18, 47, 49, 52, 61, 66, 79, 90
Soledad Canyon road, 13
Soledad Peak, 13, 17
Soledad Rhyolite, 16, 17, 46, 47, 49, 51, 52, 68, 77
South Canyon, 58
southeastern Utah, 35
southern Colorado, 35
southern Rockies, 36
specularite, 69
sphalerite, 84, 85, 86, 87
Squaw Mountain, 52, 53
  lineation, 52
  potash metasomatism, 53
  tuff, 17, 47, 51, 52, 53, 66, 77
  vitrophyre, 53
Stevenson-Bennett mine, 20, 21, 27, 38, 41, 42, 43, 57, 61, 84, 85, 86
  Bennett orebody, 85
  Page orebody, 85
  Stevenson orebody, 83, 85
stromatolites, 35
stromatolitic algae, 31
Sugarloaf dome, 63
Sugarloaf Peak, 14, 15, 17, 60, 64, 84, 90
Sugarloaf Peak quartz monzonite porphyry, 18, 60, 63, 69, 83, 84, 85, 86, 89, 90
  age, 63
  contacts, 63
  hydrothermal effects, 63
  miarolitic cavities, 64

tacite, 88
tellurium, 87
tetradymite, 84, 85, 86
Texas Canyon, 21, 57, 61, 84, 85
thickness of Paleozoic and Cenozoic strata, 28
thorium, 84, 90
Torpedo mine, 19, 39, 83, 85, 86, 90
Tortugas morphostratigraphic unit, 82
Tortugas Mountain, 66, 67, 68, 74, 88
transverse valleys, 16
travertine, 41
tremolite, 69
trilobites, 29
Truth or Consequences, 81
tuffs
  Achenback Park, 17, 47, 51, 52, 57, 66
  ash-flow, 43, 46, 47, 48, 51, 65, 66, 69, 74
  Bishop, 65
  Cox Ranch, 47, 49, 50, 51
  Cueva, 16, 46, 47, 49, 50, 51, 67
  Peña Blanca, 49, 51
  Squaw Mountain, 17, 47, 51, 52, 53, 66, 77
Tularosa Basin, 13, 70, 71, 72, 75, 76, 77, 78, 79, 80

uranium, 84, 89, 90

vanadinite, 87
variation diagram, Orejon Andesite, 45
veins, 84, 85, 90
Vinton Canyon, 27
vitrophyre, 65

west-side lavas, 49, 53, 54, 56, 68
  vitrophyre, 53
  electron-microprobe analyses, 54, 55
  groundmass glass, 54
  chemical and mineral variations, 54
  modal analyses, 54
White Creek batholith, 69
White Sands Missile Range, 13, 21, 72, 73, 82, 83
wollastonite, 69
wulfenite, 85, 87

Yellowstone eruptions, 81
Yerington district, Nevada, 77
Yeso Formation, 29, 33, 35

zinc, 83, 84, 85, 86, 87, 88, 90

Contents of pocket

Microfiche—Measured sections (Appendix A)
Sheet 1—Geologic map
Sheet 2—Cross sections
Sheet 3—Columnar and short cross sections
Sheet 4—Chemical analyses (Appendix B)

Type faces: Text in 10-pt. English Times, leaded one point
References in 8-pt. English Times, leaded one point
Main heads in 24-pt. English Times

Presswork: Miehle Single Color Offset
Harris Single Color Offset

Binding: Smyth sewn

Paper: Cover on 17-pt. Kivar
Text on 70-lb. Patina matte

Ink: Cover—PMS 320
Text—Black

Press Run: 1200

DESCRIPTION OF ROCK UNITS

Qc Colluvium and alluvium of narrow valley floors—*Mostly gravelly deposits on hillslopes, ranging from young, unconsolidated material to ancient caliche-cemented debris; wide age range; few feet thick*

Qpa Piedmont slope alluvium, undifferentiated—*Includes* Qpy *and* Qpo

Qpy Younger piedmont slope alluvium—*Unconsolidated sand, gravel, silt, and loam; mostly on floors of modern arroyos, in fans below (east of) the Organ Mountains fault scarp and as fans draining major canyons on the west side of the range; as much as 25 ft thick*

Qpo Older piedmont slope alluvium—*Sand, gravel, silt, and loam, weakly to moderately cemented by caliche, especially at top; mostly as alluvial fans, trenched by modern arroyos; several generations of such fan deposits compose the map unit; as much as 25 ft thick on the mountain block*

Qcru Camp Rice Formation—*Mostly thick, carbonate-cemented boulder fanglomerate at base(*Qcrc*) and moderately cemented fanglomerate at top(*Qcrp*); also includes slope debris composed of angular boulders that accumulated along mountain fronts, which have since treated one or more miles; up to 300 ft thick on mountain blocks, probably much thicker in the subsurface east of the Organ Mountains fault*

Qcrp Piedmont slope facies of the Camp Rice Formation—*Moderately cemented fanglomerate and sandstone to poorly indurated gravelly alluvium representing youngest deposits of the Camp Rice Formation; forms highest (oldest) fans that are still widely preserved on mountain-piedmont slopes; these high fan surfaces (Jornada I surfaces) have well-developed soil carbonate or clay-rich soils in upper 2 to 3 ft; 0 to 50 ft thick on mountain blocks*

Qcrf Fluvial facies of the Camp Rice Formation—*Moderately sorted to well-sorted, gray to tan, fluvial sand containing abundant rounded clasts of chert, quartz, and siliceous volcanics derived from regions to the north of Las Cruces; interbedded clay, mudstone, and siltstone are overbank deposits; deposit represents a large fan-delta complex constructed on the floor of the Tularosa Basin by the ancestral Rio Grande as it flowed into the Hueco-Tularosa Basin through Fillmore Gap; 0 to 100+ ft thick*

Qcrc Basal conglomerate facies of the Camp Rice Formation—*Massive, weakly bedded fanglomerate and fill of mountain valleys, the oldest Camp Rice deposit; completely indurated by carbonate cementation; hard; the deposits may underlie* Qcrp *fans on piedmont toe slopes or form isolated, high-level fan remnants near Canyon mouths; 0 to 300 ft thick on mountain blocks*

Ttb Basaltic andesite of Black Hills—*Dark, vesicular basaltic andesite flows overlying Soledad Rhyolite in the Black Hills. Some flows are porphyritic. Chemical analyses indicate high K_2O (8-10% K_2O, 52-55% SiO_2), but this may be a product of potash metasomatism. Unit is not co-magmatic with Organ batholith nor with Cueva Tuff–Soledad Rhyolite sequence; it may be related to late Tertiary rifting. At least 500 feet thick*

Tbc Conglomerate member of basaltic andesite of Black Hills—*Boulder conglomerate derived from basaltic andesite and rhyolitic rocks interbedded with sandstone and conglomeratic sandstone; resembles oldest Santa Fe deposits in the region; at least 50 ft. thick*

Ta Andesite—*Dark-greenish-gray andesite or latite dikes*

Tr Rhyolite—*Massive, cylindrical rhyolite intrusive in upper Fillmore and North Canyons; locally altered, stained with limonite, and contains disseminated pyrite*

Trf Flow-banded rhyolite—*Dikes of greenish-gray to tan flow-banded rhyolite that intrude the northern part of the Organ batholith and adjacent parts of the Precambrian batholith*

Tra Rhyolite—*Dikes of rhyolite with an aplitic texture that cut the northern part of the Organ batholith and adjacent parts of the Precambrian batholith*

Thmp Hornblende monzonite porphyry—*Dikes north of Organ that contain hornblende and plagioclase phenocrysts and large (5 cm) conspicuous alkali feldspars; dikes are locally altered to quartz-sericite and are associated with sulfide mineralization*

Tm Monzonite and latite porphyry—*Includes a wide variety of porphyritic dikes and sills in volcanic and sedimentary rocks adjacent to the Organ batholith; probably all are genetically related to the batholith*

Tmg Granite of Granite Peak phase of Organ batholith—*Pale-tan to light-gray quartz monzonite composed of perthite, oligoclase, biotite, and abundant quartz; locally contains large areas of disseminated pyrite*

Trpb Rhyolite porphyry of Baylor Mountain phase of Organ batholith—*Medium-gray rhyolite porphyry containing pink perthite phenocrysts and spherical, partly resorbed quartz "eyes" in an aphanitic matrix*

Tmps Sugarloaf Peak quartz-monzonite porphyry phase of Organ batholith—*Very coarse grained porphyry containing pink perthite phenocrysts to 3 cm long in a matrix of perthite, oligoclase, quartz, biotite, and green hornblende; aplite and pegmatite dikes and quartz veins are locally common; quartz sericite alteration and disseminated pyrite is present in the unit in the Organ mining district; K-Ar date of 32.8 m.y. on biotite*

Tmpa Aplite dikes associated with Sugarloaf Peak quartz monzonite porphyry—*Sugary textured, light-colored dikes cutting* Tmps

Tmo Organ Needle quartz-monzonite phase of Organ batholith—*Gray, equigranular, coarse-grained quartz monzonite that weathers buff, brown, or red; zoned perthite and oligoclase compose most of the rock, with lesser quartz and minor biotite; forms Organ Needles*

Tmoe Fine-grained, equigranular alaskite facies of the Organ Needle quartz monzonite—*Texturally and mineralogically similar to TMO but much finer grained; up to 25 percent quartz*

Tmom Mafic facies of Organ Needle quartz monzonite—*Medium- to dark-gray, equigranular, coarse-grained, monzonite to diorite; composed of oligoclase, perthite, biotite, hornblende, and pyroxene*

Td Diorite and diorite porphyry phase of Organ batholith—*Medium-gray, fine- to medium-grained, equigranular to porphyritic rock composed of plagioclase, hornblende, quartz, and potash feldspar; the potash feldspar occurs as phenocrysts and is probably metasomatic in origin; unit forms wispy patches and autolith swarms in younger phases of the Organ batholith*

Tr Rhyolite—*Flow-banded rhyolite, largely altered to quartz-sericite and intruded by* Tmps*; found only southwest of Hardscrabble Hill*

Trq Rhyolite of Quartzite Mountain—*Sills of light-gray to pale-orange rhyolite with an aplitic texture; contains small phenocrysts of quartz, sericitized orthoclase, and biotite*

Tlt Leucocratic latite porphyry—*Light-gray to grayish-orange felsic rock with a fine-grained to aplitic texture; carries small tabular phenocrysts potash feldspar*

Tdp Andesite porphyry to diorite—*Dark-gray to greenish-gray sill of hornblende andesite porphyry grading to diorite, which contains a few percent disseminated pyrite; about 500 ft thick*

Tfw West side trachyte—*Gray, purple-gray, brown, and brick-red, porphyritic trachyte, tristanite, dacite and rhyolite flows (61-65% SiO_2, 5-7% K_2O) with minor interbedded conglomerate; unit overlies tuff of Squaw Mountain. Unit is co-magmatic with Organ batholith, Cueva Tuff and Soledad Rhyolite; 33.7 m.y.; at least 1000 ft thick*

Ts Soledad Rhyolite—*From top includes tuff of Squaw Mountain, tuff of Achenback Park, tuff of Cox Ranch, and epiclastic and air-fall beds between the tuffs; maximum thickness about 9,000 ft*

Tss Tuff of Squaw Mountain—*Massive, gray, brown, and purple-gray, pumiceous rhyolite ash-flow tuff, crystal rich locally and at top; vitrophyre locally at base; densely welded; compound cooling unit; maximum thickness about 4,600 ft*

Tet Unnamed epiclastic rocks and ash-flow tuffs—*Fluvial red, brown, and gray conglomerate, sandstone, and mudstone interbedded with tan, fine-grained vitric ash-flow tuff; minor air-fall tuff and breccia; 0 to 200 ft thick*

Tsa Tuff of Achenback Park—*Massive, gray to red-brown pumiceous rhyolite ash-flow tuff, densely welded in most places; compound cooling unit; 400 to 3,100 ft thick*

Tse Unnamed epiclastic rocks—*Fluvial conglomerate, sandstone, and mudstone derived from rhyolitic volcanic rocks; tan, purple, and red-brown; 0 to 30 ft thick*

Tsc Tuff of Cox Ranch—*Divided locally into upper and lower members; about 800 ft thick*

Tscu Upper member of tuff of Cox Ranch—*Massive, densely welded, light-gray to tan, pumiceous rhyolite ash-flow tuff; air-fall tuff and epiclastic strata locally at base; unit mapped separately only in Boulder Canyon; about 400 ft thick*

Tscl Lower member of tuff of Cox Ranch—*Tan to pink to reddish-brown, pumiceous, welded rhyolite ash-flow tuff with platy jointing; grades down into Cueva Tuff; maximum thickness about 400 ft*

Tcu Upper tuff member of Cueva Tuff—*Massive, grayish-orange, lithic-pumice rhyolite ash-flow tuff, locally containing bodies of spherulitic and flow-banded rhyolite; generally non-welded; grades into overlying tuff of Cox Ranch; about 400 ft thick*

Tcp Peña Blanca tuff member of Cueva Tuff—*Massive, gray to pale-purple, sanidine-rich rhyolite ash-flow tuff; densely welded; dated 33.0 m.y. by K-Ar on sanidine; 0 to 220 ft thick*

Tce Unnamed epiclastic member of Cueva Tuff—*Reddish-brown to grayish-orange fluvial conglomerate, sandstone, and breccia derived from rhyolitic volcanic rocks; maximum thickness about 80 ft*

Tc Unnamed ash-flow tuff member of Cueva Tuff—*Pale-pink crystal-vitric ash-flow tuff present only at Peña Blanca and Boulder Canyon; 0 to 75 ft thick*

Tcl Lower tuff member of Cueva Tuff—*Massive gray, purple-gray, tan- or red-weathering, lithic-pumice ash-flow tuff, mostly non-welded; locally comprises more than one cooling unit; air-fall breccia and epiclastic rocks at the base in several places; maximum thickness about 600 ft*

Tcf Flow-banded rhyolite member of Cueva Tuff—*Gray to tan, dense, flow-banded to spherulitic rhyolite locally present at base and upper part of the Cueva Tuff; unit is mixed with and grades into pumiceous rhyolite ash-flow tuff; maximum thickness several hundred feet*

To Orejon Andesite—*Interbedded andesitic flows, lahar breccia, and other volcaniclastic rocks, generally dark-gray, greenish-gray or purple-gray; conspicuous epidote alteration in all outcrops; Orejon on Hardscrabble Hill may be intrusive; about 2,000 ft thick*

Tot Basal tuff member of Orejon Andesite—*Siliceous tuff-breccia composed of siliceous volcanic clasts and lesser schist, gneiss, and granitic fragments; unit not everywhere present; maximum thickness about 100 ft*

Tus Unnamed sandstone—*Tan-weathering, coarse-grained arkose; present only near western mouth of Bear Canyon; about 50 ft thick*

Tlr Love Ranch Formation, undifferentiated—*At least 2,000 ft thick near Love Ranch; less than 50 ft thick elsewhere*

Tlru Upper member of Love Ranch Formation—*Pebble to boulder conglomerate, red mudstone, and sandstone derived from Abo and Hueco beds; angularly unconformable above lower member in Bear Peak fold and thrust zone; 0 to 1,000 ft or more thick*

Tlrl Limestone member of Love Ranch Formation—*Massive, gray, algal, pisolitic, fine-grained freshwater limestone; interbedded with* Tlru*; maximum thickness about 50 ft*

Tlrb Lower member of Love Ranch Formation—*Pebble to boulder conglomerate, red mudstone, and sandstone derived from Cretaceous and Hueco and Abo beds; 0 to 1,000 ft or more thick*

Km Rocks correlative with Mancos Shale and Gallup Sandstone—*Greenish-gray to olive-brown sandstone, shale, and siltstone, and gray shale containing several thin ammonite-pelecypod coquinas; Tres Hermanos Sandstone Member of Mancos, about 300 ft thick, present near middle of section; tan, massive, crossbedded sandstone correlative with Gallup Sandstone is located near the top of unit; about 1,000 ft thick*

Kds Sarten Sandstone and Dakota Sandstone—*Yellow- tan- and gray-weathering, soft sandstone, shale, and siltstone, and massive crossbedded, gray quartzite; minor pelecypod coquina: about 260 ft thick*

Pys Yeso Formation-San Andres Limestone—*Thick- to medium-bedded, light- and dark-gray, fine-grained limestone; minor beds of soft, yellow, fine-grained sandstone; may be correlative with part of the Yeso Formation or the San Andres Limestone; about 550 ft thick*

Pay Abo-Yeso Formation—*Abo Formation—reddish-brown siltstone and fine sandstone; and red, green, and gray shale; about 425 ft thick; grades up into about 125 ft of brick-red, orange, and yellow sandstone, siltstone, and shale that may be correlative with part or all of the Yeso Formation; total thickness about 550 ft*

PPm Hueco Formation, Panther Seep Formation, and Lead Camp Limestone—*Mapped only where metamorphism combined with small outcrops made identification of formations unreliable*

Pah Intertonguing Abo and Hueco Formations—*Porcellanitic shale, tan siltstone and sandstone (Abo) interbedded with dark-gray, sandy, ledge-forming fossiliferous limestone; 425 to 1,000+ ft thick*

Ph Lower and middle members of Hueco Formation, undifferentiated

Phm Middle member of Hueco Formation—*Dark-gray, yellow, brown, and orange, sandy, ledge-forming limestone containing abundant gastropods, echinoids, and algae; interbedded with soft nodular limestone and shale; 500 ft thick*

Phl Lower member of Hueco Formation—*Cliff-forming, gray limestone and platy to shaly limestone in lower part, followed upward by interbedded sandy limestone, shale, algal and oolitic limestone, chert pebble conglomerate, and fossiliferous limestone that weathers shades of brown, olive, yellow, and orange; one to three bright-orange limestone marker beds at top; 530 ft thick*

PPs Panther Seep Formation—*Brown to gray shale, sandstone, siltstone, gypsum, and fine-grained, laminated limestone; formation forms most of the fill of Orogrande Basin and grades into Lead Camp and Hueco Formations; about 2,050 ft thick*

PPlc Lead Camp Limestone—*Massive, thick- to medium-bedded, fossiliferous, cherty, gray limestone and dolomite cyclically interbedded with shale; sandstone, conglomerate, and quartzite forms local pods in lower third; formation becomes very dolomitic, shaly, and gypsiferous at top, where it weathers orange, yellow, or olive; 654 to 870 ft thick*

PMm Lower and Middle Pennsylvanian and Mississippian formations, undifferentiated—*Mapped only where limited outcrops and metamorphism made formation identification unreliable*

Pb Berino Formation—*Cyclically interbedded marine shale, fossiliferous and intraclastic limestone, micrite, and crinoidal limestone, much of which is cherty; 516 ft thick on Bishop Cap, top eroded*

Plt La Tuna Formation—*Massive, gray, cherty micrite that becomes thinner bedded toward top; 259 ft thick*

Mh Helms Formation—*Intertonguing gray marine shale, fossiliferous and oolitic limestone, and crinoidal limestone; unit interfingers with upper part of Rancheria Formation; 0 to 132 ft thick*

M Caballero, Lake Valley, Las Cruces, and Rancheria Formations, undifferentiated

Mr Rancheria Formation—*Black or dark gray, thin- to medium-bedded micrite containing up to 70 percent chert locally; upper beds consist of crinoidal limestone and limestone with brown-weathering sand laminae; 168 to 264 ft thick*

Ml Caballero, Lake Valley and Las Cruces Formations—*Caballero Formation (Kinderhook) comprises brown-weathering dolomitic siltstone in the southern and northwestern part of the map, nodular gray, fossiliferous, shaly limestone elsewhere; 6 to 28 ft thick. Lake Valley Formation (Osage) includes crinoidal limestone, cherty limestone, sandy limestone and soft platy micrite; fossils are locally prolific; 34 to 181 ft thick. Las Cruces Formation (Meramec) consists of light-gray to blue-gray-weathering black micrite in thin to medium, parallel beds; formation contains scattered black chert; 0 to 125 ft thick*

D Percha Shale and Canutillo Formation, undifferentiated

Dp Percha Shale—*Black, gray, and purplish fissile shale, with yellow-weathering fine-grained, medium-bedded limestone locally at base; 61 to 141 ft thick*

Dc Canutillo Formation—*Fissile siltstone; cherty, black limestone; and minor dolomite; 44 ft thick*

LPm Lower Paleozoic rocks—*Mostly massive, coarse-grained white marble in the South Canyon area*

OSfm Fusselman Dolomite and Montoya Group—*Massive white marble in the South Canyon area*

Sf Fusselman Dolomite—*Massive, dark-gray, cherty dolomite in northern areas; pale-tan-weathering, light-gray, massive dolomite with scattered chert in southern areas; 110 to 310 ft thick*

Om Montoya Group—*Basal tan, coarse-grained Cable Canyon Sandstone overlain by massive, dark-gray Upham Dolomite followed by cherty, light- and dark-gray Aleman Dolomite; unit is capped by light-gray, fine-grained, thin- to medium-bedded Cutter Dolomite; 368 to 470 ft thick*

Oe El Paso Group—*Thin-bedded, siliceous, sandy, orange-weathering limestone in lower third, thick- to medium-bedded gray dolomite in upper two thirds; 780 to 1,000 ft thick*

Ceb Bliss Sandstone—*Brown, gray, or black hematitic sandstone, shale, siltstone, and quartzite; 125 to 144 ft thick*

pCd Diorite-diabase—*Dikes of black to dark-gray, equigranular, medium- to coarse-grained diorite or diabase, locally altered or foliated*

pCd Amphibolite—*Sheared, foliated masses of black or greenish-black amphibolite schist in Bear Canyon; probably are equivalent to* pCd

pCr Red granite—*Red, orthoclase-rich, coarse-grained granite; most appears to be a facies of* pCg *but locally dikes of* pCr *intrude* pCg

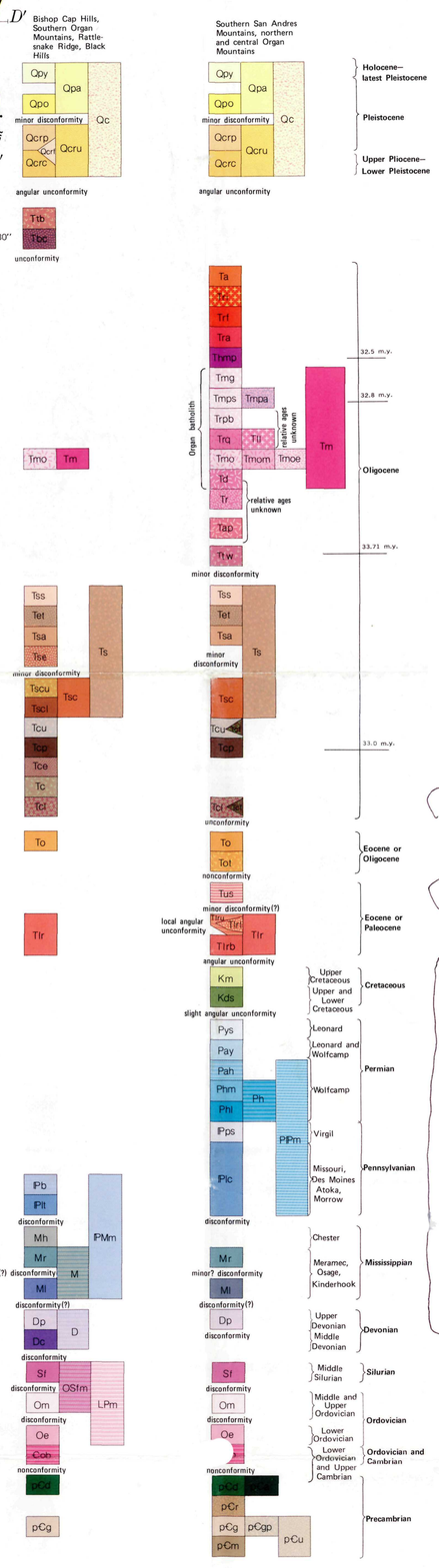
pCu Granite and metamorphic rocks, undifferentiated—*Gray, coarse-grained granite containing numerous roof pendants and xenoliths of gneiss and schist*

pCg Gray granite—*Coarse-grained, equigranular, gray granite; includes pink, medium-grained, equigranular facies near Stevenson-Bennett mine*

pCgp Gray granite, porphyritic facies—*Coarse-grained, gray granite containing phenocrysts of orthoclase up to 15 mm long*

pCm Schist—*Greenish-brown chlorite schist at northern edge of Mineral Hill*

CORRELATION OF ROCK UNITS

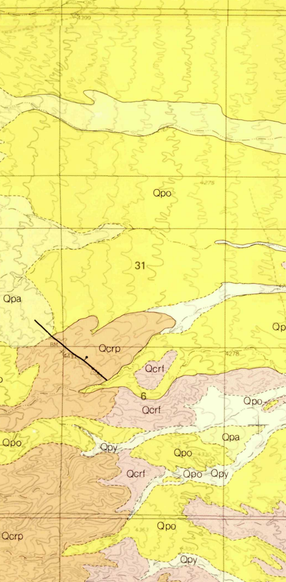


Geology by W.R. Seager 1975-1978

1:31,250

0 0.5 1 Mile 2 Miles

Contour interval 20 ft.



Map area in Doña Ana County, New Mexico.

SYMBOLS

formation contact - dashed where approximately located or uncertain, dashed-dot-dashed where gradational; arrow with direction and amount of dip

normal fault - dashed where uncertain or approximately located, dotted where buried; arrow with direction and amount of dip; ball on downthrown side

reverse or thrust fault - dashed where uncertain or approximately located, dotted where buried; arrow with direction and amount of dip; barbs on upthrown side

tear faults - arrows show relative horizontal movement; ball on downthrown side

Tmps — subcrop boundary of rock units in Organ area, approximately located on basis of drill-hole data

synclinal axis; anticlinal axis; monoclinal axis; overturned syncline axis; overturned anticline axis

apparent strike and dip of beds or lava flows; strike and dip of beds or lava flows; strike and dip of vertical beds; strike and dip of overturned beds; horizontal beds; strike and dip of joints; strike of steep or vertical joints; strike and dip of foliation in plutonic rocks; strike and dip of vertical foliation in plutonic rocks

strike and dip of foliation in ash-flow tuff or flow-banded rhyolite; arrow shows trend and direction of plunge of lineation

strike and dip of vertical foliation in ash-flow tuff or flow-banded rhyolite

shear zone in Organ batholith

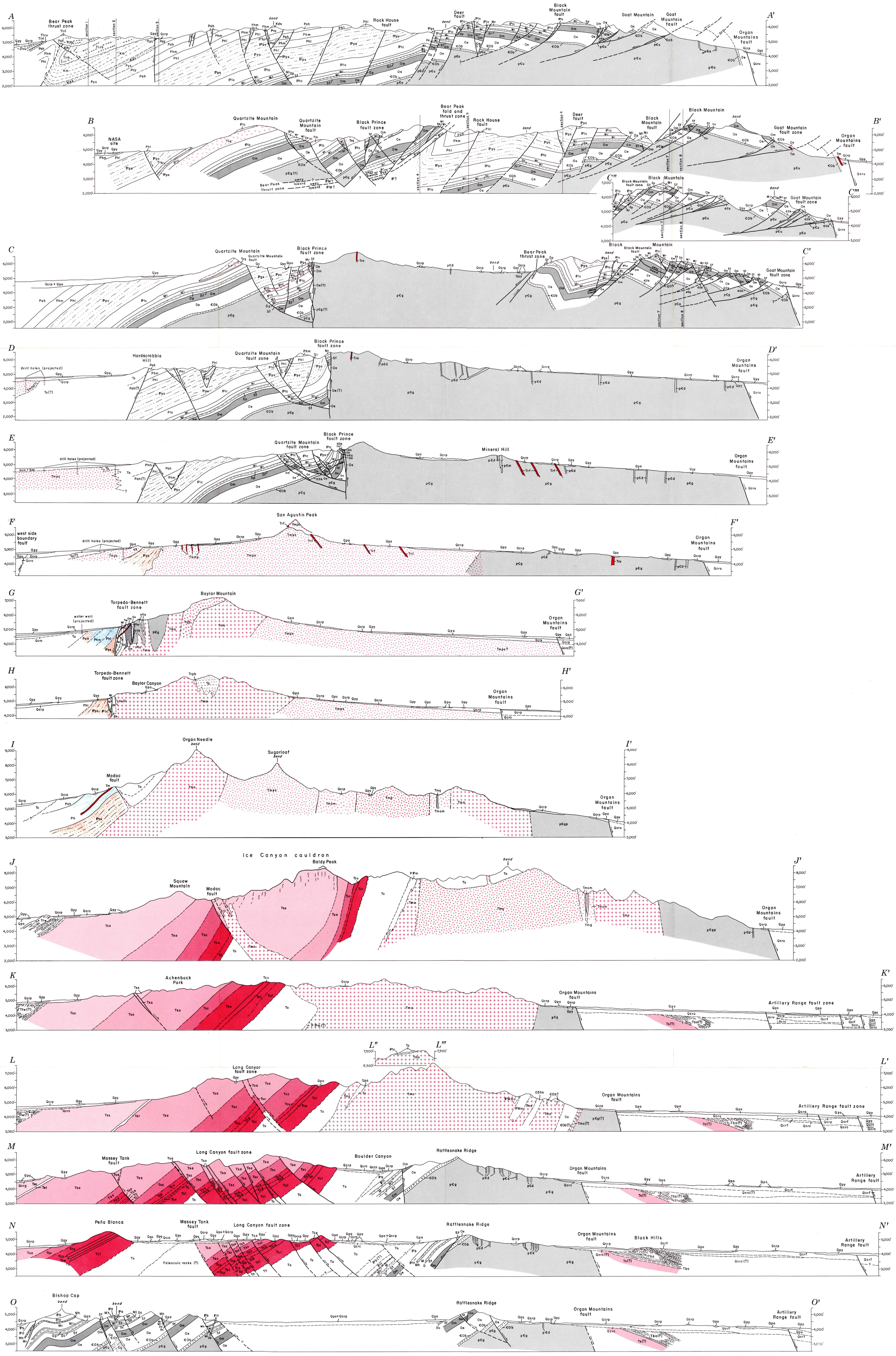
qs — areas of quartz-sericite alteration; se — areas of sericitization; L — areas of extensive limonite staining

landslide areas; coherent gravity slide block; silicified zones; m — small marble xenoliths; g — garnetite; mine dump; quarry; shaft; prospect

GEOLOGIC MAP OF THE ORGAN MOUNTAINS AND SOUTHERN SAN ANDRES MOUNTAINS, NEW MEXICO

by William R. Seager, 1980

Williams & Heintz Map Corporation, Washington, D.C. 20027



See sheet 1 for explanation of map symbols

GEOLOGIC CROSS SECTIONS OF ORGAN MOUNTAINS AND SOUTHERN SAN ANDRES MOUNTAINS

by William R. Seager

Sea level datum

Scale 1: 31,250

1 0 1 2 3 4 5 mi

1979

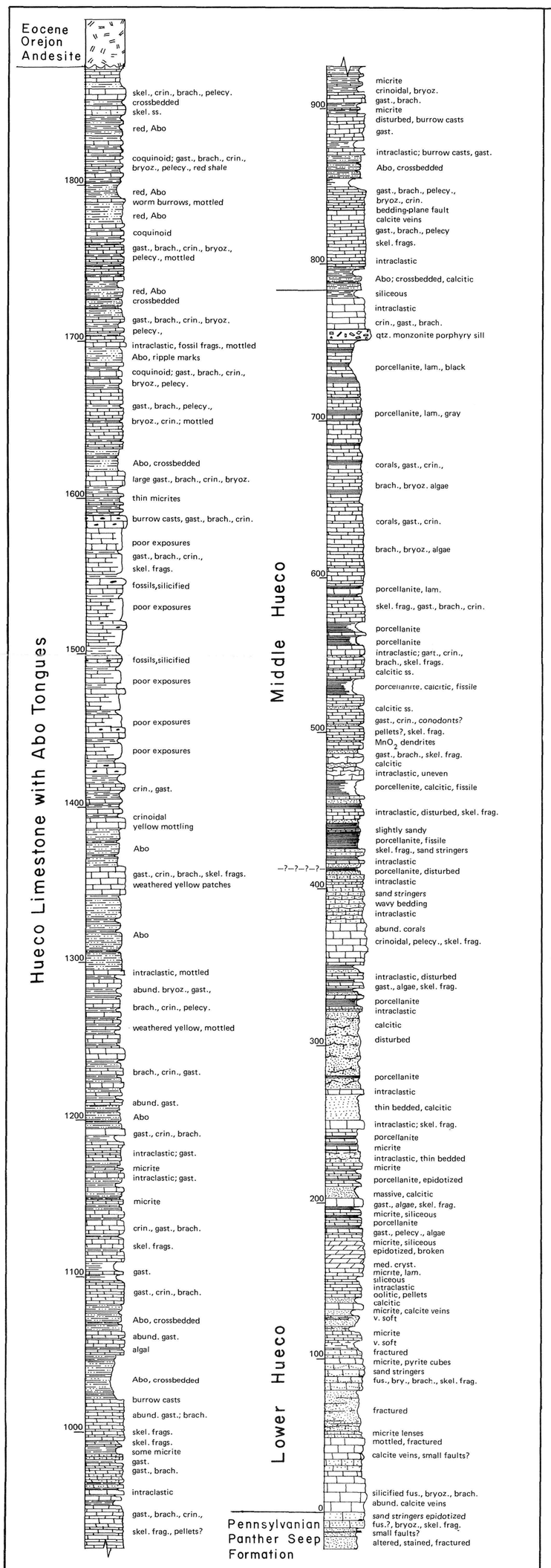


FIGURE 29—Columnar section of Wolfcampian Hueco Formation, west-central Organ Mountains, New Mexico *(by Richard E. Kelley)*.

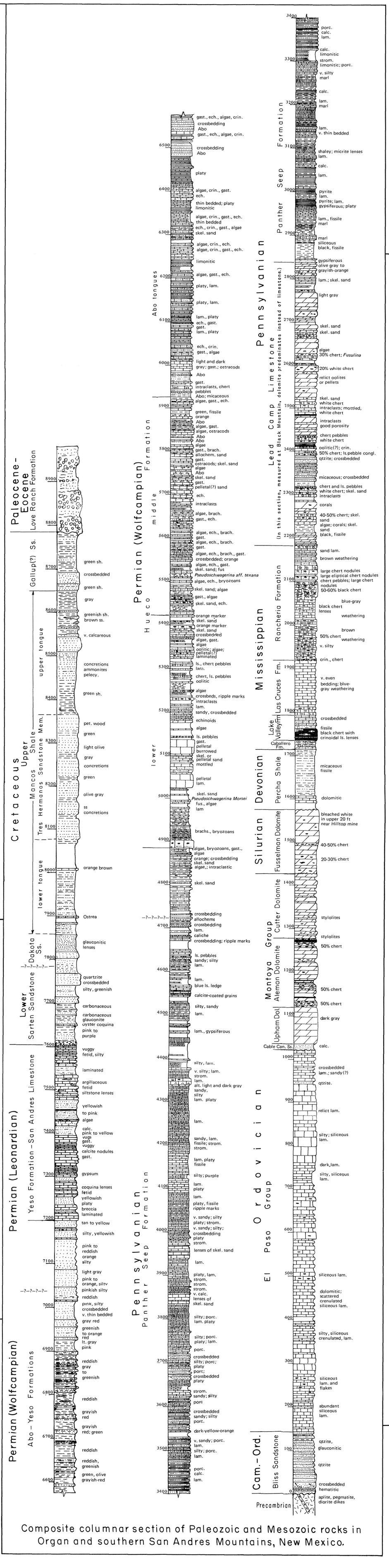
SYMBOLS

- Conglomerate
- Sandstone
- Siltstone
- Shale
- Porcellanite
- Calcareous shale or marl
- Gypsum
- Thin- to medium-bedded limestone
- Thick, massive-bedded limestone
- Limestone, nodular bedding
- Shaly limestone
- Sandy or silty limestone
- Cherty limestone
- Pebbly limestone
- Crinoidal biosparrudite
- Thin- to medium-bedded dolomite
- Thick, massive-bedded dolomite
- Cherty dolomite
- Chert
- Andesite
- Granite

ABBREVIATIONS

abund. — abundant
alt. — alternating
brach. — brachiopods
bryoz. — bryozoans
calc. — calcareous
crin. — crinoids
cryst. — crystalline
ech. — echinoids
frag. — fragments
fus. — fusulinids
gast. — gastropods
lam. — laminated
ls. — limestone
lt. — light
pelecy. — pelecypods
porc. — porcellanitic
qtz. — quartz
qtzite. — quartzite
sh. — shale
skel. — skeletal
ss. — sandstone
strom. — stromatolites
v. — very

Figures on left side of columns are in feet



Composite columnar section of Paleozoic and Mesozoic rocks in Organ and southern San Andres Mountains, New Mexico.

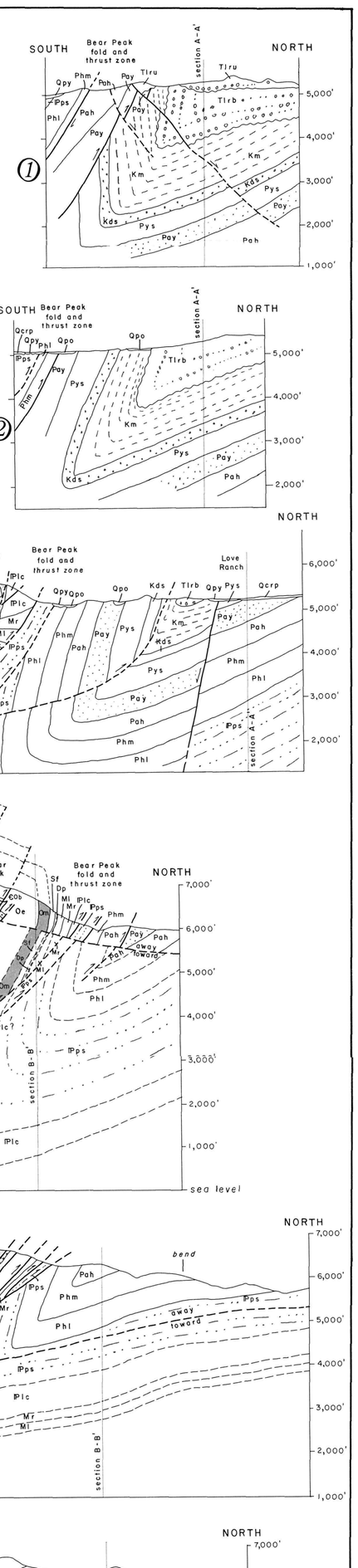
Columnar sections and
short cross sections for

Memoir 36

Geology of Organ Mountains and southern San Andres Mountains, New Mexico

by William R. Seager

1980



Geologic cross sections 1–8 along Bear Peak fold and thrust zone intersecting sections *A-A'* thru *C''-C'''* in north part of sheet 1 (no vertical exaggeration).

APPENDIX B—Chemical analyses

		Orejon Andesite		Cueva Tuff		tuff of Cox Ranch	tuff of Achenback Park			tuff of Squaw Mountain				west-side lavas							Organ batholith										Black Hills lava	
				base — top			base — top			base — top				base — top							monzo-diorite xenolith	Organ Needle quartz monzonite: alaskite facies	quartz syenite-quartz alkali feldspar syenite facies: Dunham anal.	quartz syenite-quartz alkali feldspar syenite facies	syenite facies	syenite mafic transitional	mafic facies	mafic facies: Dunham anal.	Sugarloaf Peak quartz monzonite porphyry	Sugarloaf Peak quartz monzonite porphyry: Lindgren (Dunham) anal.	granite of Granite Peak	rhyolite porphyry of Baylor Peak	Quartzite Mountain sill		
	Irvine-Baragar class field number →	dacite 78WS20	dacite 78WS11	rhyolite 78WS34	rhyolite 78WS35	rhyolite 78WS36	rhyolite 78WS37	rhyolite 78WS38	rhyolite 78WS22	rhyolite 78WS21	peralkal-rhyolite 78WS24	peralkal-rhyolite 77WS35	rhyolite 78WS25	rhyolite 78WS13	tristanite 78WS18	rhyolite 78WS17	trachyte 78WS12	dacite (vitrophyre) 78WS14	trachyte 78WS15	79WS9	78WS41	77WS77	78WS40	78WS47	78WS46	78WS45	78WS44	78WS42	78WS43	78WS39	78WS27	77WS166	77WS165
CHEMICAL ANALYSES (recalculated without CO_2 and Fe_2O_3 adjusted where needed so that $Fe_2O_3 = TiO_2 + 1.5$)	SiO_2	63.94	61.43	71.84	75.75	76.06	75.11	74.59	74.31	71.93	71.61	70.51	68.53	65.26	61.42	64.46	63.79	63.28	63.52	65.95	56.30	77.33	66.01	68.74	67.30	61.74	61.27	57.18	56.13	62.57	61.64	67.57	72.42	72.16	57.06	52.39
	TiO_2	.64	1.00	.18	.06	.10	.13	.12	.14	.05	.24	.52	.41	.46	1.06	.61	.73	1.08	.79	.89	1.25	.20	.66	.47	.35	.51	1.08	1.28	1.53	.75	1.31	.42	.30	.17	.73	1.10
	Al_2O_3	19.56	19.52	15.24	13.04	13.11	13.55	13.79	14.39	14.61	14.13	14.31	16.65	19.27	19.38	19.64	19.39	18.77	19.31	16.36	18.58	12.45	18.08	15.46	16.82	18.10	17.75	18.22	18.19	17.14	15.91	17.02	14.02	15.43	18.93	20.05
	Fe_2O_3	2.16	2.58	1.66	1.55	1.60	1.64	1.62	1.64	1.62	1.78	2.07	1.93	1.98	2.59	2.14	2.24	2.63	2.31	2.38	2.77	1.10	2.19	1.96	1.87	2.03	2.60	2.78	3.04	2.24	2.82	1.90	1.80	1.69	2.28	2.69
	FeO	1.61	1.60	.18	.10	.09	.14	.18	.05	.22	.30	.61	.22	.16	1.40	.36	.23	.82	.35	1.18	3.62	—	1.59	1.65	.65	2.33	2.62	3.28	4.57	2.39	3.18	.82	—	.23	3.66	4.59
	MnO	—	—	—	—	—	—	—	—	—	—	.07	—	—	—	—	—	—	—	.60	—	.02	—	.03	—	—	—	.06	—	.09	—	.08	—	—	—	—
	MgO	.52	.41	.03	.02	.04	.04	.12	.15	.14	.31	.24	.20	.35	.19	.46	.50	.34	.52	.94	2.69	.06	.23	.76	.33	.84	1.36	2.86	3.14	1.66	1.92	.40	.27	.20	.41	.64
	CaO	3.85	3.48	.28	.08	.10	.36	.29	.52	1.26	.38	.59	.44	.43	3.38	1.33	1.81	2.38	2.02	2.41	5.39	.08	.94	1.04	1.31	2.27	3.20	3.94	5.35	3.63	3.98	1.45	.69	.38	3.18	6.24
	Na_2O	4.40	4.26	4.28	4.50	3.28	3.16	3.80	3.54	2.85	5.23	4.88	5.07	4.62	5.53	5.85	5.83	5.01	5.92	4.44	6.12	3.23	3.86	4.71	5.87	6.79	5.56	6.23	4.41	5.06	4.18	5.06	5.13	2.09	3.20	2.97
	K_2O	3.32	5.73	6.32	4.91	5.62	5.86	5.48	5.25	7.33	6.04	6.17	6.54	7.45	5.05	5.15	5.48	5.69	5.26	4.72	3.29	5.50	6.43	5.16	5.49	5.38	4.57	4.24	3.53	4.57	4.52	5.37	5.07	7.64	10.53	9.33
	P_2O_5	—	—	—	—	—	—	—	—	—	—	.03	—	—	—	—	—	—	—	.11	—	.02	—	.03	—	—	—	.06	—	—	.45	—	.22	—	—	—
	total	100.00	100.01	100.01	100.01	100.00	99.99	99.99	99.99	100.01	100.02	100.00	99.99	99.98	100.00	100.00	100.00	100.00	100.00	99.98	100.01	99.99	99.99	100.01	99.99	99.99	100.01	100.01	100.01	100.01	100.00	100.01	100.00	99.99	99.98	100.00
CIPW NORM	Q	16.56	6.10	22.14	30.58	35.17	33.45	30.65	32.30	24.44	18.35	17.84	12.80	8.39	2.82	7.20	4.25	6.76	3.85	15.06	—	37.27	16.57	18.05	9.26	—	3.46	—	.89	6.45	10.44	13.54	22.30	29.62	—	—
	C	1.72	—	.86	.19	1.44	1.35	1.08	1.94	—	—	—	.45	2.80	—	2.04	.57	.05	.20	—	—	1.08	3.07	.32	—	—	—	—	—	—	—	.26	—	3.05	—	—
	Or	19.60	33.83	37.32	28.98	33.21	34.63	32.38	31.03	43.34	35.70	36.45	38.62	44.03	29.81	30.44	32.38	33.63	31.09	27.89	19.46	32.49	38.02	30.47	32.42	31.78	26.97	25.04	20.86	26.98	26.69	31.71	29.94	45.12	62.24	47.34
	Ab	37.25	36.04	36.19	38.06	27.79	26.72	32.16	29.94	24.08	39.03	39.26	42.90	39.14	46.77	49.47	49.35	42.38	50.09	37.60	41.87	27.37	32.65	39.84	49.68	50.15	47.01	41.60	37.28	42.78	35.33	42.82	43.39	17.68	7.97	—
	An	19.12	17.23	1.38	.39	.50	1.80	1.44	2.59	5.42	—	—	2.16	2.15	13.18	6.58	9.00	11.81	10.04	10.77	13.49	.27	4.65	4.95	3.35	3.04	10.01	9.25	19.42	10.59	11.34	7.17	.28	1.86	6.18	13.81
	Lc	—	—	—	—	—	—	—	—	—	—	—	—	—	—	—	—	—	—	—	—	—	—	—	—	—	—	—	—	—	—	—	—	—	—	6.12
	Ne	—	—	—	—	—	—	—	—	—	—	—	—	—	—	—	—	—	—	—	5.38	—	—	—	—	3.95	—	6.01	—	—	—	—	—	—	—	10.38	13.61
	Ac	—	—	—	—	—	—	—	—	—	4.57	1.82	—	—	—	—	—	—	—	—	—	—	—	—	—	—	—	—	—	—	—	—	—	—	—	—
	Di	—	.03	—	—	—	—	—	—	.67	1.48	2.02	—	—	2.59	—	—	—	—	.39	10.63	—	—	—	2.56	6.77	4.69	8.18	5.43	5.93	4.37	—	.76	—	8.27	11.65
	Wo	—	.01	—	—	—	—	—	—	.34	.78	1.03	—	—	1.28	—	—	—	—	.20	5.54	—	—	—	1.31	3.44	2.45	4.29	2.81	3.10	2.28	—	.41	—	4.01	5.69
	En	—	.01	—	—	—	—	—	—	.17	.59	.59	—	—	.49	—	—	—	—	.11	3.79	—	—	—	.73	1.81	1.77	3.16	1.82	2.16	1.59	—	.35	—	.94	1.59
	Fs	—	.01	—	—	—	—	—	—	.16	.11	.39	—	—	.82	—	—	—	—	.08	1.30	—	—	—	.53	1.53	.46	.72	.81	.68	.50	—	—	—	3.32	4.37
	Wo	—	—	—	—	—	—	—	—	—	—	.11	—	—	.22	—	—	—	—	—	—	—	—	—	—	—	—	—	—	—	—	—	—	—	—	1.47
	Hy	1.41	2.29	.11	.13	.10	.14	.43	.37	.33	.20	—	.50	.88	—	1.14	1.25	.85	1.29	3.97	—	.15	.61	2.57	.18	—	2.05	—	8.66	2.59	4.19	1.80	.32	.65	—	—
	En	1.29	1.02	.07	.05	.10	.10	.30	.37	.17	.17	—	.50	.88	—	1.14	1.25	.85	1.29	2.24	—	.15	.58	1.89	.11	—	1.63	—	6.00	1.97	3.18	.99	.32	.51	—	—
	Fs	.12	1.27	.03	.08	—	.04	.13	—	.16	.03	—	—	—	—	—	—	—	—	1.73	—	—	.03	.68	.08	—	.42	—	2.66	.62	1.00	.82	—	.14	—	—
	Fo	—	—	—	—	—	—	—	—	—	—	—	—	—	—	—	—	—	—	—	2.80	—	—	—	—	.39	—	3.48	—	—	—	—	—	—	.30	—
	Fo	—	—	—	—	—	—	—	—	—	—	—	—	—	—	—	—	—	—	—	2.03	—	—	—	—	.20	—	2.78	—	—	—	—	—	—	.06	—
	Fa	—	—	—	—	—	—	—	—	—	—	—	—	—	—	—	—	—	—	—	.77	—	—	—	—	.19	—	.70	—	—	—	—	—	—	.23	—
	Cs	—	—	—	—	—	—	—	—	—	—	—	—	—	—	—	—	—	—	—	—	—	—	—	—	—	—	—	—	—	—	—	—	—	—	—
	Mt	3.13	2.25	.06	.15	—	.08	.23	—	.56	.24	.69	—	—	1.44	—	—	—	—	3.19	4.01	—	3.17	2.85	1.06	2.94	3.76	4.03	4.40	3.25	4.09	1.43	—	.25	3.31	3.91
	Il	1.21	1.90	.34	.11	.19	.25	.23	.11	.10	.47	.98	.47	.34	2.01	.77	.49	1.73	.75	1.70	2.37	.04	1.26	.89	.67	.96	2.05	2.42	2.90	1.42	2.49	.79	.17	.33	1.39	2.09
	Hm	—	1.03	1.62	1.45	1.60	1.59	1.46	1.64	1.24	.03	.97	1.93	1.98	1.60	2.14	2.24	2.63	2.31	.18	—	1.10	—	—	1.14	—	—	—	—	—	—	.91	1.80	1.52	—	—
	Tn	—	—	—	—	—	—	—	—	—	—	—	—	—	—	—	—	—	—	—	—	—	—	—	—	—	—	—	—	—	—	—	.52	—	—	—
	Pf	—	—	—	—	—	—	—	—	—	—	—	—	—	—	—	—	—	—	—	—	—	—	—	—	—	—	—	—	—	—	—	—	—	—	—
	Ru	—	—	—	—	—	—	—	.08	—	—	—	.17	.28	—	.21	.47	.17	.40	—	—	.18	—	—	—	—	—	—	—	—	—	—	—	—	—	—
	Ap	—	—	—	—	—	—	—	—	—	—	.07	—	—	—	—	—	—	—	.26	—	.05	—	.07	—	—	—	.14	—	—	1.07	—	.52	—	—	—
	total	100.00	100.69	100.02	100.04	100.00	100.01	100.06	100.00	100.18	100.07	100.21	100.00	99.99	100.44	100.00	100.00	100.00	100.00	101.01	100.01	100.00	100.00	100.01	100.32	99.98	100.00	100.01	99.98	99.99	100.01	100.43	100.00	100.08	100.04	100.00
MOL NORM	Q	15.31	5.60	20.49	28.43	33.01	31.38	28.59	30.18	22.81	16.87	16.45	11.74	7.66	2.57	6.55	3.86	6.20	3.50	13.85	—	35.00	15.36	16.68	8.43	—	3.17	—	.82	5.92	9.71	12.40	20.59	27.81	—	—
	C	1.87	—	.94	.20	1.59	1.49	1.19	2.14	—	—	—	.49	3.02	—	2.18	.61	.05	.21	—	—	1.19	3.35	.35	—	—	—	—	—	—	—	.28	—	3.38	—	—
	Or	19.57	33.51	37.28	29.09	33.64	35.07	32.60	31.30	43.66	35.42	36.29	38.23	43.44	29.81	29.88	31.76	33.33	30.50	27.69	19.08	32.94	38.05	30.40	31.84	31.00	26.66	24.48	20.78	26.72	26.79	31.34	29.84	45.72	61.99	47.31
	Ab	39.48	37.90	38.38	40.55	29.88	28.72	34.37	32.05	25.75	41.10	41.49	45.07	40.98	46.77	51.53	51.38	44.59	52.16	39.62	43.57	29.45	34.69	42.20	51.79	51.92	49.32	43.16	39.41	44.96	37.64	44.91	45.91	19.01	8.38	—
	An	19.10	17.08	1.37	.40	.50	1.83	1.45	2.61	5.47	—	—	2.14	2.13	13.18	6.46	8.83	11.71	9.85	10.70	13.23	.28	4.65	4.94	3.29	2.97	9.90	9.04	19.35	10.49	11.39	7.09	.28	1.89	6.16	13.81
	Lc	—	—	—	—	—	—	—	—	—	—	—	—	—	—	—	—	—	—	—	—	—	—	—	—	—	—	—	—	—	—	—	—	—	—	6.24
	Ne	—	—	—	—	—	—	—	—	—	—	—	—	—	—	—	—	—	—	—	6.20	—	—	—	—	4.54	—	6.90	—	—	—	—	—	—	—	12.16	15.99
	Ac	—	—	—	—	—	—	—	—	—	4.37	1.74	—	—	—	—	—	—	—	—	—	—	—	—	—	—	—	—	—	—	—	—	—	—	—	—
	Di	—	.03	—	—	—	—	—	—	.65	1.49	1.97	—	—	2.42	—	—	—	—	.38	10.41	—	—	—	2.46	6.43	4.65	8.05	5.37	5.88	4.38	—	.78	—	7.65	10.89
	Wo	—	.01	—	—	—	—	—	—	.32	.75	.99	—	—	1.21	—	—	—	—	.19	5.20	—	—	—	1.23	3.21	2.32	4.02	2.68	2.94	2.19	—	.39	—	3.83	5.45
	En	—	.01	—	—	—	—	—	—	.19	.65	.66	—	—	.53	—	—	—	—	.12	4.13	—	—	—	.79	1.96	1.94	3.43	2.01	2.37	1.77	—	.39	—	1.04	1.76
	Fs	—	.01	—	—	—	—	—	—	.14	.09	.33	—	—	.68	—	—	—	—	.07	1.08	—	—	—	.44	1.26	.38	.59	.68	.57	.42	—	—	—	2.79	3.69
	Wo	—	—	—	—	—	—	—	—	—	—	.10	—	—	.20	—	—	—	—	—	—	—	—	—	—	—	—	—	—	—	—	—	—	—	—	1.41
	Hy	1.53	2.18	.11	.13	.11	.15	.45	.42	.32	.21	—	.55	.96	—	1.24	1.36	.93	1.40	3.92	—	.17	.67	2.66	.18	—	2.14	—	8.87	2.68	4.39	1.76	.35	.11	—	—
	En	1.43	1.12	.08	.06	.11	.11	.33	.42	.19	.19	—	.55	.96	—	1.24	1.36	.93	1.40	2.46	—	.17	.65	2.09	.11	—	1.78	—	6.63	2.16	3.54	1.08	.35	.08	—	—
	Fs	.10	1.06	.03	.07	—	.04	.11	—	.13	.03	—	—	—	—	—	—	—	—	1.45	—	—	.02	.57	.06	—	.35	—	2.24	.52	.85	.68	—	.03	—	—
	Fo	—	—	—	—	—	—	—	—	—	—	—	—	—	—	—	—	—	—	—	2.98	—	—	—	—	.38	—	3.78	—	—	—	—	—	—	.26	—
	Fo	—	—	—	—	—	—	—	—	—	—	—	—	—	—	—	—	—	—	—	2.36	—	—	—	—	.23	—	3.22	—	—	—	—	—	—	.07	—
	Fa	—	—	—	—	—	—	—	—	—	—	—	—	—	—	—	—	—	—	—	.62	—	—	—	—	.15	—	.56	—	—	—	—	—	—	.19	—
	Cs	—	—	—	—	—	—	—	—	—	—	—	—	—	—	—	—	—	—	—	—	—	—	—	—	—	—	—	—	—	—	—	—	—	—	—
	Mt	2.26	1.60	.04	.11	—	.05	.17	—	.40	.17	.49	—	—	1.02	—	—	—	—	2.28	2.84	—	2.29	2.05	.75	2.07	2.68	2.84	3.16	2.32	2.96	1.02	—	.04	2.38	2.82
	Il	.89	1.38	.25	.08	.14	.19	.17	.08	.07	.34	.72	.34	.25	1.45	.55	.35	1.26	.54	1.23	1.70	.03	.92	.65	.48	.69	1.49	1.74	2.12	1.03	1.83	.57	.13	.25	1.02	1.54
	Hm	—	.71	1.13	1.01	1.13	1.12	1.02	1.16	.87	.02	.67	1.33	1.36	1.10	1.47	1.53	1.82	1.58	.13	—	.78	—	—	.78	—	—	—	—	—	—	—	.63	1.25	.80	—	—
	Tn	—	—	—	—	—	—	—	—	—	—	—	—	—	—	—	—	—	—	—	—	—	—	—	—	—	—	—	—	—	—	—	.44	—	—	—
	Pf	—	—	—	—	—	—	—	—	—	—	—	—	—	—	—	—	—	—	—	—	—	—	—	—	—	—	—	—	—	—	—	—	—	—	—
	Ru	—	—	—	—	—	—	—	.06	—	—	—	.12	.20	—	.14	.32	.12	.27	—	—	.13	—	—	—	—	—	—	—	—	—	—	—	—	—	—
	Ap	—	—	—	—	—	—	—	—	—	—	.06	—	—	—	—	—	—	—	.21	—	.04	—	.06	—	—	—	.12	—	—	.89	—	.43	—	—	—
	total	100.01	99.99	99.99	100.00	100.00	100.00	100.01	100.00	100.00	99.99	99.98	100.01	100.00	98.52	100.00	100.00	100.01	100.01	100.01	100.01	100.01	99.98	99.99	100.00	100.00	100.01	99.99	100.00	100.00	99.98	100.00	100.00	99.01	100.00	100.01
	wt. norm	33.92	32.34	3.66	1.02	1.75	6.32	4.28	7.95	18.38	0.00	0.00	4.79	5.22	21.98	11.74	15.42	21.79	16.70	22.26	24.36	.98	12.46	11.05	6.32	5.72	17.55	18.19	34.25	19.85	24.30	14.35	.64	9.53	43.82	—
	plag (%An)																																			


NEW MEXICO BUREAU OF MINES
MINERAL RESOURCES